

LBL-8422

c.2

BIOCHEMISTRY OF SNAKE VENOM NEUROTOXINS
AND THEIR APPLICATION TO THE STUDY OF THE SYNAPSE

Michael Robert Hanley
(Ph. D. thesis)

November 1978

RECEIVED
LAWRENCE
BERKELEY LABORATORY

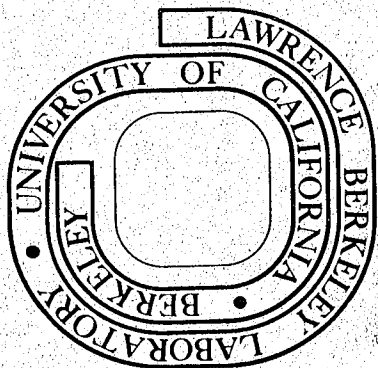
JAN 29 1979

LIBRARY AND
DOCUMENTS SECTION

Prepared for the U. S. Department of Energy
under Contract W-7405-ENG-48

TWO-WEEK LOAN COPY

*This is a Library Circulating Copy
which may be borrowed for two weeks.
For a personal retention copy, call
Tech. Info. Division, Ext. 6782*



LBL-8422

c.2

LEGAL NOTICE

This report was prepared as an account of work sponsored by the United States Government. Neither the United States nor the Department of Energy, nor any of their employees, nor any of their contractors, subcontractors, or their employees, makes any warranty, express or implied, or assumes any legal liability or responsibility for the accuracy, completeness or usefulness of any information, apparatus, product or process disclosed, or represents that its use would not infringe privately owned rights.

BIOCHEMISTRY OF SNAKE VENOM NEUROTOXINS
AND THEIR APPLICATION TO THE STUDY OF THE SYNAPSE

By

Michael Robert Hanley

ABSTRACT

The crude venom of the Formosan banded krait, Bungarus multicinctus, was separated into eleven lethal protein fractions. Nine fractions were present in sufficient concentrations to permit detailed studies, and were purified by three sequential chromatographic steps to final homogeneous toxins, designated α -bungarotoxin, β -bungarotoxin, and toxins 7, 8, 9A, 11, 12, 13, 14. On the basis of literature results and functional studies, three of the toxins, α -bungarotoxin, 7, and 8, were identified as post-synaptic curarimimetic neurotoxins, which inactivate neuromuscular transmission by preventing the binding of the neurotransmitter acetylcholine to its target receptor. The remaining toxins were identified as pre-synaptic neurotoxins, which inactivate neuromuscular transmission by blocking acetylcholine release.

α -Bungarotoxin, toxin 7, and toxin 8 are all highly stable basic polypeptides of ~ 8000 daltons molecular weight. The stability is due to the five disulfides which cross-link the toxins into compact and fairly rigid structures. By hydrodynamic and spectroscopic measurements, the toxins are asymmetric and have a high content of reverse turns (" β -bends") and β -sheets. Sensitive and insensitive regions of the proteins, in terms of biological activity, were identified by selective chemical modifications of amino acid side-chains. Two aromatic residues near α -bungarotoxin's hypothetical active site, tryptophan-28 and tyrosine-54, were studied by spectroscopic techniques as monitors of α -bungarotoxin's conformation and interaction with the acetylcholine receptor of Torpedo californica.

The pre-synaptic toxins fell into two structural groups: toxin 9A and 14 which were single basic chains of $\sim 14,000$ daltons, and β -bungarotoxin, and toxins 11 thru 13 which were composed of two chains of ~ 8000 and $\sim 13,000$ daltons covalently linked by disulfides. Spectroscopic and hydrodynamic studies indicated that these toxins were all spherical proteins rich in ordered secondary structures, both α -helix and β -structure. β -bungarotoxin was studied structurally and functionally after several selective chemical modifications. The single tryptophan of β -bungarotoxin was used to monitor the toxin's binding to model liposomes of defined compositions.

In the effort to further develop α -bungarotoxin's already extensive use as a neurobiological tool, two specific problems were addressed: whether iodinated α -bungarotoxin was functionally equivalent to a tritiated derivative, and whether there were unique features of curarimimetic toxin recognition by toxin-binding sites in rat brain. Tritiated α -bungarotoxin obeyed simple bimolecular reaction kinetics in its binding to membrane-bound acetylcholine receptor, but diiodinated toxin exhibited more complicated kinetics that suggested it either altered the receptor or itself experienced a concentration-dependent change in state. The data were interpreted as favoring the latter explanation inasmuch as diiodinated toxin appeared to undergo a concentration-dependent self-association to a dimer. It was suggested that this self-association complicated the interpretation of kinetic experiments and therefore that results based upon the use of iodinated toxins should not be used as a basis for models of the toxin-receptor interaction. As reported in the literature, radiolabeled α -bungarotoxin derivatives bound to a small population of saturable sites in rat brain. A closely-related toxin, dendrotoxin 4.7.3, was radiolabeled and shown to bind to twice the number of tritiated α -bungarotoxin sites in rat brain, and to an equivalent number on Torpedo californica acetylcholine

receptors. Because dendrotoxin 4.7.3 can block a nicotinic synapse in vertebrate brain and α -bungarotoxin cannot, a simple model was proposed to explain this observation, based upon the presence of extra sites to which dendrotoxin could bind and α -bungarotoxin could not.

All the pre-synaptic neurotoxins were shown to have intrinsic calcium-dependent phospholipase A activities. The pre-synaptic toxins were studied in terms of their binding and enzymatic selectivity on model unilamellar liposomes prepared from either tissue-extracted or purified lipids. Under certain conditions, intact synaptic membranes were hydrolyzed more rapidly than protein-free extracted synaptic-lipid liposomes which in turn, were hydrolyzed more rapidly than any other tested liposomes. It was suggested that both lipid and protein components contributed to this enhanced catalytic preference. By the change in the intensity and wavelength of the fluorescence emission maximum of β -bungarotoxin's single tryptophan, it was shown that the toxin bound to acidic lipids in the rank order of selectivity of phosphatidyl serine > phosphatidic acid > phosphatidyl inositol, and that the molar potency of phosphatidyl serine in eliciting this change was greatly enhanced by the addition of both calcium and total brain gangliosides. From these results, it was speculated that cell-surface arrays of phosphatidyl serine/glycolipids created high affinity target sites for β -bungarotoxin to which it could bind in high density, and further, that these arrays would be found in close association with membrane proteins mediating transport functions. The rapid accumulation of damage near membrane proteins inactivates their functioning and leads to the inhibition of the sodium pump, blockade of uptake sites, and a loss of membrane polarization. Single-chain toxins 9A and 14 were found to be qualitatively different from the two-chain toxins in their ability to block the functioning of Torpedo californica acetylcholine receptors, and were quantitatively different

in their enzymatic and membrane-disruptive activities. It was suggested that the presence of the light chain confers added selectivity to two-chain pre-synaptic toxins.

β -Bungarotoxin was shown to be an extremely potent neuronal lesioning agent with stereotaxic injection into defined regions of rat brain. There was no apparent selectivity for cholinergic over non-cholinergic neurons, nor for nerve terminals over cell bodies. Within 1 day, 1 nanogram of the toxin could produce an extensive focal degeneration of neurons in the corpus striatum, the dentate gyrus of the hippocampus, and the diagonal band of the septum, but caused little damage to the substantia nigra. The lesioning activity correlated with peripheral lethality since a non-toxic phospholipase from another snake venom did not cause lesions with stereotaxic administration. It was suggested that β -bungarotoxin can be considered a useful new histological tool, which may exhibit some regional selectivity.

In summation, detailed new information has been reported on the structures and functions of pre- and post-synaptic snake neurotoxins. This information has been used to develop new neurobiological applications of the toxins as selective synaptic tools.

Wm. F. J. Brown
Chairman of Thesis Committee

10-27-1978
Date

TABLE OF CONTENTS

ACKNOWLEDGMENTS	iii
ABBREVIATIONS	v
DEDICATION	vi
I. INTRODUCTION	1
i. Snake Venoms and Toxins	2
ii. The Skeletal Neuromuscular Junction: The Model for the Chemical Synapse	10
iii. Electroplaques	13
II. PURIFICATION OF THE BUNGAROTOXINS	16
Introduction	17
Methods.	20
Results.	23
Discussion.	35
References.	37
<hr/>	
III. PHYSICAL AND CHEMICAL CHARACTERIZATION OF THE BUNGAROTOXINS	40
Introduction	41
Methods.	46
Results.	51
Discussion.	74
References.	81
IV. SPECTROSCOPIC STUDIES OF THE BUNGAROTOXINS	84
Introduction	85
Methods.	88
Results.	92
Discussion.	122

IV. (con.)	
References.	132
V. APPLICATIONS AND FUNCTIONAL STUDIES OF THE α -TOXINS	135
Introduction	136
Methods.	141
Results.	150
Discussion.	184
References.	195
VI. APPLICATIONS AND FUNCTIONAL STUDIES OF THE β -TOXINS	200
Introduction	201
Methods.	205
Results.	210
Discussion.	236
References.	245
VII. SUMMARY AND PERSPECTIVES	249

ACKNOWLEDGMENTS.

My deepest thanks go to all of the following:

To Prof. H.Fraenkel-Conrat for his wit, candor, insight, and all-too-accurate advice, but most of all for his constant example of all that is excellent in science.

To Prof. Melvin Calvin for his enthusiasm, support, and creation of the unique multidisciplinary community of LCB.

To Dr.E.L.Bennett for introducing me to neuroscience, for advice, attention to detail, and lasting commitment to the Sierra Club.

To Drs. Piers Emson, Ron Lukasiewicz, and Tzyy-Wen Jeng for being excellent scientists, hard-working collaborators, and frank and intelligent critics.

To Hiromi Morimoto, Marie Hebert, and Ann Orme for clear thinking, superb work, and infectious enthusiasm ... proof that mere credentials do not a scientist make. (I would like to particularly thank Marie and Hiromi for their large contributions to work in this thesis on toxicology, enzymatic assays, and chromatography.)

To Profs. Gunther Stent, Reg Kelly, John Gerhart, Bob Zucker, and David Cole for setting me straight, providing ideas, being receptive but critical, and contributing in large measure to my professional maturation.

To Drs.Vesna Eterovic and Bill Vaughan for their early guidance and perspectives, encouragement, and assistance with learning techniques.

To second floor gang #1- Steve Cooper, Lynn Austin, Joe Landolph, Bob Blankenship, and Paul Hartig-for playing it straight, doing good work, and being fine friends.

To second floor gang #2-Clark Lagarias, Connie Oshiro, Craig Hodges,

and Anne McGuire- for hard work and good fun and the creation of an atmosphere that will be hard to beat, both personally and professionally. To the Neurobiology Group for being a home-away-from-home for a wayward biochemist with peculiar interests, both inside and outside the lab. To Marilyn Taylor, Marlyn Amann, and the others of the LCB secretarial and support staff for their unending assistance. And to Ethel LeFall for good coffee and conversation.

I would like to acknowledge the Division of Environmental and Biomedical Research of the U.S. Dept. of Energy, and the U.S. Public Health Service for their financial support.

ABBREVIATIONS.

A ₂₈₀	Absorbance at 280 nm
AChE	Acetylcholinesterase
α-Bgt	Alpha-bungarotoxin
β-Bgt	Beta-bungarotoxin
BSA	Bovine serum albumin
CD	Circular dichroism
CM	Carboxymethyl
CMF	Crude mitochondrial fraction
Ddt	Dendrotoxin 4.7.3
DMS	Dimethyl sulfoxide
d-TC	D-tubocurarine
DTT	Dithiothreitol
GABA	γ-amino butyric acid
HNB	2-Hydroxy-5-nitrobenzyl
³ H-α-Bgt	Tritiated alpha-bungarotoxin
¹²⁵ I-α-Bgt	Iodinated alpha-bungarotoxin
MCD	Magnetic circular dichroism
nAChR	Nicotinic acetylcholine receptor
NBS	N-bromosuccinimide
PA	Phosphatidic acid
PhA	Phospholipase A
PI	Phosphatidyl inositol
PMSF	Phenylmethylsulfonyl fluoride
PS	Phosphatidyl serine
SDS	Sodium dodecyl sulfate
UV	Ultraviolet

-vi-
DEDICATION.

为
人
民
服
务

"Serve the People", Chairman Mao, 1944.

CHAPTER I.
INTRODUCTION.

I. INTRODUCTION.

i. SNAKE VENOMS AND TOXINS.

Every animal venom is a natural pharmacopoeia. Venoms are complex mixtures of diverse biologically-active components (1). When the venoms are fractionated, the purified agents which possess deleterious (toxic) activities are known as toxins. For many decades, fractionation of venoms into active ingredients was aimed at identifying useful clinical compounds or explaining the physiological basis of the toxic activities. In some cases, agents with direct clinical utility have been identified, such as the clotting factors from some snake venoms (2). More recently, the successful description of toxic actions at the cellular level has led, particularly in the neurosciences (3), to the growing awareness of the significance of "selective toxicity" for basic research. Evolution has endowed individual toxins with exquisite selectivity, potency, and often but not always, stability to guarantee their biological success. Snake toxins are singularly apt examples, and it is precisely these characteristics which have focused concerted study on the biochemistry and implementation of snake toxins as pharmacological tools. Prior to this reconsideration of snake toxins as tools, however, considerable research had already been undertaken, motivated by either the desire to develop treatments for snakebite, or to understand the unusual physical chemistry of these small, stable, and highly active polypeptides.

Venoms contain both toxic and non-toxic components that are generally amino acids or proteins. For snake venom research, the greatest interest has been in the toxic components which, to date, have all been polypeptides (1,4). The first clear demonstration that a snake toxin was a protein was the crystallization of crotoxin by Slotta and Fraenkel-Conrat in 1938 (5). Over fifty purified snake neurotoxins have been sequenced and, towards increas-

ingly refined structural information, the first three-dimensional crystal structures of snake toxins have very recently become available (6,7).

Interest in the non-toxic components has focused on venom enzymes. Most, if not all, venom enzymes can be considered degradative and contributory to the overall toxicity of a crude venom (8). It is thought that the degradative enzymes participate by improving tissue penetration by the toxins, as well as by cooperative actions with certain toxins (8). Several biochemically useful classes of enzymes have been isolated from snake venoms, including phospholipases for membrane research, phosphodiesterases for nucleic acid sequencing, and proteases for protein chemistry. Work reported herein will be overwhelmingly focused on the neurotoxic proteins of snake venoms, and will deal only superficially with non-toxic constituents.

The major families of poisonous snakes are shown in Table I-1. Snakes from the Elapid and Hydrophid families are uniformly and exclusively neurotoxic in the action of their crude venoms (1), whereas Crotalid and Viperid snake venoms vary from neurotoxic to necrotic to cardio- or vasoactive (1,9). Considerably more information is available on the structures and activities of the toxins from Elapid and Hydrophid venoms.

The toxins from Elapid and Hydrophid venoms are all quite rapid in their lethal action, causing death within minutes in most cases. This rapidity is the first toxicological clue to their action on excitable tissues, although this should not be taken as a suggestion that mere speed constitutes a diagnostic test for neurotoxicity. Subsequent physiological research has established that the toxicological hints are not misleading and, indeed, that the toxins from these venom families work on excitable membranes. The major categories of snake toxins are shown in Table I-2. The most prevalent toxins are the post-synaptic ("curarimimetic" or " α -type") neurotoxins. Many such toxins have been purified and sequenced, and a picture of strik-

TABLE I-1

POISONOUS SNAKE FAMILIES

Family	Common Names	Toxic Activities
Elapidae	Cobras, Kraits, Mambas	Neurotoxins, Cytotoxins [*] , Toxic Phospholipases A ₂ , Necrotoxins
Hydrophiidae	Sea snakes	Neurotoxins, Myotoxins
Crotalidae	Rattlesnakes, Pit vipers	Neurotoxins, Cardiotoxins [*] , Hemorrhagic factors, Necrotoxins, Hemotoxins, Toxic Phospholipases A ₂
Viperidae	True vipers	Neurotoxins, Cardiotoxins [*] , Hemorrhagic factors, Necrotoxins, Hemotoxins, Toxic Phospholipases A ₂

* The cytotoxins of Elapidae venoms are referred to in the text as "cardiotoxins". However, they are called "cytotoxins" here to differentiate them from the structurally and functionally distinct cardiotoxins of Crotalid and Viperid species.

TABLE I-2
FUNCTIONAL CATEGORIES OF SNAKE TOXINS

Activity	Examples	Occurrence
Post-Synaptic (Curarimimetic, α -Type)	Cobrotoxin, α -Bungarotoxin	Elapidae, Hydrophiidae
Cardio- or Cytotoxin	Cobramine	Elapidae
Toxic Phospholipases A ₂ (includes Pre-Synaptic, β -Type)	β -Bungarotoxin, Crotoxin	Elapidae, Crotalidae Viperidae
Sodium Channel Toxins	Crotamine	Crotalidae

ing structural conservation has emerged (10). In Figure 1-1, the primary structures of these neurotoxins have been aligned for maximum homology, and then collapsed into a schematic diagram of conserved features. Note that the disulfide positions and the positions of several charged or aromatic residues are invariant. Curarimimetic toxins can be subdivided into two classifications based upon size; Type I ("short") neurotoxins of 6800-7000 daltons, and Type II ("long") neurotoxins of 7800-8200 daltons.

The next most prevalent toxin type is the cardio- or cytotoxin. These toxins appear to work indiscriminately on any cell membrane by discharging its resting potential (11). Until recently, there was a confusion surrounding these toxins owing to the plethora of biological activities they appeared to possess; now known to arise from this single cause. Thus, cardiotoxins have been called "skeletal muscle depolarizing factor", "cobramine", "direct lytic factor", or "membrane-active polypeptides". Various membranes vary in their in vivo sensitivity to these toxins; cardiac muscle and erythrocytes being unusually sensitive. Consequently, these venom components are generically known as cardiotoxins because their heart-stopping action accounts for their lethality. Like curarimimetic toxins, cardiotoxins have a highly conserved primary structure which, intriguingly, is very closely related to that of the curarimimetic neurotoxins. Indeed, Figure 1-1 has included sequence data for cardiotoxins and indicates residues common to both toxin classes. The invariance of the disulfide positions is the most significant aspect of this homology. Nevertheless, in spite of their strong resemblance to curarimimetic toxins, cardiotoxins have no post-synaptic activity because they lack critical amino acid residues.

The third major toxin type is the toxic phospholipase A₂ (E.C.3.1.1.4). Until a few years ago, this category would have been called "pre-synaptic" neurotoxins. However, this designation obscures the fact that there are other structurally-related toxic phospholipases A₂ that did not have the

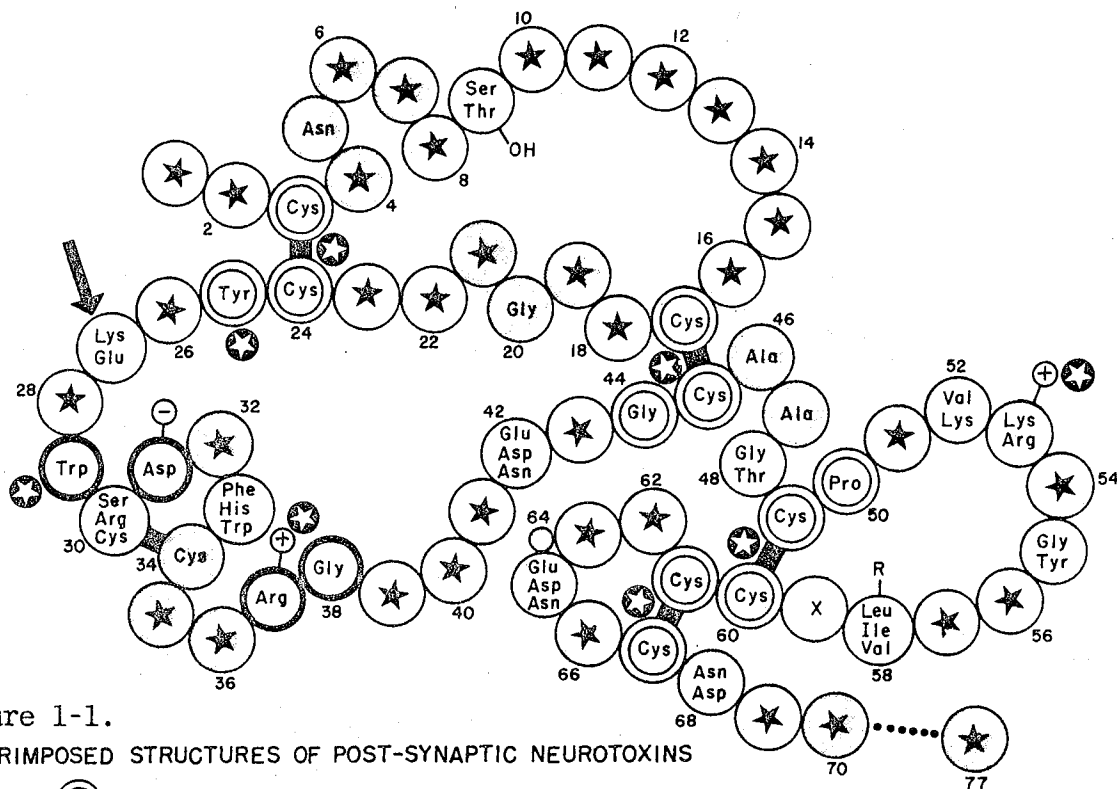


Figure 1-1.
 SUPERIMPOSED STRUCTURES OF POST-SYNAPTIC NEUROTOXINS

- - Common to all neuro- and cardiotoxins
- ◐ - Common only to neurotoxins
- ⊖ - Deletable residues (lacking in some toxins)
- ⊕ - Residues vital for toxic action (modification abolishes toxicity)
- ★ - Variable residue

pre-synaptic nerve ending of the neuromuscular junction as their toxic target. For years, the role of various isoenzymes of phospholipase A₂, known to be present in high levels in snake venoms, in the lethality of the crude venom was debated (8). For example, they appeared to potentiate the action of cardiotoxins (8) but have no intrinsic toxicity. Within the last five years, it has become clear that there are both toxic and non-toxic forms of phospholipase A₂, and that the former may be either selective for a particular tissue or widely disruptive (12). Toxic phospholipases A₂ have been identified that are directed to the nerve terminals of the skeletal neuromuscular junction ("pre-synaptic" or "β-type"), muscle sarcoplasmic reticulum, kidney glomeruli, erythrocytes, and lungs (12). Other than the in vitro enzymatic specificity and some sequence homology, little has been discovered about the similarities or differences of these toxins that account for their tissue selectivity. Similarly, little is known about the differences between toxic and non-toxic variants of the enzyme.

Although it has not been detected in any Elapid or Hydrophid venom, I have included the final category of snake toxin working on an excitable membrane, the axonal toxin. To date, only two have been described and only in Crotalid venoms. These toxins appear to work by selectively activating the axonal and muscle membrane sodium channels, leading to an irreversible depolarization (13). One of these, crotamine, has been sequenced (14).

An evolutionary scheme, based upon sequence relationships, has been put forward by Prof. C.Y.Lee. In Figure 1-2, the scheme shows the evolution of contemporary toxins from ancestral proteins that are universal constituents of salivary glands. The scheme is primarily based upon the observation that the disulfide positions have apparently been retained in toxic phospholipases A₂ compared to cardiotoxins, in turn compared to curarimimetic neurotoxins.

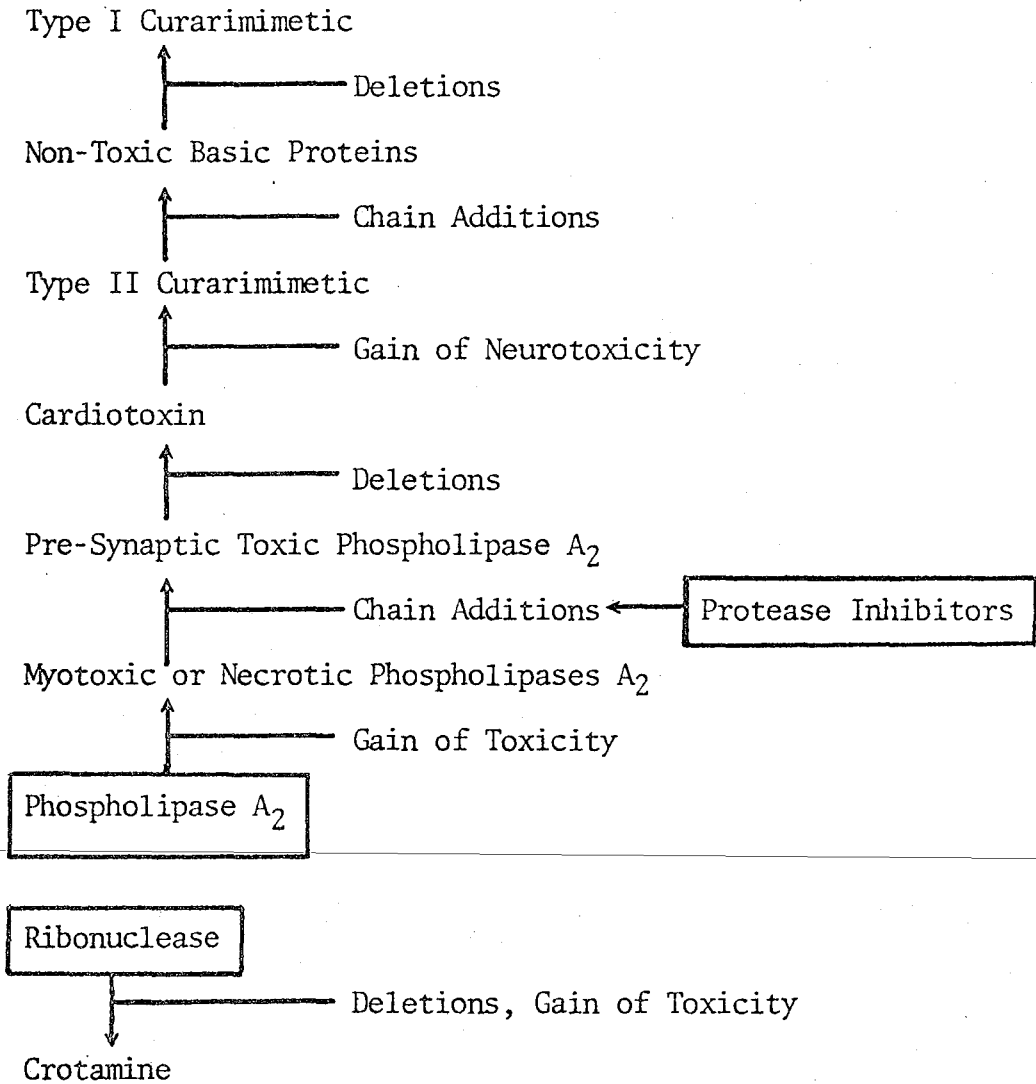


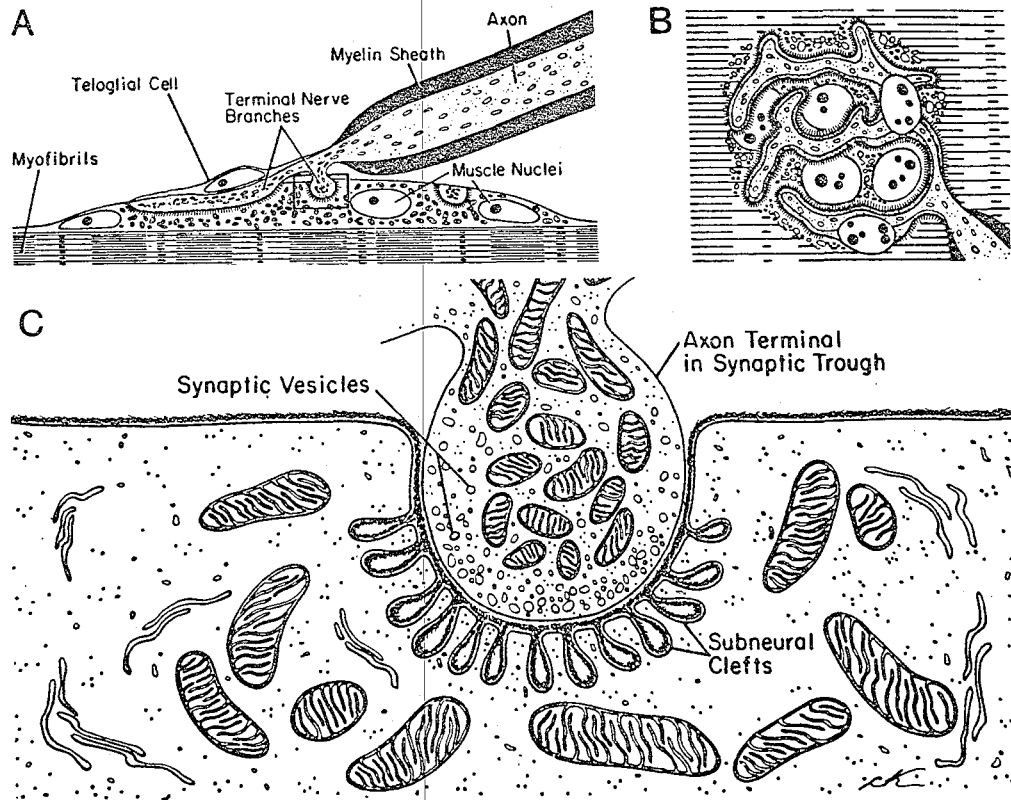
Figure 1-2. Proposed evolution of snake venom toxins from ancestral salivary gland proteins (in boxes). (Prof.C.Y.Lee,National Taiwan University)

ii. THE SKELETAL NEUROMUSCULAR JUNCTION: THE MODEL FOR THE CHEMICAL SYNAPSE

When considering the number of possible target sites, it is obvious that both the most potent toxins, and the largest number of toxins, from snake venoms are directed to the neuromuscular junction of voluntary muscle. On reflection, this is hardly surprising because inactivation of this junction causes an immediate flaccid paralysis and, in view of its accessibility to the circulation, this site is the most vulnerable point in the nerve-muscle system. There are very few centrally acting toxins and only one of these, apamin from bee venom (15), occurs in a venom. Thus, it appears that there is a strong evolutionary tendency to select for neuromuscular-junction toxins in animal venoms. Indeed, scorpion, spider, fish, and mollusc venoms all contain toxic proteins directed to this site (16).

From the standpoint of venom research, this is fortuitous, because the neuromuscular junction is the best understood chemical synapse in terms of its anatomy, physiology, and pharmacology, and many of our basic ideas of synaptic transmission have been derived from it. Consequently, snake toxin investigations have the advantage of a large background literature on their target site. In practice, one does not simply learn about neurotoxin mechanisms without learning about neuromuscular junction events. The scope of neurotoxin research therefore extends into the arena of the chemistry and physiology of synaptic transmission. It is no surprise that protein neurotoxins have been most highly refined as tools by application to the study of the neuromuscular junction. Thus, it is important to review the current knowledge of the neuromuscular junction and toxin interference with its functioning.

In Figure 1-3, a diagram of the neuromuscular junction illustrates the important features of its organization. It basically consists of a differentiated portion of the muscle surface into which the axonal ending fits, separated by a gap of 60-80 nm. The nerve ending is depolarized by a nerve impulse travelling down the motorneuron axon, leading to the activation of



XBL 764-1125
 Figure 1-3. Mammalian skeletal neuromuscular junction. A: Side view of a single junction at low magnification. B: Surface view of terminal branching of a motorneuron onto a muscle. C: EM view.

voltage-sensitive calcium channels. The resulting calcium influx constitutes the primary signal for secretion, as in other exocytotic systems (17). By an unknown mechanism, calcium ions trigger the release of neurotransmitter, acetylcholine, in increments of a basic packaging unit known as a "quantum". (It is currently assumed that the ultrastructural correlate of a quantum is a synaptic vesicle, although there are some difficulties with this interpretation (18)). Acetylcholine diffuses across the cleft to interact with binding molecules on the muscle, or post-synaptic, surface. These binding molecules are known as nicotinic acetylcholine receptors and are, in effect, chemosensitive ion channels. In response to neurotransmitter (or neurotransmitter analogues known as "agonists"), the receptors open channels which let both sodium and potassium ions redistribute, creating a depolarization or "generator potential" which then triggers the excitable muscle membrane to fire an impulse. Acetylcholine diffuses away from the receptors, which are now known to be concentrated in a narrow band at the top of the junctional folds (19), to the interior of the folds, wherein it is hydrolyzed to acetate and choline by the enzyme acetylcholinesterase. The transmission machinery is very parsimonious in its use of materials and scavenges the liberated choline, for acetylcholine resynthesis, by a pre-synaptic high-affinity uptake system (20). Likewise, synaptic vesicle membrane is thought to be recycled by its integration with the pre-synaptic membrane during exocytosis, and then subsequent reformation from coated vesicle and reticular intermediates (21).

Curarimimetic toxins interfere with normal transmission at the post-synaptic surface by interacting with the acetylcholine receptor. This interaction is extremely specific and very strong (dissociation constants range from 10^{-9} to 10^{-11} M for α -toxins). As a result of α -toxin binding, acetylcholine is unable to bind and thus activate the receptor (22). This

type of non-depolarizing neuromuscular block is qualitatively identical to that produced by the curare alkaloids (23); hence the term "curarimimetic" toxins. The specificity and tenacity of toxin binding has enabled their widespread use as natural affinity ligands for the labelling and isolation of the acetylcholine receptor (24).

The pre-synaptic toxins are a sub-class of the toxic phospholipases A₂ that block neuromuscular transmission by interfering with acetylcholine release. So far, all of the purified β -type toxins appear to have three phases in their pre-synaptic block; an initial depression, a secondary facilitation, and then a slow (60-90 min) decline in both spontaneous and evoked transmitter release (25). Neurally evoked transmitter release fails before spontaneous release activity has ceased. The involvement of the phospholipase A₂ activity in this block has been inferred (26), but a specific mechanism has yet to be worked out.

iii. ELECTROPLAQUES.

Although the skeletal neuromuscular junction is the best model for the physiology and anatomy of chemical synapses, it has not been possible to obtain sufficient material for its biochemical study. Fortunately, there exists an evolutionary homologue of muscle tissue in the electric tissues of marine animals ("electroplaques").* This tissue is densely innervated by acetylcholine-using ("cholinergic") nerve endings and thus constitutes a rich source of both pre- and post-synaptic material. The pre-synaptic preparations include purely cholinergic pre-synaptic nerve terminals, isolated by centrifugation from tissue homogenates, which are able to function in vitro (27), and cholinergic synaptic vesicles (28). Post-synaptic membranes can be isolated, made to reseal into vesicles which can retain radiotracer ions, and remain chemically excitable by cholinergic agonists (29).

These "excitable vesicles" or "microsacs" constitute a biochemical test system analogous to muscle, and it is assumed that there is considerable reciprocity of results obtained in one system in extension to the other. Previous studies have shown that by either biochemical (i.e., excitable vesicles) or physiological (i.e., direct electrical recording) testing, electroplaques tissue responds to neurotoxins in a similar fashion to the neuromuscular junction (30); although one exception has recently been described (31).

* The most frequently used specimens for electric tissue sources have been various species of electric ray (Torpedo or Narcine), and the electric eel (Electrophorus electricus).

REFERENCES.

1. Mebs, D. (1973) *Experientia*, 29, 1328.
2. Jimenez-Porras, J.M. (1970) *Clin.Toxicol.*, 3, 389.
3. Von Hahn, H.P., and Honegger, C.G. (1973) *Experientia*, 30, 2.
4. Lee, C.Y. (1972) *Ann.Rev.Pharmacol.*, 12, 265.
5. Slotta, K.H., and Fraenkel-Conrat, H.F. (1938) *Ber.Deut.Chem.Ges.*, 71, 1076.
6. Low, B.W., Preston, H.S., Sato, A., Rosen, L.S., Searl, J.E., Rudko, A.D., and Richardson, J.S. (1976) *Proc.Nat.Acad.Sci.*, 73, 2991.
7. Tsernoglou, D., and Petsko, G.A. (1977) *Proc.Nat.Acad.Sci.*, 74, 971.
8. Zeller, E.A. (1977) *Experientia*, 33, 143.
9. Tu, A.T., Venoms:Chemistry and Molecular Biology, John Wiley and Sons, New York, 1977.
10. Tu, A.T. (1973) *Ann.Rev.Biochem.*, 42, 235.
11. Condrea, E. (1974) *Experientia*, 30, 121.
12. Eaker, D. (1978) International Symposium on Proteins, Taipei, Taiwan.
13. Chang, C.C., and Tseng, K.H. (1978) *Brit.J.Pharmacol.*, 63, 551.
14. Laure, C.J. (1975) *Hoppe-Seyler's Zeit.Physiol.Chem.*, 356, 213.
15. Habermann, E. (1972) *Science*, 177, 314.

16. Zlotkin, E. (1973) *Experientia*, 29, 1.
17. Douglas, W.W. (1974) *Biochem.Soc.Symp.*, 39, 1.
18. Krnjevic, K. (1974) *Physiol.Rev.*, 54, 418.
19. Fertuck, H.C., and Salpeter, M.M. (1974) *Proc.Nat.Acad.Sci.*, 71, 1376.
20. Potter, L.T. (1970) *J.Physiol.*, 206, 145.
21. Heuser, J.E., and Reese, T.S. (1973) *J.Cell Biol.*, 57, 315.
22. Lester, H.A. (1972) *Mol.Pharmacol.*, 6, 623.
23. Jenkinson, D.H. (1960) *J.Physiol.*, 152, 309.
24. Fewtrell, C.M.S. (1976) *Neuroscience*, 1, 249.
25. Chang, C.C., Lee, J.D., Eaker, D., and Fohlman, J. (1977) *Toxicon*, 15, 571.
26. Strong, P.N., Goerke, J., Oberg, S.G., and Kelly, R.B. (1976) *Proc.Nat. Acad.Sci.*, 73, 178.
27. Dowdall, M.J., and Zimmerman, H. (1977) *Neuroscience*, 2, 405.
28. Carlson, S.S., Wagner, J.A., and Kelly, R.B. (1978) *Biochemistry*, 17, 1188.
29. Kasai, M., and Changeux, J.-P. (1971) *J.Mem.Biol.*, 6, 1.
30. Changeux, J.-P., Kasai, M., and Lee, C.Y. (1970) *Proc.Nat.Acad.Sci.*, 67, 1241.
31. Hanley, M.R. (1978) *Biochem.Biophys.Res.Communs.*, 82, 392.

CHAPTER II.
PURIFICATION OF
THE BUNGAROTOXINS.

II. INTRODUCTION.

The venom of the Formosan banded krait, Bungarus multicinctus, is one of the most popular and extensively studied venoms of any animal species. The reason for this interest is the historical and continuing significance of its major toxins, α -bungarotoxin (α -bgt) and β -bungarotoxin (β -bgt) as models of two functional classes of snake neurotoxins, pre- and post-synaptic. As a result, both α -bgt and β -bgt have been studied in detail (1,2,4,5,7,9) and sequenced (3,6). However, there are functional relatives of these neurotoxins in the same venom which have not received as much attention. Pharmacological studies of these other toxins (collectively known as "bungarotoxins") on vertebrate neuromuscular junctions (1,2,4) indicated that they fell into two classes; " α -type" similar to α -bungarotoxin, and " β -type" similar to β -bungarotoxin. One goal of the complete purification of the family of bungarotoxins was to examine the structural basis for the pharmacological similarity. The longer range goal was to initiate the detailed functional study of the purified toxins for possibly novel aspects of their superficially similar actions.

Apart from interest in the less-studied bungarotoxins, a complete purification of the venom components offered the advantage of a standard reproducible isolation procedure for individual toxins that could be applied in different laboratories. The need for such a procedure is evident from the literature. α -Bgt has been routinely prepared by an initial fractionation of the crude venom on carboxymethyl- (CM-) Sephadex, followed by a second chromatography on CM-cellulose, using elution by linear salt gradients in each step (1-3, 7). In Table II-1, the range of purification procedures and the evidence for purification or accurate identification of a given toxin is presented. Clearly, the evidence for purification or

TABLE II-1

SUMMARY OF BUNGAROTOXIN PURIFICATIONS.

Ref.	Toxins Purified	Purification Methodology ¹	Purity Criteria	Identification ²
1	All	1) Gradient elution (.05-1 M NH ₄ OAc) from CM-Sephadex CAE (pH 7.4) 2) Stepwise elution from CM-Cellulose		3
2	All	1) as (1) 2) Rechromatography as (1)	None	Alignment NMJ-block
4	β -Type Toxins 10 thru 13	1) Gradient elution (.05-.4 M NaCl) from CM-Sephadex 2) Sephadex G50 3) Repeat step #1	PAGE (pH 4.3;7.6) Rechromatography	Alignment NMJ-block Amino acid anal.
8	α -Bgt	1) Column electrofocusing (pH 3-10) 2) as (1)	Rechromatography IF	³ H-ACh binding inhibition
9	α -Bgt	1) Starch gel electrophoresis 2) Gradient elution (.05-1 M NH ₄ OAc) from CM-Cellulose	N-terminal anal. IF	NMJ-block Amino acid anal.
10	α -Bgt	1) Sephadex G50 2) Gradient elution (0-1 M NaCl) from CM-Sephadex	Rechromatography SDS-PAGE	None
11	α -Bgt	1) Gradient elution (0-1 M NaCl) from SP-Sephadex 2) Repeat step #1 with gradient elution .2-.5 M NaCl	PAGE (pH 4.3)	None
12	β -Bgt	1) as (1)	Gel filtration SDS-PAGE IF	NMJ-block Amino acid anal.
13	β -Bgt	1) Gradient elution (.05-1 M NH ₄ OAc) from CM-Cellulose CAE (pH 7.4) 2) Sephadex G75 3) Repeat step #1 with gradient elution .5-.7 M NH ₄ OAc		NMJ-block Amino acid anal.
14	β -Bgt	1) Sephadex G50 2) Gradient elution (.35-1 M NaOAc) from SP-Sephadex	PAGE (pH 4.3)	NMJ-block
17	β -Bgt	1) Gradient elution (.5-.95 M NH ₄ OAc) from CM-Sephadex	SDS-PAGE Ultracentrifugation	None

Footnotes to Table II-1.

- ¹Steps are listed starting with initial fractionations of the crude venom. "As (1)" refers to the use of the identical chromatographic conditions as in reference 1, step #1 in this Table.
- ²Identification procedures include both pharmacological tests (NMJ-block, ³H-ACh binding inhibition) which do not distinguish between structurally different toxins, and chemical methods (alignment, amino acid anal.) which do. NMJ-block, determines pre- vs. post-synaptic activity and time course of blocking effect on isolated nerve-muscle preparation; ³H-ACh binding inhibition, determines post-synaptic activity by ability to antagonize binding of ³H-ACh to electric tissue cholinergic receptor; alignment, determines chromatographically equivalent toxins by matching of experimental chromatography profile with literature; amino acid anal., amino acid composition analysis.
- ³This paper is used as the basis for subsequent identifications. " α -Bgt" and " β -bgt" are defined here.

Abbreviations used: anal., analysis; α -bgt, α -bungarotoxin; β -bgt, β -bungarotoxin; CAE, cellulose acetate electrophoresis; CM-, carboxymethyl; IF, isoelectric focusing; NMJ, neuromuscular junction; PAGE, polyacrylamide gel electrophoresis; SDS-PAGE, sodium dodecyl sulfate gel electrophoresis; SP-, sulfopropyl.

identification is often weak or absent, and, in some cases, persistent contaminants are still detectable (13). The dangers of incomplete purification or contamination are the detection of the biological activity of the contaminant in screening tests (15,16), or the unreliability of quantitative studies. The failure to properly characterize a toxin can give rise to a persistent mistaken identification, such as the confusion surrounding a " β -bgt" isolated by Livengood et al (17), which is unequivocally NOT the true β -bgt which has been sequenced (6), but rather our toxin 14 (18). Because toxin 14 is both structurally and functionally distinct from true β -bgt, the attribution of its properties to β -bgt has introduced a dangerous confusion into the literature.

This chapter describes the purification of the toxic fractions of Bungarus multicinctus crude venom, and the evidence for their homogeneity and freedom from cross-contamination.

METHODS.

i. Fractionation of Crude Venom. Lyophilized crude venom (Miami Serpentarium) was dissolved in 0.05 M ammonium acetate buffer (pH 5.0) and centrifuged at 39,000 X g for 15 min at 4°C. The small precipitate was discarded and the supernatant was applied to a 2.5 X 85 cm CM-Sephadex C50 (Pharmacia) column. The column was washed with 0.05 M ammonium acetate until the absorbance at 280 nm had returned to baseline (monitored by a Chromotronic Model 220 flow-thru UV monitor). Adsorbed proteins were eluted by a linear gradient of 0.05 M (pH 5.0) to 1 M (pH 7.0) ammonium acetate (1), and twelve discrete peaks of absorbance at 280 nm were obtained. More strongly retained proteins were then eluted by true chromatography using 1 M (pH 7.0) ammonium acetate, and four final peaks of absorbance at 280 nm were collected. The results described are a composite of data derived from nine separate preparative fractionations of several

different lots of lyophilized B.multicinctus crude venom. Chromatographic details are provided in the figure legends. In all cases, columns were run at 4°C and elution monitored by A₂₈₀ in the flow-thru monitor.

ii. Purification of CM-Sephadex Fractions. For the first experiments, pure α-bgt was obtained from fraction 3 by rechromatography on CM-cellulose (Whatman) (1,7). For later experiments, all fractions were treated to the same protocol. Fractions were desalted and concentrated by pressure dialysis (Amicon UM-2 filter) to 1-2 mL. The concentrated material was then chromatographed on a 2.6 X 40 cm Sephadex G50 (fine) column using upward elution with 0.1 M ammonium acetate (pH 6.8). The major chromatographic peaks, which were in all cases potent lethal toxins (18), were pooled, desalted, and concentrated. These fractions, which for convenience were numbered as in the initial chromatography (7), were applied to a 2.5 X 20 cm Bio-Rex 70 (Bio-Rad, 200-400 mesh, sodium form) column, rinsed with 150 mL of 0.05 M sodium acetate buffer (pH 6.0), and eluted with a linear gradient of 0 to 1.0 M sodium chloride in the same buffer. Quantitative measurements of the lethality to mice were made after each purification step (7,18). Final fractions were desalted, concentrated, and either lyophilized, or stored frozen in a dilute neutral buffer. Lyophilized components were stored dessicated at -20°C.

iii. Assay of Enzymatic Activities. Acetylcholinesterase (EC 3.1.1.7) was determined by the method of Ellman et al (19). The substrate was acetylthiocholine at a final concentration of 6×10^{-4} M. As a blank for each determination, identical assays were done in the presence of 10^{-5} M eserine (an anticholinesterase). Hyaluronidase (EC 4.2.99.1) was measured by the turbidimetric method of DiFerrante (20) with hyaluronic acid at several concentrations. Phosphomonoesterase (EC 3.1.3.1) activity was measured with p-nitrophenyl phosphate as a substrate following the method of Lowry (21). Nucleotide pyrophosphatase (NADase, EC

3.6.1.9) was determined by the method of Kornberg and Pricer (22) with 8 or 27 mM β -NAD. Phospholipase A (EC 3.1.1.4) was measured by the titrimetric method of Saito and Hanahan (23). Proteolytic activities were screened using azocasein (24). Arginine esterase was measured by the hydrolysis of BAPNA (N-benzoyl-DL-arginine-p-nitroanilide hydrochloride) which produces a product absorbing at 405 nm. Proteinase inhibitor assays employed BAPNA as a synthetic substrate for purified trypsin (Sigma Type XI) to which assay aliquots were added (24).

iv. Electrophoresis. Phenol:acetic acid:urea polyacrylamide gels were prepared by an adaptation of the procedure of Takayama et al (25). Sodium dodecyl sulfate:urea gels were prepared by the method of Eipper (26). Sodium dodecyl sulfate (SDS) cylindrical and slab gels were prepared according to Laemmli (27). Polyacrylamide slab gels were prepared by increasing the concentration of acrylamide in the direction of migration. A linear gradient of acrylamide (10-20% or 17.5-20%), with the ratio of acrylamide to bisacrylamide 20:1 (w/w), was cast as the separating gel and overlaid by a 5% stacking gel. 10-50 μ g of protein were applied, and were pre-treated by boiling for 2 min with or without β -mercaptoethanol (5% v/v). Gels were then stained in all cases by the procedure of Fairbanks et al (28).

v. Isoelectric Focusing. Isoelectric focusing in a pH 3-10 gradient was performed according to the procedures of Vesterberg (29), Fawcett (30), and Trump and Singer (31) using both chemical and photopolymerization for the polyacrylamide support (7.5% and 10% gels). The pH profile was determined by slicing a control gel (containing no protein) into 2 mm sections which were then incubated in 250 μ L of deionized water overnight (under a nitrogen barrier to prevent pH changes in the basic region from atmospheric carbon dioxide), and the pH measured with a microelectrode (Microelectrode Inc. Micro-Combination pH Probe). Proteins

were fixed and rinsed free of ampholines in 10% trichloroacetic acid over four days with repeated changes, and then stained by Coomassie Blue (28). When elution of the focused protein was desired, fixation was omitted and the gel was sliced and incubated as above, or the segments corresponding to focused protein were electrodialed free of the gel and concentrated into a dialysis bag (32).

vi. Lethality Determinations. Lethality of fractions during purification or of purified toxins was determined by subcutaneous or intraperitoneal injections into 25-40 g mice (7). Fractions were termed "non-toxic" if none of five test mice died at limiting doses of 5 to 10 $\mu\text{g/g}$ mouse. Further details of toxicological methods are given in Chapter V Methods.

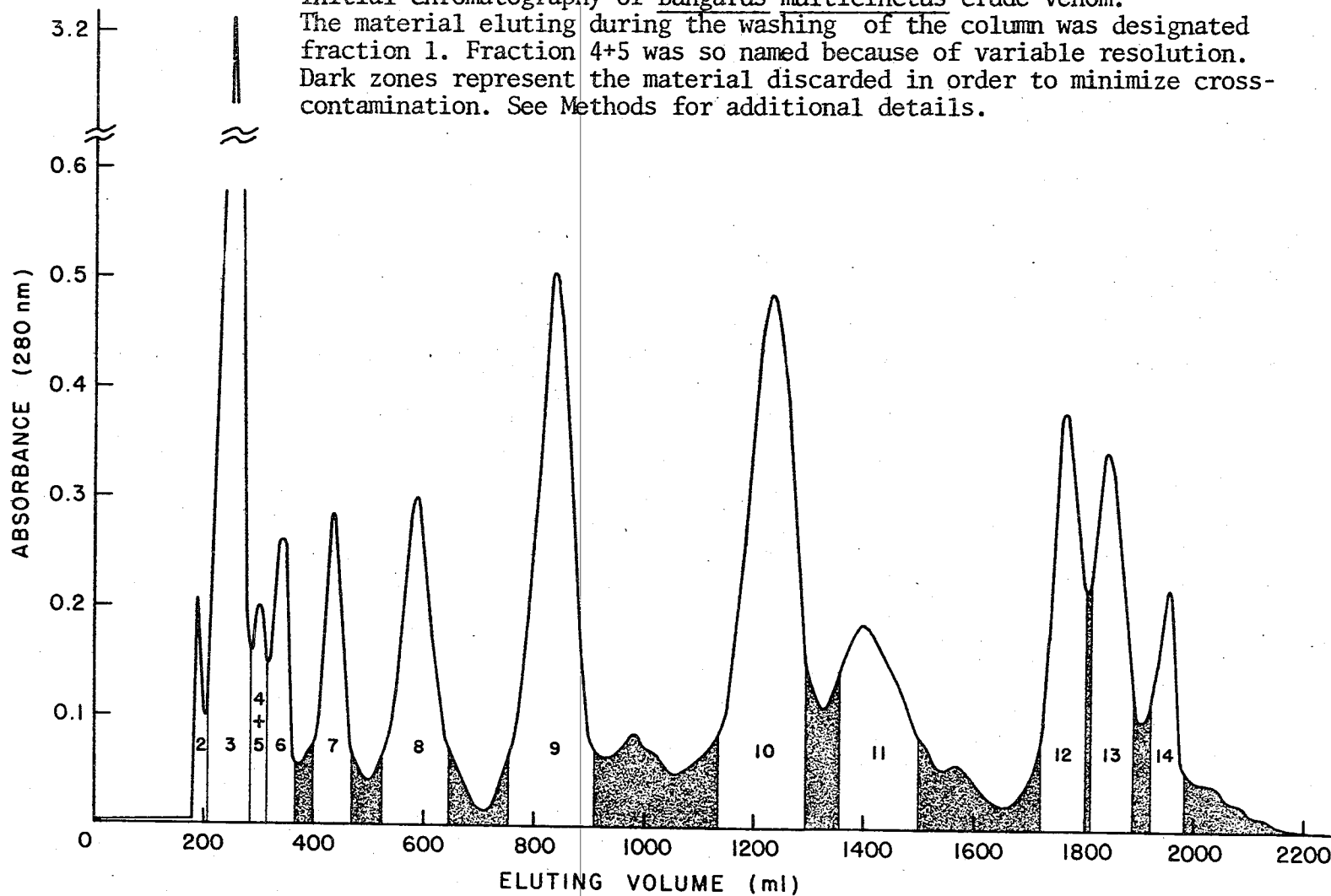
RESULTS.

Initial fractionation by gradient elution, followed by ion-exchange elution of tightly-bound components at a single high salt concentration, separated the crude venom into thirteen A_{280} peaks (Figure 2-1) on CM-Sephadex. A small amount of non-protein material, tentatively identified as guanosine (7), was removed by column washing. The subsequent A_{280} peaks were all protein, as judged by UV absorption and fluorescence spectra (7), and positive Lowry reactions. The approximate yields of each fraction are indicated in Table II-2. $\sim 85\%$ of the total A_{280} could be recovered with the protein fractions. The predominant component, fraction 3, contained 30% of the total A_{280} -absorbance in the crude venom. The next most abundant fractions were 9 and 10, each containing $\sim 12\%$ of the total absorbance. Using the peak positions for alignment, comparison of the initial chromatogram to earlier published figures (1,2) identified fraction 3 as containing α -bgt and fraction 10 as containing β -bgt. These classifications were subsequently confirmed by amino acid analyses (see Chapter III) which were compared to the known sequence-derived compositions (3,6).

Figure 2-1

Initial chromatography of Bungarus multicinctus crude venom.

The material eluting during the washing of the column was designated fraction 1. Fraction 4+5 was so named because of variable resolution. Dark zones represent the material discarded in order to minimize cross-contamination. See Methods for additional details.



XBL741-5000

TABLE II-2

FRACTIONATION OF CRUDE BUNGARUS
MULTICINCTUS VENOM ON CM-SEPHADEX

Fraction	Absorbance units (at 280 nm)	Recovery of fractions %Recovery recovered in each fraction
1	33	9
2	4	1
3	106	27
4 + 5	5	1
6	10	3
7	14	4
8	23	6
9	45	12
10	48	12
11	21	5
12	23	6
13	20	5
14	9	2
Discarded	26	7

Data from chromatographic run #2. The supernatant prepared from 355 mg of crude lyophilized venom was chromatographed (containing 387 absorbance units at 280 nm; 31 absorbance units were discarded with a small precipitate after centrifugation).

Patterns of the distributions of enzyme activity levels (Table II-3) resembled that reported by Lee et al (1). No proteolytic or proteolytic inhibitor activities were found in the crude venom or the chromatographic fractions. A thrombin-like arginine esterase was detected in fraction 4+5 (so designated because of variable chromatographic resolution). After CM-Sephadex separation, fractions 2 thru 7 were the most heavily contaminated with enzymatic activities, whereas fractions 9 thru 11 contained only traces of nucleotide pyrophosphatase and acetylcholinesterase. The electrophoretically pure α -bgt obtained upon rechromatography of fraction 3 on CM-cellulose (1,7) was completely free of any of the assayed enzymatic activities. When 10-40 μ g of each fraction was subjected to SDS-gel electrophoresis on 10% gels, they appeared substantially homogeneous, with the exceptions of fractions 2 and 4+5, which appeared to have multiple high molecular weight components (attributable to the enzymes detected by the assays in Table II-3). All other fractions were 90-100% low molecular weight proteins (Figure 2-2). Higher gel loading visualized small amounts of higher molecular weight contaminants in some fractions.

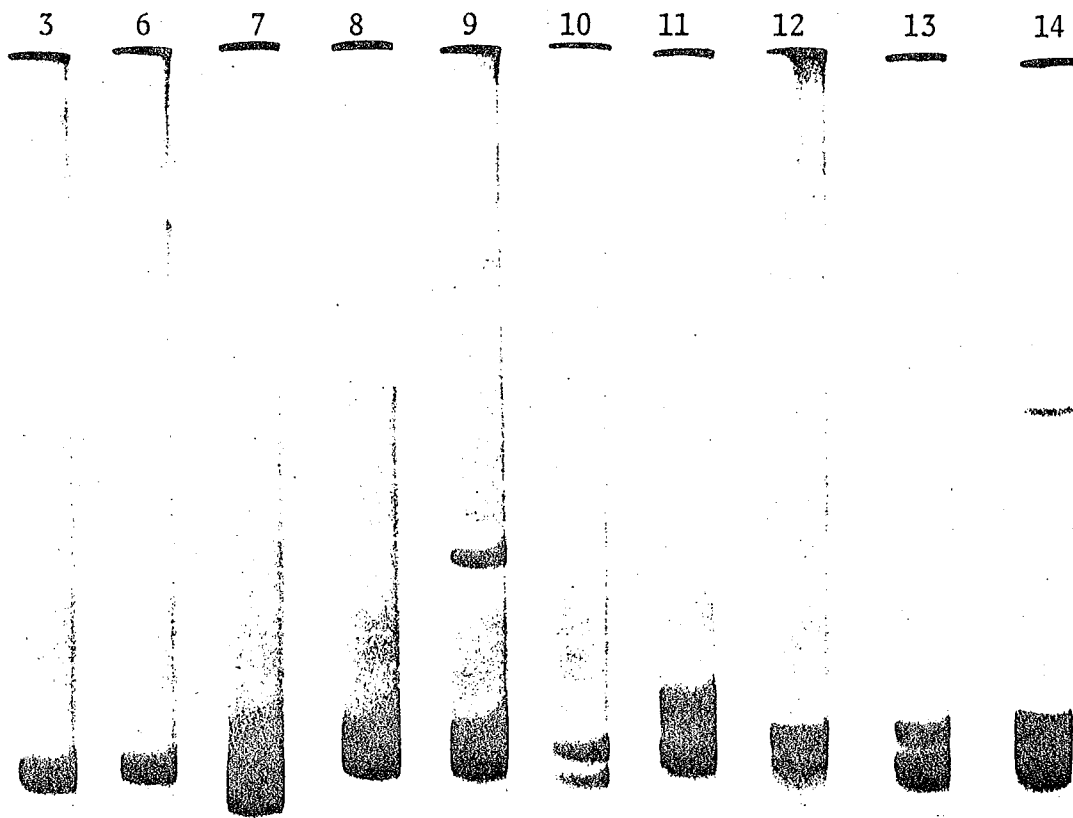
To select for toxins over contaminants of different molecular weights, the initial protein fractions were rechromatographed on Sephadex G50 (Figure 2-3). Fractions 3 and 6 thru 8 contained several protein components, including non-toxic material at the void volume. A small, tryptophan-containing peptide, whose properties are consistent with other identified snake venom peptides (33), was detected in fraction 6. The major components of fractions 3 and 6 thru 8 were all highly lethal and eluted in identical volumes, calibrated to an apparent molecular weight of 15-16,000 daltons. Fraction 9 had two major components, one toxic (9A) and one non-toxic (9B). 9B was identified as a nerve growth factor by its ability to stimulate neurite outgrowth from embryonic chick ganglia or from dissoci-

TABLE II-3
 ENZYMATIC ACTIVITIES IN THE INITIAL FRACTIONS OF THE VENOM OF B. MULTICINCTUS

Fraction	$\mu\text{mol hydrolyzed/mg protein}\cdot\text{min}$			PME (nmol/ mg \cdot min)	HLD ($\mu\text{g}/$ mg \cdot min)	ArgE ($\mu\text{mol}/\text{min}\cdot$ mg of protein)
	AChE	PhA*	NADase			
2	12	12.3	0.1	6.7		
3	37	24.0	4.8	4.3		
α -Bgt						
4+5	739	3.2	10.5	7.3		8.4
6	80		0.1	19.9		0.5
7	2		trace	17.3		
8	trace		trace	6.5		
9	trace		trace			
10	trace		trace			
11	trace					
12	trace				3.2	
13	trace				6.0	
14	trace				25.0	

* Activity was assayed in the medium of Saito and Hanahan (23) and gave no detectable levels in 9 to 14. However, addition of sodium deoxycholate to these fractions stimulated an endogenous phospholipase activity (4,5). These data have not been included for the β -toxins' fractions because they are a misleading gauge of contamination. Abbreviations: AChE, acetylcholinesterase, PhA, phospholipase A, NADase, nucleotide pyrophosphatase, PME, phosphomonoesterase, HLD, hyaluronidase, ArgE, arginine esterase. See Methods for assays.

Figure 2-2
SDS-gel electrophoresis of fractions after CM-Sephadex chromatography.
Fraction No.



XBB 759-6652A

Twenty μg protein was applied in 20 μL of Laemmli solution (27) for fractions 3 and 6 only. All others were run with 40 μg protein in 40 μL Laemmli solution. These are 12% gels run at 4 ma/gel. Stained and destained as in Methods.

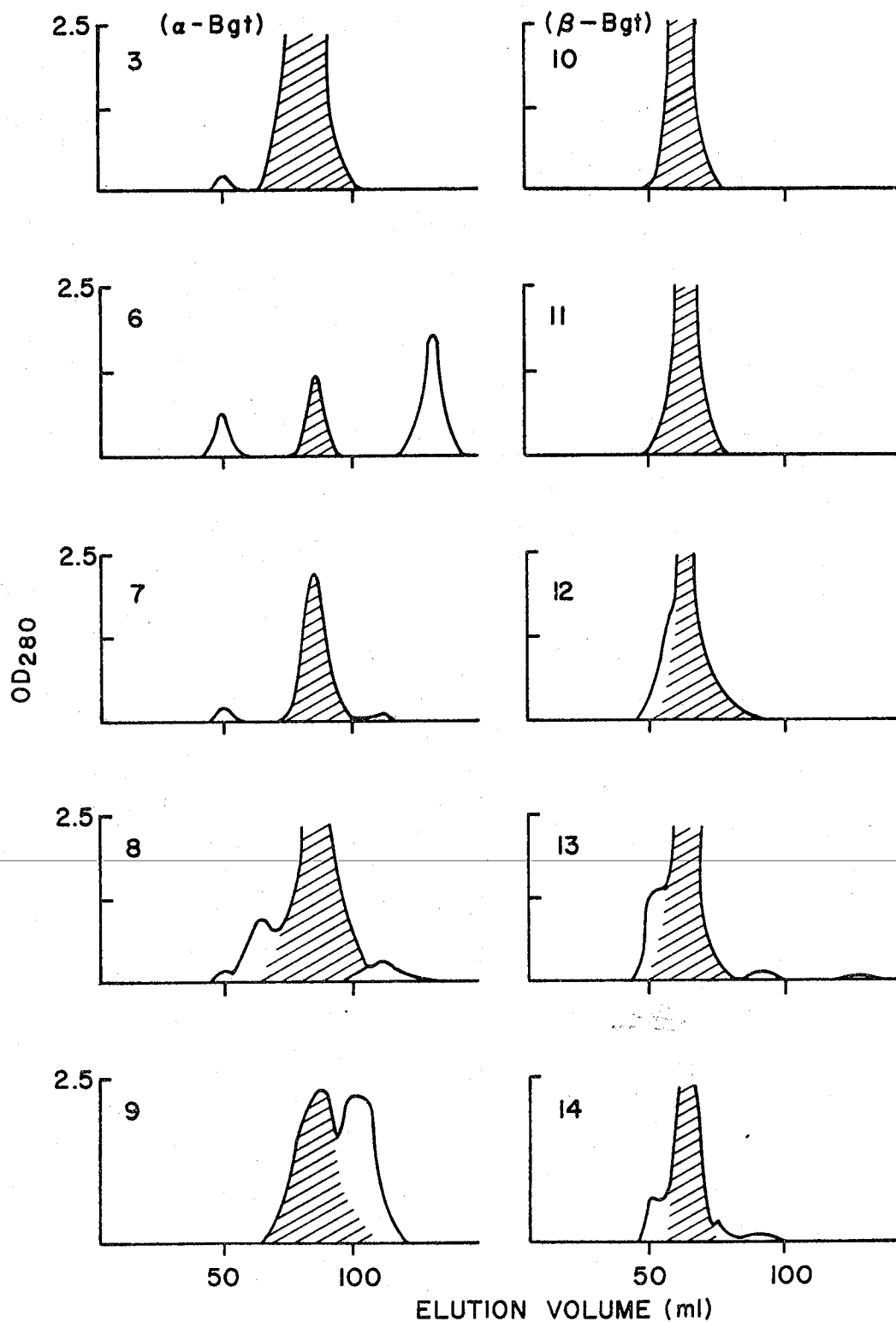


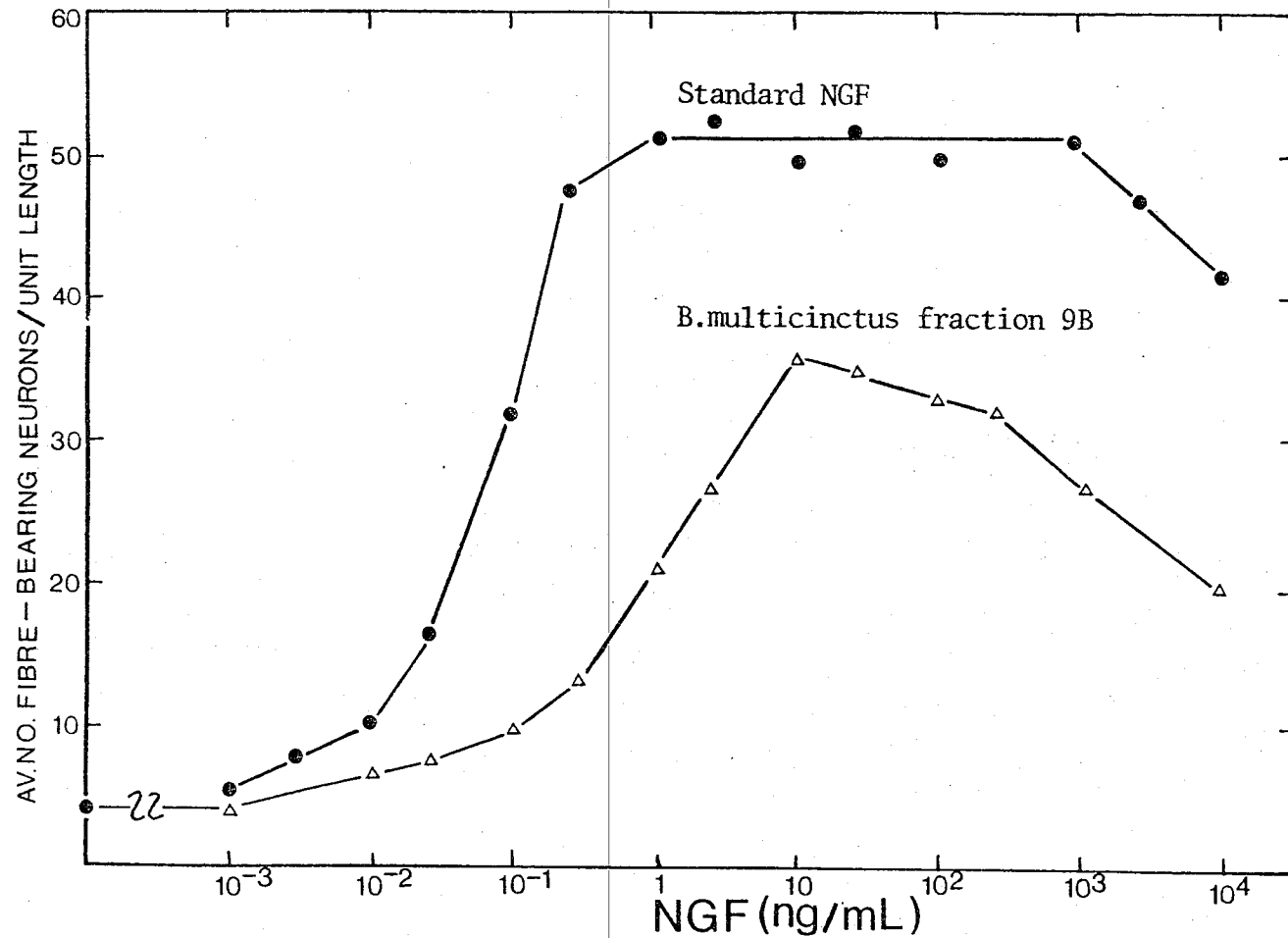
Figure 2-3. Sephadex G50 gel filtration of fractions from XBL 769-9629 initial chromatographic step. Hatched peaks indicate the components that were lethal to mice. Concentrated samples from the CM-Sephadex chromatography were run on a 2.6 X 40 cm column at 16 mL/hr with upward elution. Fractions of 4 mL were collected. The ordinate indicates the absorbance records from the flow-through monitor.

ated chick ganglionic neurons (Figure 2-4). Fractions 12 thru 14 had varying degrees of contamination by minor proteins of both higher and lower molecular weights. The toxins of fractions 10 thru 14 eluted at an identical gel position calibrated to an apparent molecular weight of 20-22,000 daltons. In all cases, preparative gel filtration on Sephadex G50 gave quantitative recovery of the applied protein.

After the G50 step, gel isoelectric focusing indicated persistent cross-contamination in several fractions (Figure 2-5). Accordingly, fractions were repurified on the basis of charge using gradient elution from the cation exchanger Bio-Rex 70 (Figure 2-6). In fractions 7 and 8, and 10 thru 12, the presence of more than one toxic component and correspondence of the minor component elution positions with the major components of other fractions indicated that cross-contamination had been significant. The major proteins obtained after this step were all highly toxic with quantitative characteristics of their toxicology consistent with those of previously described neurotoxins (1,2) in the venom (see Chapters V and VI). Rechromatography of these fractions on gel filtration (G50, G75, Bio-Gel P30) or cation exchange resins (Bio-Rex 70, CM-cellulose) gave single protein components of constant specific lethal activity. Gel electrophoretic or gel isoelectric focusing techniques also indicated homogeneity of the final products (Figure 2-7). Subsequent chemical and hydrodynamic analyses supported the chromatographic evidence of purification to homogeneity (see Chapter III). For simplicity, the final toxins were given the same sequential numbering as in their initial chromatographic fractions from the CM-Sephadex column, with the exceptions of 9A, α -bgt, and β -bgt. Contaminants, with the exception of the nerve growth factor (9B), were not given systematic identifications or further purified.

Selective gel staining indicated that no purified toxin was a glyco- or lipoprotein.

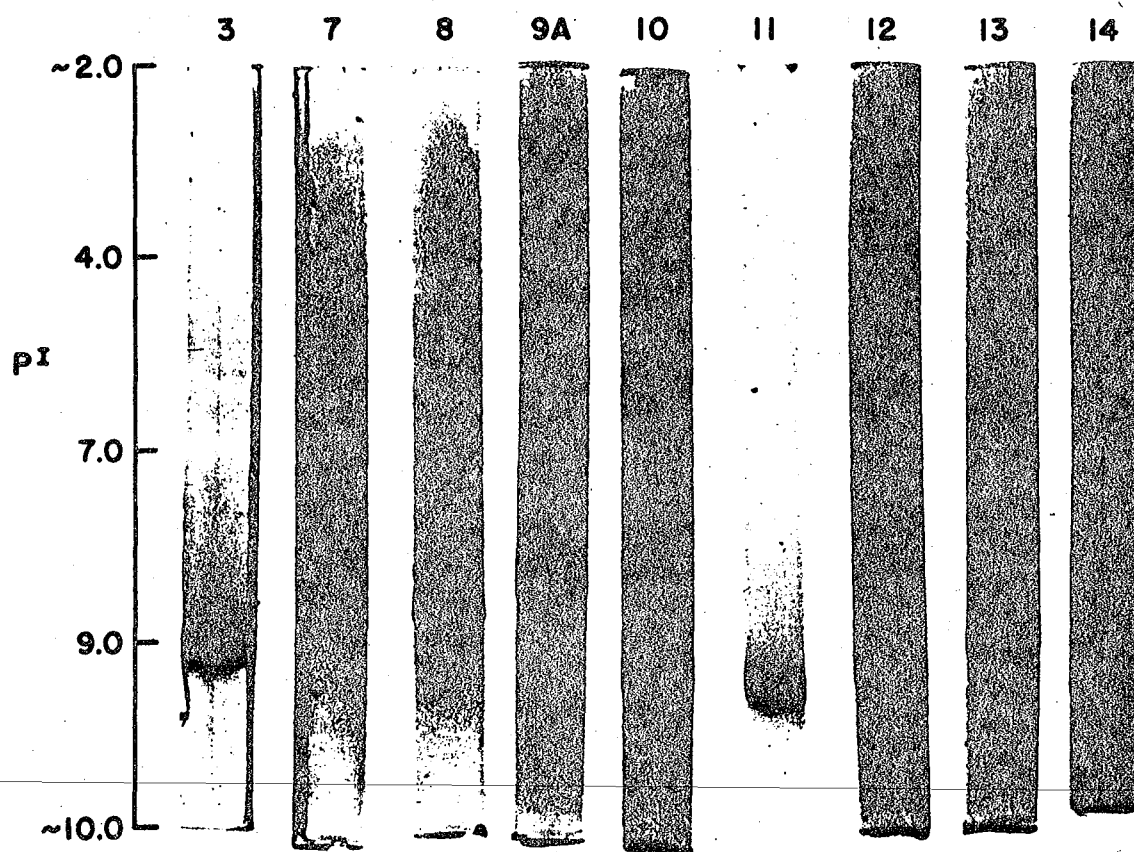
Figure 2-4



Nerve growth factor (NGF) assays of fraction 9B and standard mouse NGF using the dissociated chick ganglionic neuron method (Greene, L.A. (1974) Neurobiol., 4, 286). At each concentration, fibre-bearing neurons were counted across the diameters of five replicate wells on Falcon plates and were averaged.

Figure 2-5

Gel isoelectric focusing of fractions after Sephadex G50 chromatography. Forty μ g protein were focused in each gel for 1 hr at 100V and then 2 hrs at 200V. Gels were fixed, rinsed, stained, and destained as in Methods.



XBB 763-2142A

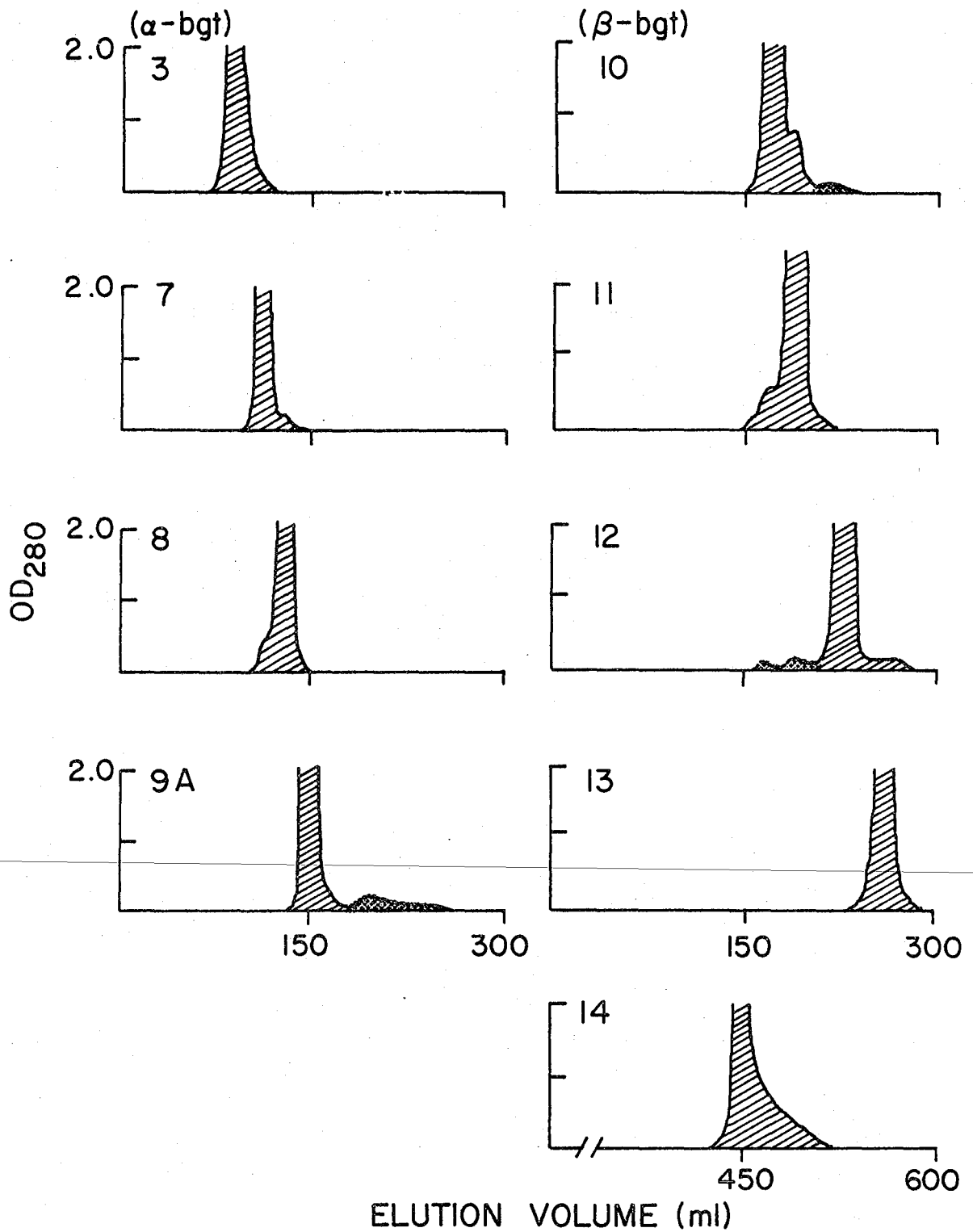
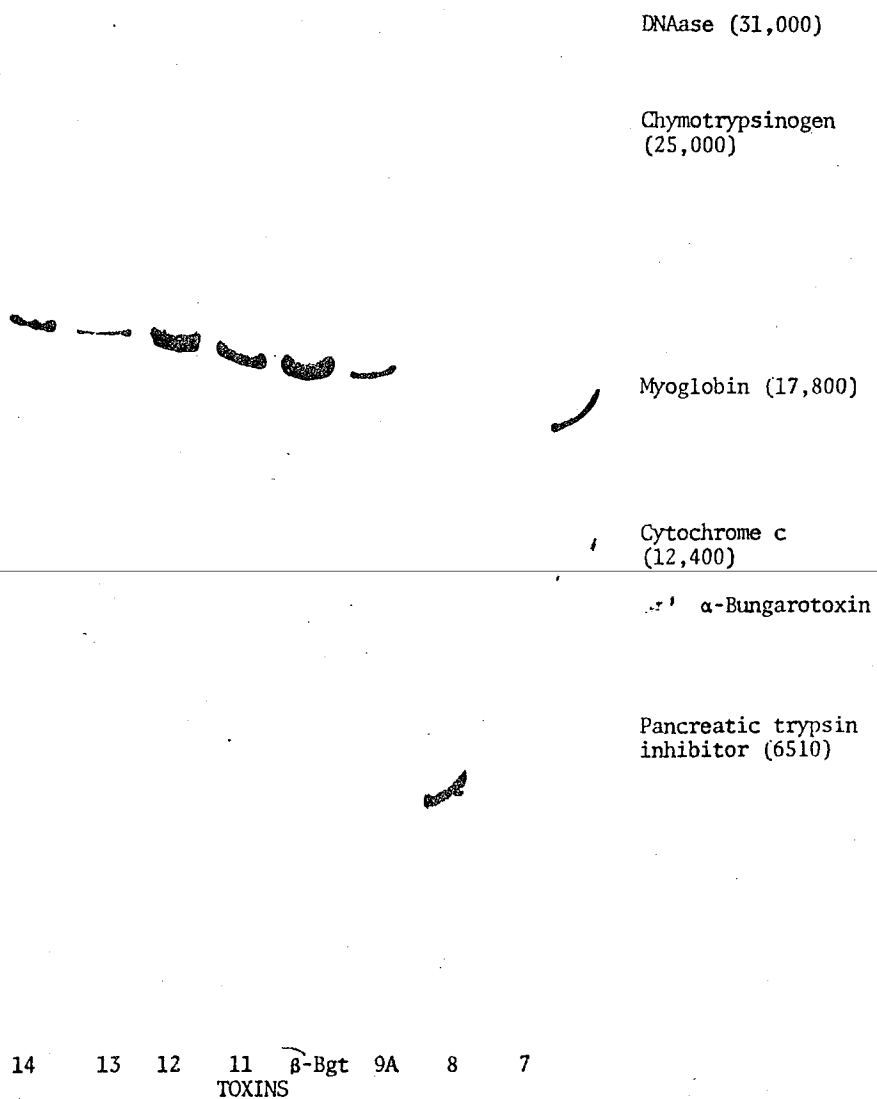


Figure 2-6. Rechromatography of Sephadex G50 fractions on XBL 774-4334 Bio-Rex 70. Hatched peaks were lethal to mice and were pooled. Cross-hatched peaks were discarded. Column was prepared and run as in Methods at 20 mL/hr.

Figure 2-7. Sodium dodecyl sulfate gradient slab gel (10-20%) electrophoresis of final purified toxins. Twenty μ g of each toxin or standard was loaded into each lane after dissociation by boiling in Laemmli solution minus a reducing agent.



Stability and Storage of Purified Toxins. Lethality of the individual toxins was stable to extreme conditions such as acid pH, high temperature (85°C), non-reducing denaturants (8 M urea, 6 M guanidine hydrochloride), and brief exposure to non-precipitating organic solvents (trifluoroethanol, chloroform). The native toxins are relatively resistant to the action of various proteases* (trypsin, chymotrypsin, pepsin, carboxypeptidases, aminopeptidases). The toxins can be stored either frozen or lyophilized. There is no tendency for any of the toxins to aggregate on freeze-drying (34), but the toxins do form less active aggregates with repeated freezing and thawing from buffered solutions. They are soluble at all pHs, unless damaged (see below).

The toxic activities are susceptible to cystine cleavage by either reducing agents or basic pH. The toxins 9A thru 14 are much more sensitive to alkaline damage and will be denatured irreversibly by exposure to pH >10. The toxins α -bgt and 6 thru 8 can be stored at up to pH 12 without suffering irreversible damage. Alkaline denaturation is immediately detectable by an increase in turbidity indicative of reduced solubility. Control experiments allowing bacterial growth in toxin solutions did not give proteolytic damage, but did produce apparent deamidation of asparagine and glutamine residues, because a mixture of isoelectric point variants was obtained after such treatment without a change in the amino acid compositions of the altered species.

DISCUSSION.

The natural heterogeneity of the toxins from Bungarus multicinctus venom makes it an ideal source for the purification of either α -type or β -type toxins. However, with partially purified toxins, subsequent pharma-

* <20% quantitative lethality loss

cological and biochemical studies may be quantitatively, or worse, qualitatively compromised. α -Bgt can be obtained in high yield and purity after only two chromatographic steps (1,2,7). On the other hand, experience with the other bungarotoxins has established that obtaining them free of cross- and non-toxic contamination requires more extensive repurification (18). β -Bgt is a good example. Several purification schemes have been used to obtain the predominant component of the crude venom that has a pre-junctional-blocking activity on isolated nerve-muscle preparations (12-14). One study (12) declared β -bgt "pure" after a single chromatographic resolution of the crude venom into only six apparent components, unlike the thirteen noted here (18), which makes it likely that the properties described are an average of the closely-related β -type fractions 10 thru 13 (4). Another study (13) reported a persistent contaminant of their β -bgt preparation detectable on cellulose acetate electrophoresis amounting to 5% of the total; although the poor sensitivity of this electrophoretic technique compels consideration of the "5%" estimate as a minimum value. In both of these cases, subsequent chemical and physiological work has clearly shown that both of these groups are working with true β -bgt (1,6). However, one group (17) has reported a " β -bgt" that is the most basic fraction of the crude venom, strongly adsorptive to cation exchangers, and near 11,000 daltons in molecular weight (35). Without an amino acid analysis, its identity cannot be unequivocally ascertained, but its size, electrophoretic, and chromatographic behavior are all inconsistent with its identification as true β -bgt, but are consistent with the description of toxin 14 (18). As a single chain toxin resembling notexin (18), 14 does not have the important covalent two-chain structure that is found in true β -bgt (5,6,18) and its homologues, toxins 11 thru 13 (4,18). Moreover, 14 has a unique and peculiar pharmacology, exhibiting both pre-

and post-synaptic effects on the neuromuscular junction (2), and the myotoxic effects previously seen with notexin (36). To further confuse the literature, this toxin is absent from the crude venom of some commercial suppliers (37,38). Consequently, this example offers strong evidence for the need for a reproducible set of identification procedures and/or a standard, reliable purification scheme, such as the one reported here.

Until recently, post-synaptic snake toxins appeared to differ only in their potencies on different test systems, and in the degree of reversibility. However, the pitfalls of incomplete purification can even be suffered in such an apparently similar group of toxins. A study on the responsiveness of the chick ciliary ganglion to blocking by α -bgt (16) showed that the active component was not in fact true α -bgt, but rather a contaminating α -toxin which we are currently trying to identify. Thus, cross-contamination can confuse the identification of new activities with the wrong purified toxin. Fraction 9, for example, can contain as much as 30% cross-contamination with α -type fraction 8 after the initial chromatography (18). Thus, it seems that the post-junctional activity detected in the fraction (2) is possibly attributable to the failure to purify away post-synaptically active contaminants.

Based upon their elution order on the same chromatographic system (1, 2) and their gel filtration behavior, toxins 6 thru 8 are assigned to a group similar to α -bgt, and toxins 11 thru 14 to a group similar to β -bgt. At this stage, toxin 9A is not classifiable.

REFERENCES.

1. Lee, C.-Y., Chang, S., Kau, S., and Luh, S.-H. (1972) *J.Chromatog.*, 72, 71.
2. Dryden, W.F., Harvey, A.L., and Marshall, I.G. (1974) *Eur.J.Pharmacol.*, 26, 256.

3. Mebs, D., Narita, K., Iwanaga, S., Samejima, Y., and Lee, C.Y. (1972) Hoppe-Seyler's Zeit.Physiol.Chem., 353, 243.
4. Abe, T., Alema, S., and Miledi, R. (1977) Eur.J.Biochem., 80, 1.
5. Kondo, K., Narita, K., and Lee, C.Y. (1978) J.Biochem., 83, 91.
6. Kondo, K., Narita, K., and Lee, C.Y. (1978) J.Biochem., 83, 101.
7. Eterovic, V.A., Hebert, M., Hanley, M.R., and Bennett, E.L. (1975) Toxicol., 13, 37.
8. Eldefrawi, M.E., and Fertuck, H.C. (1974) Anal.Biochem., 54, 63.
9. Clark, D.G., Macmurchie, D.D., Elliott, E., Wolcott, R.G., Landel, A.M., and Raftery, M.A. (1972) Biochemistry, 11, 1663.
10. Potter, L.T. (1974) Meths.Enzymol., 32, 309.
11. Ong, D., and Brady, R.N. (1974) Biochemistry, 13, 2822.
12. Kelly, R.B., and Brown, F.H. (1974) J.Neurobiol., 5, 135.
13. Wernicke, J.F., Oberjat, T., and Howard, B.D. (1974) J.Neurochem., 22, 781.
14. Kato, A.C., Pinto, J.E.B., Glavinovic, M., and Collier, B. (1977) Can. J.Physiol.Pharmacol., 55, 574.
15. Lee, C.Y., and Chen, Y.M. (1977) Toxicol., 15, 395.
16. Chiappinelli, V.A., and Zigmond, R.E. (1978) Proc.Nat.Acad.Sci., 75, 2999.

17. Livengood, D.R., Manalis, R.S., Donlon, M.A., Masukawa, L.M., Tobias, G.S., and Shain, W. (1978) Proc.Nat.Acad.Sci., 75, 1029.
18. Hanley, M.R., Eterovic, V.A., Hawkes, S.J., Hebert, A.J., and Bennett, E.L. (1977) Biochemistry, 16, 5840.
19. Ellman, G.L., Courtney, K.D., Andres, V., and Featherstone, R.M. (1961) Biochem.Pharmacol., 7, 88.
20. DiFerrante, N. (1956) J.Biol.Chem., 220, 303.
21. Lowry, O.H. (1957) Meths.Enzymol., 4, 366.
22. Kornberg, A., and Pricer, W.E. (1950) J.Biol.Chem., 182, 763.
23. Saito, K., and Hanahan, D.J. (1962) Biochemistry, 1, 521.
24. Fritz, H., Trautschold, I., and Werle, E., in Methods of Enzymatic Analysis, Vol.2, ed. by Bergmeyer, J., Academic Press, New York, 1974, p 1064.
25. Takayama, K., Maclellan, D., Tzagoloff, A., and Stoner, C. (1966) Archs.Biochem.Biophys., 114, 223.

26. Eipper, B.A. (1974) *J.Biol.Chem.*, 249, 1407.
 27. Laemmli, U. (1970) *Nature*, 227, 680.
 28. Fairbanks, C., Steck, T., and Wallach, D. (1971) *Biochemistry*, 10, 2606.
 29. Vesterberg, O. (1972) *Biochim.Biophys.Acta*, 257, 11.
 30. Fawcett, J. (1968) *FEBS Lett.*, 1, 81.
 31. Trump, G., and Singer, S.J. (1970) *Proc.Nat.Acad.Sci.*, 66, 411.
 32. Braatz, J.A., and McIntire, K.R. (1977) *Prep.Biochem.*, 7, 495.
 33. Tu, A.T., Venoms:Chemistry and Molecular Biology, John Wiley and Sons, New York, 1977.
 34. Karlsson, E., Eaker, D., Fryklund, L., and Kadin, S. (1972) *Biochemistry*, 11, 4628.
 35. Donlon, M.A., Tobias, G.S., Shain, W., and Catravas, G. (1975) *Neurosci.Abstracts*, 5, 649.
 36. Harris, J.B., Johnson, M.A., and Karlsson, E. (1975) *Clin. Exp. Pharmacol.Physiol.*, 2, 383.
 37. Dryden, W.F., Harvey, A.L., and Marshall, I.G. (1973) *J.Pharm.Pharmacol.*, 25, 125.
 38. Narita, K. (Osaka University, Japan), personal communication, May,1978.
-

CHAPTER III.
PHYSICAL AND CHEMICAL
CHARACTERIZATION OF THE BUNGAROTOXINS.

III. INTRODUCTION.

From the purification steps, it was clear that the bungarotoxins shared physical similarities, size and charge, in correspondence with their pharmacological classification. Thus, predictably, the differences in biological activities between α - and β -type toxins arose from differences in protein structures. However, the relation between structure and function cannot be addressed without a much more specific description of physical and chemical characteristics of the purified toxins. The structural heterogeneity of the α - and β -type bungarotoxins permits the search for generic features of the two functional classes.

In the case of the curarimimetic toxins, the availability of over thirty primary structures has identified an invariant "core" sequence homology (see Figure 1-1). Without exception, such toxins are highly basic polypeptides of 6000-8000 daltons, cross-linked by four to five disulfides(1, 2). As noted in Chapter I, the toxins can be subdivided into Type I and Type II (Table III-1). Within the last two years, the first two X-ray diffraction structures at 2.5-2.8 Å resolution were published of the Type I neurotoxins, erabutoxin a (3) and erabutoxin b (4), and it is presumed that Type II neurotoxins will not differ dramatically from this structure (5). Earlier sequencing work, identifying invariant residues, and later chemical modification studies, implicating particular residues in function (reviewed in ref.6), pinpointed lys-27, lys/arg-53, trp-29, asp-31, arg-37, and gly-38 as key residues*. The X-ray structures revealed that asp-31 and arg-33 (numbers for the erabutoxins) are situated at the end of an elongated loop maintained spatially by β -pleated sheets, and occupy positions in space consistent with their functional groups mimicking the two charged ends of

* Using the numbering of Figure 1-1 in which individual toxins have been aligned to give a composite sequence of maximum homology.

TABLE III-1
 PHYSICAL AND BIOLOGICAL COMPARISON OF TYPE I
 AND TYPE II CURARIMIMETIC NEUROTOXINS

	Mol.Wt.	No.Residues	Disulfides	N-Terminal	nAChR K_d *
Type I	6800-7000	60-62	4	Leu, Met, Arg	0.02-0.1 nM
Type II	7800-8200	71-74	5	Ile, Thr, Arg	0.5-5.0 nM

* Equilibrium dissociation constant determined by competition against ^3H -Naja nigricollis toxin α with solubilized Torpedo acetylcholine receptor (nAChR). Data taken from ref. 10.

the acetylcholine molecule (5). Because five of the six invariant residues occupy the same sequence loop, it is speculated that residues 31 and 33 (asp-31 and arg-37 in the general numbering) provide recognition specificity for the acetylcholine receptor, and that the others contribute to the stabilization of that interaction (5,6). Type II toxins differ from Type I toxins in the addition of a short, disulfide-bridged loop in the region of residues 30-35. Intriguingly, this extra loop is placed in the very middle of the hypothesized recognition site. Thus, comparative studies of a variety of Type I and Type II neurotoxins may be expected to figure prominently in a critical evaluation of the recognition site hypothesis. Curarimimetic bungarotoxins should therefore be carefully studied for their potential utility in the development of toxin structure-function principles.

Structural variants of α -bgt may not only enable us to learn more about toxin structure and activity, but may also prove useful in investigating their target site, the nicotinic acetylcholine receptor (nAChR). For example, the variation in the reversibility of toxin-nAChR binding was significant in the choice of toxins to be immobilized on affinity columns for receptor purification (7); α -bgt retaining solubilized receptor so well that nAChR yields were halved (8). For the preparation of radioactive toxin derivatives of high specific activity, some toxins prove unsuitable for particular labelling procedures, such as iodination, because of their inactivation (9). Moreover, natural differences in toxin primary structure can be exploited to describe sensitive or insensitive sequences wherein residue substitution affects the affinity for the nAChR (10). A tantalizing possibility is that some curarimimetic toxins may distinguish between tissue-specific forms of nAChR, such as has been reported for the synaptic blocking activity of some α -toxins in central nervous systems of vertebrates (11) and invertebrates (12).

Likewise, variability in β -toxin structure may be put to good advantage in understanding both the toxin and its target site. For example, the variation in the quantitative toxic potency of β -bungarotoxins (13) may have a correlate in variation in their in vitro phospholipase activity (see Chapter VI). Initial indications from chromatographic behavior suggested that toxins 9A and 14 should be examined closely for their relationship to the very similar β -toxins 10 thru 13 (14). The limited range of pre-synaptic toxins that have been studied in detail requires that more such toxins be purified and characterized before general principles may be recognized. The current difficulties in interpreting β -toxin structures are revealed in Table III-2, which summarizes important observations about the four best examples. In all cases, a core structure homologous to the family of phospholipase A_2 enzymes has been found. However, three of the examples have additional subunits, the significance of which is not understood; particularly since one of the examples is functionally equivalent but has only the core phospholipase chain. It has been suggested that the additional chains could participate in directing or modifying the binding behavior or enzymatic activity of the active subunit (see Chapter IV; 15,16).

Both notexin and β -bungarotoxin have been sequenced. β -Bgt is composed of a highly basic light chain (7000 daltons), which has some sequence homology to protease inhibitors (17), and a less-basic heavier chain (13,500 daltons) which has the core structure homology to phospholipase enzymes (18). Several studies have implicated the enzymatic activity in its mechanism of neuromuscular blockade (19,20), but the means by which β -bgt achieves its apparent pre-synaptic specificity is not known. One hypothesis is that β -bgt is an "affinity enzyme" directed to the pre-synaptic terminal by a binding specificity, perhaps arising from the enigmatic non-phospholipase subunit (20).

TABLE III-2

STRUCTURAL FEATURES OF PRE-SYNAPTIC SNAKE VENOM NEUROTOXINS

Toxin	Iso. Pt.	Mol. Wt.	-S-S-	Comments
Crotoxin complex	4.5	22,000	14	Subunit synergism, myotoxic
Crotoxin A	3.8	10,000	7	3 Chains (41, 35, 14 amino acids)
Crotoxin B [*]	8.8	12,000	7	1 Chain, low toxicity
β -Bungarotoxin	9.4	20,500 ^{**}	10	2 Chains linked by 1 -S-S-, highest pre-synaptic selectivity
Light Chain	8.8	7000 ^{**}	3.5	Protease inhibitor sequence homology
Heavy Chain [*]	7.5	13,500 ^{**}	6.5	
Notexin [*]	Basic	13,600 ^{**}	7	Myotoxic
Taipoxin complex	5.0	57,800	22	Subunit synergism, myotoxic
Taipoxin α [*]	>10	14,600	7	Low toxicity
Taipoxin β [*]	7.0	16,300	7	
Taipoxin γ [*]	2.5	26,900	8	Contains carbohydrate

* Sequence homology with one another and with other phospholipases A₂

** From primary structures. The exact molecular weight of β -bungarotoxin from sequencing (18) was not available until much of the work reported in this Chapter was completed.

To contribute to these issues, further characterization of the individual bungarotoxins was undertaken. It should be noted that the toxin of fraction 6 was not studied in detail because of limited amounts in the crude venom.

METHODS.

i. Sodium Dodecyl Sulfate (SDS) Gel Electrophoresis. SDS cylindrical and slab gels were prepared according to Laemmli (21). For cross-linking, 200 μ g of lyophilized protein was dissolved in 200 μ L of 0.2 M triethanolamine (pH 8.5) containing 100 μ g dimethyl suberimidate (Pierce Chemical) and incubated for three hrs at 25^o C (22). The cross-linked products and standards were then solubilized and separated by Laemmli SDS-gels. For reduction and alkylation of cross-linked proteins, 100 μ g of protein was incubated for 17 hrs in 0.2 M sodium borate buffer (pH 9.0) with 1% (v/v) mercaptoethanol. One mg of iodoacetic acid^{*} in the same buffer was added and the protein incubated for another hr at 25^oC. The reduction and alkylation steps were performed under an argon barrier, and all samples were incubated in the dark to prevent photodecomposition. Gels were stained as in Chapter II Methods.

ii. Isoelectric Focusing. Polyacrylamide gel isoelectric focusing in a pH 3-10 (ampholines from Pharmacia) gradient was performed as described in Chapter II Methods. For accurate measurements of isoelectric points (pIs), results obtained using polyacrylamide gels were confirmed by focusing in glycerol gradients. In 0.8 X 15 cm glass tubes, linear gradients of 5-50% (v/v) glycerol were prepared containing 2% pH 8-10 ampholytes (Brinkmann pHysolytes) and 30-50 μ g of purified toxins. Gradients were supported in individual tubes by polymerized 1 cm plugs of 15% polyacrylamide. Samples

^{*} Pierce Chemical. Recrystallized three times from 1:1 v/v ether:hexane.

were focused at 300v for 18 hrs at 4°C. Samples were removed by pumping the gradient out with 80% glycerol injected through a needle inserted in the plug. Fractions of 0.25 mL were collected by a Gilson MicroFractionator with continuous absorbance (A_{280}) monitoring by a flow-through UV recorder. The pH of collected fractions was measured by a combination microelectrode at 4°C under a nitrogen barrier.

iii. Analytical Gel Filtration. In addition to data collected during preparative gel filtration of fractions (see Chapter II), analytical gel filtration was executed on Sephadex G50 (fine) and Sephadex G75 (fine) in 2.5 X 110 cm columns. Elution was with dilute sodium phosphate buffer (pH 7.4).

iv. Amino Acid Analysis. Toxins (1 to 1.5 mg) were hydrolyzed with 1 mL constant boiling HCl (Pierce Chemical) in sealed glass tubes maintained at $110 \pm 1^\circ$ C in a Dow Corning 550 oil bath. Prior to sealing, tubes were flushed twice with dry nitrogen and evacuated to < 20 μ m Hg. Hydrolyses were run for 20-22, 44, and 68-72 hrs. Hydrolysates were analyzed in a Beckman model 120C amino acid analyzer using the two-column system of Spackman et al (23). Values for serine, threonine, cystine, tyrosine, and histidine were corrected to zero time, owing to decomposition, and values for valine, leucine, isoleucine, alanine, glycine, and phenylalanine were extrapolated to plateau levels at long hydrolysis times, owing to incomplete liberation at shorter hydrolysis intervals. In cases where an appreciable decomposition of cystine occurred, the values for proline were also corrected to zero time since cysteine is coeluted with proline in the chromatographic system.* The best integral fit of amino acid residues to the experimental data was obtained by a computer analysis (24). Results were weighted to give different reliabilities to different amino acids,

* Its presence can be detected by the ratio of absorbances at 570 and 440 nm which is normally 7.56 and 1.46 for the ninhydrin derivatives of proline and cysteine respectively.

based on their acid stability, and to account for either absolute or percentage errors.

Independent amino acid composition analyses, including tryptophan, were obtained by hydrolysis in 4N methanesulfonic acid (Pierce Chemical) at 115°C for 22 hrs after the procedure of Simpson *et al* (25). Tryptophan values were confirmed by oxidation with N-bromosuccinimide in both the presence and absence of urea (26), and by magnetic circular dichroism (see Chapter IV). Total sulfur was obtained by X-ray fluorescence (see below) and compared with values of cystine plus methionine. Titration with DTNB was used for the detection of free sulfhydryls (27).

Carboxymethylated-reduced toxins (CM-toxins) were prepared by reducing 3 to 5 mg protein dissolved in 1 mL of 0.1 M tris base (pH 8.5) with a hundred-fold molar excess of solid dithiothreitol over protein at 25°C overnight. Sufficient iodoacetic acid was then added to quench the free sulfhydryls and prevent reoxidation (all manipulations were done under a nitrogen barrier to further minimize reoxidation). Iodoacetic acid was added in 100 µL of 0.1 M tris base titrated to pH 8.5. Samples were incubated for 1 hr in the dark at 20°C, and were then acidified to pH 3.0. Carboxymethylated derivatives were isolated by gel filtration on a 1.6 X 50 cm Sephadex G10 (fine) column equilibrated with 10% acetic acid. The CM-toxins were lyophilized and stored dessicated. Cystine content was checked by acid hydrolysis of CM-toxins and quantitation of the carboxymethylcysteine liberated (28).

v. X-Ray Fluorescence (performed by Dr.A.Hebert). Total sulfur content of the protein samples was determined with a nondispersive vacuum soft X-ray spectrometer (29). The spectrometer features six anodes which provide characteristic X-rays for sample excitation and determinations of the elements from oxygen to iron. The present experiments were primarily aimed

at a sulfur determination, and only a brief examination was made to insure the absence of Na, Mg, Al, Si, P, Cl, K, and Ca at $\mu\text{g/g}$ protein levels. Analysis used 50 μL of aqueous solution or a homogeneous suspension containing 14-53 μg protein. An important consideration in performing vacuum soft X-ray analyses is the amount of incident radiation which may be converted to heat in the sample. This is especially true of biological samples which may contain easily decomposed or volatile components. Repeated analyses with several of the toxins over periods of hours revealed no detectable sample deterioration or decline in measured sulfur content.

vi. Analytical Ultracentrifugation. A Beckman Model E analytical ultracentrifuge was used with a Schlieren optical system for sedimentation velocity runs, and with a Rayleigh interference fringe optical system for sedimentation equilibrium determinations. The velocity runs were performed at 20° C and 56,100 rpm with a double sector quartz window cell employing an aluminum-filled Epon centerpiece. Samples were prepared from lyophilized toxins in 0.2 M NaCl/0.2 M tris base (pH 8.5) at four to five concentrations from 0.5-20 mg/mL. The dissolution buffer was used to establish the baseline. Schlieren patterns were recorded at 32 min intervals on Kodak Metallographic plates and were read on a Gaertner Scientific microcomparator. The sedimentation coefficients (S-values) were calculated from the migration rates of the maximum ordinates of the Schlieren peaks. S-values were extrapolated to infinite dilution to correct for concentration dependence.

The sedimentation equilibrium experiments were performed at temperatures and rotor speeds as noted in Table III-6, with a double sector sapphire window cell employing an aluminum-filled Epon capillary-type synthetic boundary centerpiece. Samples were prevented from sedimenting by 0.02 mL of FC-43 oil in the sample sector. Initial solute concentrations were determined using the same sample material as for the equilibrium runs and

replacing the reference solution. Equilibrium was ascertained by measuring fringe shifts at intervals of five hrs and was established in all cases within 24 hrs. Interference fringes were recorded on Kodak Spectroscopic II-G plates and were measured by conventional procedures (30). Molecular weights were calculated by the method of Chervenka (30), but were not corrected to infinite dilution.

Diffusion coefficients were measured at 20°C and 4609 rpm using a double sector quartz window cell with an aluminum-filled Epon capillary-type synthetic boundary centerpiece. Interference fringes were recorded as for equilibrium runs at 8 min intervals. Plates were measured and data analyzed by standard procedures (30).

vii. Fluorescence Polarization. All fluorescence measurements were made on a Hitachi-Perkin-Elmer MPF 2A fluorimeter. Samples were prepared in 0.02 M ammonium acetate buffer (pH 7.5) at 12.7 μ M for α -bgt and 4.9 μ M for β -bgt. α -Bgt was excited at 285 nm and emission recorded at 342 nm, and β -bgt was excited at 286 nm and emission recorded at 338 nm. Slit-widths were 8 nm in all cases. Polarization measurements were made under two conditions; "isothermal" and "isoviscous". Isothermal measurements were made at 20°C (temperature control by jacketed cuvette holders) and the solution viscosity was varied by the addition of 10-60% sucrose (w/v). Isoviscous measurements were made in 80% glycerol (v/v) and the temperature was varied from 10 to 90°C. For α -bgt, both intrinsic (tryptophan) and extrinsic (dansyl) fluorescence were used for polarization experiments, whereas for β -bgt, only intrinsic fluorescence was used. α -Bgt was labelled by dansyl chloride by incubating 10 mg of purified toxin in 1 mL of 0.02 M sodium borate buffer (pH 8.0) with 10 μ L of a 10 mM stock solution (freshly prepared) of cycloheptaamylose-dansyl chloride complex (Pierce Chemical) in the same buffer for 4 hrs at 4°C. Dansyl-labelled α -bgt was isolated

from unreacted dye by gel filtration on a 1.6 X 25 cm Sephadex G10 column with elution by distilled water. Dansylated- α -bgt was then resolved into homogeneously-labelled species by cation exchange chromatography on a 2.5 X 5 cm Bio-Rex 70 column with elution by 0-0.2 M NaCl gradient in 0.05 M sodium acetate (pH 6.0). Six mg of monolabelled dansyl- α -bgt* was obtained (60% overall yield). Although the derivative could be a mixture of singly-labelled species modified at different residues, a single exponential relaxation was observed in the lifetime of the dansyl- α -bgt extrinsic fluorescence, suggesting that if multiple species exist, the dansyl groups are in equivalent environments. Fluorescence lifetime measurements were made on an instrument designed in this laboratory (31), using procedures for data acquisition and manipulation described elsewhere (32). Viscosities for sucrose and glycerol solutions at various temperatures were taken from the literature (33).

viii. N-Terminal Determination. Thirty nmol of purified toxins were dansylated and hydrolyzed as described by Gros and Labouesse (34) with the modifications of Zanetta et al (35). Dansyl amino acids were chromatographed on 3 X 3 cm Schleicher and Schuell polyamide sheets with two-dimensional development in 3% formic acid followed by benzene:acetic acid (9:1 v/v). To resolve dansylaspartic acid and dansylglutamic acid, a subsequent re-development in the second dimension with ethyl acetate:methanol:acetic acid (20:1:1 v/v) was used. Unknowns were identified by comparison to standard dansyl amino acids (Pierce Chemical). No attempt was made to quantitate yields of N-terminal amino acids.

RESULTS.

i. Molecular Weights and Chain Structures by SDS-Gels. In SDS-gel systems

* Determined by ninhydrin reactivity against a native α -bgt standard.

in the absence of reducing agent, single bands were observed for all purified toxins, with the exception of 14 (Table III-3). With reduction, however, toxins β -bgt and 11 thru 13 split into two electrophoretic bands calibrated to lower molecular weights. Since these toxins migrated as single components in both SDS:urea and phenol:acetic acid:urea gel systems (see Chapter II), the strongly dissociative agents SDS, urea, and acid pH are ineffective in producing the two-chain structures noted with cysteine-reducing conditions. This constitutes preliminary evidence for the maintenance of the constituent chains by interchain disulfides in the native molecules. Toxins 9A and 14 migrated in non-reducing SDS-slab gradient gels at calibrated molecular weights roughly twice those obtained under reducing conditions. This might suggest that these toxins were also disulfide cross-linked. However, the incorporation of 4M urea into the SDS-gel system dissociated the dimers without reduction. Therefore, toxins 9A and 14 apparently interact to homodimeric structures under non-reducing SDS-gel conditions, but can be dissociated by the addition of urea. These gel results are summarized in Table III-3.

The initial results with SDS-gels obtained during the purification procedure (Figure 2-2) suggested that these toxins might be difficult to accurately analyze by conventional SDS-gel techniques because, like the anomalously-behaving histones (35), they were small and highly basic. Several more elaborate gel approaches were used. Estimates of the unreduced molecular weights were obtained by calibration of a linear gradient SDS-slab gel. Toxin 7 migrated in a similar fashion to α -bgt, but toxin 8 appeared unusually small (≤ 5000 daltons). All of the toxins 9A to 14 were calibrated to weights of 20-22,000 daltons. Reduction of toxins 7 and 8 did not alter their apparent molecular weights, indicating that they were single polypeptide chains like α -bgt. Smaller chains were observed in all

TABLE III-3

MOLECULAR WEIGHTS OF BUNGAROTOXINS AND THEIR CONSTITUTENT POLYPEPTIDE CHAINS

<u>Toxin</u>	<u>SDS-slab^a gradient gel</u>	<u>Reduced/SDS-slab^a gradient gel</u>	<u>DMS/SDS^b disc gel</u>	<u>Reduced/alkylated^b DMS/SDS disc gel</u>	<u>SDS-Urea disc gel</u>
α -bgt	8000	8000	8400	8100	8200
7	8000	8000	8700	7800	8100
8	5000	5000	7000	68000	7600
9A	21,000	11,500	16,000	14,500	12,500
β -bgt	21,500	8500 11,500	8500 18,000	6000 15,000	21,000
11	20,500	7000 11,500	9000 18,500	6800 15,000	21,000
12	21,000	7000 11,500	8400 18,000	7000 15,000	21,500
13	21,500	7000 12,500	7600 13,500	7200 14,000	22,000
14	21,500	11,300 12,000 12,500	11,500	11,000	14,000

^a Measured with acrylamide gradients from 17.5 to 20% (2 experiments), and 10 to 20% (1 experiment).

^b Measured on 12% and 15% Laemmli (21) SDS-gels. DMS, dimethyl suberimidate.

^c Measured on 12% and 15% Laemmli (21) SDS-gels incorporating 4M urea (recrystallized) in gel and solubilizing solutions.

the toxins 9A thru 14 upon reduction, as noted earlier. Toxins 11 thru 13 and β -bgt had chains of similar weights; 7000-8500 daltons for the light chain and 11,500-12,500 daltons for the heavier chain. Toxins 9A and 14 migrated as single chains of 21-21,500 daltons without reduction, and 11,300-12,500 daltons with reduction. Toxin 14 gave three separate bands upon reduction of 11,300, 12,000 and 12,500 daltons.

The cross-linking procedure of Davies and Stark (22) gave another indication of oligomeric structures in β -bgt and 11 thru 13, but gave calibrated molecular weights that were uniformly higher than in other SDS-gel systems. This is frequently observed with cross-linked proteins, even when calibrated against cross-linked standards (22). To reduce the overall charge on the cross-linked molecules, unchanged by dimethyl suberimidate cross-links, they were reduced and carboxymethylated and electrophoresed against comparably treated standards. Values for the heavy and light chains in the two-chain toxins, and the single chains of the other toxins, were all lower. These gel results are tabulated with the previous data in Table III-3.

ii. Isoelectric Focusing. The purified toxins were all highly basic ($pI \geq 8.8$) in either gel or glycerol gradient isoelectric focusing. The focused basic proteins were also lethal to mice with the same toxic symptoms and potency as the unfocused purified toxins. The addition of 4M urea gave multiple closely-spaced bands, which may be attributable to either carbamylation (36) or reversible association of the ampholines with pH-dependent conformations (37) produced by partial denaturation with urea. The pI s of the individual toxins are shown in Figure 3-4.

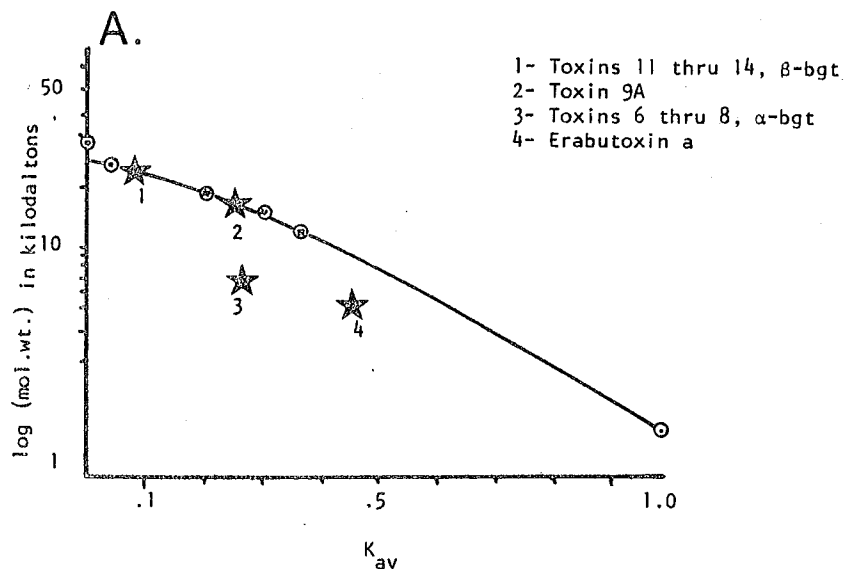
iii. Analytical Gel Filtration. The results from preparative gel filtration of the toxins were confirmed by analytical scale (0.25-1.0 mg) gel filtration on Sephadex G50 or G75, or Bio-Gel P30. Toxins 7, 8, and α -bgt were all calibrated to molecular weights twice that expected from their behavior in

gel electrophoresis, or from α -bgt's sequence. To investigate whether this was attributable to dimerization under the mild conditions used, partitioning behavior was checked with the following elution media; 5% acetic acid, 0.2 M NaCl/0.05 M ammonium acetate (pH 7.0), 0.5 M NaCl/0.05 M Tris base (pH 8.5), and 4 M urea/0.05 M ammonium acetate (pH 7.0); and the elution positions (K_{av}) were not altered. This behavior was also independent of the column matrix, since either Sephadex or Bio-Gel supports gave the same results in terms of calibrated molecular weights, although there was adsorption to Bio-Gel P30 (~70-80% yields with pronounced trailing of peaks). These data indicated that the α -toxins were not forming dimers, but were partitioning on the gel like larger molecules. Examination of the calibration graph for molecular weight (Figure 3-1A) indicated that toxins 9A thru 14 fell on the line established by globular protein standards, but, assuming monomeric molecular weights, α -toxins did not. Thus, the assumption that the gel partition coefficient K_{av} (38) is related to molecular weight is inappropriate for the α -toxins. This assumption relies on the calibration standards and unknowns having the same hydrodynamic shape; thus, the discrepancy in the α -toxins might be due to non-globular shapes. It has been shown that gel filtration data are more rigorously expressed in terms of Stoke's radius (39) and, accordingly, a second calibration curve based on this parameter was used (Figure 3-1B). α -Toxins gave an apparent Stoke's radius of 16-17 $\overset{\circ}{\text{A}}$, 9A gave 17-18 $\overset{\circ}{\text{A}}$, and the remaining toxins all gave 22-23 $\overset{\circ}{\text{A}}$. These results are presented in Table III-4.

iv. Ultracentrifugation. Sedimentation values (S-values) for the purified toxins were determined at 20 $^{\circ}$ C and extrapolated to infinite dilution to correct for concentration dependence. Five of the toxin correction plots are shown in Figure 3-2. Both α -bgt and β -bgt appear homogeneous and free from pronounced self-association because their concentration correction

Figure 3-1

Calibration of Sephadex G50 column according to molecular weight. Standards are listed below. Points are 0 and 1.0 on the K_{av} axis are the void volume and total bed volume respectively.



Calibration of Sephadex G50 column according to Stoke's radius. Values **B.** for standards were taken from the literature (33,39).

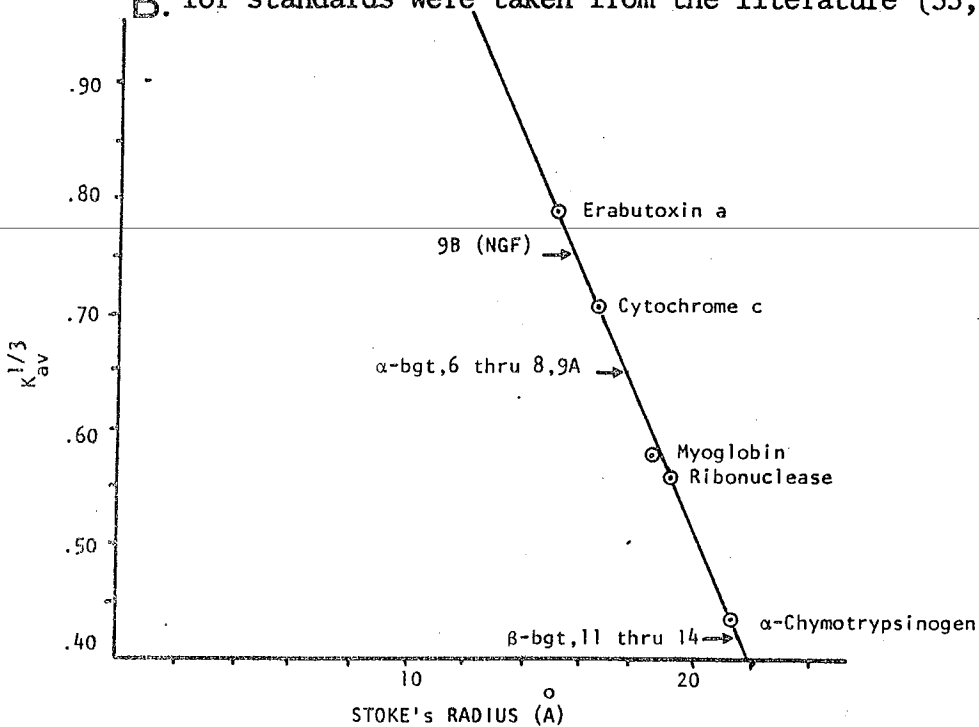


TABLE III-4

SUMMARY OF GEL FILTRATION DATA OF BUNGAROTOXINS

Fraction	Neurotoxic ^a act.	Earlier Names ^b		K _{av} ^c		App ^d mol wt	Stoke's radius
		Lee	Dryden	Sephadex G-50	Bio-Gel P30		
3(α-Bgt)	α type	II ₂	5c	0.28	0.21	15,000-16,000	16.5 Å
7	α type	III ₁	7	0.28	0.21	15,000-16,000	16.5 Å
8	α type	III ₂	8	0.28	0.21	15,000-16,000	16.5 Å
9A	β type	IV ₂	9	0.28	0.17	15,000-17,500	17.5 Å
10(β-Bgt)	β type	V	10	0.12	0.14	20,000-21,000	22 Å
11	β type			0.11	0.13	20,500-21,500	22 Å
12	β type	VI	11	0.10	0.12	21,000-21,000	22 Å
13	β type	VII	13	0.11	0.13	20,500-21,500	22 Å
14	β type	VIII	12	0.08	0.10	22,000-23,000	22 Å

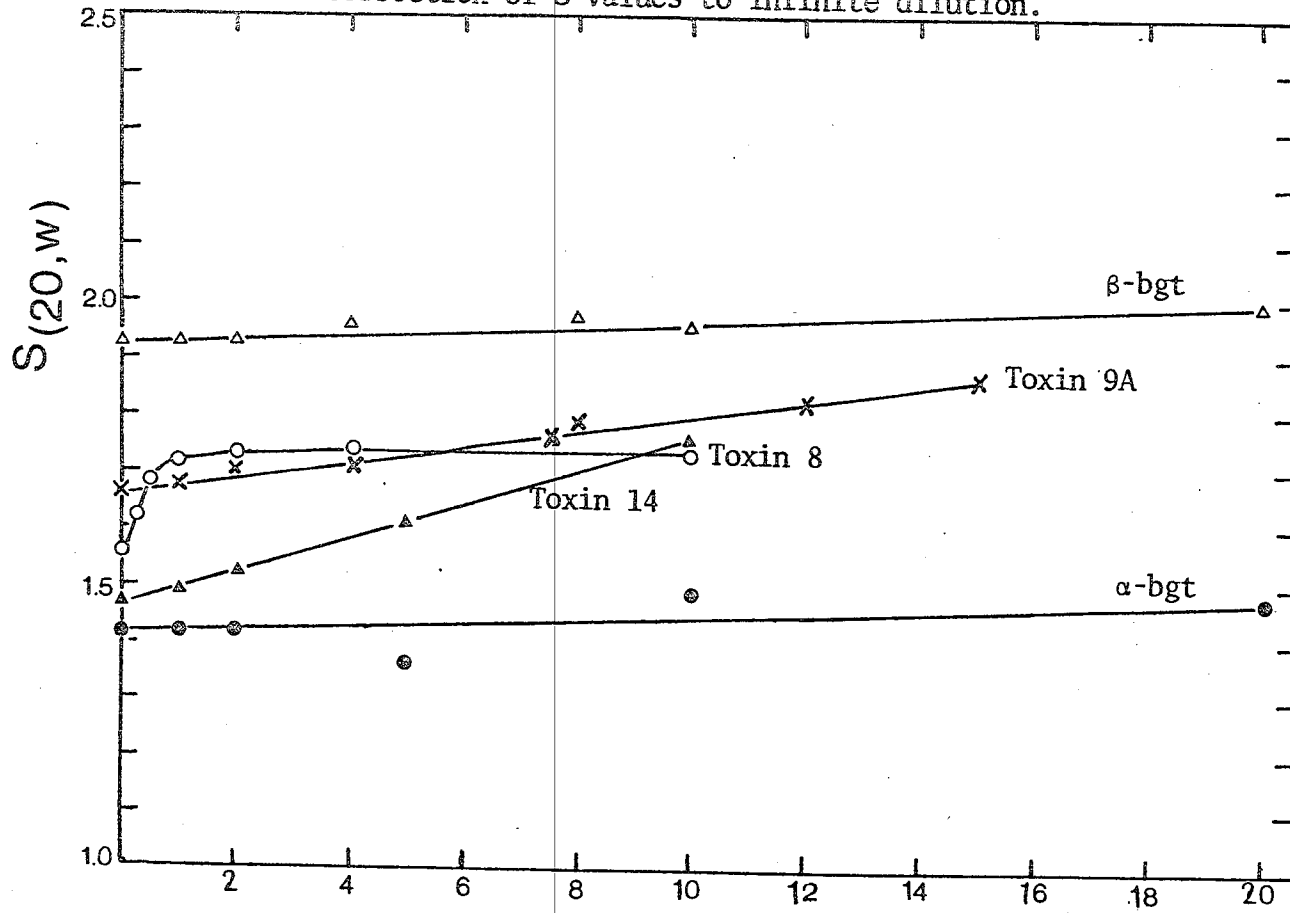
^aActivities defined by toxicology (13) and pharmacological studies (51,52).

^bFrom Lee et al. (51), Dryden et al., (52).

^cK_{av} is defined as $(V_e - V_o) \cdot (V_t - V_o)^{-1}$, where V_e is the elution volume of the peak concentration of a solute; V is the void volume (indicated by blue dextran); V_t is the total volume (indicated by potassium dichromate) (38).

^dFrom calibration curve of K_{av} vs. (molecular weight) using chymotrypsinogen, myoglobin, lysozyme, ribonuclease, cytochrome c, pancreatic trypsin inhibitor, and insulin as standards.

Figure 3-2
Correction of S-values to infinite dilution.



$S(20,w)$ = S-value at 20°C and viscosity of water. Points on the ordinate are extrapolated.

lines have slopes near zero. Toxins 8, 9A and 14 all appear to undergo aggregation as the concentration is increased. Both 9A and 14 give linear $S_{(20,w)}$ vs. C plots, but 8 gives a saturating (at 1 mg/mL) hyperbolic plot. Using partial specific volumes estimated from the amino acid compositions (40), and measured diffusion coefficients, molecular weights were calculated for the toxins from their S-values. Toxins 6 thru 8 were very similar to α -bgt, 9A and 14 were both near 13,000 daltons, and β -bgt plus 11 thru 13 were all \sim 21-22,000 daltons. These data are summarized in Table III-5.

Sedimentation equilibrium experiments gave molecular weights in good agreement with the sedimentation velocity results (Table III-6). Examination of the log C vs. r^2 plots again suggested self-interaction of 8 and 14.

v. Fluorescence Polarization. α -Bgt and β -bgt were selected for intensive study by fluorescence polarization because this technique is very sensitive to axial asymmetry (41) and the behavior of these two toxins was expected to be predictive for the majority of the other bungarotoxins. In Figure 3-3, the Perrin plots of the fluorescence polarization as a function of either temperature or viscosity are shown. These plots are a graphical method for solving for the molecular volume, V, using the Perrin equation (42);

$$\frac{1}{P} = \frac{1}{P_0} + \left(\frac{1}{P_0} - \frac{1}{3}\right) \cdot \left(\frac{R\tau}{V}\right) \cdot \frac{T}{\eta}$$

where P is the polarization observed, P_0 is a constant derived from linear extrapolation to the ordinate, R is the gas constant, T is the absolute temperature, η is the viscosity, τ is the fluorescent lifetime, and V is the volume of the fluorescent rotational unit. Graphically, the slope gives $\left(\frac{1}{P_0} - \frac{1}{3}\right) \cdot \frac{R\tau}{V}$ and the y-intercept gives $\frac{1}{P_0}$. Using the single tryptophan of α -bgt as the monitor, the intrinsic-fluorescence polarization was determined isothermally using a series of sucrose solutions of known viscosity (Figure 3-3A). The results gave a good fit to a straight line and

TABLE III-5

SUMMARY OF SEDIMENTATION VELOCITY EXPERIMENTS

Toxin	$S_{(20,w)} \times 10^{-13}{}^a$	Diffusion Coefficient $\times 10^{-7}$	Partial Specific Vol. b	Molecular Weight c
3 (α -Bgt)	1.41	15.7*	.723	7900
6	1.52	15.0	.710	8500
7	1.38	15.7	.711	7400
8	1.56	15.0*	.708	8700
9A	1.66	10.0*	.700	13,500
10 (β -Bgt)	1.92	8.2*	.724	20,700
11	2.04	8.2	.706	20,600
12	2.07	8.2	.702	20,600
13	2.17	8.2	.710	22,200
14	1.47	10.0	.717	12,650

* Measured directly

^a Corrected to infinite dilution

^b Estimated from amino acid composition

^c Calculated from substitution into the Svedburg equation:

$$MW = \frac{R \cdot T \cdot S}{D(1 - v_p)}$$

$$T = 293^\circ K$$

$$R = 8.313 \times 10^7$$

p assumed as 1

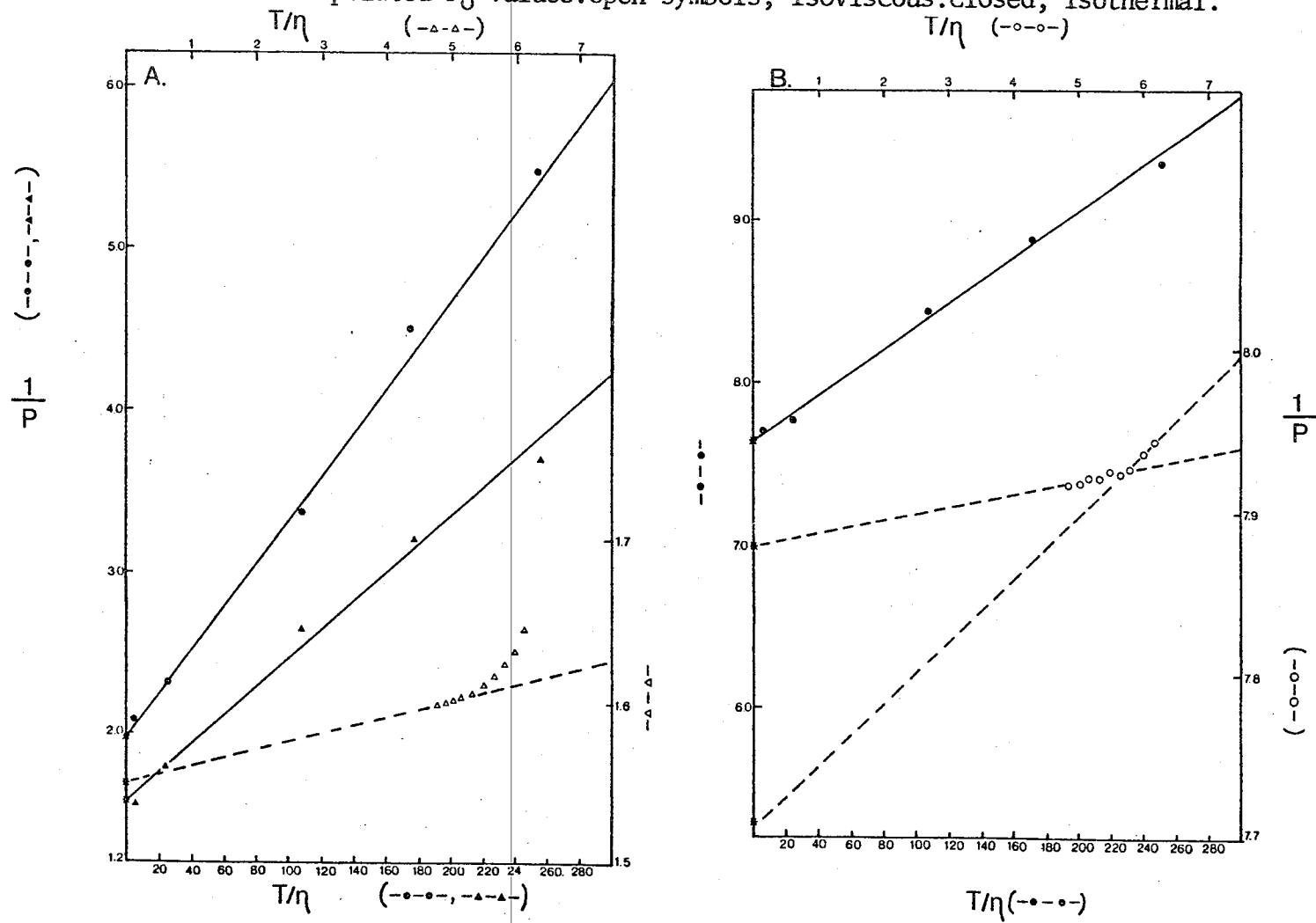
TABLE III-6

SUMMARY OF SEDIMENTATION EQUILIBRIUM EXPERIMENTS

<u>Toxin</u>	<u>Equilibrium Rotor Speed</u>	<u>Concentration (mg/ml)</u>	<u>Mol. Wt.</u>	<u>Limiting Mol. Wt.*</u>	
				<u>Meniscus</u>	<u>Bottom</u>
α -Bgt	25,980	1.5	8000	straight line	
7	25,980	1.5	8400	straight line	
8	25,980	1.0	11,000	7800	15,800
9A	20,410	1.0	14,800	13,300	17,100
β -Bgt	19,160	2.0	21,500	straight line	
11	19,160	1.3	21,700	straight line	
12	19,160	1.5	22,100	20,700	25,400
13	19,160	1.6	22,900	straight line	
14	20,410	1.5	12,400	11,900	16,500

* molecular weights calculated using the limiting slopes of the $\log C$ vs. r^2 plots at the meniscus and bottom of sample cell. Upward curvature suggests heterogeneity or self-association and downward curvature suggests thermodynamic non-ideality (30).

Figure 3-3
 Perrin plots of fluorescence polarization data.
 A: α -bgt, B: β -bgt. Asterisks on the ordinate mark
 extrapolated P_0 values. Open symbols, isoviscous. Closed, isothermal.



were used, together with the experimentally determined emission lifetime, to calculate the molecular weight from the molecular volume (43). The calculated molecular weight, 4130, is half that of α -bgt, therefore the tryptophan chromophore must be capable of independent rotation. This might be expected since the intrinsic fluorescence spectrum (13, see Chapter IV) has $\lambda_{\text{max}} = 342$ nm; consistent with partial exposure of the residue to the solvent. Moreover, the X-ray data for erabutoxin shows the homologous tryptophan to be partly immobilized (4). Consequently, a monolabelled dansyl derivative of α -bgt was prepared to provide a suitable extrinsic marker-fluorophor. The isothermal Perrin plot of the dansyl- α -bgt gave a satisfactory fit to straight line, although there was detectable curvature towards the T/η axis; attributable to either asymmetry or heterogeneity of the fluorescent species (43). Solving for the molecular weight, a value of 11,520 daltons was obtained. Because the consequences of thermal perturbation on the protein structure and fluorescent lifetime are unpredictable (44), isoviscous polarization measurements are less reliable than those under isothermal conditions. Indeed, the Perrin plot using temperature variation shows pronounced curvature away from the T/η axis; evidence of thermally-provoked accelerated motion of either the fluorophor or its immediate protein environment. Nonetheless, the use of the limiting slope in the Perrin equation gave a molecular weight of 9110. The fact that both isothermal and isoviscous polarization measurements gave higher apparent molecular weights, using the extrinsic dansyl probe, than the true weight of ~ 8000 daltons suggested the rotational unit was asymmetric, in keeping with the deviation from globular protein behavior detected in gel filtration. Using the calculated rotational relaxation time ρ_0 (see Table III-7), axial ratios for standard shapes can be determined from theoretical curves generated by Weber (45). If α -bgt is assumed to be a prolate ellipsoid,

its axial ratio is 6-to-1, and if α -bgt is assumed to be an oblate ellipsoid, its axial ratio is 4.5-to-1. These values confirm the presence of tertiary asymmetry.

The isothermal Perrin plot of β -bgt's intrinsic fluorescence gave a straight line (Figure 3-3B). From this plot and the measured fluorescent lifetime, an apparent molecular weight of 21,370 daltons was calculated, in good agreement with values from other techniques. This suggests that the single tryptophan of β -bgt is rotating with the correlation time of the entire protein and must therefore be immobilized. This is consistent with the observed Stoke's shift of the emission maximum to $\lambda_{\text{max}} = 338 \text{ nm}$, which indicates a strongly hydrophobic environment around the tryptophan. Interestingly, when the temperature is raised to 80°C , the measured fluorescent lifetime increases substantially (2.5 to 7.5 nsec) and the steady-state emission maximum is shifted to 334 nm. Thus, the tryptophan chromophore is apparently shifted to an even more hydrophobic environment upon heating and, as a result, remains immobilized upon heating. The isoviscous Perrin plot is biphasic, showing a transition to more rapid rotation between 70° and 80°C . The calculated molecular weights corresponding to the two slopes of the graph are 20,120 daltons for the lower temperature segment, and 12,150 daltons for the higher temperatures. There is no suggestion of molecular asymmetry from previous results or the characteristics of the Perrin plots for β -bgt. The axial ratio of β -bgt assuming a prolate ellipsoid is 1-to-1, and assuming an oblate ellipsoid is 2-to-1. Thus, it is likely that β -bgt and closely-related bungarotoxins do not differ appreciably from a spherical hydrodynamic approximation.

The fluorescence polarization measurements and calculated results are shown in Table III-7.

vi. Amino Acid Composition. Tables III-8 and III-9 summarize the data for

TABLE III-7
FLUORESCENCE POLARIZATION DATA AND CALCULATED RESULTS

A. Data

<u>α-Bgt</u>					
Condition	$1/p_0^a$	Slope of Perrin plot ^b	τ^c	V^d	$\rho_H(20,w)^e$
Isothermal, Intrinsic	1.96	$1.38 (10^{-4})$	4.2	4130	5.0
Isothermal Extrinsic	1.60	$0.88 (10^{-4})^f$	9.6	11,520	14.0
Isoviscous, Extrinsic	1.55	$0.98 (10^{-4})^f$	8.8 (80°)	9110	
<u>β-Bgt</u>					
Isothermal, Intrinsic	7.63	$0.71 (10^{-4})$	2.5	21,370	24.9
Isoviscous, Intrinsic (biphasic)	7.88 7.71	$0.78 (10^{-4})$ $3.80 (10^{-4})$	2.5 (20-70°) 7.5 (80°)	20,120 12,150	

B. Calculated Results

	\bar{v}	ρ_0^g	Mol. Wt. ^h 8900	ρ_H/ρ_0	Axial Ratios ⁱ	
					Prolate	Oblate
α -Bgt	.723	6.4	11,260	2.18	6.1	4.5:1
β -Bgt	.724	16.7	19,650 20,770	1.49	1:1	2:1

^aFrom the y-intercept of the Perrin plots (Figure 3-3)

^bFrom Figure 3-3

^cFluorescent lifetime measured directly at 20° C (unless otherwise indicated) in nsec

^dMolecular volume (in cc). Calculated from $V=(1/p_0-1/3) \cdot R\tau \cdot (\text{slope})^{-1}$

^eRotational correlation time in nsec at 20° C and viscosity of water

^fLimiting slopes at y-intercept for curved Perrin plots

^gRotational correlation time for hard sphere in nsec. Calculated from $\rho_0 = (\text{Mol. Wt.}/1.23) (10^{-3})$

^hCalculated from $MW=V \cdot (H + v)^{-1}$ where H =hydration=.3g/g protein for both toxins

ⁱAxial ratios are for prolate or oblate ellipsoid model structures using the theoretical equations of Weber (45)

TABLE III-8

AMINO ACID COMPOSITION OF BUNGAROTOXINS (FRACTIONS 7 through 14)*

	Fraction 7		Fraction 8		Fraction 9A		Fraction 10		Fraction 11		Fraction 12		Fraction 13		Fraction 14	
	Moles Mole	Integer	Moles Mole	Integer	Moles Mole	Integer	Moles Mole	Integer								
Lys	5.23	5	6.42	6	7.90	8	13.18	13	14.32	14	15.77	16	18.88	19	12.92	13
His	1.15	1	1.34	1	2.77	3	4.82	5	5.79	6	6.06	6	6.25	6	3.21	3
Arg	4.77	5	5.76	6	10.82	11	14.05	14	14.11	14	15.12	15	17.26	17	8.71	9
Asp	8.50	9	8.91	9	18.13	18	23.01	23	22.27	22	22.77	23	23.86	24	12.08	12
Thr	7.11	7	5.62	6	9.27	9	10.28	10	11.30	11	11.19	11	10.17	10	6.94	7
Ser	3.44	4	3.79	4	4.40	4	3.42	4	6.93	7	6.83	7	5.97	6	5.32	5
Glu	5.10	5	5.98	6	8.39	8	12.29	12	11.82	12	12.09	12	13.21	13	7.86	8
Pro	5.00	5	1.89	2	5.28	5	6.94	7	8.18	8	7.84	8	9.82	10	6.07	6
Gly	4.55	5	2.97	3	12.63	13	17.72	18	15.97	16	16.09	16	16.29	16	8.20	8
Ala	3.26	3	2.15	2	9.24	9	11.38	11	10.87	11	10.64	11	11.35	11	5.92	6
$\frac{1}{2}$ -Cys	9.78	<u>10</u>	9.94	<u>10</u>	14.04	<u>14</u>	16.29	<u>16</u>	20.18	<u>22</u>	22.13	<u>30</u>	20.78	<u>26</u>	12.57	<u>12</u>
Val	2.70	<u>3</u>	1.82	<u>2</u>	2.29	<u>2</u>	5.00	<u>5</u>	4.54	<u>5</u>	3.69	<u>4</u>	5.58	<u>6</u>	3.93	<u>4</u>
Met	1.00	1	0.94	1	1.61	2	1.95	2	1.97	2	2.04	2	1.61	2	0.61	1
Ile	2.61	3	2.81	3	4.92	5	8.48	9	8.47	9	8.21	8	8.53	9	5.67	6
Leu	3.19	3	3.10	3	4.70	5	7.58	7(8)	6.32	6	5.90	6	7.61	8	4.90	5
Tyr	1.84	2	4.26	4	9.93	<u>10</u>	13.82	<u>14</u>	13.82	<u>14-15</u>	16.10	<u>16</u>	13.18	<u>14-15</u>	7.06	9
Phe	2.26	<u>2</u>	3.18	<u>3</u>	4.15	<u>4</u>	6.02	<u>6</u>	5.99	<u>6</u>	6.13	<u>6</u>	6.14	<u>6</u>	2.72	<u>3</u>
Trp	0.95	1	0.84	1	0.98	1	0.86	1	0.92	1	0.89	1	0.92	1	0.54	1
Total no. of aa/mole	74		72		131		177		186		198		204		118	
Mol wt	8300		8500		15100		20400		21500		23000		23700		13800	
N terminus	Met		Met		Asx		Arg,Asx		Arg,Asx		Arg,Asx		Lys,Asx		Asx	

* Moles of amino acid per mole of protein were calculated from the μ mole of amino acid obtained from the analyses and the μ mole of protein hydrolyzed. This last value was calculated from A_{280} of the solution to be hydrolyzed and the ϵ_{280} of the respective protein. Values for half-cystine which are underlined were obtained by subtracting the values for methionine from total sulfur content obtained from x-ray fluorescence spectrum (Table III-9). Values for tyrosine which are underlined were obtained from MCD spectra. Values are extrapolated from at least one analysis at each time point; 20-22, 44, and 68-72 h. Every fraction has more than one determination at the 20-22 h time point, including a methanesulfonic acid hydrolysis for tryptophan.

TABLE III-9

DETERMINATION OF SULFUR CONTENT OF BUNGAROTOXINS BY X-RAY FLUORESCENCE

Fraction	Moles of S/mole of protein*	Fraction	Moles of S/mole of protein*
α -Bgt	10.4	10 (β -Bgt)	17.8
7	11.8	11	24.1
8	10.2	12	31.6
9A	16.3	13	27.2
		14	13.1

* Protein molar concentration was calculated from A_{280} and the extinction coefficient.

amino acid analyses. The existence of a single tryptophan in 9A thru 14 was originally indicated by the magnetic circular dichroism spectra (see Chapter IV). Results from 22-hr methanesulfonic acid hydrolyses of the toxins agreed very closely with those obtained by HCl hydrolyses, and gave independent proof for a single tryptophan in all the purified bungarotoxins.

Except for 8 and 14, molecular weights generated from a computer program* agreed well with values from other techniques. Toxin 8 appeared smaller than α -bgt by SDS-gels, but larger by its best-fit amino acid composition. From the basic isoelectric points, the bulk of the aspartic and glutamic acid residues must be amidated to asparagine and glutamine.

Notable destruction of threonine, serine, cystine, and tyrosine was observed; therefore these values were back-extrapolated to zero time. Even with correction, the serine and threonine numbers may still be low because of their nonlinear destruction kinetics in these proteins. Comparison of the amino acid composition reported here to that derived from the amino acid sequence of β -bgt (18) shows that the serine value was correct, but that the threonine value was indeed too low (by two residues). The tyrosine content was compared with independent determinations based upon the magnetic circular dichroism spectra (see Chapter IV), and the latter values were given preference because this type of measurement can theoretically give absolute concentrations of tyrosine in the samples, independent of their conformation.

Although alanine and methionine are absent from many Elapid toxins (46), alanine (4 to 6 fraction percent) was found in all the bungarotoxins. Methionine concentrations were the lowest of all the amino acids. There were consistently higher tyrosine-to-tryptophan ratios in the β -type than in the α -type toxins. Except for the high proportion of basic residues and disulfides, the compositions of the toxins were very similar to the average calculated

* Giving the molecular weight for the best integral fit of the experimental residue moles/mole protein values.

for soluble globular proteins (47).

Complete reduction and alkylation were difficult to achieve in the β -toxins, in agreement with another report (48). Long incubation times (24-36 hrs) with a large molar excess of reducing agent in the presence of a strong denaturant (6M guanidine hydrochloride) were necessary. Carboxymethylcysteine values after acid hydrolysis were low in several instances, reflecting the known acid instability of this amino acid derivative (49). No evidence was obtained for reaction of lysines or histidines with iodoacetic acid alkylation. α -Type toxins could be reduced and alkylated satisfactorily under standard conditions.

N-terminal amino acid analyses of α -bgt gave the expected isoleucine (50). Toxins 7 and 8 gave methionine as the N-terminal, 9A and 14 gave Asx only, and each of β -bgt and 11 thru 13 gave Arg/Lys and Asx as the N-terminals.

The X-ray fluorescence determinations served two purposes: 1) an independent measurement of the total sulfur content, assumed to represent the cystine plus methionine residues; and 2) the analysis of ionic contamination. The latter was of interest to judge the success of the desalting procedure, and to screen for any tightly-bound ionic co-factors. There were no appreciable amounts of Na, Mg, Si, Cl, K, or Ca in the samples. Since the β -toxins have a calcium-binding site (see Chapter IV), which is apparently required for the maximum in vitro expression of their phospholipase A activity (see Chapter VI), the absence of calcium indicated that the binding was reversible and that toxin activity did not depend on calcium retention during purification.

Cystine content was very high in these proteins, as with other snake venom neurotoxins (2). The high proportion of disulfides accounts for their resistance to nonreducing denaturation and sensitivity to reduction (13). Free sulfhydryl groups were not found in any purified toxin. The number

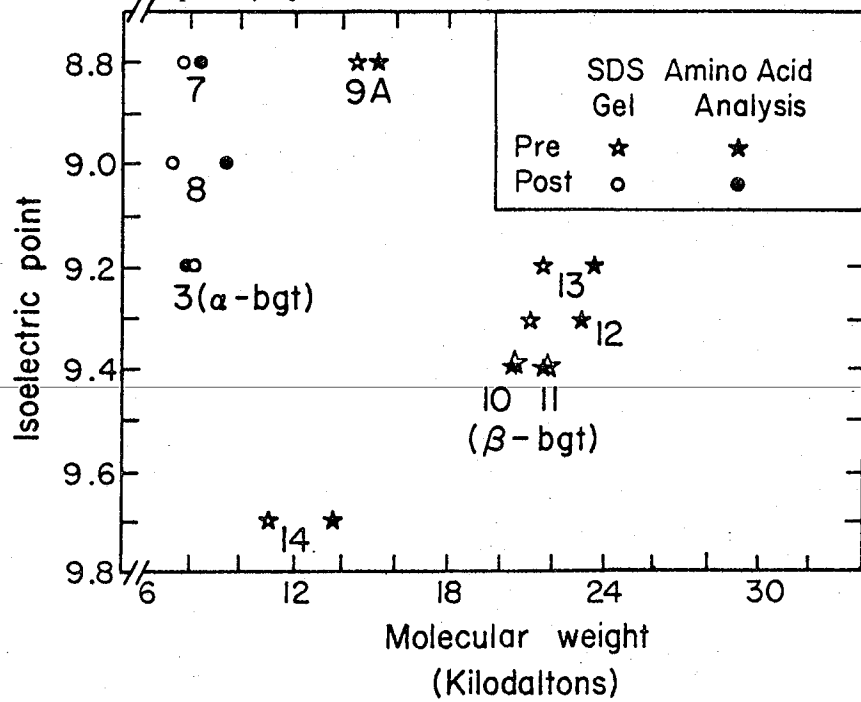
of half-cystines plus methionine agreed within 10% for the X-ray fluorescence vs. amino acid analyses for 7 and 8. 9A and 14 agreed within a single sulfur per protein. In β -bgt, only 16 half-cystines per 20,500 daltons were detected by both techniques, unlike the 20 half-cystines from the primary structure (18). Previously, this discrepancy had been attributed to the cross-contamination of β -bgt with its chromatographic neighbor, toxin 11 (14), which has 22 half-cystines. Sulfur values from X-ray fluorescence for 12 and 13 were considerably higher than the total sulfur from amino acid composition. In earlier work, the X-ray data were taken as correct (18), and the lower cystine content detected after acid hydrolysis was ascribed to incomplete compensation by the extrapolation correction to zero time. Corroboration for the higher cystine content in these toxins, however, is provided by the magnitude of a diagnostic near-UV circular dichroism signal, which is shown in Chapter IV to be sensitive to the total cystine content.

vii. Comparative Summary. Figure 3-4 indicates the isoelectric points and molecular weights (by two techniques) of the purified bungarotoxins. The figure points out the shared size and charge properties of α -bgt and 7 and 8, and β -bgt and 11 thru 13. Toxins 9A and 14 are distinctive from both classes in these physical characteristics, but are functionally classed with the other β -toxins because of previous pharmacological studies (51,52).

Table III-10 compares the amino acid compositions of α -bgt to 7 and 8, and β -bgt to determinations from other laboratories and the composition derived from the sequence. The compilation of deviations from the sequence-based composition indicates that the results reported herein were the most accurate, with the important exception of the cystine content.

Table III-11 summarizes the results for molecular weight determinations from various techniques. With the α -toxins, the gel filtration results gave anomalously high values because the toxin shape is sufficiently asymmetric

Figure 3-4
 Comparison of isoelectric points and molecular weights of purified toxins. The horizontal distance between the open and solid symbols indicates the agreement of the two methods of molecular weight estimation. The post-synaptic toxins and pre-synaptic toxins cluster separately.



XBL 774-4333

TABLE III-10

COMPARISONS WITH BUNGAROTOXIN AMINO ACID COMPOSITIONS

	A. α -Type			B. β -Bgt (*-deviation from sequence)					C. β -Type					
	α -Bgt ^a	7	8	From Sequence ^b	This Work	Ref. 51	Ref. 53	Ref. 54	11	β_2^c	12	β_3^c	13	β_4^c
Lys	6	5	6	13	13	13	13	14*	14	12	16	12	19	14
His	2	1	1	5	5	5	5	5	6	4	6	5	6	7
Arg	3	5	6	14	14	14	15*	16*	14	19	15	16	17	17
Asp	4	9	9	22	23*	22	24*	21*	22	22	23	23	24	24
Thr	7	7	6	12	10*	12	12	13*	11	15	11	12	10	12
Ser	6	4	4	4	4	6*	6*	6*	7	5	7	5	6	5
Glu	5	5	6	12	12	12	13*	13*	12	13	12	14	13	13
Pro	8	5	2	7	7	8*	8*	7	8	6	8	7	10	8
Gly	4	5	3	18	17*	16*	18	19*	16	19	16	18	16	16
Ala	5	3	2	11	11	11	12*	13*	11	14	11	13	11	12
$\frac{1}{2}$ -Cys	10	10	10	20	16*	20	20	20	22	20	30	22	26	20
Val	5	3	2	5	4*	4*	4*	6*	5	5	4	5	6	4
Met	1	1	1	2	2	2	2	2	2	2	2	2	2	2
Ile	2	3	3	9	9	8*	9	9	9	8	8	9	9	8
Leu	2	3	3	7	7	7	7	7	6	8	6	8	8	8
Tyr	2	2	4	14	14	13*	13*	15*	14-15	16	16	15	14-15	15
Phe	1	2	3	6	6	6	6	6	6	6	6	6	6	5
Trp	1	1	1	1	1	3*	4*	2*	1	2	1	2	1	2
					(5*)	(7*)	(9*)	(11*)						
Total	74	74	72	180	177	182	191	194	186	195	198	194	204	192
Mol. Wt.	7983	8350	8540	20500	20440	21110	22130	22000	21500	22000	23000	22000	23700	22000
N-terminals	Ile	Met	Met	Arg,Asn	Arg,Asx	x	x	x	Arg,Asx	x	Arg,Asx	x	Lys,Asx	x

^aFrom sequence (50)^bRef. 48^cRef. 54

TABLE III-11

COMPARISON OF MOLECULAR WEIGHTS FROM DIFFERENT TECHNIQUES

<u>Toxin</u>	<u>SDS-Slab Gradient Gels</u>	<u>Gel Filtration</u>	<u>From S-value</u>	<u>From amino acid composition</u>	<u>Sedimentation Equilibrium</u>
α -Bgt	8000	15-16,000	7900	7900	8000
7	8000	15-16,000	7400	8300	8400
8	5000	15-16,000	8700	8500	11,000
9A	21,000	15-17,500	13,500	15,100	14,800
β -Bgt	21,500	20-21,000	20,700	20,400	21,500
11	20,500	20,500-21,500	20,600	21,500	21,700
12	21,000	21-22,000	20,600	23,000	22,100
13	21,500	20,500-21,500	22,200	23,700	22,900
14	21,500	22-23,000	12,650	13,800	12,400

to invalidate the assumptions of molecular weight calibration. Toxin 8 gave an unusually wide dispersion of observed weights. With toxins 11 thru 13 and β -bgt, the agreement is very good. Toxin 9A gives a nearly dimeric molecular weight by SDS-gels, and toxin 14 gives a similar disagreement by both SDS-gels and gel filtration.

Table III-12 compiles the various hydrodynamic parameters from the different approaches. Although none of the bungarotoxins are dramatically asymmetric by their f/f_0 ratio, when corrected for the hydration contribution, the α -toxins nonetheless have an intrinsic asymmetry as demonstrated in their unhydrated f/f_0 ratios and in the axial ratios from fluorescence polarization data. The β -toxins in all cases approach the behavior of a model rigid sphere in solution.

DISCUSSION.

Based upon the various structural determinations, three distinct classes of bungarotoxins have been defined: 1) α -type single-chain toxins of ~ 8000 daltons (α -bgt, 6 thru 8); 2) β -type single-chain toxins of $\sim 14,000$ daltons (9A, 14); and 3) β -type covalent two-chain toxins of 20-22,000 daltons (β -bgt, 11 thru 13). Figure 3-4 shows that categories #1 and #3 also share similar isoelectric points. The comparisons in Table III-10 of the β -toxins' amino acid compositions with results from other groups confirm the identification of the functional activities with the toxins purified by the scheme herein. Thus, I shall assume that α -type toxins correspond to curarimimetic toxins (see Chapter V) and that β -type toxins correspond to pre-synaptic toxins (see Chapter VI). 9A and 14, however, have structural differences from the other bungarotoxins which may have functional correlates (13,51,52) and should therefore be considered potentially unique in their pharmacology, albeit, for simplicity, they will be routinely considered with the β -toxins.

TABLE III-12
COMPARISON OF HYDRODYNAMIC PARAMETERS CHARACTERIZING THE BUNGAROTOXINS

Toxin	Partial Sp. Vol. ^a	Mol. Wt. ^b	Stoke's radius	f/f_o^c	$(f/f_o)_H^d$	$(f/f_o)_A^e$
α -Bgt	.723	7938	16.5	1.26	1.12	1.13
7	.711	8000	16.5	1.26	1.12	1.13
8	.708	8600	16.5	1.23	1.125	1.09
9A	.700	14,000	17.5	1.11	1.13	0.98
β -Bgt	.724	20,500	22	1.22	1.12	1.09
11	.706	20,700	22	1.21	1.125	1.08
12	.702	21,700	22	1.20	1.13	1.06
13	.710	22,300	22	1.20	1.125	1.07
14	.717	13,000	22	1.42	1.12	1.27

^aFrom amino acid compositions in Table III-8 using procedure of Cohn and Edsall (40).

^bRounded average of results in Table III-11, except α -bgt and β -bgt which are based upon sequences and 9A and 14 which use the monomeric weights.

^cCalculated from $f/f_o = \frac{a}{[(3\bar{v}M)(4\pi N)^{-1}]^{1/3}}$ where a=Stoke's radius, \bar{v} =partial specific volume, M=molecular weight, N=Avogadro's number.

^dCalculated from $f/f_o = (f/f_o)_H \cdot (f/f_o)_A$ where $(f/f_o)_H$ =asymmetry due to hydration and $(f/f_o)_A$ = asymmetry due to unhydrated shape.

$$(f/f_o)_A = (1 + H/\bar{v}\rho)^{1/3}$$

where H=hydration (assumed to be .3 g/g protein and ρ =density (assumed to be 1.0)

Focusing on the first category, it is evident that both α -bgt and 7 are Type II toxins. 8, however, is difficult to classify on the present evidence. The size disparity of 8 measured by different techniques is the greatest for any of the bungarotoxins (Table III-11). The concentration vs. $S_{(20,w)}$ plot for 8 (Figure 3-2) suggests one complication may be a monomer-dimer equilibrium. Using a previously-developed formulation for the calculation of association constants of interacting systems from sedimentation velocity experiments (55), an apparent monomer-dimer K_d of $1.25 (10^{-6})M$ is obtained. Thus, toxin 8 should be fully dimerized under sedimentation and gel filtration conditions. In the latter technique, the K_{av} is identical to that for the monomeric, albeit structurally asymmetric, α -toxins α -bgt and 7. If the dimer-formation evidence is correct, then the gel partitioning indicates that the dimer has an indistinguishably different Stoke's radius from the monomer. It is possible that the association of two axially-asymmetric molecules could produce a symmetric dimer of roughly the same excluded volume in solution. The sedimentation equilibrium data support the idea of a reversible, concentration-dependent dimer formation because the $\log C$ vs. r^2 plot is curved upwards from the r^2 axis, suggesting self-association (30). The limiting slopes are strongly supportive of this interpretation; giving 7800 at the meniscus and 15,800 at the cell bottom (Table III-6). The molecular weights obtained from amino acid analysis, S-value, and the limiting slope in sedimentation equilibrium all gave ~ 8000 daltons for toxin 8. However, the use of SDS-slab gradient gels gave an a low estimated molecular weight of 5000 daltons. Since the accuracy of molecular weight determinations by SDS-gels depends on the binding of an equivalent proportion of the detergent by both standards and unknowns (56), it is possible that 8 binds an unusually large amount of SDS to give rise to the enhanced mobility (57). An unequivocal statement as to the size and Type I or II classification of 8 may have to await sequencing.

The α -toxins appear asymmetric in shape by several criteria. The f/f_0 ratios in Table III-12 have been divided into contributions from hydration, $(f/f_0)_H$, and intrinsic asymmetry, $(f/f_0)_A$. The α -toxins have apparently equal contributions from both terms to their overall solution shape. The f/f_0 ratios are in the normal range for globular proteins (39), but nonetheless could be consistent with axial ratios of 3 or 4-to-1. The fluorescence polarization data provides a direct and independent measure of this asymmetry, and an axial ratio of 4.5-to-1 was obtained for an oblate ellipsoid approximation (Table III-7). However, the X-ray structures of the Type I erabutoxins gave dimensions of $38 \text{ \AA} \times 28 \text{ \AA} \times 15 \text{ \AA}$ (4,5); indicating less spherical distortion than that suggested for the Type II bungarotoxins from the hydrodynamics. Further, preliminary X-ray studies of α -bgt itself have suggested it could be accommodated within an ellipsoid of $40 \text{ \AA} \times 28 \text{ \AA} \times 21 \text{ \AA}$ (58). Thus, the apparent asymmetry must come from another source. One intriguing possibility is the fact that the preliminary X-ray results indicate the C-terminal "tail" of α -bgt extends 31 \AA away from the main globular body of the toxin (58). This could add a considerable degree of anisotropy to solution structure measurements and account for the observations noted before. Another consideration is whether the hydration term asymmetry indicates any clustering of charged groups on the surface of the protein. Examination of the X-ray structures of the erabutoxins indicates that there is indeed such a clustering. The toxin surface (B-surface) opposite to the hypothetical recognition site contains a net charge of zero (five positive, five negative), whereas the recognition site surface (A-surface) contains a net charge of plus three (four positive, one negative). Examination of predicted structures for α -bgt (58,59) shows that its B-surface also has a net charge of zero (two positive, two negative) and its A-surface has a net charge of plus three (eight positive, five negative).

It might be speculated that water bound to the A-surface could be the source of the solution asymmetry and could also have a functional significance.

In interacting with the receptor, water could be released from the toxin's A-surface to contribute to the entropy in the binding thermodynamics. In this regard, it should be noted that an investigation of the binding thermodynamics of ^3H -Naja naja siamensis toxin to solubilized nAChR indicated that the reaction was driven by an unusually large entropy change (60), which required the invocation of large conformational changes, but could be alternatively explained by the release of bound water.

β -Bgt and 11 thru 13 all appear nearly spherical in solution by all techniques. In Table III-11, there is very good agreement between the various estimates of molecular weight. From Table III-12, the hydration term appears to account for the little apparent asymmetry in f/f_0 ratios, and may arise from a nonuniform distribution of charged surface residues and the resulting asymmetry of bound water, as has been speculated for the α -toxins. From Table III-10, it is clear that 11 thru 13 correspond to the β_2 thru β_4 toxins of Abe et al (54). Systematic differences can be seen in the compositions reported here and those reported by Abe et al (54), notably in the cystine and tryptophan content. The higher tryptophan content noted for β_2 thru β_4 is incorrect since the existence of single tryptophans in 11 thru 13 has been confirmed by several techniques. The cystine content, however, may be overestimated in 12 and 13 because of the use of two spectral procedures, X-ray fluorescence and circular dichroism, whose reliability for proteins has yet to be critically checked. It is unclear what the origin of such an overestimate may be, but for X-ray fluorescence, it is conceivable that it could arise from a contribution of non-protein sulfur atoms, possibly bound sulfate groups. It should be considered that erabutoxin has been shown to be capable of binding sulfate ions at its N-terminal (3).

By both isothermal and isoviscous determinations, the fluorescence polarization results for β -bgt yield accurate molecular weights (20,770 and 19,650 daltons respectively). Thus, the use of the single tryptophan as an intrinsic reporter has demonstrated trp immobilization because the trp rotates with the correlation time of the entire protein. With thermal perturbation, there is a phase transition between 70^o and 80^oC, as detected by the lowering of the correlation time. The apparent molecular weight for this new correlation time is 12,150, very near the 12,500 daltons (48) of the heavy chain which contains the tryptophan residue. This result could point to either increased independent rotation of the tryptophan chromophore, or the dissociation between the two subunits cross-linked by a disulfide, so that the heavy and light subunits were undergoing independent rotation. Since the trp steady-state fluorescence shifted to shorter wavelengths above 70^oC, with a concomitant lengthening of the fluorescent lifetime, it is unlikely that the trp residue is acquiring increased rotational freedom; rather the trp remains immobilized but rotates with the correlation time of the heavy subunit. This suggests that the globular domains of the subunits are stronger than the interaction domain between them, cross-linking notwithstanding. This type of independent segmental flexibility in disulfide-linked regions has been well-documented in fluorescence polarization studies of immunoglobulins (61).

It was previously reported that the light chain of β -type toxins (11 thru 13 and β -bgt) was refractory to N-terminal analysis (14). However, more recent experiments have indicated that the low levels of lysine and arginine previously reported (14) do in fact originate as the N-terminals of the light chains.

Both 9A and 14 appear roughly 13-14,000 daltons in SDS gels containing reducing agents or urea, but not in SDS only. In the latter condition, they

appear roughly twice as large. Thus, it appears that the toxins can form stable dimers which are not dissociated by SDS, but are nonetheless non-covalently associated. Examination of Table III-11 indicates that 9A does not normally exist as a dimer in solution, although it has an inclination towards self-association in both sedimentation velocity and sedimentation equilibrium experiments. 14, however, has a more pronounced tendency to form dimers and is dimeric under the conditions of preparative gel filtration (~10 mg/mL concentration). Analytical gel filtration experiments confirmed the concentration-dependence of its partitioning behavior. At the same concentrations, 9A and 14 form stable dimers in SDS, but may or may not do so in solution. Thus, SDS apparently induces or favors dimer formation by these toxins. This is not surprising from results in other systems. SDS can be regarded as a model of the fatty acids making up the hydrophobic domain of biological membranes (62) and, as such, can mimic a membrane-surface in its effects on isolated proteins. One example is the SDS induction of a dimer of fd virus coat protein which is analogous to a membrane-mediated effect (63). Similarly, the single-chain phospholipase A₂ from Naja naja, to which both toxins should be homologous in sequence, undergoes self-association to dimers and higher oligomers at membrane surfaces and the same self-association can be promoted by long-chain amphiphilic detergents (64). Since 9A and 14 have been shown to have similarities to the single-chain pre-synaptic toxin notexin (14), it is possible that all three toxins share with Naja naja phospholipase a sensitivity to interfacial lipid induction of dimers, which may be important to their mechanisms of membrane interaction or digestion. An interesting line of speculation is whether the high pre-synaptic selectivity of the two-chain β -toxins is related to their inability to undergo dimer formation, and whether this is brought about by a protective or modifying effect

of the light chain.

Lastly, the results in Table III-12 show that 9A and 14 have considerably different f/f_0 ratios, possibly pointing to significant differences in solution structure (see Chapter IV). Thus, although I have considered the two toxins together, this does not indicate that they are to be taken as structurally or functionally equivalent.

REFERENCES.

1. Lee, C.-Y. (1972) *Ann.Rev.Pharmacol.*, 12, 265.
2. Tu, A.T. (1973) *Ann.Rev.Biochem.*, 42, 235.
3. Tsernoglou, D., and Petsko, G.A. (1977) *Proc.Nat.Acad.Sci.*, 74, 971.
4. Low, B.W., Preston, H.S., Sato, A., Rosen, L.S., Searl, J.E., Rudko, A.D., and Richardson, J.S. (1976) *Proc.Nat.Acad.Sci.*, 73, 2991.
5. Tsernoglou, D., Petsko, G.A., and Hudson, R.A. (1978) *Mol.Pharmacol.*, 14, 710.
6. Ryden, L., Gabel, D., and Eaker, D. (1973) *Int.J.Pep.Prot.Res.*, 5, 261.
7. Potter, L.T. (1974) *Meths.Enzymol.*, 32, 309.
8. Ong, D.E., and Brady, R.N. (1974) *Biochemistry*, 13, 2822.
9. Raymond, M.L., and Tu, A.T. (1972) *Biochim.Biophys.Acta*, 285, 498.
10. Ishikawa, Y., Menez, A., Hori, H., Yoshida, H., and Tamiya, N. (1977) *Toxicon*, 15, 477.
11. Miledi, R., and Szczepaniak, A.C. (1975) *Proc.Roy.Soc.*, 190, 267.
12. Szczepaniak, A.C. (1974) *J.Physiol.*, 241, 55P.
13. Eterovic, V.A., Hebert, M., Hanley, M.R., and Bennett, E.L. (1975) *Toxicon*, 13, 37.
14. Hanley, M.R., Eterovic, V.A., Hawkes, S.J., Hebert, A.J., and Bennett, E.L. (1977) *Biochemistry*, 16, 5840.
15. Fohlman, J., Eaker, D., Karlsson, E., and Thesleff, S. (1976) *Eur.J. Biochem.*, 68, 457.
16. Habermann, E., and Breithaupt, H. (1978) *Toxicon*, 16, 19.
17. Narita, K. (Osaka University, Japan), personal communication, May, 1978.

18. Kondo, K., Narita, K., and Lee, C.-Y. (1978) *J.Biochem.*, 83, 101.
19. Wernicke, J.F., Vanker, A.D., and Howard, B.D. (1975) *J.Neurochem.*, 25, 483.
20. Strong, P.N., Goerke, J., Oberg, S.G., and Kelly, R.B. (1976) *Proc. Nat.Acad.Sci.*, 73, 178.
21. Laemmli, U. (1970) *Nature*, 227, 680.
22. Davies, G., and Stark, G. (1970) *Proc.Nat.Acad.Sci.*, 66, 651.
23. Spackman, D., Stein, W., and Moore, S. (1958) *Anal.Chem.*, 30, 1190.
24. Katz, E. (1968) *Anal.Biochem.*, 25, 417.
25. Simpson, R., Neuberger, M., and Liu, T.-Y. (1976) *J.Biol.Chem.*, 251, 1936.
26. Spande, T., and Witkop, B. (1967) *Meths.Enzymol.*, 11, 498.
27. Robyt, J., Ackerman, R., and Chittenden, C. (1971) *Archs.Biochem.Biophys.*, 147, 262.
28. Stark, G., Stein, W., and Moore, S. (1961) *J.Biol.Chem.*, 236, 436.
29. Hebert, A., and Street, K. (1974) *Anal.Chem.*, 46, 203.
30. Chervenka, C.H., A Manual of Methods for the Analytical Ultracentrifuge, Beckman Instruments, Palo Alto, California, 1969.
31. Leskovar, B., Lo, C.C., Hartig, P.H., Sauer, K. (1976) *Rev.Sci.Instrum.*, 47, 1113.
32. Hartig, P.H., Sauer, K., Lo, C.C., and Leskovar, B. (1976) *Rev.Sci. Instrum.*, 47, 1122.
33. Sober, H.A. (ed.), Handbook of Biochemistry, Chemical Rubber Company, Cleveland, Ohio, 1970.
34. Gros C., and Labouesse, B. (1969) *Eur.J.Biochem.*, 7, 463.
35. Panyim, S., and Chalkley, R. (1976) *J.Biol.Chem.*, 246, 7557.
36. Stark, G., Stein, W., and Moore, S. (1960) *J.Biol.Chem.*, 235, 3177.
37. Hare, D.L., Stimpson, D.I., and Cam, J.R. (1978) *Archs.Biochem.Biophys.*, 187, 274.
38. Ackers, G. (1975) The Proteins, 3rd edition, 1, 2.
39. Siegel, L., and Monty, K. (1966) *Biochim.Biophys.Acta*, 112, 346.
40. Cohn, E., and Edsall, J., Proteins, Amino Acids, and Peptides, Reinhold, New York, New York, 1941.

41. Brand, L., and Witholt, B. (1967) *Meths.Enzymol.*, 11, 776.
42. Perrin, L. (1926) *J.Phys.*, 7, 390.
43. Laurence, D.J.R. (1957) *Meths.Enzymol.*, 4, 174.
44. Teale, F.W.J., and Badley, R.A. (1970) *Biochem.J.*, 116, 341.
45. Weber, G. (1953) *Adv.Prot.Chem.*, 8, 415.
46. Karlsson, E. (1974) *Experientia*, 29, 1319.
47. Jukes, T.H., Holmquist, R., and Moise, H. (1975) *Science*, 189, 50.
48. Kondo, K., Narita, K., and Lee, C.-Y. (1978) *J.Biochem.*, 83, 91.
49. Gurd, F.R.N. (1972) *Meths.Enzymol.*, 25, 424.
50. Mebs, D., Narita, K., Iwanaga, S., Samejima, Y., and Lee, C.-Y. (1972) *Hoppe-Seyler's Zeit.Physiol.Chem.*, 353, 243.
51. Lee, C.-Y., Chang, S., Kau, S., and Luh, S.-H. (1972) *J.Chromatog.*, 72, 71.
52. Dryden, W.F., Harvey, A.L., and Marshall, I.G. (1974) *Eur.J.Pharmacol.*, 26, 256.
53. Kelly, R.B., and Brown, F.H. (1974) *J.Neurobiol.*, 5, 135.
54. Abe, T., Alema, S., and Miledi, R. (1977) *Eur.J.Biochem.*, 80, 1.
55. Gilbert, L.M., and Gilbert, G.A. (1973) *Meths.Enzymol.*, 27, 273.
56. Reynolds, J.A., and Tanford, C. (1970) *J.Biol.Chem.*, 245, 5161.
57. Frank, R.N., and Rodbard, D. (1975) *Archs.Biochem.Biophys.*, 171, 1.
58. Spencer, S. (1977) Ph.D. Thesis, California Institute of Technology.
59. Dufton, M.J., and Hider, R.C. (1977) *J.Mol.Biol.*, 115, 177.
60. Maelicke, A., Fulpius, B.W., Klett, R.P., and Reich, E. (1977) *J.Biol.Chem.*, 252, 4811.
61. Weltman, J.K., and Edelman, G.M. (1967) *Biochemistry*, 6, 1437.
62. Reynolds, J.A., and Tanford, C. (1970) *Proc.Nat.Acad.Sci.*, 66, 1002.
63. Nozaki, Y., Reynolds, J.A., and Tanford, C. (1978) *Biochemistry*, 17, 1239.
64. Roberts, M.F., Deems, R.A., and Dennis, E.A. (1977) *Proc.Nat.Acad.Sci.*, 74, 1950.

CHAPTER IV.
SPECTROSCOPIC STUDIES
OF THE BUNGAROTOXINS.

IV. INTRODUCTION.

Several aspects of the bungarotoxins make them promising experimental objects for spectroscopic study. There is not only the intrinsic interest in the toxin structures, but also their potential utility as more general protein models for spectral interpretation. The first important feature is the limited content of spectrally-active aromatic residues, tryptophan, tyrosine, phenylalanine, and histidine. The α -toxins each have a single tryptophan and no more than four tyrosines, three phenylalanines, and two histidines. The β -toxins have a higher content of the latter three residues, but also have single tryptophans. Thus, the interpretation of the spectra of native and chemically-modified derivatives may be expected to be simpler than in larger proteins, and ideally, could allow the complete assignment of the individual contributions from particular amino acids. The second useful aspect is the stability of the toxins arising from their high content of disulfides. Both the stability and degree of internal cross-linking further predicts a restricted conformational flexibility, another advantage for spectral interpretation. In these respects, the toxins resemble polypeptide protease inhibitors and lysozyme which have been frequently used as model proteins for spectroscopy (1,2). A third advantage is the availability of the target protein for the α -toxins, the nicotinic acetylcholine receptor (nAChR), in a purified or enriched membrane-bound form (3). Thus, spectroscopic studies may be extended from α -toxins themselves to their interaction with their target.

The two spectroscopic techniques emphasized in this Chapter are fluorescence and circular dichroism (CD) spectroscopy. Fluorescence properties have already been used for polarization measurements described in

the previous Chapter. Steady-state and fluorescence lifetime analyses contribute particularly to knowledge of the tryptophan environments. In the α -toxins, the single tryptophans are invariant residues located in the proposed receptor-recognition site (4) and may be expected to act as sensitive reporters of conformational perturbations in this region, or as general monitors of the overall toxin integrity. In the β -toxins, the single tryptophans may be used as internal conformational reporters, as well as monitors of the interaction with target sites. Moreover, chemical modification has suggested that the single tryptophan of β -bgt may have an important role in both its lethal and enzymatic activities (5).

Circular dichroism spectroscopy can provide two different types of information depending on whether measurements are taken in the far-ultraviolet (<250 nm) or the near-ultraviolet (250-350 nm). The far-UV CD is dominated by the contributions of peptide bonds in repeating, optically-active secondary structures (6), and provides an index of the proportions of ordered secondary structures (7). It can thus be considered a monitor of the global structure of a protein. The near-UV CD, on the other hand, consists of contributions from tyrosine, tryptophan, and disulfides (8), and, although harder to interpret (8), constitutes an independent technique for assessing the environments of these residues. Thus, fluorescence and CD spectra can prove complementary in describing environmental changes around the tyrosine and tryptophan chromophores. The high disulfide content of the toxins makes their near-UV spectra interesting, because little is known about how protein folding can affect the intrinsic chiroptical properties of cystine (8,9). Similarly, little systematic information is available on the influence of local residues on the CD signals generated by aromatic groups. The possibility of correlating CD signals with identified amino acid residues would be a significant advance

in both toxin and protein spectroscopy research.

There has been little previous application of spectroscopy to the study of snake venom neurotoxins. To date, there have been isolated studies using fluorescence (10), infrared (11), Raman (12), circular dichroism (13), and nuclear magnetic resonance (14) spectroscopies. More extensive use of these approaches has been made with the cardio-toxins, because their targeting to biological membranes in general permits the design of simplified model systems for concerted spectral study (15). Thus, at the very least, the studies reported here provide useful background data on the spectral behavior of two different functional classes of snake toxins.

There is another context in which the detailed examination of the far-UV CD may prove useful. Far-UV CD is represented as a linear combination of three basic structures: α -helix, β -pleated sheets, and residual structure termed "random" (7,16). In recent years, there has been an intensive effort directed to predicting regions of secondary structures from the amino acid sequence of a protein (17). Because of the ease of their application, the predictive rules of Chou and Fasman (18) have been most frequently used. In view of the availability of both primary structures for α -bgt and β -bgt and the X-ray structure for the α -toxin erabutoxin (19,20), it is possible to correlate the predictions with the observations by CD, and, in turn, to compare both of these to the crystal structure. Previous studies of α -bgt have suggested that it is largely composed of β -structure, and contains no α -helix (21), and of β -bgt have suggested that it has contributions from both α -helix and β -structure (21,22). The CD observations on the β -toxins can also be compared to those on non-toxic PhA enzymes, to detect any systematic differences.

METHODS.

i. Ultraviolet Absorption Spectroscopy. Absorption spectra in the ultraviolet (UV) were all taken on a Cary 118C recording spectrophotometer using matched 1 cm cuvettes and the automatic slit setting. For solvent perturbation studies, experimental samples were dissolved as a lyophilized powder in 20% ethylene glycol (v/v, redistilled Eastman reagent grade) in 0.05 M sodium phosphate (pH 7.0) and references were toxins in buffer alone. Baseline corrections were made by the use of tandem cells (23).

ii. Fluorescence Spectroscopy. All spectra were recorded on a Hitachi-Perkin Elmer MPF 2A recording fluorimeter using the blue-sensitive Hamamatsu R106 photomultiplier and 6 nm emission and excitation slitwidths. Excitation and emission wavelengths are given in Figure legends. The quantum yields were calculated from $q = S_p \cdot q_{trp} \cdot (S_{trp})^{-1}$ where S_p and S_{trp} are the areas under the corrected emission spectra (taken on a Hitachi-Perkin Elmer MPF-3L fluorimeter calibrated against a standard of anthracene in ethanol) of the toxins and of tryptophan solutions having the same absorbances at the excitation wavelength; and q_{trp} = fluorescence quantum yield of a neutral aqueous solution of tryptophan = 0.20. Fluorescence quenching measurements were made using I^- as an anionic quencher and Cs^+ as a cationic quencher. The quenching in all cases obeyed the Stern-Volmer law; giving straight lines in Stern-Volmer plots (24) of $Q = I_0(I-1)^{-1}$ vs. quencher concentration. The linearity is further evidence for homogeneity inasmuch as it indicates a single population of identically-behaving tryptophans. The line slope gives the Stern-Volmer constant K_{SV} which is used to calculate the relative accessibility by the following equation; $L = [K_{SV}(\text{protein}) \cdot q_{trp}] \cdot [K_{SV}(\text{trp}) \cdot q_{\text{protein}}]^{-1}$ (10). Quenching determinations followed the standard literature procedure (24).

iii. Circular Dichroism and Magnetic Circular Dichroism. Circular dichroism (CD) and magnetic circular dichroism (MCD) measurements were made on an instrument designed in this laboratory (25). Spectra were recorded from 190 to 250 nm (far-UV) and 250 to 350 nm (near-UV) at 0.1 nm intervals using a scan speed of 0.25 nm/sec and an instrumental time constant of 0.3 sec. For the far-UV CD, samples were approximately 0.01% protein (w/v), or 10-13 μM for the α -toxins and 2-5 μM for the β -toxins, in 0.02 M sodium phosphate (pH 7.0) in 0.1 cm pathlength cells, and for the near-UV CD, samples were 0.1% protein (w/v) in 1.0 cm pathlength cells. Instrumental slitwidths were 1.0 mm for the far-UV and 0.5 mm for the near-UV. For MCD spectra, samples were prepared as described by Barth et al (26) in buffered 6 M guanidine hydrochloride (Heico, ultra-pure spectral grade) and were 0.1% protein (w/v) in 1.0 cm pathlength cells using a 2.0 mm instrumental slitwidth. For CD and MCD of both the samples and references, ten passes through the experimental wavelength region were signal-averaged by on-line computer and stored as sample-reference computer library files for subsequent manipulation and plotting. The CD intensity was calibrated using a 1 mg/mL D-10-camphorsulfonic acid standard (prepared gravimetrically from material twice recrystallized from benzene and stored in vacuo) and is expressed as $\Delta\epsilon(\text{M}\cdot\text{cm})^{-1} = (\epsilon_L - \epsilon_R)(\text{M}\cdot\text{cm})^{-1}$. The MCD intensity is expressed as $\Delta\epsilon/H(\text{M}\cdot\text{cm}\cdot\text{T})^{-1}$ where $T = \text{one Tesla} = 10^4$ gauss, and the magnetic field strength of the electromagnet was calibrated (~ 1.4 T) with a potassium ferricyanide standard (25). CD and MCD results can be converted to mean residue ellipticity (8) by $[\theta]_{\text{MRW}}(\text{deg}\cdot\text{cm}^2)(\text{decimol})^{-1} = 3305 \times \Delta\epsilon \times (n)^{-1}$ where $n = \text{number of amino acid residues in the protein}$.

Protein concentrations were determined using absorbance at 280 nm and reported extinction coefficients for the toxins (27, see Table IV-5), or,

in the case of modified proteins, by weighing the lyophilized toxin (stored over P_2O_5 in vacuo). Molecular weights were assumed to be those derived from amino acid compositions (see Chapter III).

iv. Chemical Modifications. N-bromosuccinimide (NBS) oxidations followed the protocol of Spande and Witkop (28). Stepwise additions of NBS were monitored by changes in the absorbance (A_{280}) until the change of absorbance with incremental addition reached a plateau. The NBS additions were not continued beyond the plateau region because of potential damage to residues other than tryptophan and peptide bond cleavage (28). The reaction was performed on 1 mg of purified toxin in 3.0 mL of 0.1 M sodium acetate buffer (pH 3.0) and was quantitated spectrophotometrically (28). An independent quantitation and check on the specificity of the reaction was made by hydrolyzing 0.5 mg desalted and lyophilized NBS-oxidized toxins in 4 N methanesulfonic acid. Tryptophan values agreed within 5% by the two procedures, and there was no apparent degradation of other amino acids.

Iodinated α -bgt derivatives were prepared using ICl in a non-enzymatic procedure. To a solution at a final concentration of 1.4 M HCl, containing 1 mole-equivalent of potassium iodate, 2 mole-equivalents of potassium iodide were added, yielding iodine, >95% of which is rapidly converted to ICl. One volume of ICl mixture was then added to the appropriate quantity of α -bgt in five volumes of 3.2 M ammonium chloride (pH 8.9), and incubated at 20°C for 30 to 60 min. The molar ratio of toxin to ICl and the final pH of the reaction mixture may be varied so as to favor yields of diiodo- or monoiodo- α -bgt. Formation of the diiodinated derivative is favored when the toxin is exposed to greater than twofold molar excess of ICl and/or the pH is lower than 8.0. Monoiodo-toxin is the primary product when there is an excess of toxin over ICl and at pH greater than 8.0. Iodinated α -bgt

was desalted by chromatography on a 1.5 X 35 cm Sephadex G10 (medium) column equilibrated in 0.05 M sodium phosphate buffer (pH 6.5). The void volume peak was pooled and applied to a 2 X 30 cm CM-cellulose (Whatman CM-52) column equilibrated in 0.05 M sodium phosphate buffer (pH 6.5) and iodinated derivatives were eluted with a 0-0.08 M sodium chloride gradient in the same buffer. Derivatives eluted in the order diiodinated, unlabelled (or tritiated), and monoiodinated (29) and were pooled, desalted, and stored frozen in the same buffer. Proteolytic digests of radioactively-labelled derivatives established that only one tyrosine was labelled in the mono- and diiodinated toxins (29).

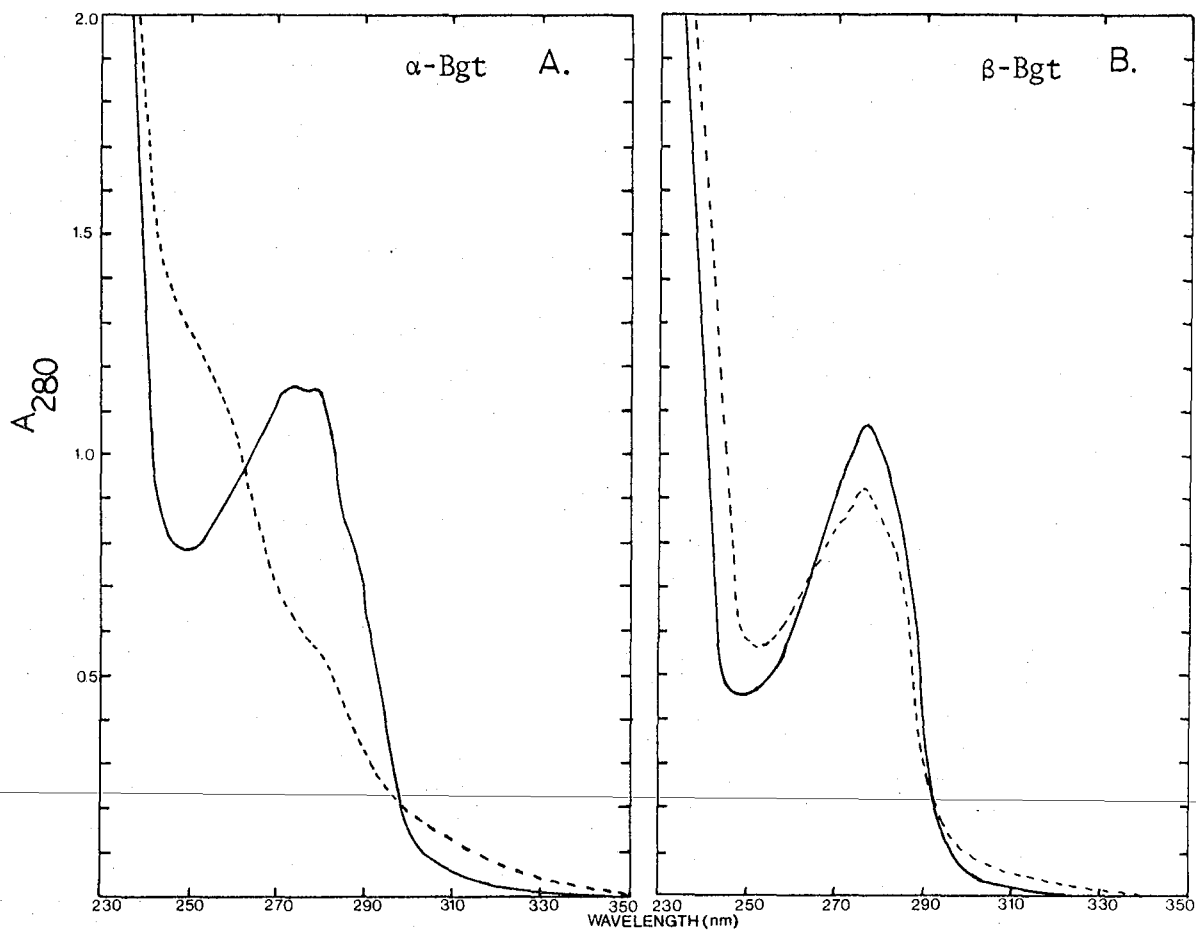
Selective chemical reduction of disulfides was performed in two ways. The first method, by analogy to the catalytic tritiation of radioactively-iodinated α -bgt (30), used catalytic hydrogenation of iodinated α -bgt. Iodinated α -bgt in 0.5 mL sodium phosphate buffer (pH 7.4) was frozen and 10 mg of palladium (10%) on powdered charcoal (Matheson, Coleman, and Bell) added. The thawed toxin solution was hydrogenated for 60 min at 400 mm Hg and then flushed with nitrogen. The catalyst was separated from the solution by a desk centrifuge and washed once with 1 mL distilled water. The combined supernatants were lyophilized, redissolved in 0.05 M sodium phosphate buffer (pH 6.5) and chromatographed on a 2 X 20 cm CM-cellulose column with a linear salt gradient (0-0.1 M). The individual peaks of A_{280} were desalted, lyophilized, and then hydrolyzed for amino acid composition analyses. Fractions showing a specific loss of sulfur-containing amino acids were then taken for further spectral analysis. The second method used reduction by dithiothreitol (DTT). α -Bgt was dissolved to a final concentration of 1 mg/mL in 3 mL of 0.1 M sodium borate buffer (pH 9.0). Twelve μ M DTT was added as a solid and the reaction allowed to proceed for 15 min at 20°C. Twenty-five μ M recrystallized iodoacetic acid (Pierce Chemical)

were added in 0.1 M sodium borate at pH 9.0 to a final concentration of 25 μ M and the incubation continued for 30 min in the dark at 20°C. The alkylated products were desalted by gel filtration on Sephadex G10 and lyophilized. The modification of disulfides was quantitated by the yield of carboxymethylated cysteine detected after acid hydrolysis (31).

RESULTS.

i. Ultraviolet Absorption and Fluorescence Spectroscopy. The UV absorption spectra are characteristic of tryptophan-containing proteins for all the bungarotoxins. Figure 4-1 shows representative spectra of α -bgt and β -bgt. The extent to which the single tryptophans contribute to the observed spectra can be seen to be very different, because NBS oxidation of α -bgt (Figure 4-1A) largely eradicates the peak between 270 and 290 nm, leaving only a shoulder; whereas the oxidation of β -bgt's tryptophan has little effect (Figure 4-1B). Solvent perturbation studies (Table IV-1) indicate that 1 tyr is fully exposed to the solvent in α -bgt, and that the other tyr and the single trp residue are partially or fully buried, and the same general result is found for toxins 7 and 8. For β -bgt, 2 to 3 tyr out of a total of 14 are fully exposed to the solvent. The other tyr residues and the single tryptophan are unavailable to the ethylene glycol perturbant. This is consistent with the NBS requirement for full oxidation of the trp in β -bgt, 8 moles NBS/ mole tryptophan (see Figure 4-5), which should be contrasted to the 2 to 4 moles normally required for fully exposed trp residues (28). An independent estimate for the degree of tyr exposure can be made by investigation of the first derivative of the absorbance spectrum (32). Using this approach, 1 tyr is exposed and 1 buried in α -bgt and roughly half of the tyr in β -bgt are exposed. A similar disagreement between the two methods was also seen for tyr exposure estimates

Figure 4-1
Ultraviolet absorption spectra of native and N-bromosuccinimide (dashed lines) modified α - and β -bgt. Concentration was 1 mg/mL in all cases (pH 7.0).



XBL 789-4227

TABLE IV-1

SOLVENT PERTURBATION STUDIES OF THE EXPOSURE OF TRP AND TYR

<u>Toxin</u>	<u>Tryptophan Exposure</u> *		<u>Tyrosine Exposure</u> *	
	<u>Percent</u>	<u>No. Residues</u>	<u>Percent</u>	<u>No. Residues</u>
α -Bgt	20	None	66	1.3
7	16	None	60	1.2
8	34	None	43	1.7
9A	45	None	32	3.2
β -Bgt	0	None	21	2.9
11	0	None	26	3.8
12	0	None	27	4.3
13	65	1	24	3.5
14	94	1	48	4.3

*

Both sample solution and references were prepared by dilution from a freshly-prepared stock in dilute neutral (pH 7.0) phosphate buffer. Samples included the perturbant 20% ethylene glycol, and the reference was protein in buffer alone. Baseline corrections were made by the use of tandem cells (23). The standard for 100% exposure was a mixture of N-acetyl-L-tryptophanamide and N-acetyl-L-tyrosinamide, at the same concentrations as the residues trp and tyr in the proteins, prepared in the same sample and reference solutions. The percentage exposure was determined by the relative intensities of the samples against the standards (23). Values <50% are taken as "none" and >50% are taken as "1" for the single trp residues. Fractional values reflect partial accessibility to the perturbant.

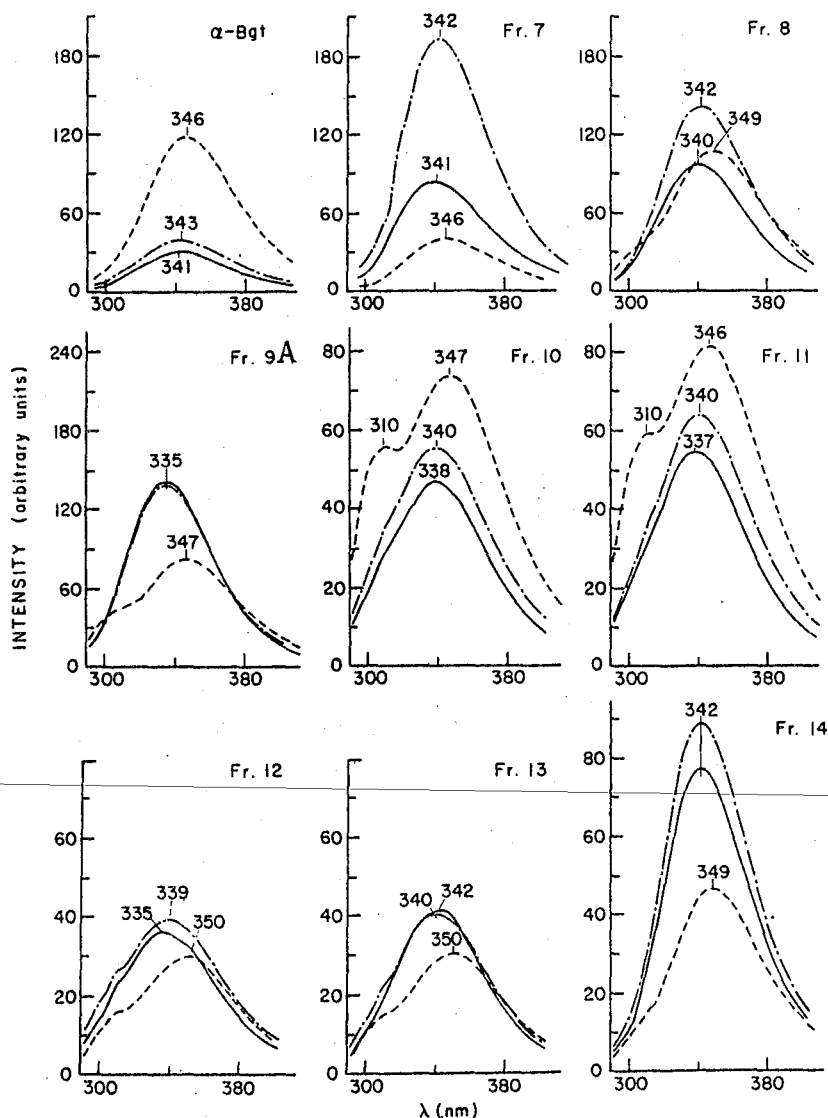
in ribonuclease (32) and was attributed to the formation of hydrogen-bonds between phenolic chromophores so as to mimic a "water" environment with tyr residues in the interior of a protein. The fluorescent spectrum of the NBS-modified derivatives of both toxins gave a similar emission intensity, suggesting that only a small proportion of the larger number of tyr in β -bgt are unquenched. Toxin 14 has the highest proportion of exposed residues, and differs from the pattern of the other β -toxins.

The fluorescent emission spectra are typical for tryptophan-containing proteins (Figure 4-2). α -Toxins had emission maxima at longer wavelengths than β -toxins (340-341 nm vs. 335-338 nm) in keeping with the results for tryptophan accessibility by absorbance or chemical modification techniques. Toxins 13 and 14 were unusual among the β -toxins in that their emission maxima were at 340 and 342 nm respectively. Emission intensity varied among the toxins and was greatest for 9A and lowest for 12 and 13 on a molar basis. Tyrosine fluorescence ($\lambda_{\text{max}} = 303$ nm) was not observed in any of the native toxins, as is normal in trp-containing proteins (34). However, tyr presence could be detected by studying the emission ratios at 303 (tyr only) and 380 nm (trp only) with excitation at 265 and 290 nm. In Table IV-2, the results are shown. Tyr contribution could be detected in all but toxins 7 and 8 and was the largest in α -bgt. The failure to detect a tyr contribution in 7 and 8 may be attributed to the much larger proportion of trp fluorescence overshadowing the small tyr component. Alternatively, it is possible that some small sequence changes have introduced quenching environments near the tyr residues.

Partial denaturation by 8 M urea increased the fluorescent intensity and caused a slight shift of the positions of the emission maxima towards longer wavelengths, consistent with increased exposure. The urea effects

Figure 4-2

Fluorescence spectra of the bungarotoxins. All spectra are uncorrected for photomultiplier response vs. wavelength. Excitation was at 280 nm using 6 nm slitwidths. Absorbance at 280 nm was approximately 0.16 for all samples. Note the change in the intensity scale for α -bgt and toxins 7 thru 9A.



The solid lines are the native spectra (distilled water), the dashed lines are the urea-treated toxins (+8 M urea), and the dot-dashed lines are the reduced toxins (+8 M urea + 30 mM DTT). These spectra are the average of at least three determinations on three different purified preparations.

TABLE IV-2
SUMMARY OF FLUORESCENCE PROPERTIES OF THE BUNGAROTOXINS^a

Toxin	Emission Maximum (nm)	Bandwidth (nm)	Relative Tyr Contribution ^b	
			Native	Reduced ^c
α -Bgt	340-342	60	1.6	3.1
7	340-342	60	0.9	3.3
8	340-342	60	1.1	4.5
9A	338-340	65	0.9	7.6
β -Bgt	335-338	70	0.9	8.4
11	335-338	70	0.8	8.2
12	335-338	70	1.1	8.9
13	340-341	60	1.5	8.3
14	342-344	70	1.1	7.4

a

Uncorrected for photomultiplier response vs. wavelength. Summary of three to five separate measurements.

b

Emission spectra were obtained using excitation at 265 nm or 290 nm. In both cases, the ratio of the intensity at 303 nm (I_{303}) and that at the maximum (I_{max}) were calculated.

$$[(\text{ratio of excitation at 265 nm}) - (\text{ratio at 290})]$$

Relative tyr contribution =

$$\frac{\text{---}}{(\text{ratio at 290 nm})}$$

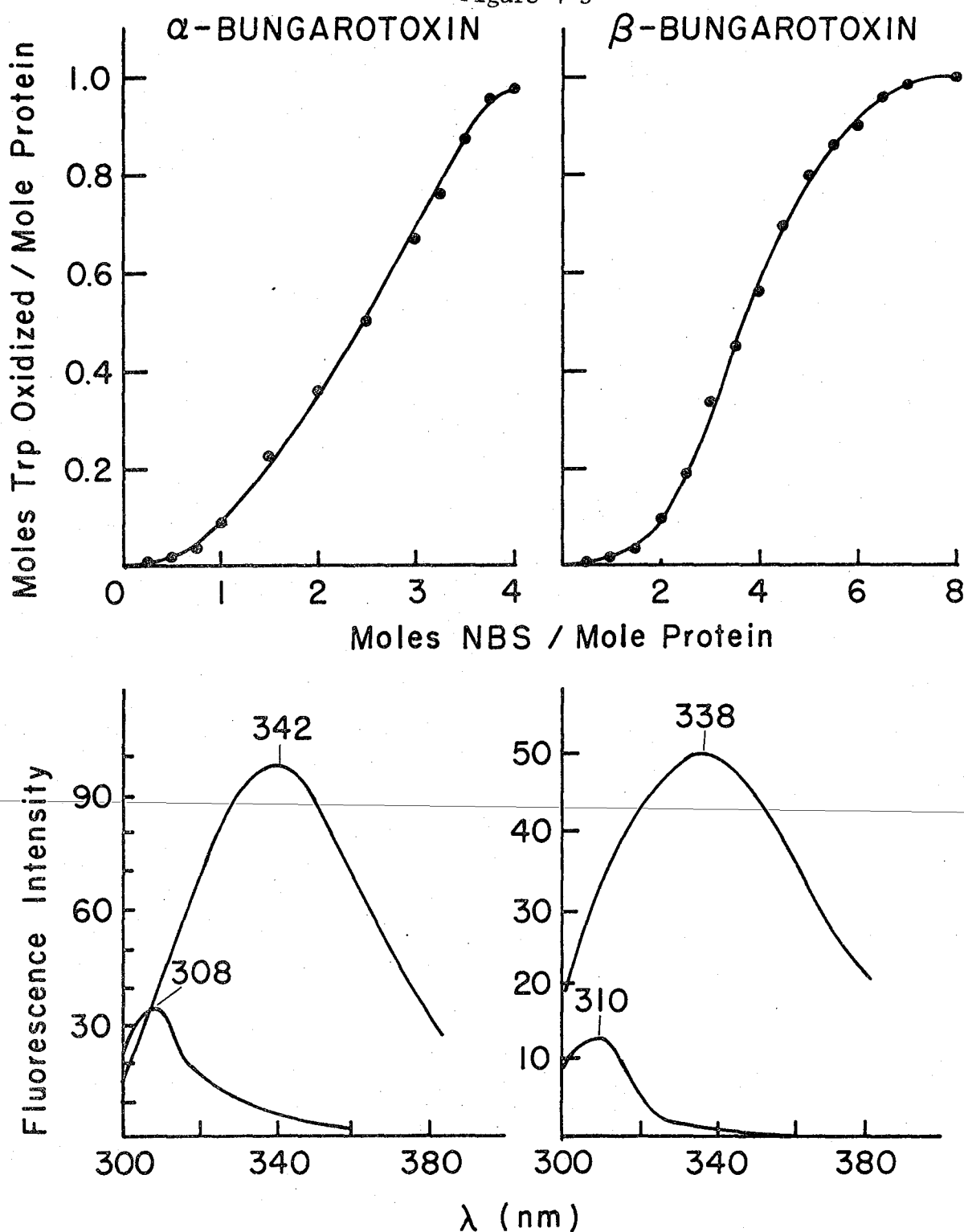
c

As in legend to Figure 4-2.

were completely reversible. Addition of the reducing agent DTT caused a further increase in the exposure of the chromophores, as judged by the further shift of the λ_{\max} to 346-350 nm, increased bandwidth, and the appearance of tyr shoulders in the 300-310 nm region. The shoulders were not artifacts of Raman scattering since their emission maxima were not altered by changing the excitation from 280 to 260 nm. Oxidation of the single trp in both α -bgt and β -bgt abolished the characteristic spectra and led to spectra indicative of residual tyr fluorescence (Figure 4-3).

Quantitative studies of several fluorescence parameters characterizing α -bgt and β -bgt (Table IV-3) strongly reinforced other evidence for differences in the trp environments. α -Bgt exhibited two emission lifetimes, 0.9 and 4.2 nsec, using an interference filter exciting at 289 nm. The fastest relaxation was attributed to tyr because it could be selectively eliminated by N-acetyl imidazole modification of the exposed tyr. Thus, the single relaxation observed for β -bgt might have a faster component attributable to tyr which is not resolved by the curve-fitting program (35). If the single exponential is exclusively due to trp, the shorter lifetime in an apparently more hydrophobic domain than that of the α -bgt trp is not consistent with the trend towards longer lifetimes shown by indole model compounds in apolar solvents (36). This might point to collisional quenching mechanisms shortening the lifetime; this is consistent with the low quantum yield. The quantum yields for both toxins are quite low, but within the range observed for proteins (37). The examination of the sequences show that trp residues are within 4 residues of disulfides in both cases, and cystine is known to be a very effective quencher of trp fluorescence (38). The accessibility to external quenchers indicates that the environment around the α -bgt trp is relatively cation-rich because I^- is much more effective than Cs^+ . An abundance of basic residues can

Figure 4-3



Fluorescence spectra of NBS-oxidized α -bgt and β -bgt. Spectra were recorded using 0.1 mg of desalted and lyophilized native or modified toxins in 1 mL cuvettes. Note that the NBS-oxidized toxins have reduced intensity and emission maxima shifted to wavelengths characteristic of tyr emission. NBL 763 5762

TABLE IV-3
 QUANTITATIVE ASPECTS OF INTRINSIC FLUORESCENCE OF α - AND β -BUNGAROTOXINS

	<u>Lifetime (nsec)</u> ^a	<u>Q_{trp}</u> ^b	K_{sv} ^c		L^d	
			<u>I⁻</u>	<u>Cs⁺</u>	<u>I⁻</u>	<u>Cs⁺</u>
α -Bgt	0.9, 4.2 ^e	0.11	2.4	0.08	0.70	0.20
β -Bgt	2.5	0.07	0.74	0.45	0.34	1.79

a

Fluorescence lifetimes were determined using single-photon counting and data analysis on a system designed in this laboratory (35). Excitation was at 289 nm using a Baird narrow band interference filter and emission was filtered through a Kodak 18A filter passing 300-400 nm.

b

Quantum yield relative to trp determined as in Methods.

c

K_{sv} = Stern-Volmer constant (24) for quenching.

d

Relative accessibility to quenchers calculated as in Methods by equation developed in ref.10.

e

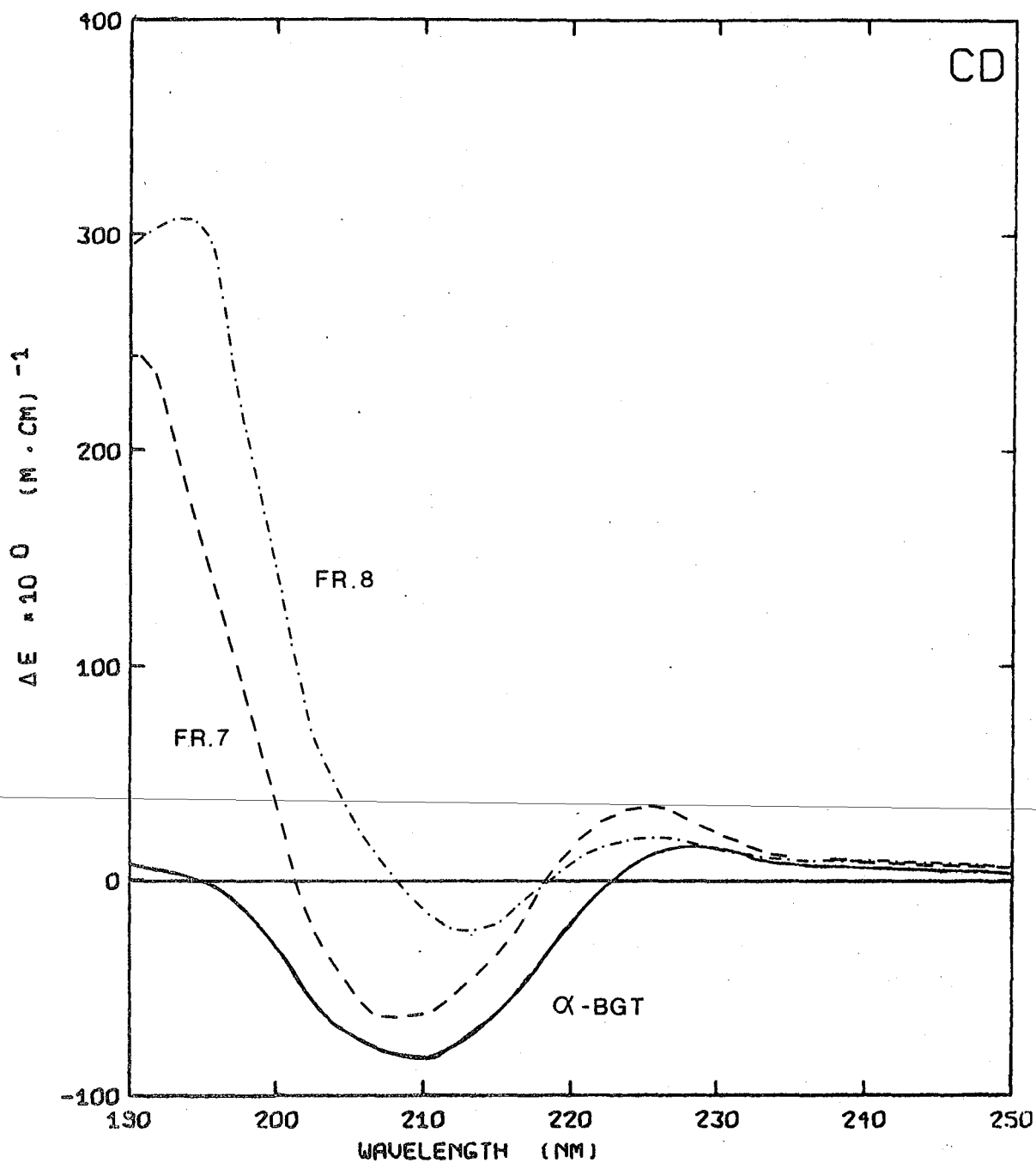
Two lifetimes were observed after exponential resolution of fluorescence decay. The fastest lifetime corresponds to tyr since it can be eliminated by acetylation of the residue with N-acetyl imidazole.

be seen near the trp in the predicted X-ray structure (4). The reverse is true of β -bgt because it is more responsive to Cs^+ than I^- . The sequence of β -bgt's heavy chain shows a large proportion of acidic residues in close proximity to the single trp.

ii. Circular Dichroism and Magnetic Circular Dichroism Spectroscopy. In keeping with other experimental evidence, the toxins' CD spectra segregated into the recurring three classes: α -bgt, 7 and 8, 9A and 14, β -bgt and 11 thru 13. The far-UV CD spectra of the α -toxins are shown in Figure 4-4. All three display a weak minimum at 210 to 215 nm and a weaker maximum at 220 to 230 nm. α -Bgt approaches zero below 200 nm, but 7 and 8 each have very strong positive bands in this region. These spectra are all indicative of high proportions of β -type structures (pleated sheets and four-residue bends (39)). This is emphasized by computing the proportions of ordered secondary structures by two techniques (7,40), shown in Table IV-4. By both procedures, almost half of each toxin is organized into β -type structures, with no evidence for the presence of any α -helix. The very strong signal at 194 nm, and the shift (210 to 213 nm) and intensity attenuation of the negative extremum in toxin 8 are consistent with the replacement of β -sheet structures by an increased proportion of β -bends, as compared to the other two α -toxins.

The far-UV CD of the β -toxins are distinguishable into the two groups, 9A and 14, and β -bgt and 11 thru 13. The greater signal intensities in the latter group presumably reflect contributions from the light chain to the overall structures (Figure 4-5). Nonetheless, the spectra are similar in qualitative shape, suggesting they share a considerable proportion of α -helix or helical-like structure. Signal intensities in the 200 to 220 nm wavelength region increase in the order, 13>12=11> β -bgt, which corresponds to the rank order of their relative molecular weights. Thus, the larger the

Figure 4-4
Far-UV circular dichroism spectra of α -toxins.
Experimental conditions are given in Methods.



XBL 775-4399

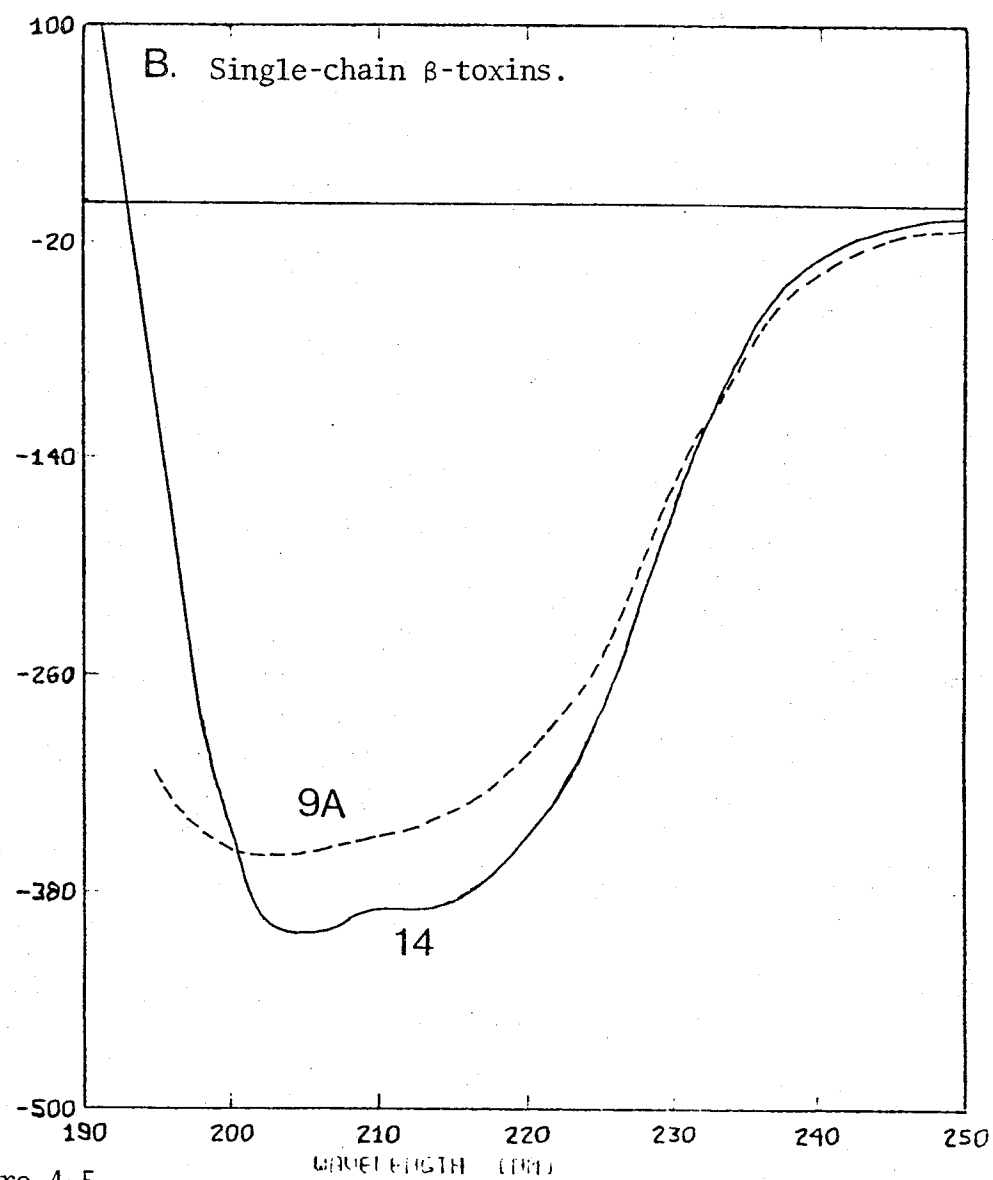
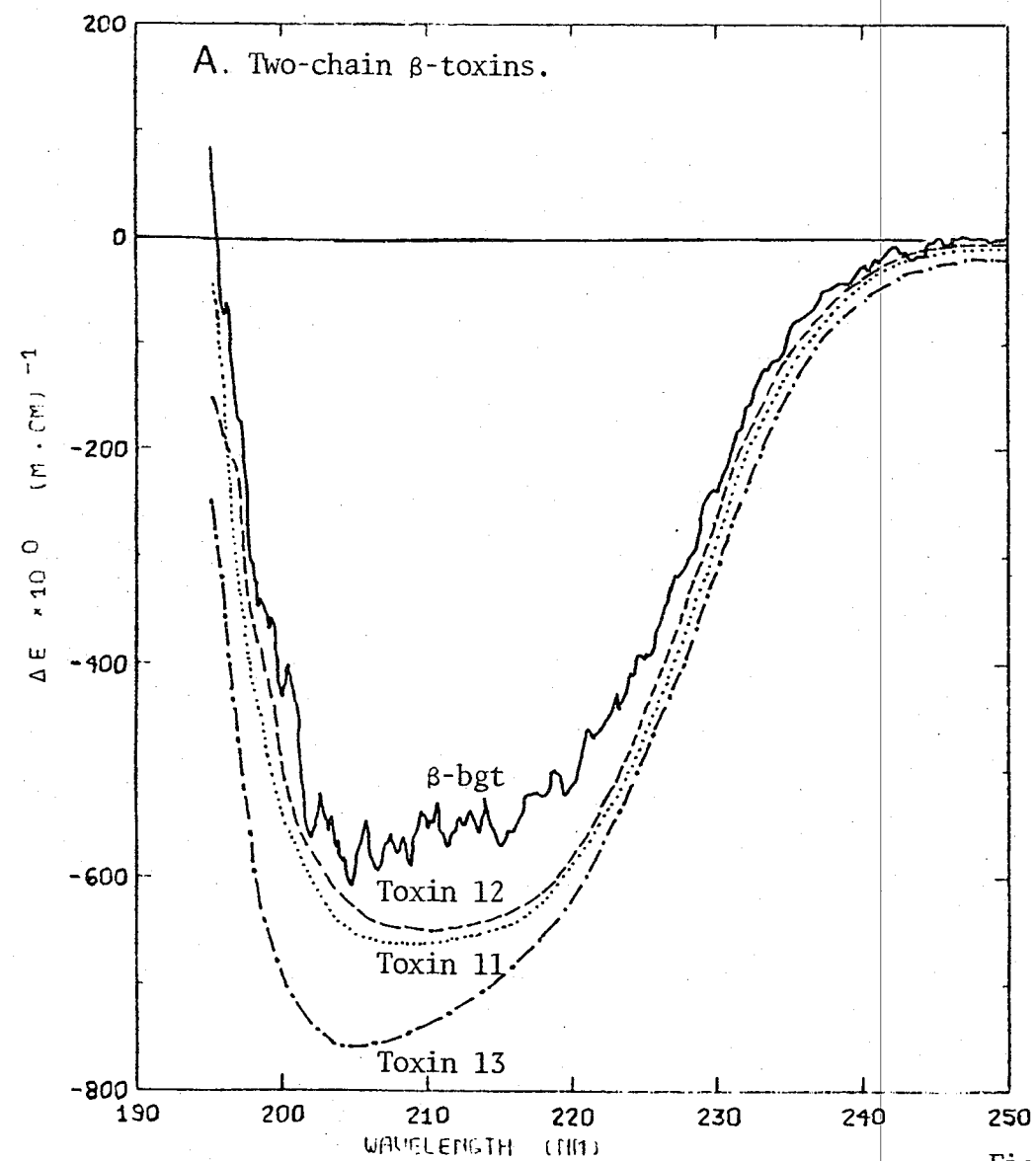


Figure 4-5
Far-UV circular dichroism spectra of β -toxins.

toxin, the greater the proportion of ordered structure. The additional residues in the larger toxins are apparently added to existing secondary structure domains, although subtle differences in the spectral shapes indicate that there may be qualitative as well as quantitative differences in the secondary structures of this group. From Table IV-4, it is apparent that the proportion of α -helix decreases and the proportion of β -structure increases from β -bgt to toxin 13, and that all of these four toxins have over half of their secondary structure in ordered forms. 9A and 14 have half the helical content of the two-chain β -toxins and a larger proportion of β -structure.

Although it gives no conformational information, MCD is a useful technique for obtaining an independent measure of the tryptophan and tyrosine content of proteins (26). In agreement with chemical results reported in Chapter III, single trp residues were found in every toxin. A representative spectrum at each of the two reference pHs is shown in Figure 4-6. In addition, the experimental spectra are compared to a model mixture of N-acetyl-L-tyrosinamide and N-acetyl-L-tryptophanamide at the same concentrations as the residues in the β -bgt sample. The close agreement confirms the accuracy of the residue quantitation. By using the MCD determination of tryptophan concentration, extinction coefficients were calculated for the toxins, assuming that the measure of the single trp concentration was directly applicable as the toxin concentration. In Table IV-5, these extinction coefficients are reported on both a molar and weight basis. Quantitative amino acid analyses confirmed that these ϵ_{280} values could be no more than 5% in error (using the molecular weights derived from amino acid compositions).

The near-UV CD spectra for the α - and β -toxins are different and toxin 7 and β -bgt are presented as representative examples in Figure 4-7. The

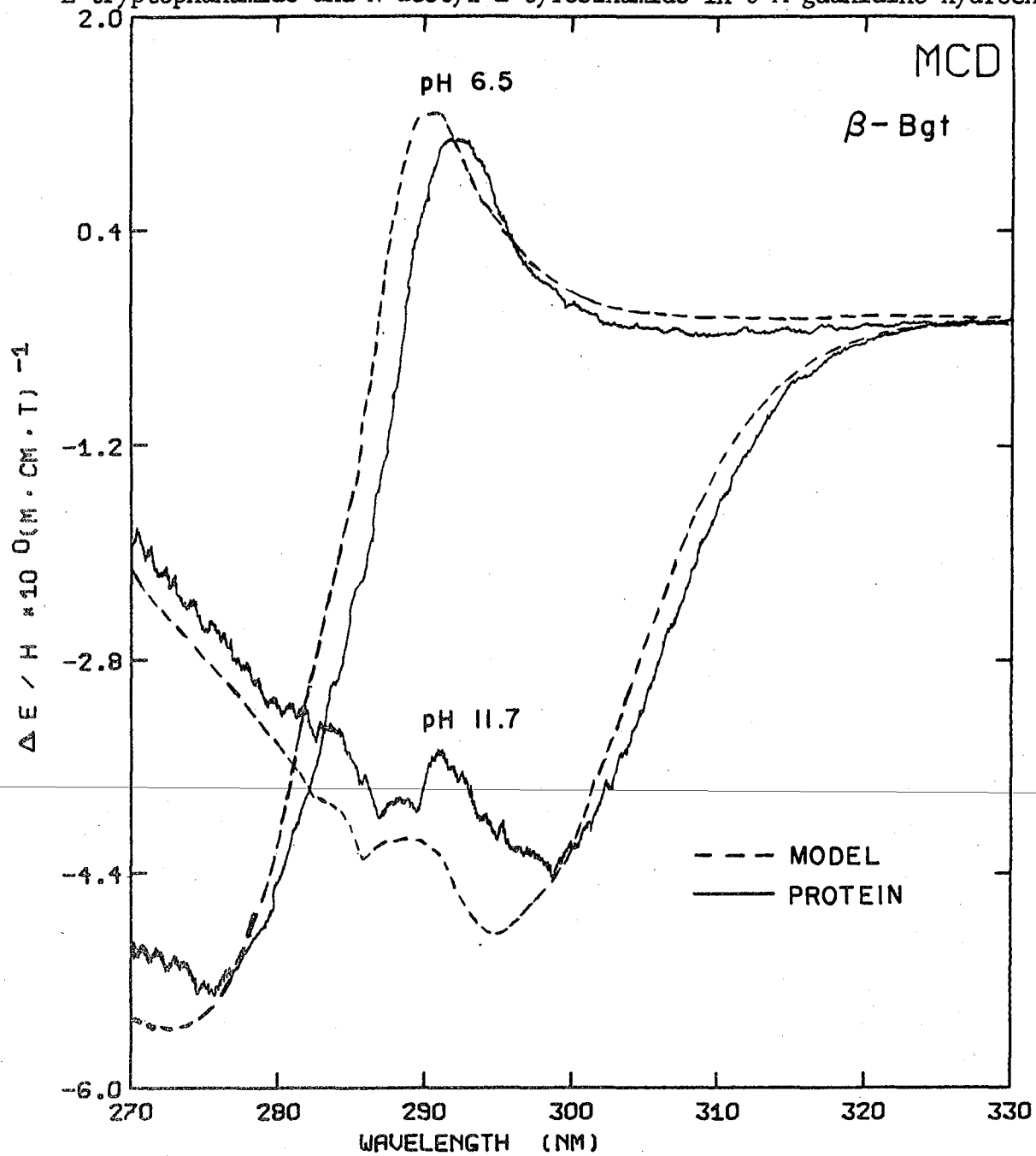
TABLE IV-4
SECONDARY STRUCTURE ESTIMATES FROM FAR-UV CIRCULAR DICHROISM DATA

Toxin	Method of Analysis						
	Greenfield & Fasman (7)			Chen et al (40)			
	<u>α-helix</u>	<u>β-structure</u>	<u>random</u>	<u>α-helix</u>	<u>β-structure</u>	<u>random</u>	<u>β-bend</u>
α -Bgt	None	60	40	None	55	40	5
7	None	60	40	None	55	40	5
8	None	60	40	None	50 30*	40 50*	10 20*
9A	22	38	40	20	26	54	None
β -Bgt	43	17	40	40	18	42	None
11	51	16	33	65	10	25	None
12	50	16	34	63	10	27	None
13	60	10	30	80	None	20	None
14	26	34	40	29	21	50	None

*

This estimate was based upon a blue-shifted β -bend (12 nm) standard curve. The exact fit that results may suggest that the reported β -bend spectrum (39) is an unsatisfactory model for these toxins.

Figure 4-6
Magnetic circular dichroism spectra of β -bgt and model mixture of N-acetyl-L-tryptophanamide and N-acetyl-L-tyrosinamide in 6 M guanidine hydrochloride.



XBL 763-5767

TABLE IV-5
TYR-TRP RATIOS AND EXTINCTION COEFFICIENTS OF BUNGAROTOXINS

<u>Toxin</u>	<u>Tyr/ Trp^a</u>	<u>Integral Value</u>	<u>ϵ_{\max}^b (mM cm)⁻¹</u>	<u>$A_{280}^{0.1\%c}$ (cm)⁻¹</u>
α -Bgt	2.2	2	10.5	1.32
7	2.2	2	10.9	1.31
8	4.0	4	13.5	1.59
9A	10.2	10	21.3	1.41
β -Bgt	13.7	14	29.6	1.45
11	14.5	14-15	29.8	1.39
12	16.1	16	35.4	1.54
13	14.5	14-15	34.2	1.44
14	8.9	9	20.1	1.46

a

Method of calculation based upon Barth et al (26).

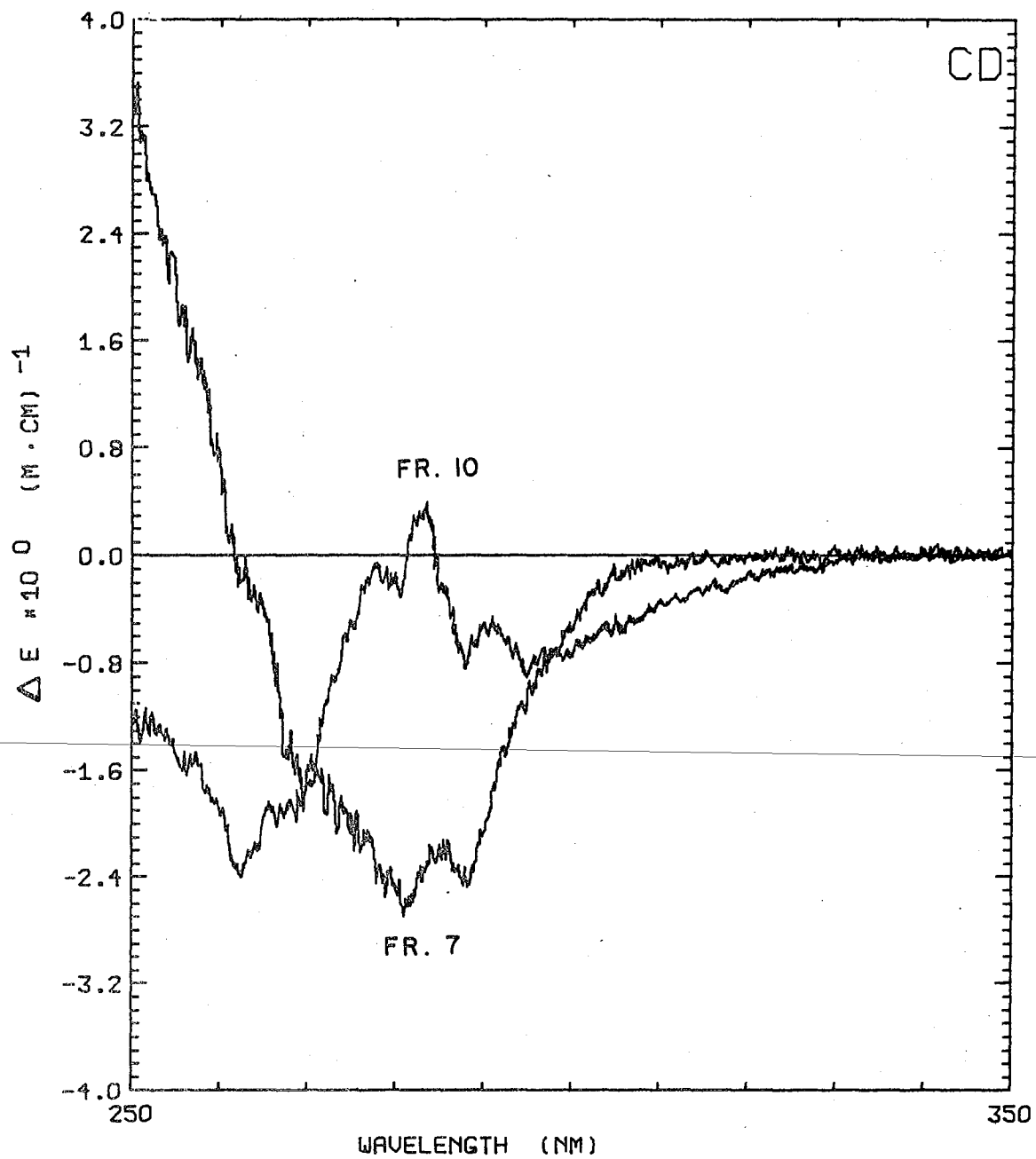
b

Maximum was 278-279 nm for α -toxins and 277-278 nm for β -toxins.

c

These values were calculated from the values for ϵ_{280} and molecular weight estimates from Table III-8.

Figure 4-7
Near-UV circular dichroism spectra of representative
 α -(Fr.7) and β -(Fr.10= β -bgt) toxins.



XBL 763-5766

α -toxins' CD did not differ appreciably except that the intensity of the broad negative extremum at 280 to 290 nm increased in the order $8 > 7 > \alpha$ -bgt. The near-UV CD of toxins 9A thru 14 were similar, except that toxin 14 exhibited none of the vibronic fine structure in the region 270 to 300 nm and had only a broad negative band with a peak between 260 and 270 nm. This broad negative band was found in all the β -toxins, and was assigned to disulfides because of its intensity, wavelength maximum, band shape, and resistance to guanidine hydrochloride denaturation (9,41). Plotting the $\Delta\epsilon_{262}$ intensity as a function of the molar percentage of disulfide content generated a straight line (Figure 4-8), suggesting that its intensity is a direct measure of the proportion of disulfides. Extrapolation of the line to the ordinate indicated that the cystine band was superimposed on a positive band of constant intensity in all the β -toxins. The positive band's existence was experimentally confirmed by subtracting the spectra in 6 M guanidine hydrochloride from the native spectra for each toxin to eliminate the cystine contribution. The resulting difference spectrum had a positive extremum between 260 and 270 nm.

One approach to assigning the near-UV CD signals depends on the identification of the true contributing bands by gaussian curve resolution (8). The approach used here is the elimination of particular signals by selective chemical modification of chromophores or by environmental perturbation. Of course, the far-UV CD must be routinely monitored to insure that modification of a particular residue does not disrupt the global structure. The first modification was the oxidation of the single trp in the α -toxins. In Figure 4-9, the effect of this and several other modifications are shown. Trp eradication leads to the abolition of the negative trough between 280 and 290 nm, and the appearance of masked weaker signals. Accordingly, the

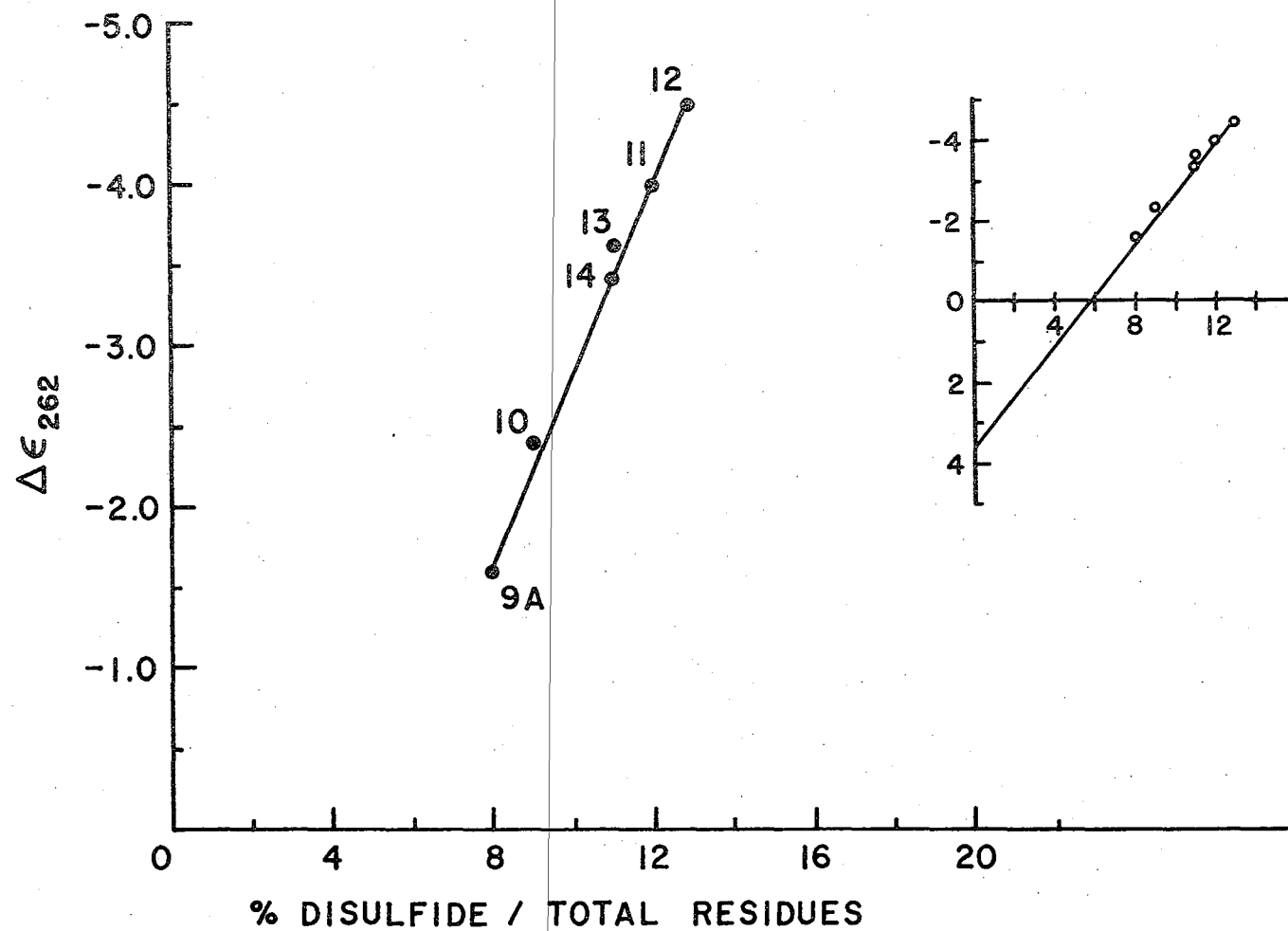
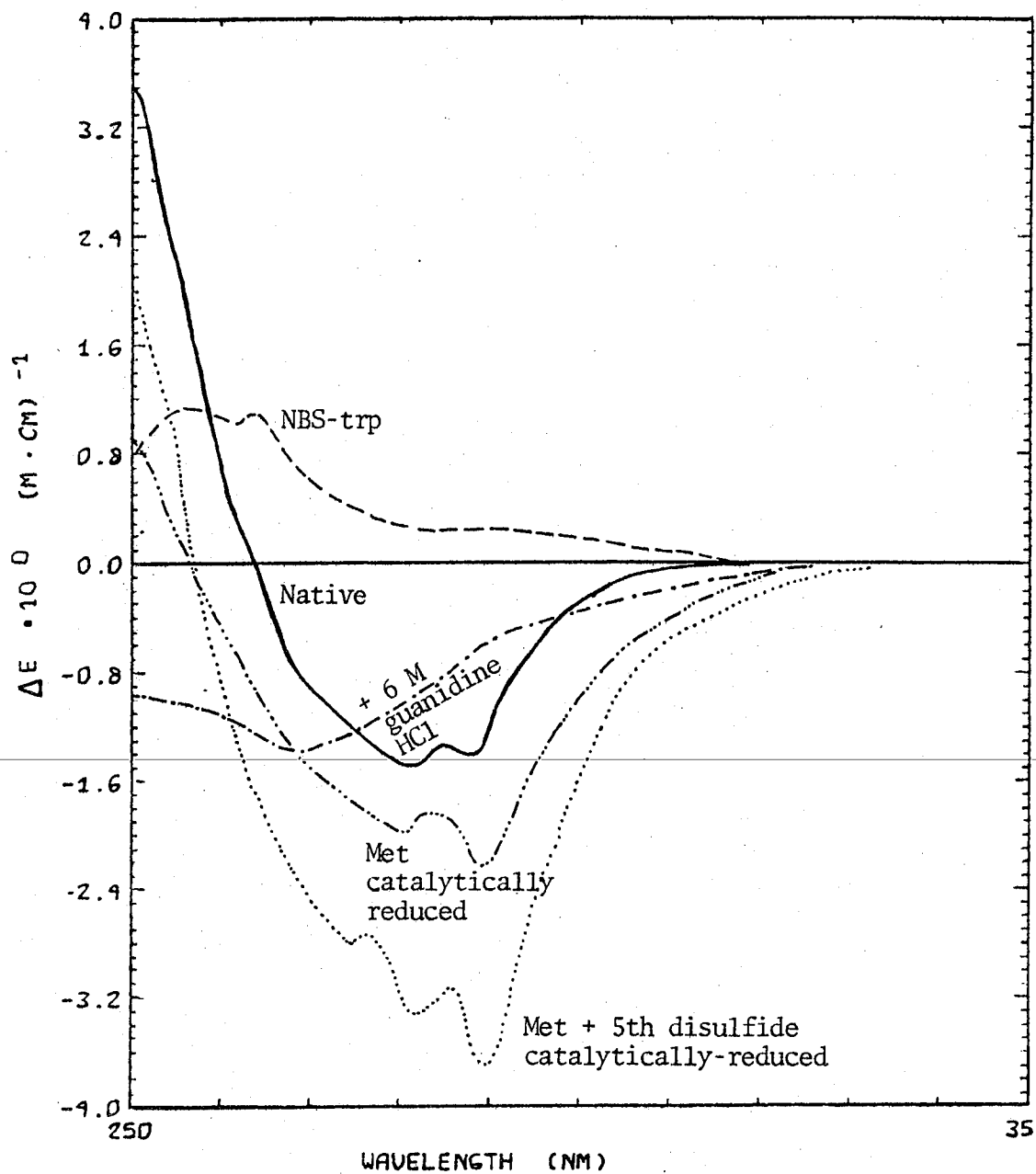


Figure 4-8
 Correlation of intensity of CD signal at 262 nm with mole-percentage of cystines.
 Inset shows extrapolation of line to ordinate.

XBL 764-5804

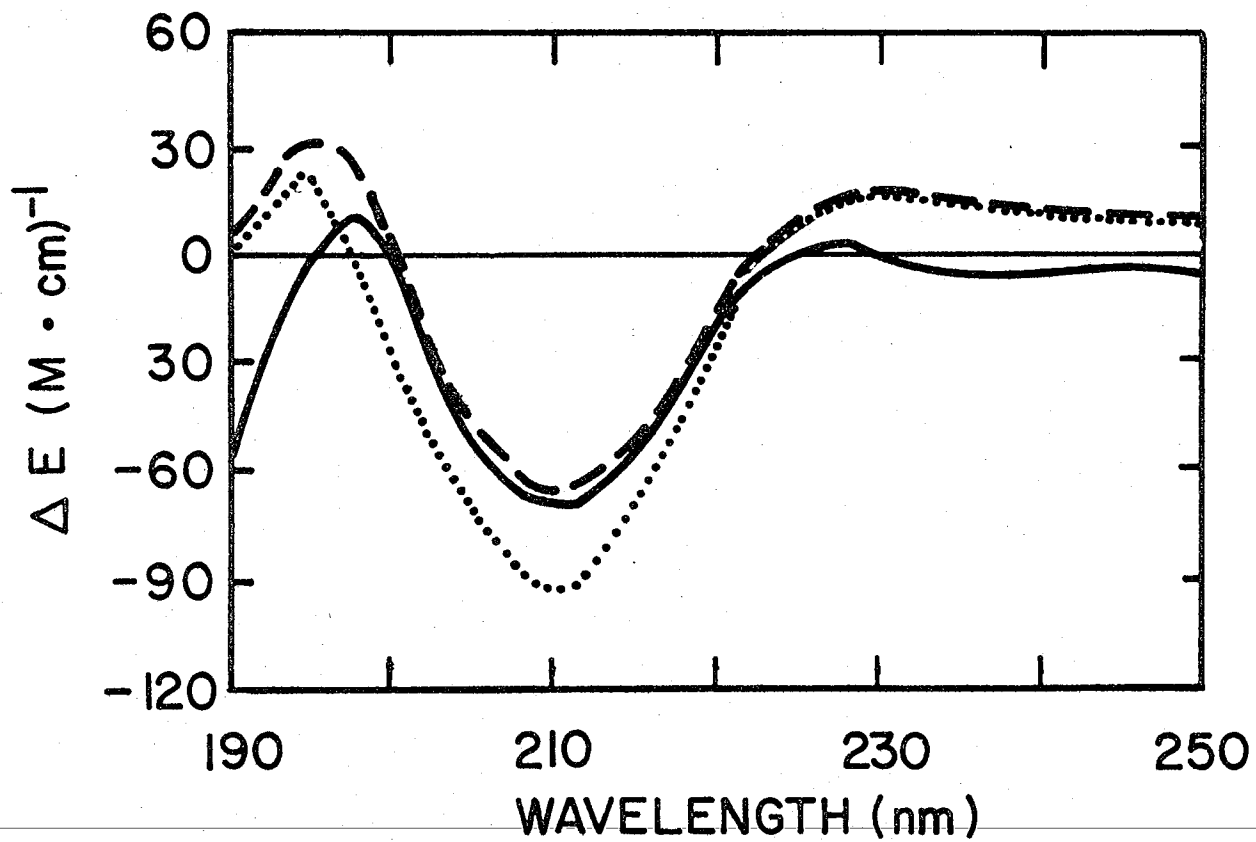
Figure 4-9
Effects of perturbants and chemical modifications on near-UV CD spectrum
of α -bgt. All spectra are at pH 7.0.



strong negative extremum is assigned to the trp. Abolition of secondary structure by 6 M guanidine hydrochloride leads to a broad negative band which is assigned, as with the β -toxins, to cystine. Catalytic reduction produced several derivatives which were resolved chromatographically. One product had lost only its single met by its reduction to α -amino butyrate (determined by amino acid analysis, see ref. 42). Because the met residue is next to the trp, it is not surprising that the negative extremum, assigned to the trp, is affected by this modification; its intensity is increased. Another product of the catalytic reduction had undergone further damage and had lost exactly one cystine in addition to the met. From comparative studies (43), it is known that the "fifth" disulfide, which differentiates Type II from Type I neurotoxins, is particularly sensitive to reduction and can be selectively opened. Thus, it is likely that this disulfide has been reduced to the two additional ala residues detected in amino acid analysis of this derivative. Its cleavage leads to the weakening of all the near-UV bands as compared to reduced-met derivative, but the negative extremum is slightly more intense than in the native toxin. The data are consistent with loosening of the structure around the tyr chromophores, but not the trp.

Iodination of α -bgt by the ICl method has been shown previously to give chromatographically resolvable mono- and diiodinated derivatives of a single exposed tyr (29). Subsequent cyanogen bromide cleavage of the modified toxin has identified tyr₅₄ as the altered residue (44). In Figure 4-10, the far-UV CD of the mono- and diiodinated derivatives are shown. The 50% reduction in the intensity at the negative extremum, and the increased negative ellipticity below 200 nm are both consistent with a reduction in the proportion of ordered structures and their replacement

Figure 4-10
Far-UV circular dichroism spectra of native (dotted line), monoiodinated (dashed line), and diiodinated (solid line) α -bgt derivatives.



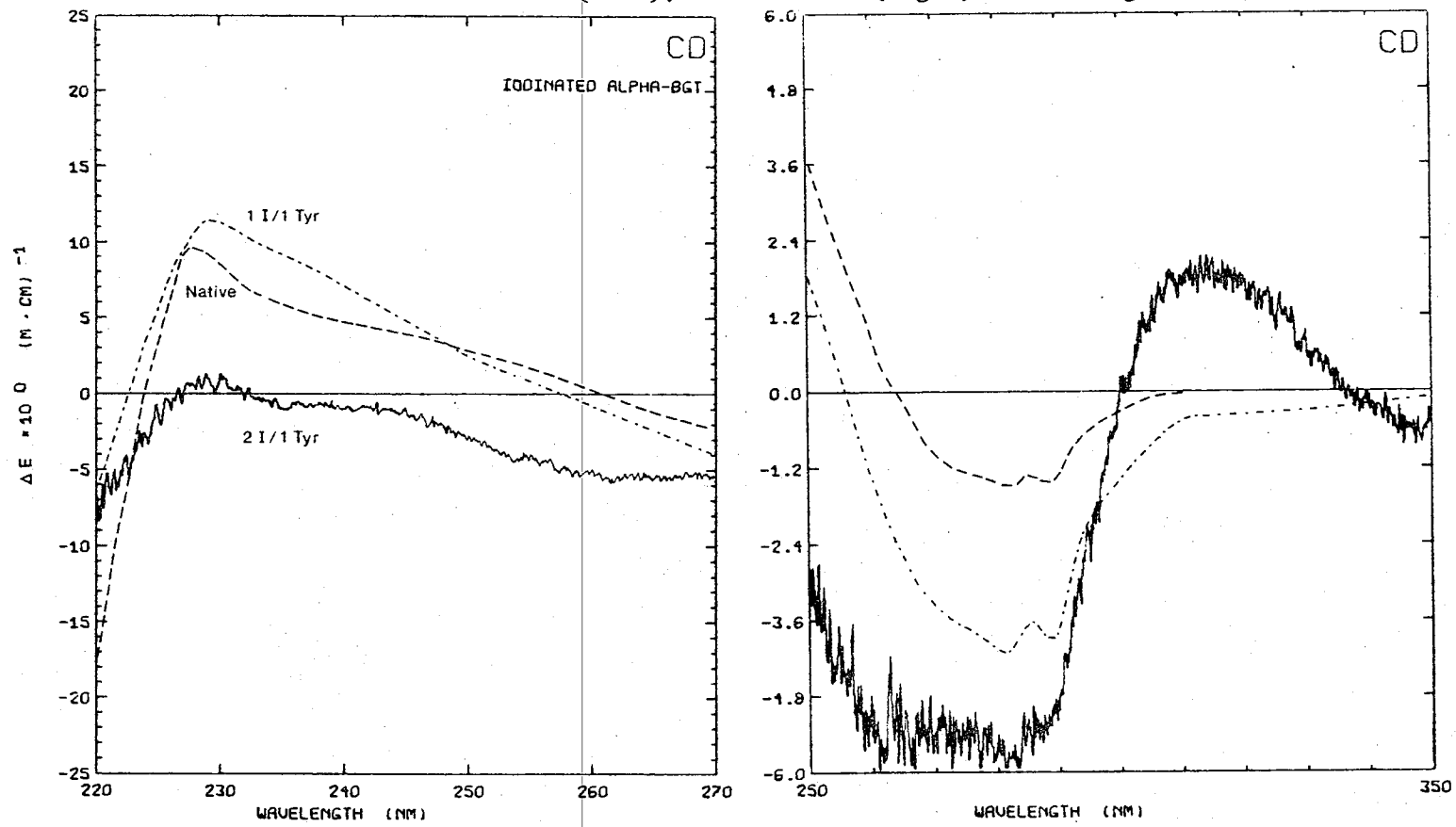
XBL 779-4607

by random coil (7,40). Thus, diiodination of tyr₅₄ leads to a partial delocalized denaturation (see also Chapter V). The altered spectrum is also independent of experimental pH, so the disruptive influence of diiodination is not the result of the reduced pK_a of the diiodophenolic group and its ionization at neutral pH, but rather is a steric effect from the bulkiness of the iodine atoms. The near-UV CD of the iodinated derivatives are compared to the native toxin in Figure 4-11. The signal at 220 to 230 nm is abolished with diiodination. Mono-iodination leads to an increase in the 280-290 negative band, and diiodination further increases its intensity. Diiodination also produces a new band above 300 nm which corresponds to the transition detectable in the UV absorption spectrum of diiodo-tyr (29).

Fewer modifications were explored with β -bgt because the greater complexity of its aromatic amino acid content and its near-UV CD spectrum make complete and unequivocal band assignment unlikely. Modification of the single trp by NBS leads to very little change, in agreement with the UV absorption data (Figure 4-12). Addition of 6 M guanidine hydrochloride leaves only the \sim 260 nm band previously assigned to cystines. The solvent perturbation results suggested that a small number of the total tyr residues should be responsive to change in the external solvent. Accordingly, the exposed tyr residues were ionized by raising the pH to 9.0. The negative band between 260 and 270 nm was increased, the positive extremum at 295 nm was increased, and a new positive band appeared below 250 nm. These effects are all consistent with the ionization of tyr residues and suggest that a positive contribution to the neutral pH spectrum between 260 and 270 nm is attributable to exposed tyr.

A summary of the band assignments for the toxins' near-UV CD is given in Table IV-6.

Figure 4-11
Effects of iodination on mid-UV (left), and near-UV (right) CD of α -bgt. All spectra were at pH 7.0.



XBL 774-4335

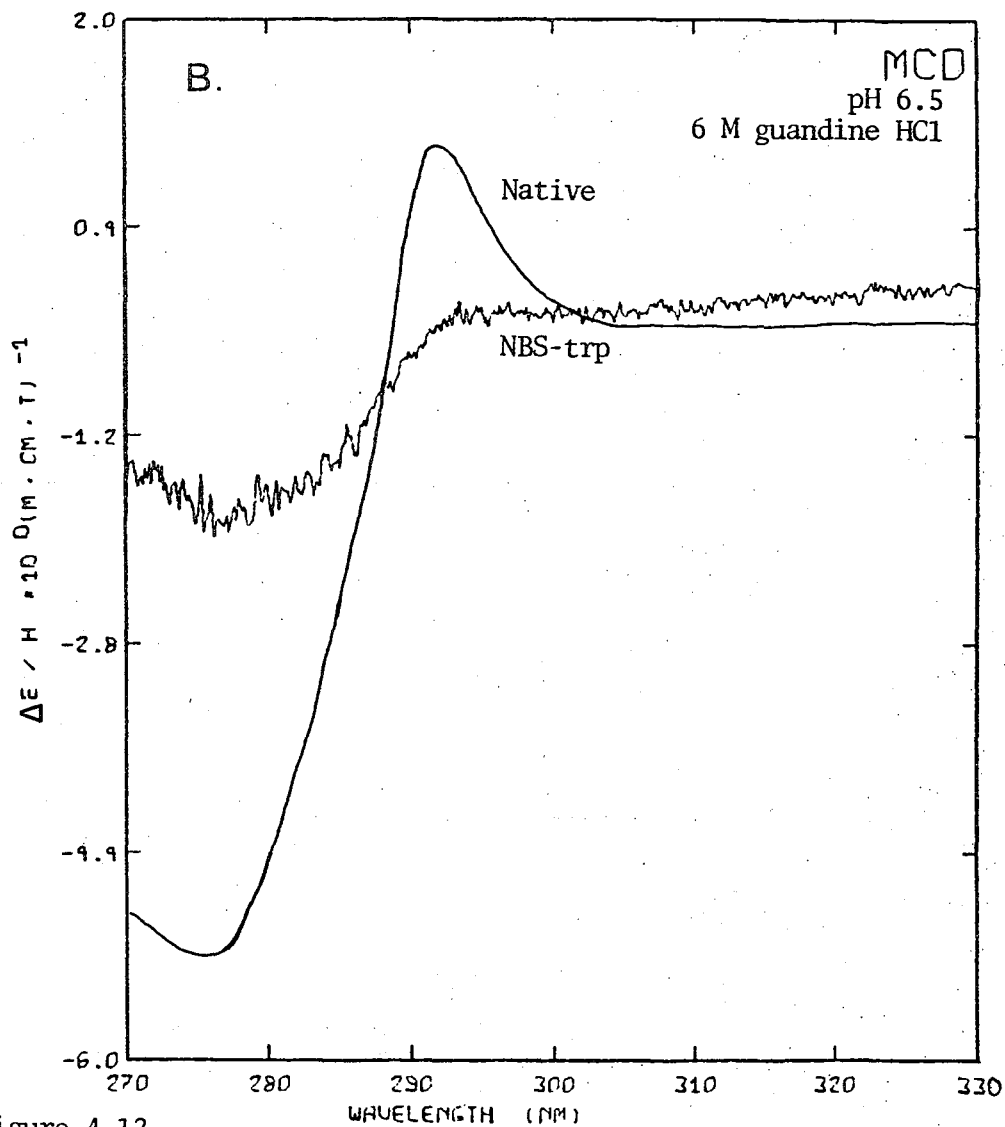
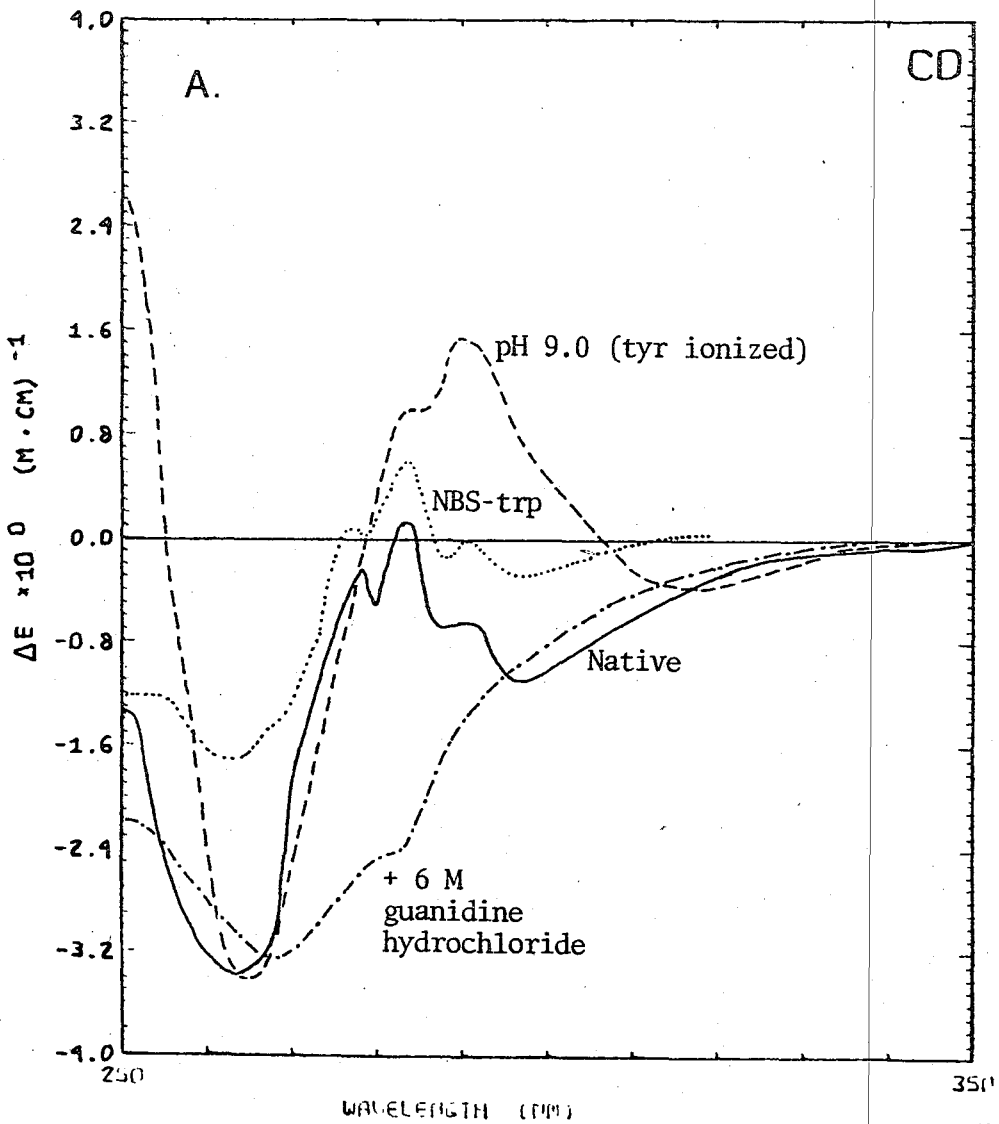


Figure 4-12 Effects of perturbants and chemical modifications on near-UV CD and MCD of β -bgt.

TABLE IV-6
NEAR-UV CD BAND ASSIGNMENTS FROM CHEMICAL MODIFICATIONS OF α - AND β -BGT

	<u>Extremum Wavelength (nm)</u> *	<u>Assignment</u>
α -Bgt	228 (+)	Tyr-54
	230 (+)	Tyr-24
	266 (+)	Tyr-54
	268 (-)	Cystines
	285 (-)	Trp-28
β -Bgt	260 (+)	Phe
	269 (-)	Cystines
	276 (+)	Tyr (exposed)
	282 (+)	Tyr (exposed)
	284 (+)	Trp
	290 (+)	Tyr (buried)
	292 (+)	Trp

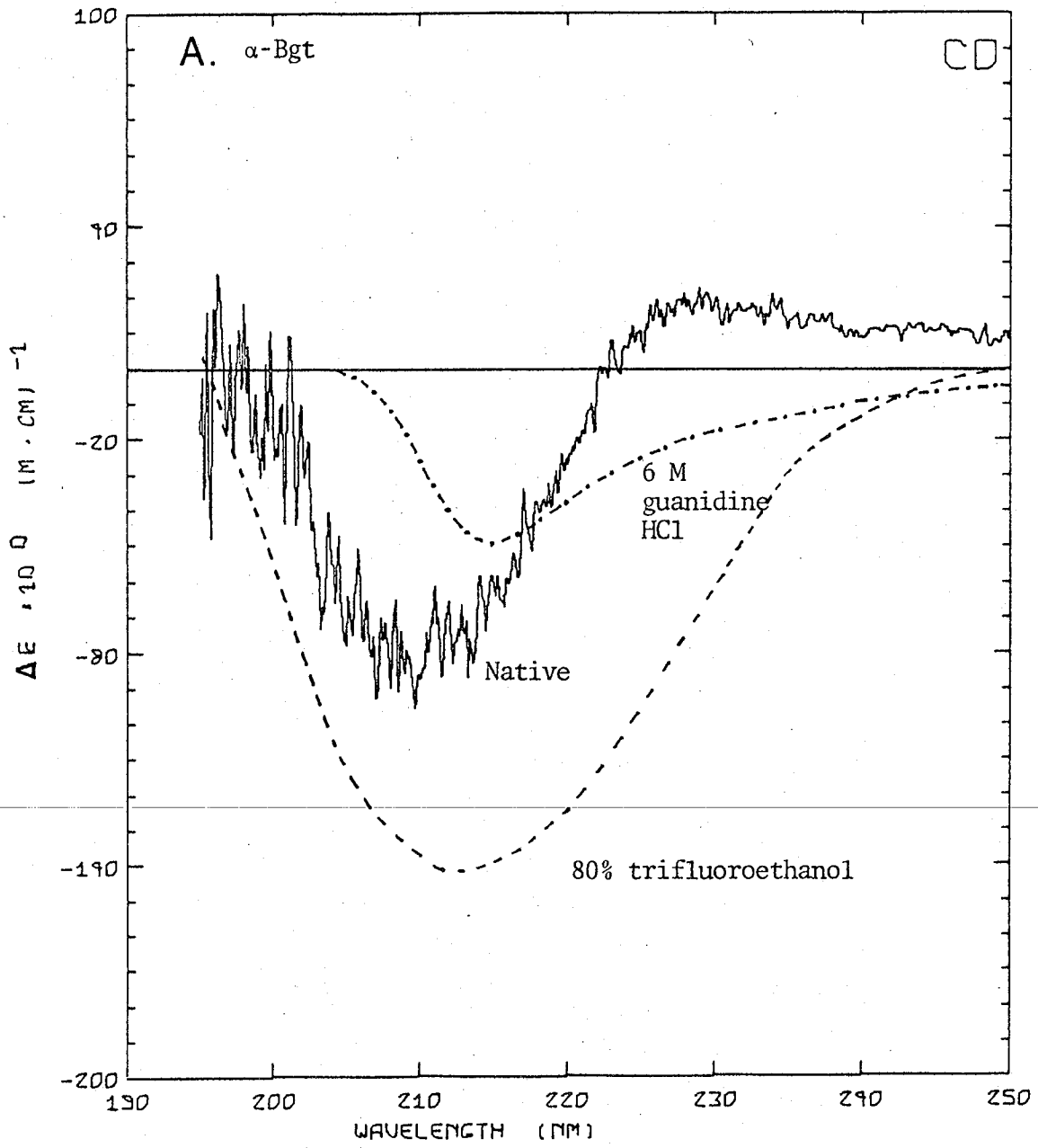
*

Values are given for wavelength position of maximum intensity in difference spectra of native vs. chemically-modified derivatives. These are not therefore the band positions of resolved Gaussian bands or of apparent bands in native spectra. Numbers in parantheses indicate the signal sign.

The effects of two perturbants on the global structures of the toxins were examined in order to identify differences in stability or flexibility between functional types. α -Bgt, β -bgt, and toxin 14 were taken as the representative toxins for study. The addition of 6 M guanidine hydrochloride abolished ordered secondary structure in all cases (Figure 4-13). Eighty percent trifluoroethanol has been shown to be a solvent that mimics membrane environments in its stabilization of intrinsic membrane protein conformations (45). Because the toxins are membrane-targeted proteins, the influence of this solvent on conformation was explored. The results are indicated in Figure 4-13. The far-UV CD spectra of toxin 14 and α -bgt were increased in intensity over a wavelength region consistent with the addition of α -helix. β -Bgt, however, exhibited a different spectrum, suggesting the conversion of secondary structures to β -forms. The effects of both guanidine hydrochloride and 80% trifluoroethanol were completely reversible in every instance.

The ion sensitivity of the toxins was explored using their CD spectra. No evidence was obtained for spectral modification of α -bgt by any cation or anion at 10 mM. Both toxin 14 and β -bgt were sensitive to divalent cations in the order $\text{Ca}^{+2} \approx \text{Mn}^{+2} \approx \text{Zn}^{+2} \approx \text{Eu}^{+2} > \text{Ba}^{+2} > \text{Sr}^{+2} > \text{Mg}^{+2}$. The addition of 10 mM CaCl_2 augmented the near-UV CD signal intensity without an effect on the far-UV CD (see Figure 4-14). The enhancement of the entire near-UV region suggests that no particular reporter chromophores were preferentially affected, rather that the Ca^{+2} binding appeared to stiffen the toxin in general. Scatchard plots of calcium binding to β -bgt and toxin 14 (Figure 4-14B) gave dissociation constants of 140 μM and 62.5 μM respectively, which is consistent with values for calcium binding to notexin (46) and a non-toxic phospholipase A (47). The data show a slight tendency towards positive cooperativity (Hill numbers ≈ 1.5), but suggest a single set of sites.

Figure 4-13
Effects of perturbants on far-UV CD spectra.



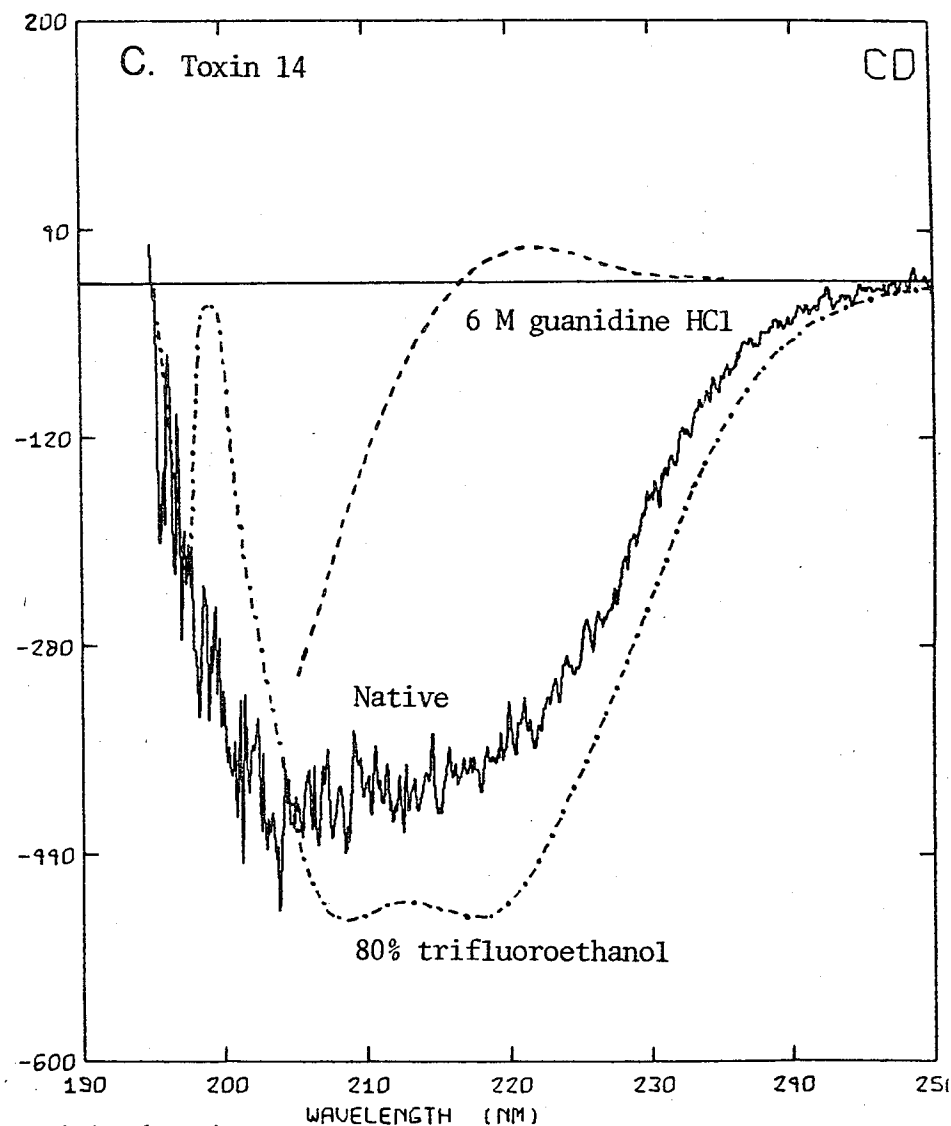
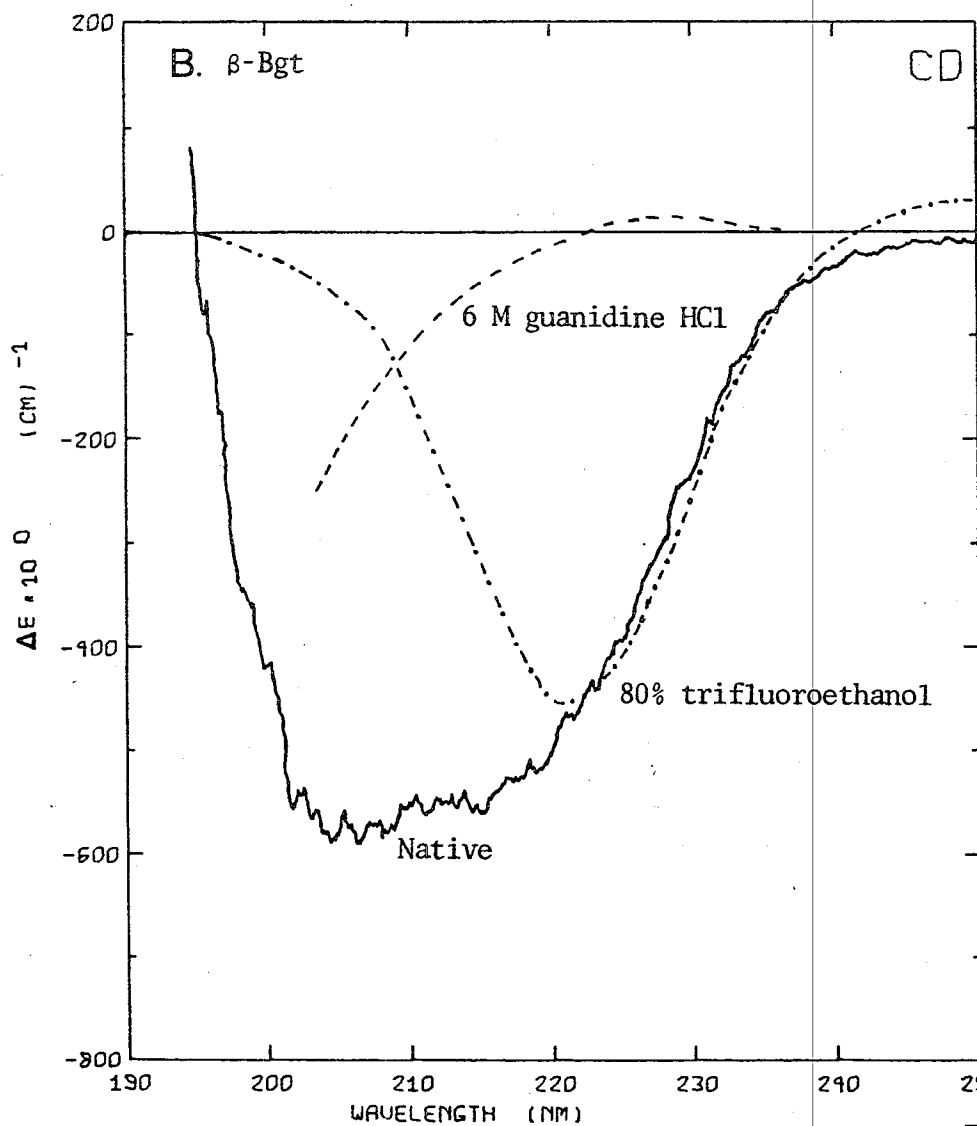
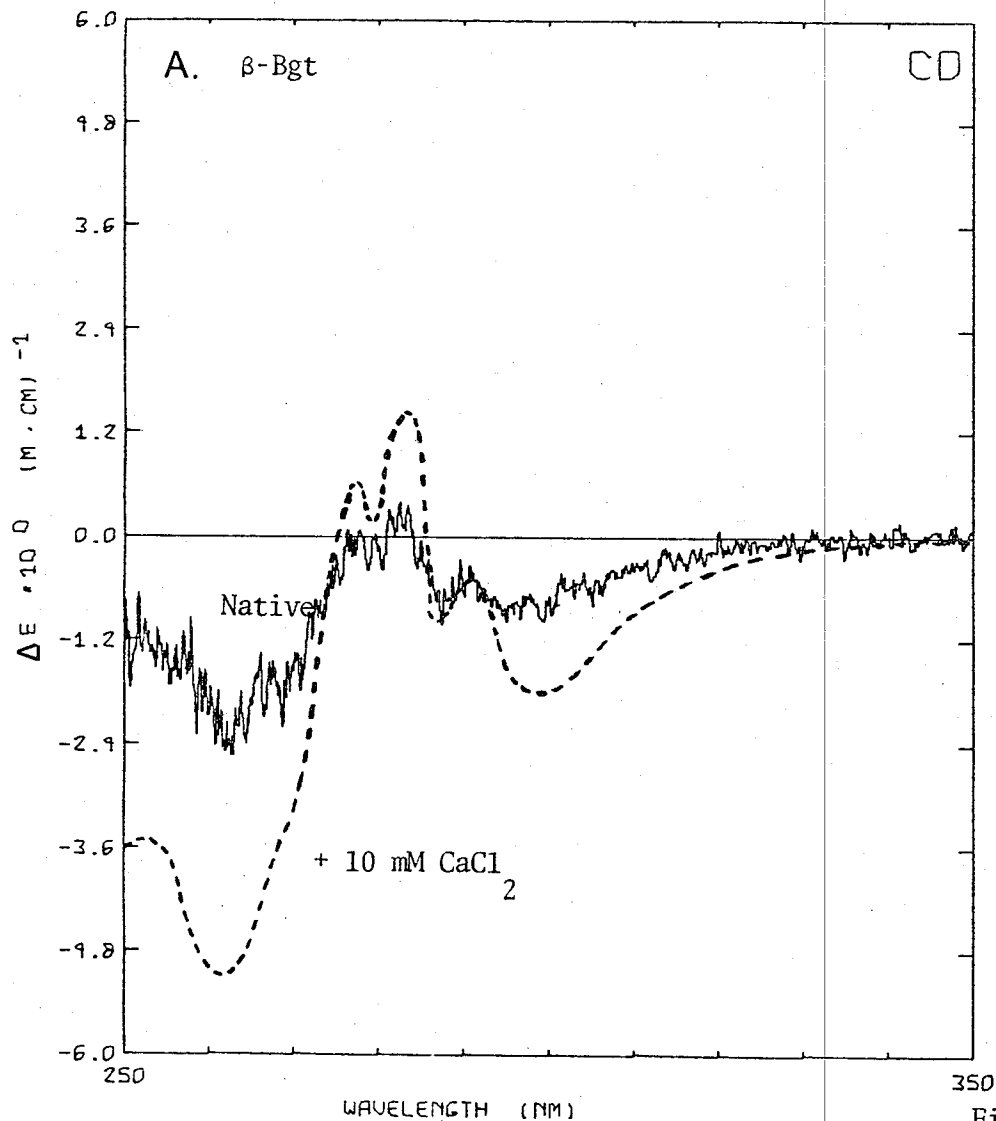


Figure 4-13 (con.)



A) Calcium binding effects on near-UV CD of β -bgt. Samples are in 20 mM Tris (pH 8.0).

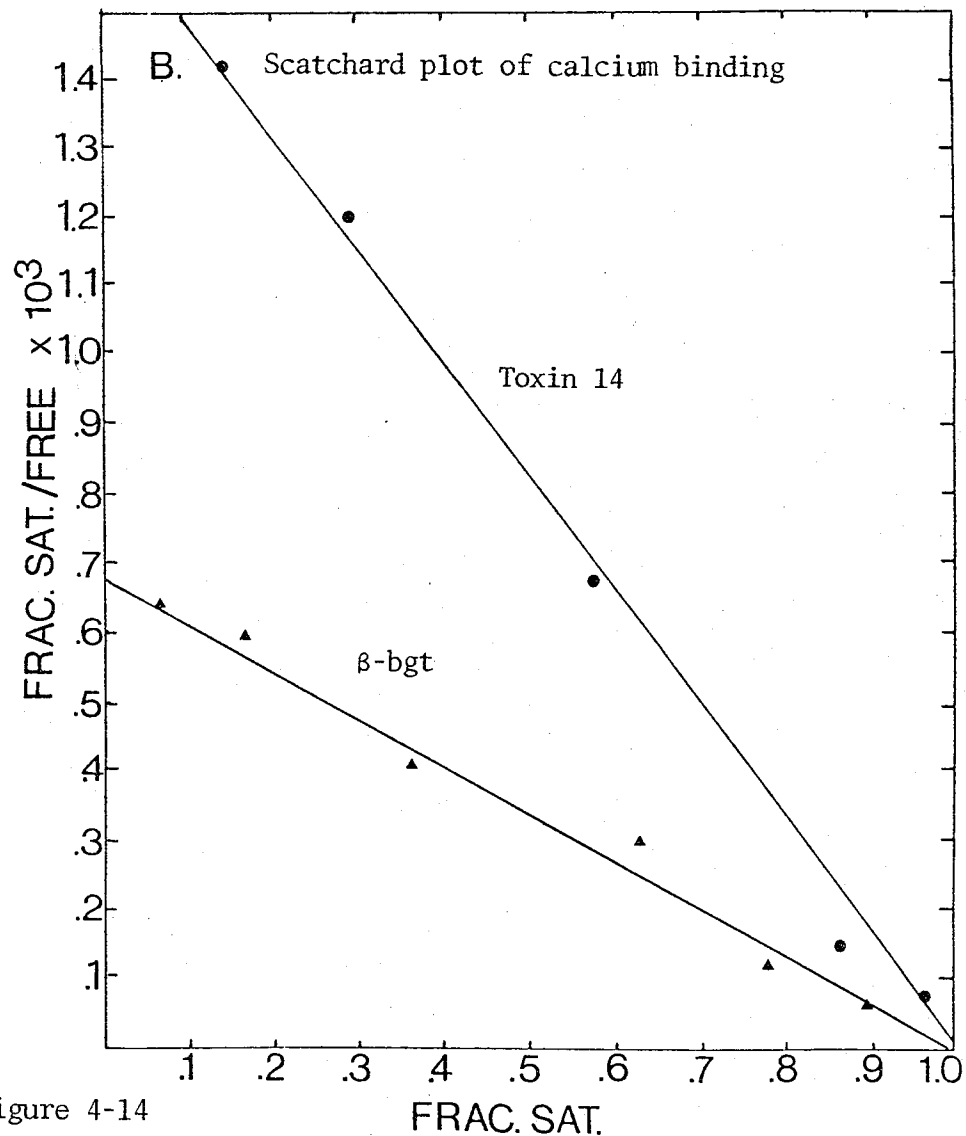


Figure 4-14

B) Scatchard plot of calcium binding from changes in the intensity of near-UV CD signals. Both 262 nm and 298 nm were used as reference positions without altering the results.

DISCUSSION.

The spectroscopic properties of the bungarotoxins confirm the structural classification into three groups. The α -toxins (α -bgt,7,8) are all exclusively composed of β -sheets and β -bends, and are dominated in their UV absorption, fluorescence, and near-UV CD spectra by the single trp residues. The single-chain β -toxins (9A,14) have nearly equal proportions of α -helical and β -structures, while the other β -toxins (β -bgt, 11 thru 13) have larger apparent contributions from α -helix and a more limited amount of β -structure.

The α -toxins are particularly interesting to consider in some detail because of the secondary structure predictions from their sequences (48, 49) and the X-ray structures. The predictive results have pointed to unique patterns of the distribution of predicted β -bends and β -structure in individual sequences which nonetheless converge to a basic form (48, 49). The basic forms for Type I and Type II neurotoxins differ in detail from one set of predictive results (48) to another (49), but consist of a repeating pattern of β -sheets hinged by a large number of reverse turns (β -bends), with little or no α -helical structure. The predictive results are compared to the experimental in Table IV-7. One difference between Type I and Type II toxins has been proposed (48), based upon the predicted secondary structures, which is that the latter have a significant amount of pleated sheets, whereas the former have none. This hypothesis would point to toxins 7 and 8 being Type II toxins because of their high proportion of measured β -structure. Examination of the predicted vs. the experimental results show that the predictive method often includes an element of α -helix which is not experimentally found. One possibility, previously suggested by Chou and Fasman for the conformation of glucagon

TABLE IV-7
COMPARISONS OF SECONDARY STRUCTURE ESTIMATES FROM EXPERIMENTAL AND PREDICTIVE METHODS FOR α -TOXINS

Toxin	Experimental (CD)					Predictive (ref.18)				
	α -helix	β -structure	random	β -bend	Ref.	α -helix	β -structure	random	β -bend	Ref.
α -Bgt	None	55	40	5		None	30	5	65	[48]
cobrotoxin	None	90	10	None	[13]	10 None	55 18	35 37	None 45	[63] [48]
Hemachatus hemachatus toxin II	None	80	20	None	[63]	10	40	50	None	[63]
Naja haje annulifera C14	None	80	20	None	[63]	10	30	60	None	[63]
Naja nivea β	None	80	20	None	[63]	10	40	50	None	[63]
Naja haje oxiana II	None	90	10	None	[63]	10	50	40	None	[63]
erabutoxin b	None*	90*	10*	None*	[63]	None None	45 27	55 21	None 52	[63] [48]
Type I Toxin Average						None	None	42	58	[48]
Type II Toxin Average						None	32	9	59	[48]

* From X-ray diffraction (20): 40% β -structure and 26% β -bends, with no α -helix.

(50), is that the region predicted as α -helical, residues 40 to 47 (49), has a potential to assume this structure and will do so only if altered by experimental perturbation (e.g., 80% trifluoroethanol) or a natural interaction (e.g., with the receptor in its hydrophobic environment). Another difference between the two methods is the larger proportion of β -structure suggested by CD. Since the CD results are converted to an estimate of ordered secondary structure by comparison with model polypeptides (7) or empirically-derived reference spectra (40), it is possible that these models are not suitable for the toxins. One complication in the toxin structures is the high density of disulfides which confers a compactness that restricts intramolecular contacts. Another is that the CD intensity of ordered secondary structures is dependent upon the number of residues involved in generating a given structure. That is, the longer the portion of the polypeptide chain organized into a repeating form, the stronger the intrinsic optical activity (40). Thus, the long lengths of β -sheet found in model polypeptides (7) may not be an accurate model for the CD properties of the shorter segments of interrupted β -structure found in the toxins (19,20).

The spectrum used in curve-fitting for the β -bends was derived from a model polypeptide (39), whose spectral features, negative extrema at 192 to 199 nm and 222 to 227 nm and a positive extremum at 208 nm, were in agreement with a theoretical prediction (51). However, it has been proposed that the observed β -bends may be blue-shifted in the positions of the diagnostic extrema by as much as 10 nm in α -toxins (13). Thus, the estimated secondary structures in Table IV-4 would have to be revised if this were established. One example is the alternative proportional breakdown given for toxin 8 assuming a blue-shifted reference spectrum for β -bends (see Table

IV-4). With this assumption, the reproduced CD curve fits the experimental curve exactly.

The current results improve on an earlier CD study of α -bgt (21). In the far-UV, α -bgt was previously reported to have a negative extremum centered at 216 nm. Using highly purified toxin, the negative extremum has been shown to be centered at 210 nm, and that the cross-over point is not at 210 nm, but rather at 196 nm.

The near-UV CD is dominated by the negative trough attributed to the single trp. Superimposed on this are cystine and tyrosine contributions. The cystine residues are apparently insensitive to the conformational state of the toxin since their chiroptical properties are unaffected by non-reducing perturbants. This agrees with results from laser Raman scattering studies of sea snake Type I neurotoxins in which the disulfides were shown to share an equivalent stereogeometry and be unaffected by chaotropic denaturation (urea, guanidine hydrochloride), but distorted by thermal denaturation (52).

The origin of the positive band between 220 and 230 nm has been a source of controversy, being variously attributed to a mixture of aromatic residues (13), a β -bend (13), tyr residues (53), or a tightly-constrained disulfide loop (54). Its abolition by diiodination suggests that it is largely derived from the exposed tyr₅₄, although the shoulder at slightly longer wavelengths, which persists after iodination, may be a weaker contribution from the buried invariant tyr. The 220-230 CD band is very sensitive to perturbation in the toxin structure in the recognition site loop. Selective reduction of the fifth, Type II-toxin specific disulfide or oxidation of the trp leads to weakening of its intensity. The indications are that selective chemical introduction of reporter groups into this tyr would produce an even more sensitive monitor of toxin structure changes.

α -Bgt can be reversibly denatured by exposure to high concentrations (>4 M) of guanidine hydrochloride. However, the residual spectrum has unusual characteristics which are not attributable to a random coil spectrum. Unlike the random coil model spectrum, the experimental CD does not grow increasingly negative below 210 nm, but rather reverses to approach zero. This spectrum cannot be interpreted with present information, but it can be speculated that it arises from restriction of the denaturant-induced expansion by the high density of disulfide cross-links. The addition of the perturbant 80% trifluoroethanol abolishes the tyrosine assigned band between 220 and 230 nm and increases the far-UV CD negative ellipticity. An identical response to trifluoroethanol was reported for the Type II Naja nigricollis toxin α (55). The Type I neurotoxin erabutoxin b, however, formed increasing proportions of α -helix with increasing concentrations of trifluoroethanol (55). Thus, Type II toxins are unresponsive to helical induction by trifluoroethanol owing to an increased rigidity. The loss of the 220-230 nm band suggests it is capable of independent flexibility from the rest of the Type II toxin. Similar conclusions have been reached by other groups working with homologous Type II toxins (4,55, 56). The flexibility monitored by the 220-230 nm band is very likely, as discussed earlier, confined to the recognition site, and may be important for either orienting residues in the initial encounter with the receptor, or for reorienting them for stabilization of the complex.

Comparison of the fluorescence data with that from a previous toxin study (10) indicates that α -bgt has a similar quantum yield and accessibility to external quenchers as the Type II neurotoxin from Naja naja oxiana. The Type I neurotoxin from the same venom has a higher quantum yield and lower accessibility to I^- quenching. The cause of the low quantum yield in Type II toxins may be the proximity of positively charged groups

to the trp.

The fluorescence properties of β -bgt and the steady-state fluorescence of its homologues 11 thru 13 point to immobilization of the single trp residues in hydrophobic environments, which are nevertheless susceptible to external quenchers. The selectivity of Cs^+ over I^- indicates an accumulation of negative charges in the vicinity of the trp. The ability of external quenching ions to perturb buried residues has been reported before and attributed recently to conformational "flickering" of the protein structure, permitting brief exposures of the interior residues to the exterior (57). This is intriguing inasmuch as the trp is found in the N-terminal region of the heavy chain of β -bgt, and the N-terminal end of related phospholipases has been implicated in lipid interface binding (58). As there is evidence that this binding domain is retained in β -bgt (see Chapter VI), the flickering of the N-terminal region detected by the trp may be indicative of considerable independent conformational mobility in this part of the toxin. One can speculate that the dynamics of the lipid recognition site show a capability for multiple conformations which could be significant in the stabilization of binding to appropriate target membranes or the release from inappropriate membranes.

The predominant element of secondary structure from curve-fitting analysis of the far-UV CD is α -helix. As the toxins increase in size from β -bgt to toxin 13, so the estimated content of helix also increases. Comparison of the experimental structure estimates with those derived from the Chou-Fasman predictive method shows a much larger proportion of α -helix in experimental estimates (see Table IV-8). The same disagreement was noted for non-toxic phospholipase A enzymes, and was attributed to spectral mimicry of helix by uncharacterized "other asymmetric structures" (59). Evidence in favor of this interpretation for the β -toxins is the fact that

TABLE IV-8
COMPARISONS OF β -TOXINS AND SNAKE PHOSPHOLIPASE A ISOENZYMES BY EXPERIMENTAL AND PREDICTIVE TECHNIQUES
FOR SECONDARY STRUCTURES

Toxin	Experimental (CD)			Ref.	Predictive (ref.18)			Ref.
	α -helix	β -structure	random		α -helix	β -structure	random	
β -Bgt	34,40	18	42	[21]	7 ^a	36 ^a	57	[64]
1.Heavy chain	x	x	x		10	33 ^a	57	[64]
2.Light chain	x	x	x		None	40	60	[64]
Notexin	x	x	x		8 ^a	25 ^a	67	[60]
Crotoxin	38	45	17	[60]	x	x	x	
1.Crotoxin A	6	41	53	[60]	x	x	x	
2.Crotoxin B	15	39	46	[60]	x	x	x	
<u>Phospholipase A</u>								
Naja melanoleuca	16,17,20 ^b	40	~40	[65]	x	x	x	
Bitis gabonica	22	45	33	[66]	20	36	44	[66]
Vipera ammodytes								
1.Toxic Enzyme ^b	21	32 ^a	47	[67]	x	x	x	
2.Non-toxic Enzyme ^b	28	33 ^a	39	[67]	x	x	x	

a

Recalculated from the literature.

b

Isoenzymes found in the same venom.

the far-UV CD negative extrema are blue-shifted from the diagnostic positions of the comparable extrema for model α -helix; the 222 nm minimum is found below 220 nm and the 200 nm cross-over point is found below 200 nm (7,16). However, the study on non-toxic phospholipases noted that the helical-imitating structures were insensitive to the disruptive effect of 7 M guanidine hydrochloride (59), which is unlike the denaturation induced by lower concentrations of guanidine hydrochloride in β -bgt. Without further analysis by independent spectral methods, the predictive-experimental disagreement cannot be resolved.

The far-UV CD for the β -toxins are similar to that reported for the related phospholipolytic neurotoxin, crotoxin (60). Previous reports on the CD of β -bgt gave helical estimates of 34% (21) and 23% (22), in fair agreement with the values reported here. Other features of the earlier near- and far-UV CD spectra are qualitatively and, in most respects, quantitatively close to the data in this study.

Both the absorbance and the near-UV CD spectra indicate that the β -bgt trp is almost spectrally silent. Thus, although it is in a unique fluorescence environment, its absorbance properties are overshadowed by the large number of tyr residues. The near-UV CD for β -bgt is generated by tyr chromophores in several environments superimposed on a background band from the intrinsic chirality of the disulfides.

As has been noted for notexin (46) and non-toxic phospholipases (47,61), the aromatic residues of β -bgt report on the interaction with divalent cations. The addition of 10 mM calcium causes a general enhancement of the near-UV CD and a quenching of the intrinsic fluorescence. Investigation of the dose-potency of a variety of divalent cations has shown good agreement with results on the cation interaction with Naja naja phospholipase A (61). Because of the quantitative preference for calcium, it is assumed

that these spectral perturbations are evidence for a physiologically-relevant calcium binding site, such as has been inferred from chemical modification (5,62) and extrinsic fluorescence studies (62). The site-binding constant of 140 μM is in excellent agreement with the value of 150 μM reported earlier (62), and with values for notexin (46) and non-toxic phospholipases (47,61). The tendency of the dose-potency of calcium to exhibit positive cooperativity cannot be considered significant without independent evidence from direct binding studies using ^{45}Ca . Because the present data favors only a single calcium-binding site on the toxin (62), the steepness of the calcium effect should not be attributed to the presence of a second site. An alternative is that calcium may mediate the tendency of toxin molecules to undergo dimer formation, such as been already shown for the role of divalent cations in the self-association of Naja naja phospholipase A (61).

Toxins 9A and 14 must again be considered separately because, although their fluorescence and CD spectra have certain features in common with the two-chain β -toxins, they are in many respects spectrally different. Their far-UV CD were found to have a much larger contribution from β -structure than in the two-chain toxins. This clear difference in secondary structures could point to functional differences, and this point is considered in detail in Chapter VI. On the other hand, the near-UV CD in toxin 9A in particular is very similar to that for the two-chain toxins. This shows that the dominant contribution to the near-UV CD in the latter group must arise from the heavy chain, and that the light chain is spectrally muted in this wavelength region. The larger proportion of ordered secondary structure in the two-chain toxins must arise from either the direct contribution of the light chains or their modification of the structures of the

heavy chains. The subunits of crotoxin show the same type of CD behavior (60).

Both 9A and 14 have calcium-binding sites as do the two-chain β -toxins. The site-binding constant for toxin 14 is stronger than that reported for most phospholipases A_2 . Moreover, the rank order of divalent cation potency, and the nature of the spectral consequences of different cations, are not like those observed with β -bgt. The cation-binding sites of 9A and 14 differ from those in the two-chain toxins.

In yet another respect, toxins 9A and 14 differ from the two-chain family. The perturbant 80% trifluoroethanol has been shown to reproduce the conformation of several membrane-bound proteins outside the membrane environment and has consequently been reported as a model for the effects of membrane environments on spectral characteristics (45). β -Bgt is shifted to an enriched β -structure conformation in response to this treatment, whereas toxin 14 becomes more helical in its ordered structure content. Interestingly, toxin 14 at high concentrations assumes a conformation very similar to that induced by trifluoroethanol in β -bgt. Furthermore, the addition of low concentrations of amphiphilic, fatty acid-like detergents can also induce a β -structure form in toxin 14. Both high concentrations of toxin 14 and amphiphilic detergents have been shown to induce dimer formation (Chapter III). Thus, the self-association of 14, speculated to be the first step in its interaction with membranes, reproduces an experimentally-induced conformation of β -bgt. Accordingly, it is possible that a conformational shift to the β -structure-form is significant for a transition from a delivery structure to a membrane-bound structure, and that this transition is linked to either binding or catalytic activities on target membranes. This behavior is strongly reminiscent of that described for crotoxin (60), which also undergoes membrane-mediated conformation changes.

REFERENCES.

1. Brunner, H., Holz, M., and Jering, H. (1974) *Eur.J.Biochem.*, 50, 129.
2. Bradbury, J.H., and Norton, R.S. (1976) *Mol.Cell.Biochem.*, 13, 113.
3. Briley, M.S., and Changeux, J.-P. (1977) *Int.Rev.Neurobiol.*, 20, 31.
4. Tsernoglou, D., Petsko, G.A., and Hudson, R.A. (1978) *Mol.Pharmacol.*, 14, 710.
5. Strong, P.N., Heuser, J.E., and Kelly, R.B. in *Cellular Neurobiology*, ed. by Hall, Z.W., Kelly, R.B., and Fox, C.F., Alan R. Liss, Inc., New York, New York, 1977, p 227.
6. Beychok, S. (1966) *Science*, 154, 1288.
7. Greenfield, N., and Fasman, G.D. (1969) *Biochemistry*, 8, 4108.
8. Strickland, E.H. (1974) *CRC Crit.Rev.Biochem.*, 2, 113.
9. Casey, J.P., and Martin, R.B. (1972) *J.Am.Chem.Soc.*, 94, 6141.
10. Buklova-Orlova, B., Burstein, E.A., and Yukelson, L.Y. (1974) *Biochim. Biophys.Acta*, 342, 275.
11. Yang, C.C. (1967) *Biochim.Biophys.Acta*, 133, 346.
12. Yu, N.-T., Lin, T.-S., and Tu, A.T. (1975) *J.Biol.Chem.*, 250, 1782.
13. Chen, Y.-H., Lo, T.-B., and Yang, J.T. (1977) *Biochemistry*, 16, 1826.
14. Lauterwein, J., Wuthrich, K., Schweitz, H., Vincent, J.-P., and Lazdunski, M. (1977) *Biochem.Biophys.Res.Communs.*, 76, 1071.
15. Dufourcq, J., and Faucon, J.-F. (1978) *Biochemistry*, 17, 1170.
16. Chen, Y.-H., Yang, J.T., and Martinez, H.M. (1972) *Biochemistry*, 11, 4120.
17. Sternberg, M.J.E., and Thornton, J.M. (1978) *Nature*, 271, 15.
18. Chou, P.Y., and Fasman, G.D. (1974) *Biochemistry*, 13, 222.
19. Tsernoglou, D., and Petsko, G.A. (1977) *Proc.Nat.Acad.Sci.*, 74, 971.
20. Low, B.W., Preston, H.S., Sato, A., Rosen, L.S., Searl, J.E., Rudko, A.D., and Richardson, J.S. (1976) *Proc.Nat.Acad.Sci.*, 73, 2991.
21. Hamaguchi, K., Ikeda, K., and Lee, C.-Y. (1968) *J.Biochem.*, 64, 503.
22. Kelly, R.B., and Brown, F.H. (1974) *J.Neurobiol.*, 5, 135.
23. Herskovits, T.T. (1967) *Meths.Enzymol.*, 11, 748.

24. Lehrer, S.S. (1971) *Biochemistry*, 10, 3254.
25. Sutherland, J.C., Vickery, L.E., and Klein, M.P. (1974) *Rev.Sci.Instrum.*, 45, 1089.
26. Barth, G., Bunnenberg, E., and Djerassi, C. (1972) *Anal.Biochem.*, 48, 471.
27. Hanley, M.R., Eterovic, V.A., Hawkes, S.J., Hebert, A.J., and Bennett, E.L. (1977) *Biochemistry*, 16, 5840.
28. Spande, T., and Witkop, B. (1967) *Meths.Enzymol.*, 11, 498.
29. Lukasiewicz, R., Hanley, M.R., and Bennett, E.L. (1978) *Biochemistry*, 17, 2308.
30. Eterovic, V.A., Aune, R.G., and Bennett, E.L. (1975) *Anal.Biochem.*, 68, 394.
31. Stark, G., Stein, W., and Moore, S. (1961) *J.Biol.Chem.*, 236, 436.
32. Matsushima, A. Inoue, Y., and Shibata, K. (1975) *Anal.Biochem.*, 65, 362.
33. Brandts, J.F., and Kaplan, L.F. (1973) *Biochemistry*, 12, 2011.
34. Teale, F.W.J. (1960) *Biochem.J.*, 76, 381.
35. Hartig, P.H., Sauer, K., Lo, C.C., and Leskovar, B. (1976) *Rev.Sci. Instrum.*, 47, 1122.
36. DeLauder, W.B., and Wahl, P.H. (1971) *Biochim.Biophys.Acta*, 243, 153.

37. Eisinger, J., and Navon, G. (1969) *J.Chem.Phys.*, 50, 2069.
38. Steiner, R.F., and Kirby, E.P. (1969) *J.Phys.Chem.*, 73, 4130.
39. Brahms, S., Brahms, J., Spach, G., and Brack, A. (1977) *Proc.Nat.Acad. Sci.*, 74, 3208.
40. Chen, Y.-H., Yang, J.T., and Chou, K.H. (1974) *Biochemistry*, 13, 3350.
41. Takagi, T., and Izutsu, T. (1974) *J.Biochem.*, 75, 441.
42. Perlstein, M.T., Atassi, M.Z., and Cheng, S.H. (1971) *Biochim.Biophys. Acta*, 236, 174.
43. Chicheportiche, R., Vincent, J.-P., Kopeyan, C., Schweitz, H., and Lazdunski, M. (1975) *Biochemistry*, 14, 2081.
44. Hanley, M.R., Lukasiewicz, R., and Bennett, E.L. (1978) *Biochemistry* (submitted).
45. Long, M.M., Urry, D.W., and Stoekenius, W. (1977) *Biochem.Biophys.Res. Commun.*, 75, 725.

46. Halpert, J., Eaker, D., and Karlsson, E. (1976) FEBS Lett., 61, 72.
47. Pieterse, W.A., Volwerk, J.J., and DeHaas, G.H. (1974) Biochemistry, 13, 1439.
48. Hseu, T.-H., Liu, Y.-C., Wang, C., Chang, H., Hwang, D.-M., and Yang, C.C. (1977) Biochemistry, 16, 2999.
49. Dufton, M.J., and Hider, R.C. (1977) J.Mol.Biol., 115, 177.
50. Chou, P.Y., and Fasman, G.D. (1975) Biochemistry, 14, 2536.
51. Woody, R.W. in Peptides, Polypeptides, and Proteins, ed. by Blout, E.R., Bovey, F.A., Goodman, M., and Lotan, N., John Wiley and Sons, New York, New York, 1974, p 338.
52. Tu, A.T., Jo, B.H., and Yu, N.-T. (1976) Int.J.Pep.Prot.Res., 8, 337.
53. Woody, R.W. (1978) Biopolymers, 17, 1451.
54. Yoshida, C. Yoshikawa, M., and Takagi, T. (1976) J.Biochem., 80, 449.
55. Menez, A., Bouet, F., Tamiya, N., and Fromageot, P. (1976) Biochim. Biophys.Acta, 453, 121.
56. Drake, A.F., Dufton, M.J., and Hider, R.C. (1977) FEBS Lett., 83, 202.
57. Eftink, M.R., and Ghiron, C.A. (1975) Proc.Nat.Acad.Sci., 72, 3290.
58. Van Dam-Mieras, M.C.E., Slotboom, A.J., Pieterse, W.A., and DeHaas, G.H. (1975) Biochemistry, 14, 5387.

59. Jirgensons, B., and DeHaas, G.H. (1977) Biochim.Biophys.Acta, 494, 285.
60. Hanley, M.R. (1978) Biochemistry (in press).
61. Roberts, M.F., Deems, R.A., and Dennis, E.A. (1977) J.Biol.Chem., 252, 6011.
62. Abe, T., Alema, S., and Miledi, R. (1977) Eur.J.Biochem., 80, 1.
63. Visser, L., and Louw, A.I. (1978) Biochim.Biophys.Acta, 533, 80.
64. Kondo, K., Narita, K., and Lee, C.-Y. (1978) J.Biochem., 83, 101.
65. Joubert, F., and Van Der Walt, S.J. (1975) Biochim.Biophys.Acta, 379, 317.
66. Viljoen, C.C., Visser, L., and Botes, D.P. (1976) Biochim.Biophys.Acta, 438, 424.
67. Gubensek, F., and Lapanje, S. (1974) FEBS Lett., 44, 182.

CHAPTER V.

APPLICATIONS AND FUNCTIONAL
STUDIES OF THE α -TOXINS.

V. INTRODUCTION.

The class of post-synaptic neurotoxins is one of the best examples of the successful application of toxins as investigative aids. Due to their specificity in binding to the nicotinic acetylcholine receptor (nAChR), the α -toxins have become important in a number of imaginative applications, several of which are listed in Table V-1.

Their most extensive use has been in the identification and purification of the nAChR. Although their curare-like action had been recognized earlier, it was a catalytic paper of Changeux et al (1) that first demonstrated their utility as naturally-occurring affinity labels. Research focused initially on the receptor-rich electric organs, but it soon became evident that, with few modifications, the technology could be applied to the study of the nAChR in other tissues, particularly muscle (2,3). Subsequently, there appeared reports on the occurrence of a significant and reproducible, but extremely low level of a toxin-binding component in vertebrate brain (4,5). More recently, α -toxin sites have been identified in cultured cell lines (6,7), sympathetic ganglia (8), parasympathetic ganglia (9), adrenal medulla cells (10), retina (11), thymus cells (12), and invertebrate ganglia (13,14). The obvious and tempting inference is that these sites correspond to homologues of the peripheral nAChR. However, physiological investigations have shown no blocking activity of α -bgt on central nervous system nicotinic synapses of the cat (15) and frog (16) spinal cords, on sympathetic ganglion neurons (17) or on an excitable cell line (18). In marked contrast to these results, histochemical studies at the light and electron microscope levels have revealed the predicted distribution of the α -toxin-binding molecules in neural

TABLE V-1
APPLICATIONS OF α -TOXINS

1. nAChR identification, assay, quantitation, and localization. (1,38,40)
2. nAChR purification by affinity columns using immobilized toxins. (55,68)
3. In vitro and in vivo histology of receptor sites using radiolabeled or fluorescent toxin derivatives. (62)
4. Ultrastructural location of nAChR using radiolabeled, ferritin-conjugated, or peroxidase-conjugated derivatives. (71,72,88)
5. Monitoring of in vitro binding-state changes as a model for desensitization. (24,25)
6. Neuropathology of neuromuscular diseases, particularly myasthenia gravis. (93)
7. Pharmacological screening of drugs for nicotinic receptor effects. (23,87)
8. Isolation of neurons, and nAChR-rich membranes. (76)
9. Chronic interruption of neuromuscular transmission. (2)
10. Subcellular marker for synaptic membranes. (39,70,88)

tissues (19,20). Thus, although the biochemical and localization evidence is good for the identification of nAChR in ganglia and brain, the functional failure of the toxins cannot be explained. Thus, caution must be exercised in interpreting these data. In one instance, an α -toxin, dendrotoxin 4.7.3, was shown to block nicotinic synapses in the frog spinal cord (16), and hyperpolarizing receptors in an invertebrate ganglion (21). The possibility that different α -toxins might have different binding activities to nervous tissues has been explored in this Chapter with the aim of generating an explanation for the biochemical specificity but physiological ineffectiveness.

The nature of the α -toxin binding to peripheral nAChR has been studied in detail by several groups, using different radiolabeled toxin derivatives and electroplaques or muscle tissues. It is clear that agonists and antagonists (including curarimimetic toxins) are mutually exclusive (22). α -Toxin pre-treatment prevents the binding of radiolabeled agonists such as ^3H -acetylcholine and ^3H -decamethonium, and agonist pre-treatment prevents the binding of radiolabeled toxins (23). These observations have been reproduced in the three different experimental preparations on which binding studies have been conducted: excitable vesicles ("membrane-bound nAChR"), detergent-solubilized crude nAChR, and purified solubilized nAChR. Thus, the binding responses are, to a first approximation, independent of the physical form of the receptor. However, this point has not been examined closely and some of the data reported in this Chapter speak to this question.

There is considerable disagreement as to the exact nature of toxin and small ligand sites. It is not clear whether they are separate, interconverting, or identical sites and whether they are altered by changes in receptor state or by stabilization of pre-existing states in equilibrium.

Further, several binding responses show time-dependent changes under certain conditions, suggesting dynamics that may mimic physiological events (24,25). One difficulty in integrating the present body of data is the variation in experimental conditions, particularly in the choices of tissue, physical state of nAChR, and the probing ligand. It has only rarely been considered that the choice of probing ligand might seriously affect the results. For example, decamethonium has recently been shown to have partial local anaesthetic character (26), invalidating its use in the description of pure agonists. Similarly, the choice of detergents for solubilization has been shown to be important in stabilizing different binding states of the receptor (27). Thus, a strong possibility exists that some of the literature may be physiologically irrelevant because of an idiosyncratic choice of experimental conditions.

There is extensive documentation of the reaction kinetics of radiolabeled toxins with nAChR. As with equilibrium experiments, variations in procedures and choice or preparation of radiolabeled toxin may account for some of the disagreements. The range of values for association rates, dissociation rates, and dissociation constants is listed in Table V-2. In general, the conclusion has been that the reactions are surprisingly slow considering the binding affinity, but that the slow on-rates are more than compensated for by the extremely slow off-rates ($\tau_{1/2} \geq 60$ hrs), giving an overall K_d in the nanomolar to subnanomolar range. The observed dissociation constants correspond to free energies of ~ 12 to 15 kcal/mole which place the interaction between values observed for the hemoglobin $\alpha\beta$ dimer and the very tight complexing of trypsin inhibitors with trypsin (28). The driving force for the reaction appears to be a large change in entropy (100 to 120 e.u./mole) and the enthalpy change is ~ 17 kcal/mole(22).

TABLE V-2

ON-RATES, OFF-RATES, CALCULATED AND MEASURED DISSOCIATION CONSTANTS OF α -TOXIN BINDING TO nAChR

Ref.	Tissue Source	Receptor Preparation	Radiolabeled Toxin	$k_1 M^{-1} min^{-1}$	$k_{-1} min^{-1}$	$K_d^* M$	$K_d^{app**} nM$
22	<u>Electrophorus electroplaques</u>	Purified	3H - <u>Naja naja siamensis</u>	7.6 (10^6)	9 (10^{-5}) 4 (10^{-3})	1.7 (10^{-11})	0.7-2.4
25	<u>Torpedo electroplaques</u>	Membrane-bound	[$^{125}I_1$]- <u>Naja naja siamensis</u>	0.5 (10^6)	6 (10^{-4})	1.2 (10^{-9})	X
38	<u>Electrophorus electroplaques</u>	Membrane-bound	3H - <u>Naja nigricollis</u> toxin α	30 (10^6)	2 (10^{-4})	6.7 (10^{-11})	X
54	rat muscle	Purified	[^{125}I]- α -bgt	3.0 (10^6) 7.8 (10^6)	1.14 (10^{-4}) 2.88 (10^{-3})	0.4 (10^{-11}) 3.7 (10^{-10})	X
59	<u>Electrophorus electroplaques</u>	Membrane-bound	[^{125}I]- α -bgt	0.7 (10^6)	irreversible		
73	cat muscle	Membrane-bound	[3H]- α -bgt	1-2 (10^6)	X	X	X
81	<u>Torpedo electroplaques</u>	Membrane-bound Solubilized	[$^{125}I_2$]- α -bgt	20 (10^6) 19 (10^6)	X	X	X

* $K_d = k_{-1}/k_1$ by microscopic reversibility constraint (22,25,38).

** K_d^{app} = value from direct graphical transform of saturation binding data under pre-equilibrium conditions.

METHODS.

i. Toxicology. The lethal characteristics of purified toxins were measured by subcutaneous or intraperitoneal injections into male mice. No strain differences in lethality were detected. Time to death for individual mice was always recorded. LD₅₀, LD₁₀₀, and slope functions were calculated by the method of Litchfield and Wilcoxon (29). The lethal doses were replotted on semilog graphs to measure the lethality parameters. Typically, forty to sixty mice were used for the estimation of lethality of purified toxins.

ii. Preparation of *Torpedo californica* Electroplaques Excitable Vesicles.

Vesicles enriched in nAChR ("excitable vesicles") were prepared from liquid-nitrogen frozen *Torpedo californica* electric organ (Pacific Bio-Marine, stored at -70°C) by the procedure of Hazelbauer and Changeux (30), and further purified by centrifugation onto a discontinuous gradient of 0.9/1.2 M sucrose (in 20 mM sodium phosphate buffer, pH 7.4, containing 0.02% NaN₃ and 0.1 mM PMSF) in a Beckman SW27 rotor at 25,000 rpm for 2 hrs. Vesicles were taken from the 0.9/1.2 M sucrose interface and checked for purity by negative staining electron microscopy (2% phosphotungstate).

Membranes enriched in nAChR were prepared from vesicles by osmotic rupture and pelleting at 100,000 X g for 1 hr. The resulting membrane suspension could be stored without changes in its toxin-binding properties at -70°C.

iii. Sodium-22 Efflux Assay of nAChR Function. Freshly-prepared excitable vesicles were resuspended to a final concentration of 10 mg membrane protein/mL in 0.5 M sucrose (+0.02% NaN₃ and 0.1 mM PMSF) containing 10 mM NaCl and 100 µCi of ²²NaCl (New England Nuclear, carrier free). This was equilibrated at 4°C for 16 to 18 hrs and 100 µL aliquots were diluted 80X with *Torpedo californica* Ringer (160 mM NaCl, 5 mM KCl, 2 mM CaCl₂, 2 mM MgCl₂, 3 mM NaPO₄ buffer at pH 7.2) and maintained at 4°C for 30 min

to stabilize the resting efflux (31). One hundred μL of either control (Ringer alone) or test (Ringer with experimental additions) solutions were added and incubations continued for 15 min at 4°C unless otherwise noted. At time zero, carbamylcholine (Calbiochem, carbachol) in Ringer was added to a final concentration of 0.1 mM and the efflux of ^{22}Na followed by rapid filtration of 1 mL samples at timed intervals on Millipore HAWP 02500 filters (equilibrated in cold Torpedo Ringer). Filters were rinsed with 3 X 5 mL of ice-cold Ringer, and then immediately dissolved with agitation in 10 mL of Beckman Filter-Solv. Samples were counted for vesicle-trapped ^{22}Na retained on the filters using a Packard Tri-Carb liquid scintillation spectrometer with third-channel settings optimized for ^{22}Na . Excitable vesicles had a specific toxin-binding activity of 0.5-0.7 nM ^3H - α -bgt sites/mg protein. The parameters used to characterize the efflux process are θ , the time required for the carbachol-stimulated efflux to reach 75% of the initial filter-trapped radioactivity, and θ_0 , the time required for the resting efflux to reach the 75% point (see ref.32).

iv. Preparation of Radioactively-Labeled Toxins. Iodinated species of α -bgt were prepared and purified by the protocol described in Chapter IV. The resolved species, monoiodinated ($[^{125}\text{I}]\text{-}\alpha\text{-bgt}$), diiodinated ($[^{125}\text{I}_2]\text{-}\alpha\text{-bgt}$), and unlabeled toxin were identified by their characteristic UV absorption spectra (33). Dendrotoxin 4.7.3 (gift of Dr.R.A.Shipolini, see ref.34) was radioactively-labeled by $^{125}\text{I}\text{Cl}$ using the same procedure as for $[^{125}\text{I}]\text{-}\alpha\text{-bgt}$ (33) with the modification that the CM-52 column chromatography used a 0-0.25 M NaCl gradient instead of 0-0.08 M NaCl. Monoiodinated dendrotoxin ($[^{125}\text{I}]\text{-ddt}$) was the only product isolated (elution position at $\sim 220\text{-}230$ mM NaCl). The specific activities of all iodinated toxins were determined by direct counting on a Nuclear-Chicago γ -ray counter aliquots of known concentration (determined by UV absorbance at 280 nm after cor-

rection for scattering and using $\epsilon_{280}^{0.1\%} = 1.70$ for ddt and 1.29 for α -bgt) and were confirmed by titration of the total number of specific* α -toxin with an excess of ^3H - α -bgt (10 to 100-fold molar excess) over anticipated nAChR concentrations in Torpedo membrane suspensions. Specific activities for the iodinated toxins were calculated by assuming that the specifically-bound radioactivity at saturation corresponded to the same number of sites. These specific activity values agreed within 5% in all cases. Specific activities were 100 dpm/fmol for [^{125}I]- α -bgt (= 45.5 Ci/mmol), 200 dpm/fmol for [$^{125}\text{I}_2$]- α -bgt (= 91 Ci/mmol) and 25 dpm/fmol for ^3H - α -bgt (= 11.4 Ci/mmol). Specific activities for [^{125}I]-ddt were experimentally varied between 10 and 100 dpm/fmol by dilution of the initial ^{125}I Cl by carrier KI.

^3H - α -bgt was prepared from [^{125}I]- α -bgt by catalytic exchange for tritium using the same procedure described in Chapter IV Methods for catalytic hydrogenation (see ref. 35). ^3H - α -bgt was purified by CM-52 chromatography as for the iodinated toxins.

All toxins were stored frozen at -20°C in the presence of 1 mg/mL bovine serum albumin (BSA) to prevent adsorption and limit radiolysis. Iodinated toxins retain $\sim 80\%$ of their binding activities through two half-lives, and tritiated toxin shows $>93\%$ activity for over one year.

To insure that radiolabeling did not destroy binding activity, all toxin preparations were titrated with increasing amounts of Torpedo membrane suspensions at toxin concentrations of ~ 10 nM (saturation). After overnight incubation at 20°C , the total radioactivity bound to the membranes was measured after centrifugation at 100,000 X g for 1 hr, and the remaining free concentration was measured by duplicate aliquots of the supernatant. For freshly-prepared radiolabeled bungarotoxins, 100% of the

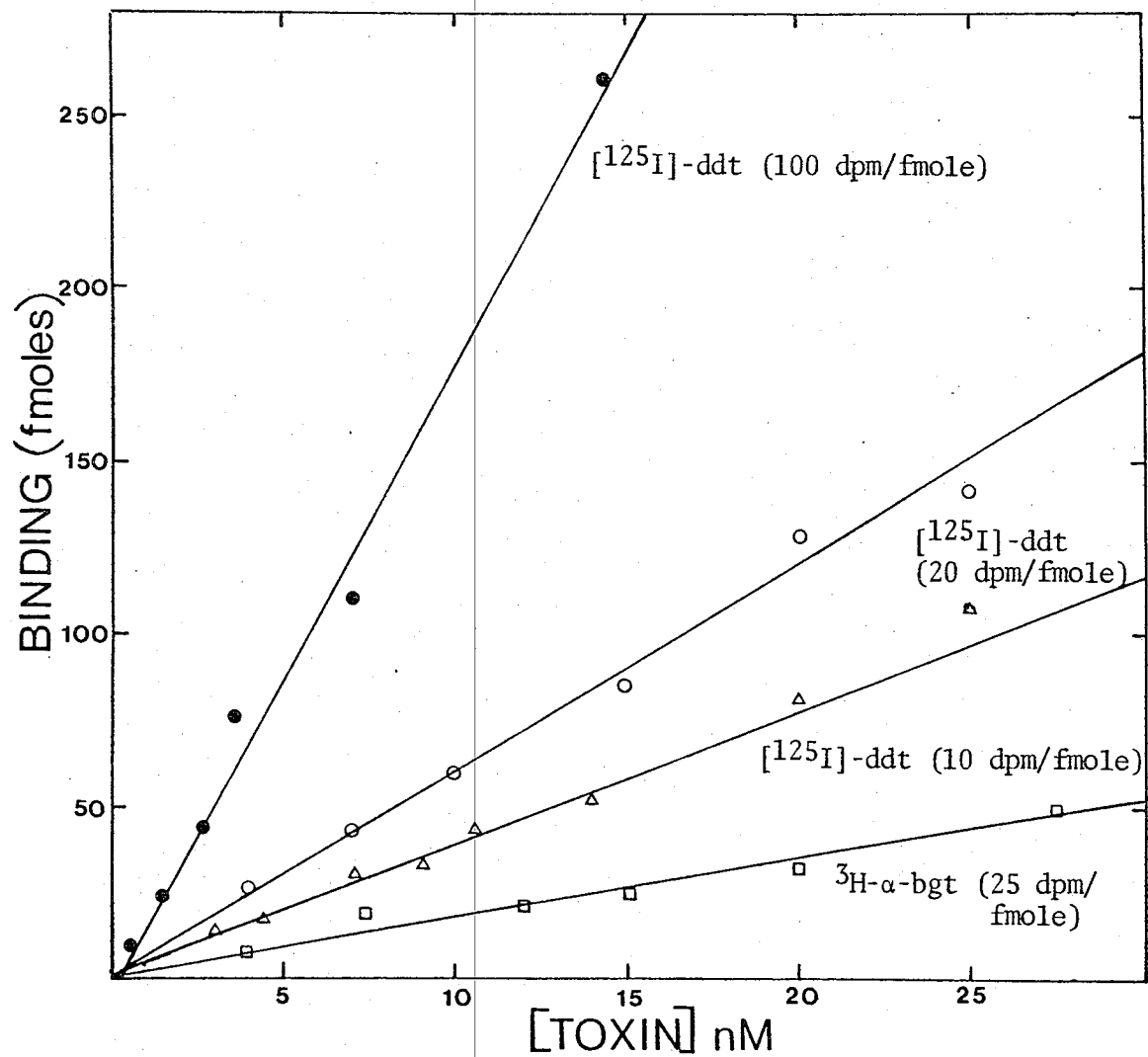
* Specific sites are defined as those given by the difference of total sites minus non-specific sites (given by pre-treatment with an excess of unlabeled toxin).

toxins was removed by nAChR excess. For [^{125}I]-ddt, the proportion varied between 40% and 60% in three preparations. The slope of the non-specific binding (see Figure 5-1) increased with increasing specific activity, but the proportion of toxin bound with receptor excess decreased. This suggested that the [^{125}I]-ddt preparations were a mixture of active and inactive species, and that the inactive species was much more non-specifically adsorptive. Accordingly, this property was used to remove inactive labeled ddt by incubating radiolabeled preparations with 1 mg/mL BSA, concentrating by lyophilization, and then chromatographing on a 1.6 X 10 cm DEAE-Sephadex column with 10 mM sodium phosphate buffer (pH 8.0). Material eluting at the void volume was [^{125}I]-ddt freed of inactivated ddt, as 100% could be bound with receptor excess. The strongly-adsorptive inactive derivative was retained as a complex with BSA on the column. Concentrations given in the Figures are total concentrations of [^{125}I]-ddt and are uncorrected for the active species. However, quantitative drug-competition experiments and dissociation constant determinations were corrected for the active concentration. To confirm that the active radiolabeled ddt was as biologically active as the unlabeled toxin, a preparation in which 60% of the [^{125}I]-ddt bound with receptor excess was progressively diluted with unlabeled ddt to give a saturation curve which was superimposable on that generated by directly varying the [^{125}I]-ddt concentration.

v. Solubilization and Purification of the Torpedo Acetylcholine Receptor.

Receptors were solubilized from nAChR-rich membranes by incubation with either 1% Emulphogene BC-720 or 1% sodium deoxycholate (added 0.1 mL per mg membrane protein) for 90 min at 4°C with constant stirring. Detergents were made up in 10 mM sodium phosphate buffer (pH 7.4) supple-

Figure 5-1
Non-specific binding of [125 I]-ddt to rat brain membranes at different specific radioactivities.



mented with 0.02% NaN₃ and 0.1 mM PMSF. After incubation, solubilization mixtures were centrifuged at 100,000 X g for 1 hr at 4°C. The supernatant was clarified through a Millipore filter and stored at 4°C. Under these conditions, 70-75% of the total membrane-bound ³H-α-bgt sites were solubilized and 22% of the total membrane protein, giving a roughly three-fold enrichment in specific binding activity.

Acetylcholine receptors were purified by the affinity column method of Schmidt and Raftery (36) from a Triton X-100-solubilized Torpedo californica crude preparation. The final product had a specific toxin-binding activity of 5 nmol/mg protein and was stored at 4°C in phosphate-buffered (pH 7.0) 0.1% Triton X-100 at ~100 μg protein/mL. The purified nAChR used in these studies was a gift of Prof. M.A. Raftery (California Institute of Technology).

vi. Preparation of Rat Brain Membranes. Wag/Rig rats (Lawrence Berkeley Laboratory breeding colony) were decapitated and chilled whole brains minus cerebellum were homogenized in 10 volumes of 0.32 M sucrose (pH 7.4 sodium phosphate buffer, 0.1 mM PMSF, 0.02% NaN₃) in a Teflon-glass homogenizer at 1000 rpm. The homogenate was centrifuged at 1000 X g for 10 min and the supernatants collected. The pellets were resuspended in 2 volumes of homogenizing medium, rehomogenized, and recentrifuged. The supernatants were pooled and the pellets discarded. The total supernatant was then centrifuged for 15 min at 17,800 X g at 4°C to yield a crude mitochondrial fraction in the pellet (which contains the bulk of synaptic membranes (37)). Crude mitochondrial fractions were then osmotically shocked by resuspension in 2 volumes of 0.02 M Tris buffer (pH 7.4) plus azide and PMSF, and pelleted at 19,000 X g for 10 min. The crude mitochondrial membrane pellet was then resuspended in 2 volumes of rat Ringer (115 mM NaCl, 5 mM KCl,

1.8 mM CaCl_2 , 1.3 mM MgSO_4 , 33 mM Tris at pH 7.4) and recentrifuged at 19,000 X g for 10 min. The resulting pellet was resuspended in rat Ringer for binding experiments. In some experiments, a total particulate fraction including microsomal membranes was prepared by taking the pooled supernatants from the first low-speed centrifugation, pelleting them at 100,000 X g for 30 min, resuspending in 2 volumes of 0.05 M sodium phosphate buffer (pH 7.4 + 0.02% NaN_3 + 0.1 mM PMSF), and then recentrifuging at 100,000 X g for 30 min. The final pellet was resuspended in rat Ringer.

vii. Solubilization of Rat Brain Membrane Proteins. Membrane proteins were solubilized from total particulate fractions by incubation in 1% Emulphogene BC-720 or 1% sodium deoxycholate for 90 min at 4°C (10% w/v suspensions). Detergents were made up in 0.05 M sodium phosphate buffer (pH 7.4) with preservative and protease inhibitor. After incubation, samples were centrifuged at 100,000 X g for 60 min. The resulting supernatant contained 20-25% of the total toxin-binding sites and 20% of the total membrane proteins, so no enrichment was achieved.

viii. Toxin Binding Assays. The binding of radioactively-labeled toxins to Torpedo nAChR-rich membranes was measured by a microfuge assay and the results confirmed by a filtration method (38). Ten μL of the membrane suspension (10 μg protein/mL) were added to 230 μL of Torpedo Ringer in polypropylene microfuge tubes. For ligand or unlabeled toxin competition studies, these additions were made 30 min prior to the addition of radioactively-labeled toxins. All samples were then incubated for 60 min at 21°C for competition studies, or for 16 to 18 hrs for equilibrium studies, followed by a 30 min chase with added unlabeled α -bgt (1 μM final concentration). Membranes were sedimented by centrifugation at 4°C for 6 to 10 min in a Beckman 152 microfuge, freed from the supernatants by aspiration

(duplicate 50 μ L aliquots were retained to check free toxin concentrations), resuspended in 250 μ L Ringer, sedimented again, and aspirated to dry pellets. Control experiments pelleted membranes at 100,000 X g in polycarbonate tubes for 60 min, and confirmed the suitability of membrane collection by the microfuge. For ^{125}I -labeled toxins, samples in γ -well tubes were counted directly in a γ -ray counter (41% efficiency). For ^3H - α -bgt, pellets were quantitatively dispersed and transferred to scintillation vials by either solubilization in Protosol overnight, 3 X extraction with trifluoroethanol, or by exhaustive rinsing with 0.1 mL aliquots of Ringer containing 2% SDS. All techniques gave values within 7%. Extracts were, in all cases, counted in 16 mL of Aquasol 2 (Packard) on a Packard Tri-Carb scintillation spectrometer (37-42% efficiency) after overnight storage to eliminate chemiluminescence.

Toxin binding to brain membranes was assayed in 250 μ L of rat Ringer with incubation for 60 min at 21°C. At the end of the incubation period, the suspension was diluted with 3 mL of a sodium phosphate buffer, and sedimented at 18,000 X g for 10 min. The pellet was resuspended and washed 3 X in order to bring the non-specific binding to a reproducible minimum. Pellets were transferred to scintillation vials by repeated washing for ^3H - α -bgt, or to γ -well tubes for counting ^{125}I -labeled toxins. Total binding levels were determined by chasing samples with an excess of native α -bgt for 30 min after the radiolabeled-toxin incubation period. Under these conditions, all specific binding sites are occupied by radiolabeled toxin, and the cold chase methodology dilutes non-specific binding to the same degree as in the non-specific binding samples (see ref. 39). Non-specific binding was defined by pre-treatment of samples with a 100X molar excess of unlabeled toxin for at least 30 min prior to the addition of radiolabeled

toxins.

Toxin binding to solubilized and purified nAChR was determined by the DE81 (Whatman) filter disk method (40). ^{125}I -labeled toxins were measured directly on the disk and ^3H - α -bgt binding was measured, after overnight desorption from the disks using 1 mL of 1N NaOH/2M NaCl, in 16 mL of Aquasol 2.

Variations on the general methodologies described in this section are indicated in Figure and Table legends.

ix. Sucrose Gradient Centrifugation. A crude particulate fraction from the brains of 4 rats was prepared by a 100,000 X g centrifugation as described in section vi. The pellet was resuspended in rat Ringer to a final concentration of 20 mg membrane protein/mL and split into 4 X 3 mL samples. Two samples were given [^{125}I]- α -bgt (10.4 nM) and the other two were given [^{125}I]-ddt (14.6 nM). In one of the samples from each pair, excess α -bgt was pre-equilibrated (10 μM) for 30 min prior to the addition of radiolabeled toxins. These samples defined non-specific binding. Radiolabeled toxins were incubated with all samples for 60 min at 22°C. Unlabeled α -bgt (10 μM) was added to the second pair of samples (total binding) for 30 min additional incubation. Samples were freed from excess unbound toxin by centrifugation at 100,000 X g for 30 min. Each pellet containing bound toxin was resuspended in 3 mL of dilute phosphate buffer.

Aliquots were checked for specific binding (total minus non-specific) and gave values of 21.3 fmol/mg protein for [^{125}I]- α -bgt and 46.6 fmol/mg protein for [^{125}I]-ddt. Each sample was then applied to a 36 mL 5-50% linear sucrose gradient prepared in dilute phosphate buffer equilibrated to 4°C. Gradients were centrifuged in a Beckman SW27 rotor at 25,000 rpm for 16 hrs at 4°C. Each gradient was fractionated into 0.65 mL samples which were tested for protein content by the Lowry method and counted

for radioactivity. Additional details are given in the Figure legend.

x. Chemical Modifications. The procedures for dansylation, N-bromosuccinimide oxidation of trp, catalytic reduction of sulfur-containing residues, dimethyl suberimidate cross-linking, and iodination of tyr residues have been given in the Chapters III and IV Methods. Additional chemical modifications of α -bgt followed literature procedures: 1) modification of trp by dimethyl-(2-hydroxy-5-nitrobenzyl) sulfonium bromide (Koshland reagent I, see ref.41, Pierce Chemical); 2) photooxidation of his by Rose Bengal (Aldrich)-sensitized illumination (42); 3) selective reduction of the fifth disulfide (Cys₂₉-Cys₃₃) by rapid quenching (20 min) of 0.1 M sodium borohydride (Fisher Scientific) reduction (43); 4) N-acetyl imidazole modification of tyr (44); and 5) 2,4-pentanedione (Aldrich) modification of arg and lys and selective arg modification by hydroxylamine restoration of lys residues (45).

RESULTS.

i. Toxicology. The quantitative aspects of the lethality of the purified toxins are indicated in Table V-3. The slopes of the mortality vs. dose curves were very steep for all toxins, giving slope functions between 1.05 and 1.20. The ratios of the LD₅₀s observed with intraperitoneal vs. subcutaneous injections were 0.5 to 0.9 for α -bgt and toxins 6 thru 9A, while for all the remaining toxins the values were between 0.14 and 0.2 (compare values in Tables V-3 and V-4). The higher ratios point to the freer access of the smaller toxins to their physiological target site, and more rapid diffusion.

As expected, the time to death was sensitive to the dose. To facilitate the comparison between toxins, the doses were normalized to their respective LD₁₀₀s. Two examples of time-to-death vs. dose curves are shown in

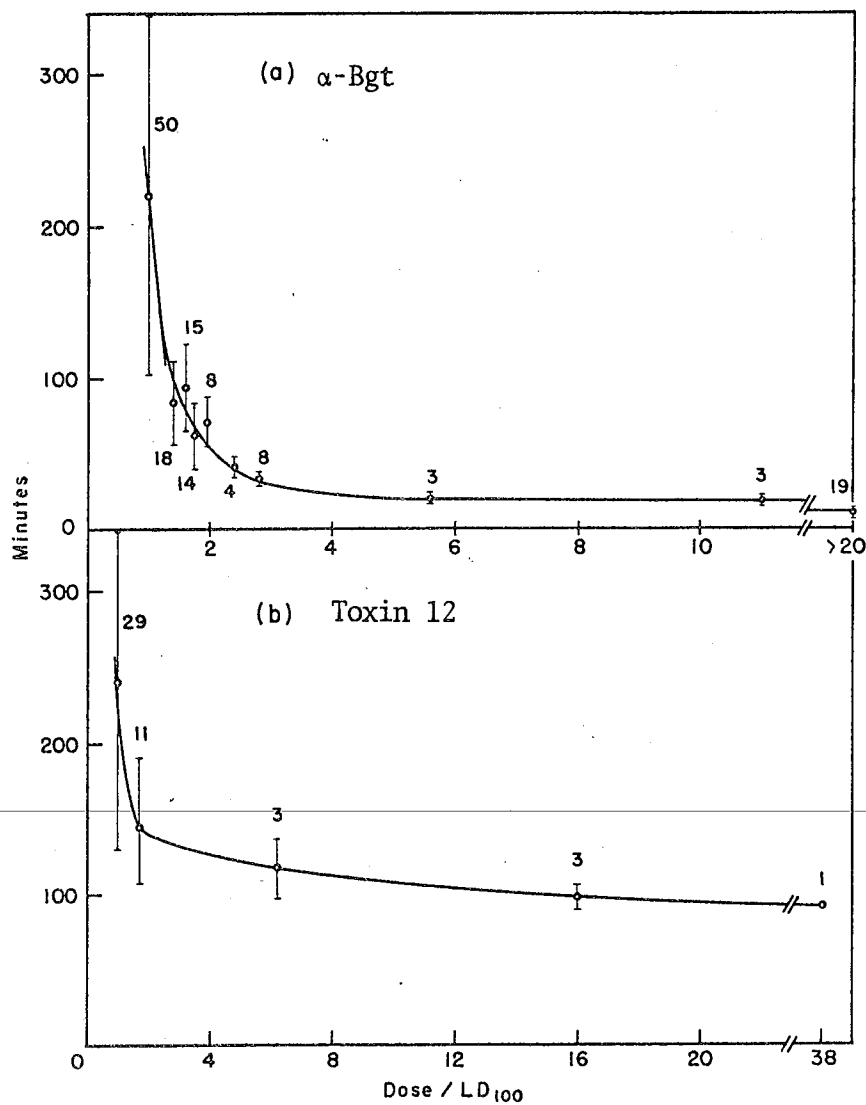
TABLE V-3
LETHALITY OF BUNGAROTOXINS AFTER SUBCUTANEOUS INJECTIONS

Toxin	(µg/g mouse)		Time to death ^a (mean ± SEM)		Minimum time to death ^b min.
	LD ₅₀	LD ₁₀₀	No.mice	min.	
α-Bgt	0.14	0.16	28	190±23	8
7	0.17	0.19	15	138±24	21
8	0.46	0.68	31	153±22	25
9A	0.25	0.55	21	500±58	117
β-Bgt	0.06	0.08	30	230±20	72
11	0.16	0.21	26	267±27	79
12	0.09	0.11	29	241±21	92
13	0.04	0.05	30	215±16	75
14	0.15	0.17	29	315±28	124

^a For doses between 0.83 and 1.25 X LD₁₀₀.

^b At the highest dose used (>15X LD₁₀₀).

Figure 5-2
Time to death vs. dose for representative α - and β -toxins.
Results are for subcutaneous injections.



XBL744-5132

Figure 5-2. At high doses, the α -toxins killed in less than 25 min. In contrast, there was an apparent latent period for the β -toxins because the time-to-death could not be reduced below 70 min at even the highest concentrations. This provides one basis for the functional division of the toxins, since all β -toxins had this characteristic latent period.

α -Toxins always killed with 5 hrs, or the mice would recover. The symptoms were flaccid paralysis and respiratory distress, as noted for other curarimimetic toxins (46). These values are compared to those reported earlier by Lee et al (47) in Table V-4. There is good agreement. Time-to-death has been used in the past to titrate cobra toxin doses (48) as the log plot of time vs dose gave a good fit to a straight line. This method is also applicable to the bungarotoxins, albeit their linear range is more limited.

Preliminary evidence was obtained for the physiological persistence of α -toxins. Injection of doses in the range of LD_0 to LD_{90} inevitably left some survivors which were given second injections one day later. It was estimated from percentage mortality and time-to-death that as much as 50% of the previous dose was present.

ii. Inhibition of Sodium-22 Efflux from Excitable Vesicles. As noted in the Introduction (Chapter I), the cholinomimetic drug stimulation of the release of trapped ^{22}Na from pre-loaded nAChR-rich vesicles constitutes a biochemical test system for the analysis of effects of compounds on nAChR function. The addition of α -bgt to a final concentration of $1\ \mu\text{M}$ completely abolished the ability of carbachol to trigger ^{22}Na release above the resting rate (see Figure 5-3). The Figure also shows that a similar concentration of the putative pre-synaptic neurotoxin crotoxin can also block the accelerated efflux. This is an example of the detection of a false-positive for a post-synaptic agent, because these vesicles

TABLE V-4
COMPARISON OF TOXINS IN THIS WORK WITH THOSE DESCRIBED BY LEE ET AL (47)

<u>Toxin</u>	<u>LD₅₀[*]</u>	<u>Lee et al Fraction</u>	<u>LD₅₀[*]</u>
α-Bgt	0.11 (0.10-0.12) ^a	II ₂	0.15 (0.10-0.22)
6	1.2 (1.1-1.3)	IV ₁	2.12 (1.40-3.20)
7	0.15	III ₁	0.25 (0.22-0.29)
8	0.41 (0.31-0.51)	III ₂	0.74 (0.69-0.80)
9A	0.15 (0.1-0.2)	IV ₂	0.28 (0.21-0.38)
β-Bgt	0.01 (0.005-0.02)	V	0.014 (0.011-0.018)
11	0.022 (0.01-0.03)		
12	0.014 (0.011-0.017)	VI	0.053 (0.039-0.072)
13	0.007 (0.005-0.009)	VII	0.016 (0.011-0.022)
14	0.045 (0.04-0.05)	VIII	0.04-0.05

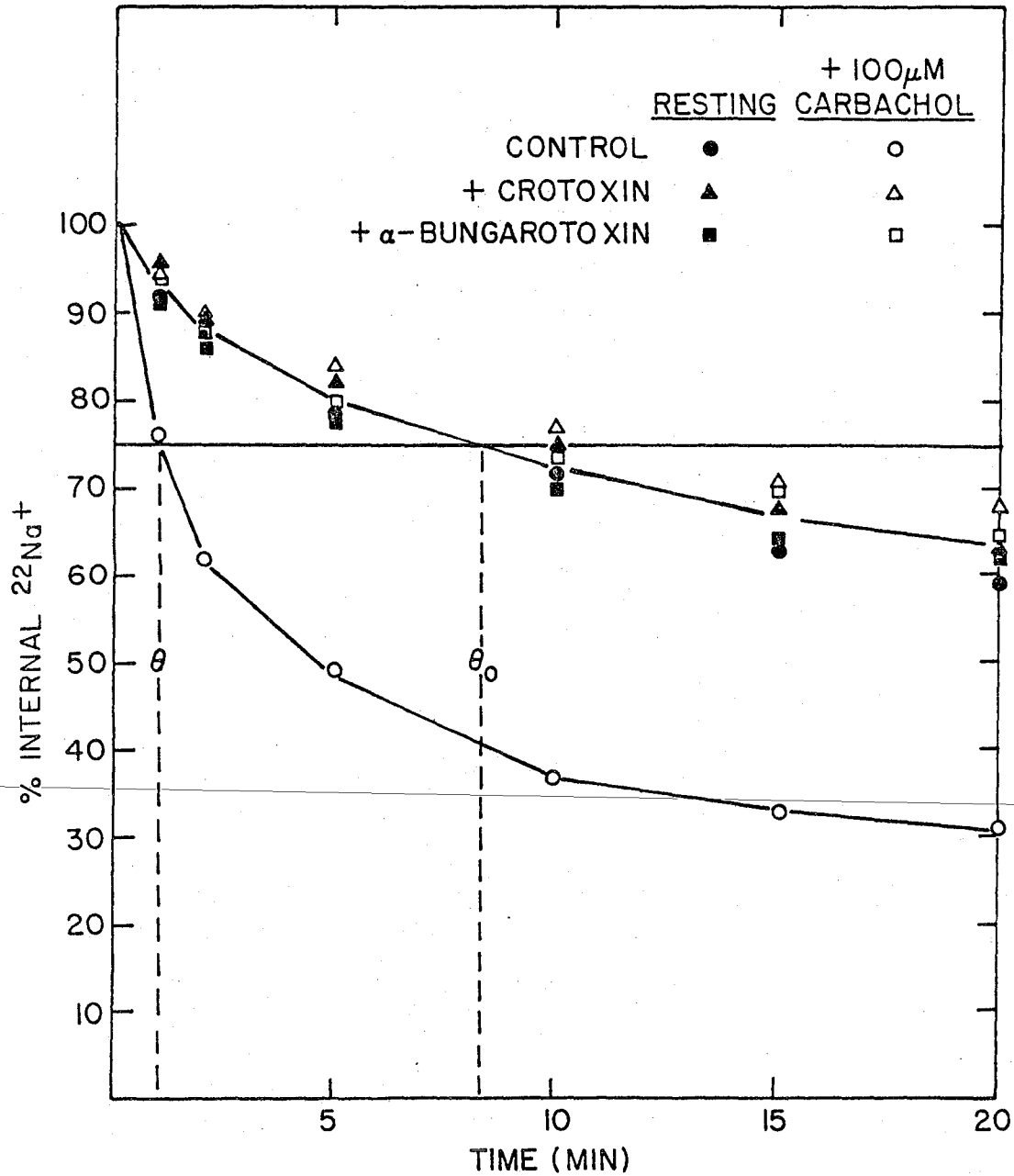
*

μg/g mouse weight by intraperitoneal injections.

a

Figures in parantheses are intervals of confidence as calculated by method of Litchfield and Wilcoxon (29).

Figure 5-3
 Resting, stimulated, and blocked efflux of ^{22}Na from pre-loaded Torpedo californica excitable vesicles. Results have been normalized to a percentage of the trapped ^{22}Na at time zero. The reference parameters (θ_0, θ) are shown.



XBL7712-4793

appear to be unusually sensitive to the phospholipolytic activity of crotoxin (49) and other snake phospholipases (50). Thus, one precaution is to insure that the effect of a blocking agent does not arise from a non-specific degradative action. By incubating the vesicles with a smaller concentration of toxin than a molar equivalent to the total number of toxin-binding sites, it was demonstrated that only partial inhibition of the efflux resulted in proportion to the expected fraction of blocked sites (Table V-5). Further, longer incubations with these sub-stoichiometric doses did not improve their antagonistic potency. These observations are unlike those seen with enzymatic disruption of excitable vesicles (49,50, see Chapter VI).

Toxins 7 and 8 also blocked the ^{22}Na efflux induced by carbachol. The characteristics of the other toxins indicated that their effects were mediated by their intrinsic phospholipase A activities in a fashion very like crotoxin (see Chapter VI for a full discussion of these data). To show that α -bgt, 7 and 8 were functionally competitive with d-tubocurarine, a known post-synaptic antagonist (51), undiluted vesicles were incubated with 0.1 mM d-tubocurarine or 1 μM α -bgt or both. Subsequent dilution of the vesicles indicated that excitability was blocked by treatment with α -bgt alone. However, dilution into medium containing 0.1 mM d-tubocurarine suppressed carbachol stimulation. These results indicate that d-tubocurarine is a rapidly reversing antagonist, unlike α -bgt which is much more persistent, and that it can protect against α -bgt blockade. Thus, α -bgt and toxins 7 and 8 are curarimimetic toxins, as earlier pieces of evidence had suggested. The ^{22}Na -efflux data are summarized in Table V-5.

iii. Radioactive Labeling of α -Bgt and Ddt. Iodinated derivatives of the two toxins were purified by ion exchange chromatography on CM-cellulose.

TABLE V-5
SUMMARY OF SODIUM-22 EFFLUX EXPERIMENTS WITH α -TOXINS

<u>Treatment*</u>	<u>θ_0(min)</u>	<u>θ(min)</u>	<u>θ_0/θ</u>
Control (10)	9.3 \pm 1.0	1.0 \pm 0.1	9.3 \pm 1.0
α -Bgt (4)	8.6 \pm 0.8	9.2 \pm 0.9	0.9 \pm 0.1
Toxin 6 (2)	8.8	9.3	1.0
Toxin 7 (2)	9.5	9.4	1.0
Toxin 8 (2)	9.9	9.0	1.1
α -Bgt (0.5 μ M) (2)	9.0	2.0	4.5
α -Bgt (0.25 μ M) (2)	8.9	1.4	6.4
α -Bgt (0.25 μ M, 60 min) (2)	9.4	1.4	6.7
α -Bgt, followed by dilution** (2)	9.0	8.8	1.0
α -Bgt/100 μ M d-TC, followed by dilution**	9.3	1.1	8.5
100 μ M d-TC, followed by dilution** (2)	9.4	0.9	10.4
100 μ M d-TC (2)	9.1	9.2	1.0

* Toxins were added for 15 min at 4°C to a final concentration of 1.0 μ M, unless otherwise noted.

**

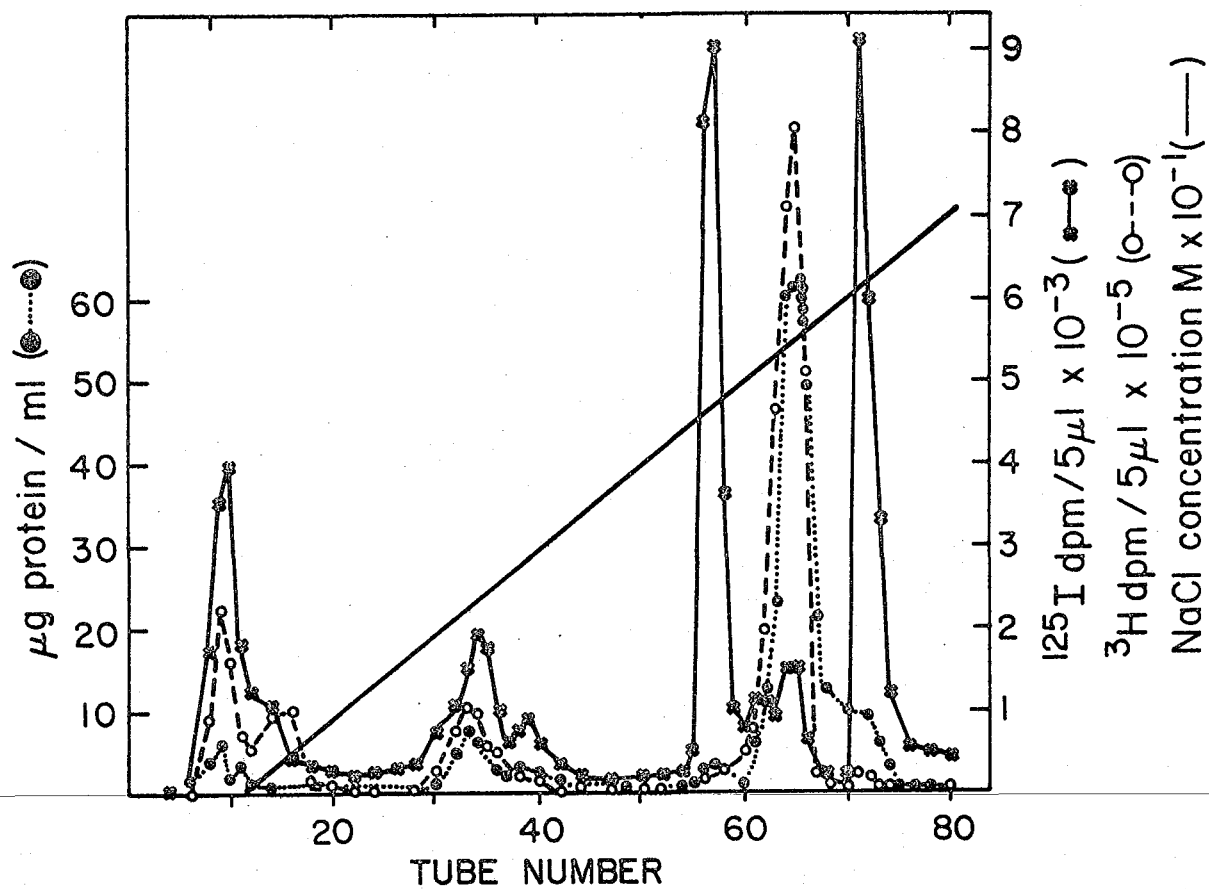
Toxins were added before dilution of 100 μ L aliquots of vesicles, and were allowed to equilibrate for 20 min. Upon dilution, concentration of α -bgt was reduced to \sim 10 nM and d-TC was reduced to \sim 1 μ M.

When ddt was iodinated, the only radiolabeled product was moniodinated. When α -bgt was modified under the same conditions, both mono- and diiodinated derivatives were produced. Figure 5-4 shows the chromatographic profile for the elution order of the radiolabeled derivatives of α -bgt. All species were well-resolved. ^3H - α -bgt and native toxin had identical elution patterns, supporting the idea that native structural properties are restored by catalytic replacement of the iodine atoms. Further support for this claim was provided by CD and UV absorption spectra of hydrogenated products from nonradioactive iodinated toxins, which were indistinguishable from native toxin. Both monoiodinated and diiodinated α -bgt have been successfully used for catalytic tritiation, with the latter yielding, as expected, a derivative of twice the specific activity of the former.

iv. α -Bgt Binding to Torpedo nAChR. As noted in the Methods, both iodinated and tritiated derivatives of α -bgt were homogeneous by radiochemical measures, physical techniques, and binding activities.

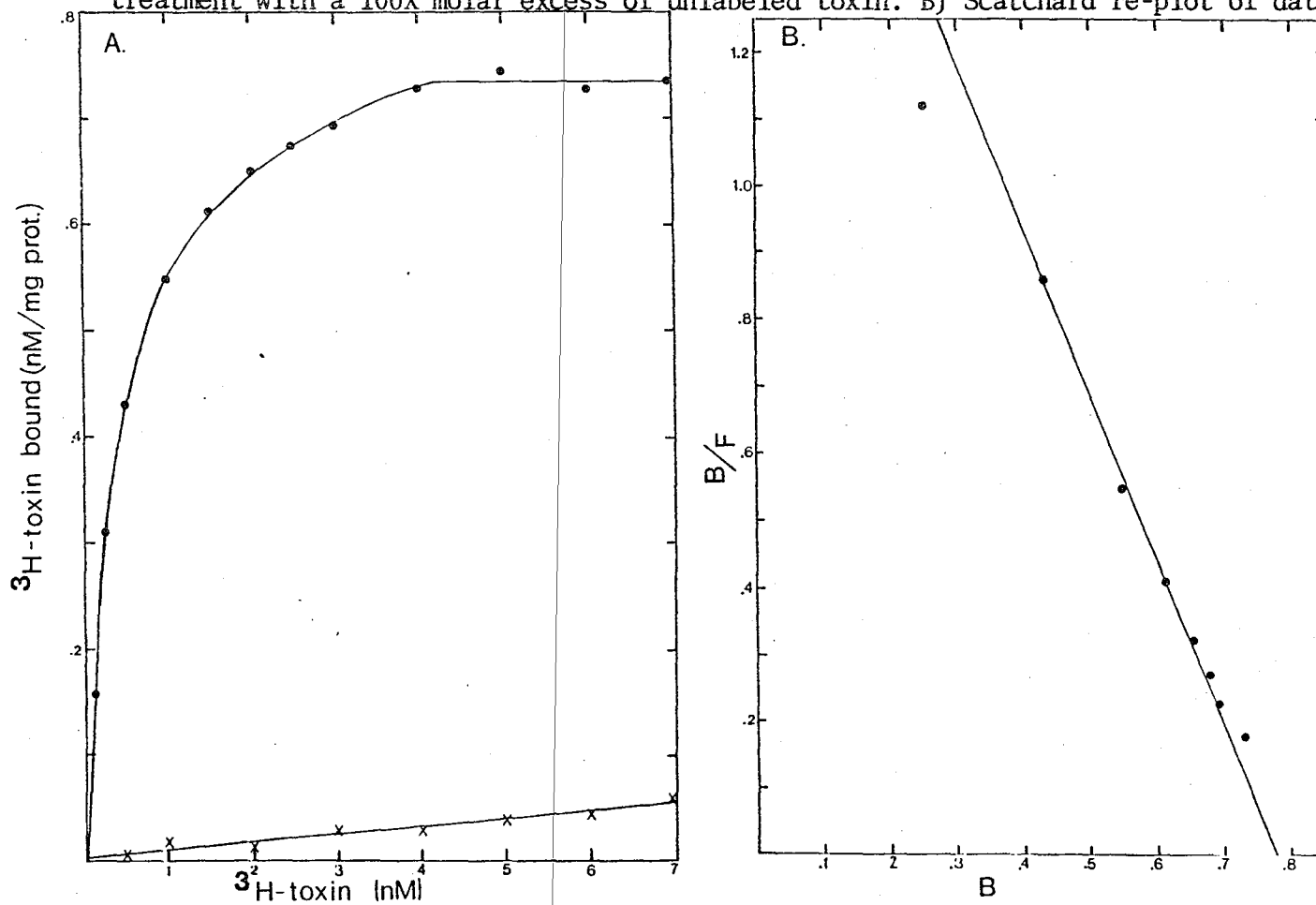
Figure 5-5 shows the saturation of a fixed concentration of Torpedo nAChR membranes by increasing concentrations of ^3H - α -bgt. The Torpedo nAChR concentration was chosen to be low enough so that significant depletion of the free concentration did not take place during the time course of the binding assay, and this was directly checked by routine monitoring of the free toxin concentration at the termination of the assay. Non-specific binding under these conditions was so low that total binding levels could be used at low toxin concentrations without correction. Replotting of the data in Figure 5-5A on a Scatchard plot (52) gives estimates of the K_d^{app} (apparent dissociation constant) from the slope, and the total number of binding sites at saturation from the x-

Figure 5-4
Elution profiles of labeled and unlabeled α -bgt with gradient chromatography from a CM-52 column. Experimental details are given in Methods.



XBL 779-4606

Figure 5-5
Saturation of ^3H - α -bgt binding to Torpedo nAChR-rich membranes. A) linear plot of specific (----) and non-specific binding (-X-X-) as a function of ^3H -toxin concentration. Specific binding was given by (total minus non-specific) where the total binding was measured after 60 min incubation at 21°C, followed by a 30 min chase with a 100X molar excess of unlabeled toxin, and the non-specific binding was defined by a 30 min pre-treatment with a 100X molar excess of unlabeled toxin. B) Scatchard re-plot of data in A).



intercept. The latter value was ~ 0.78 nM/mg protein, in good agreement with literature values on comparably enriched membranes (22, 30, 38). The K_d^{app} was ~ 0.5 nM in reasonable accord with literature figures (see Table V-2). However, the term K_d^{app} is used deliberately to indicate that this measure should not be regarded as a true dissociation constant, but should only be considered a means of indexing direct saturation binding curves conducted under the same conditions. Previous work has shown that true equilibrium is not reached when the time-dependent uptake of radiolabeled toxin reaches saturation (22, 38, 53), but rather takes many hours (38, 53). True equilibrium measurements are reported later, as are K_d s determined by kinetic methods (22, 38, 54).

Figure 5-6 shows that toxins 6 thru 8 are all antagonists of the interaction of ^3H - α -bgt with nAChR. Comparison of their potencies to that of unlabeled α -bgt shows that they inhibit binding in the order α -bgt > 7 > 8 > 6, and have parallel slopes. To investigate whether the other α -toxins are truly competitive with α -bgt binding, equilibrium saturation plots in the presence of fixed concentrations of 6 thru 8 were determined and replotted on a double-reciprocal format. An example is shown in Figure 5-7 for toxin 8. The intersection of the three straight lines on the y-intercept indicates that the rate is altered, but not the total number of sites. Thus, toxins 6 thru 8 are all competitive inhibitors of α -bgt, differing in their affinities for the receptor site. Similar conclusions have been reached using a wider range of competing snake toxins against ^3H -Naja nigricollis toxin α (53).

A large body of work indicates the mutual antagonism of α -toxin and cholinergic agonist/antagonist binding (22, 23, 55). In Figure 5-8, the inhibition of ^3H - α -bgt binding by two nicotinic agonists, acetylcholine

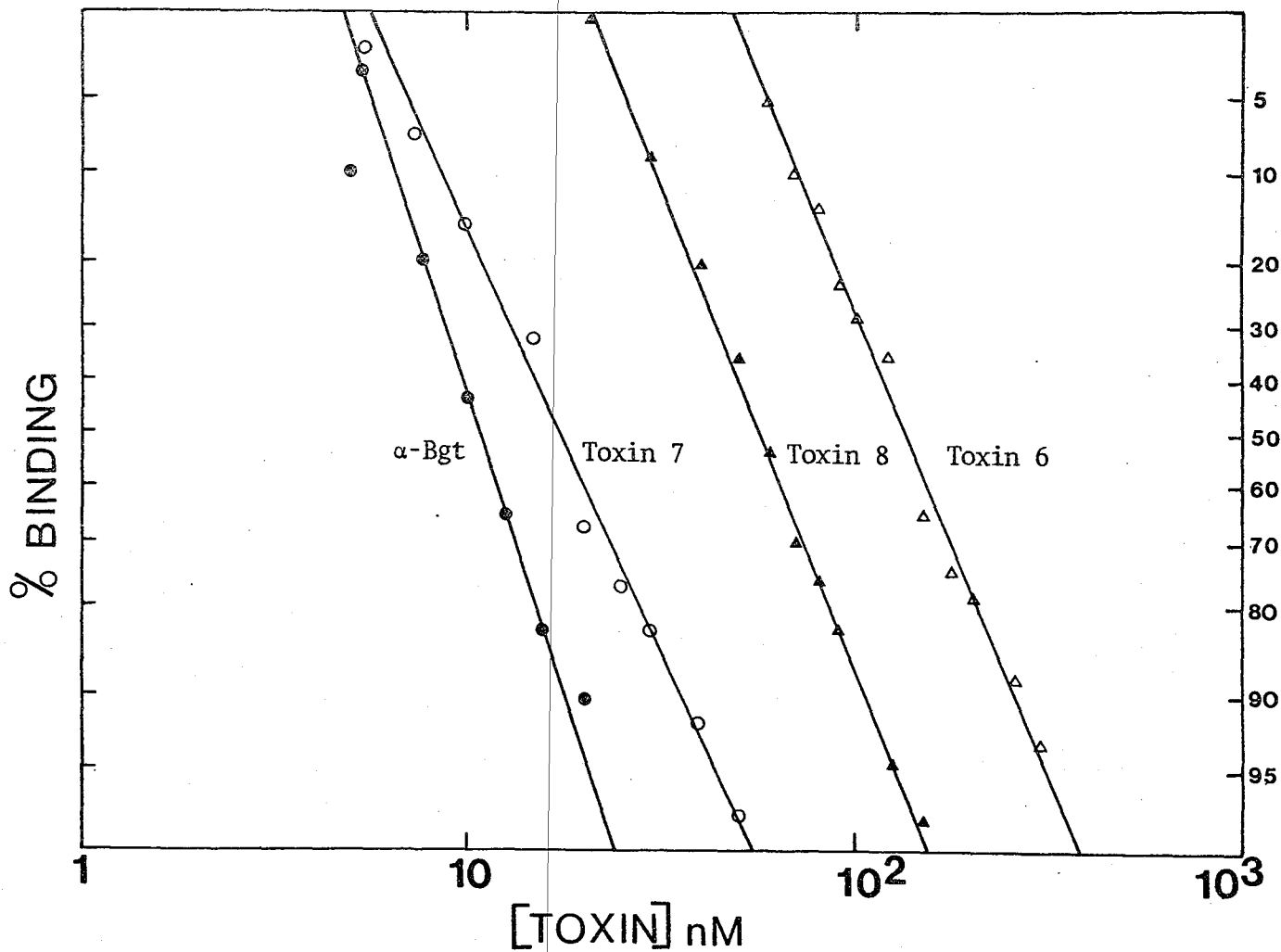


Figure 5-6
 Competition of unlabeled toxins against ^3H - α -bgt binding to Torpedo membranes. Labeled and unlabeled toxins were coincubated for 18 hrs at 21°C in 250 μL of Torpedo Ringer containing a total of 0.4 pmoles nAChR. Final concentration of ^3H - α -bgt = 10.5 nM.

Figure 5-7

Double reciprocal plot of toxin 8 competition against ^3H - α -bgt saturation binding to Torpedo membranes. Toxins were coincubated for 17 hrs at 21°C with 0.1 pmole of nAChR in 250 μL Torpedo Ringer. B-bound toxin, F-free toxin (checked by counting of aliquots of supernatant after centrifugation of incubation mixture).

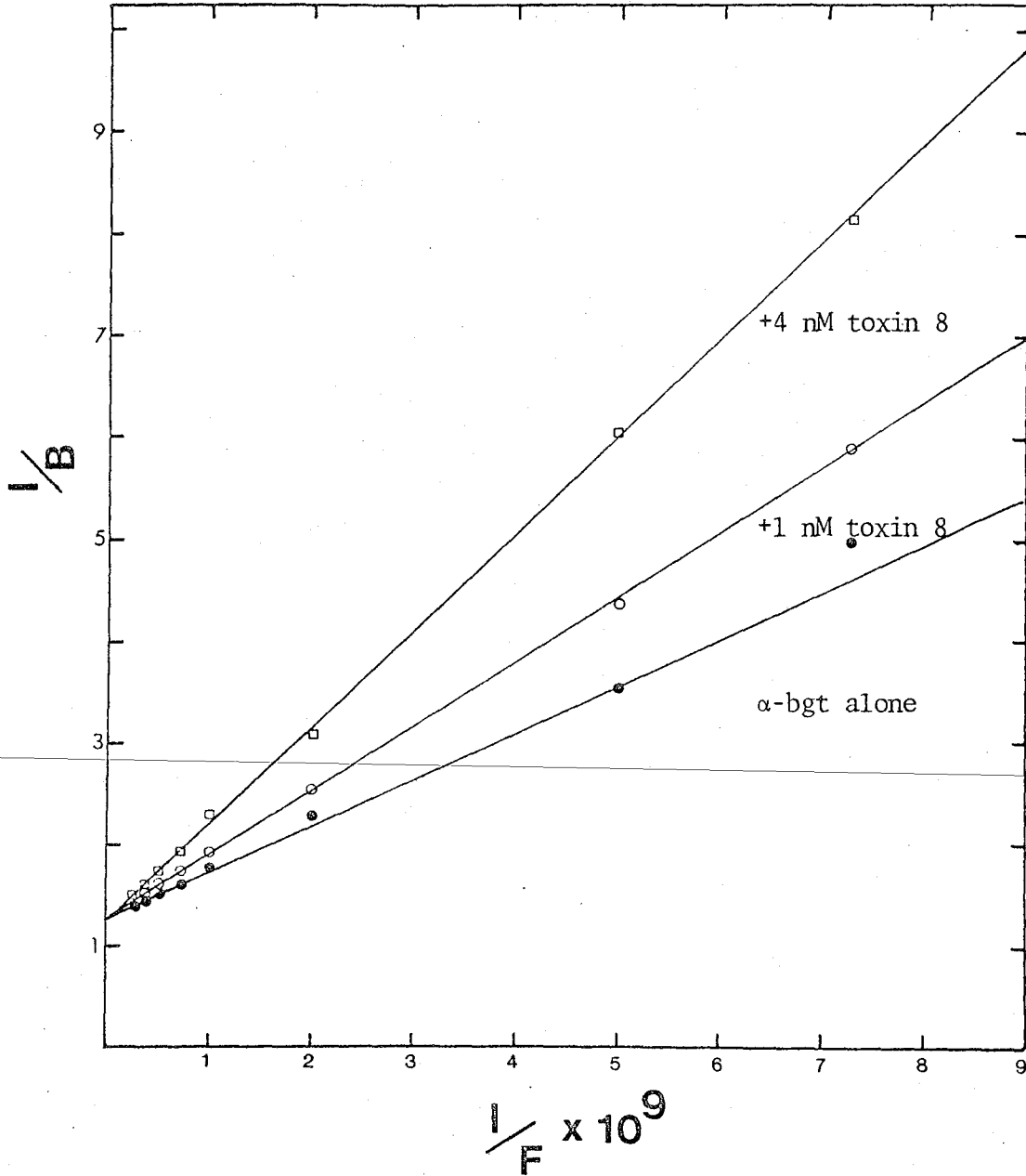
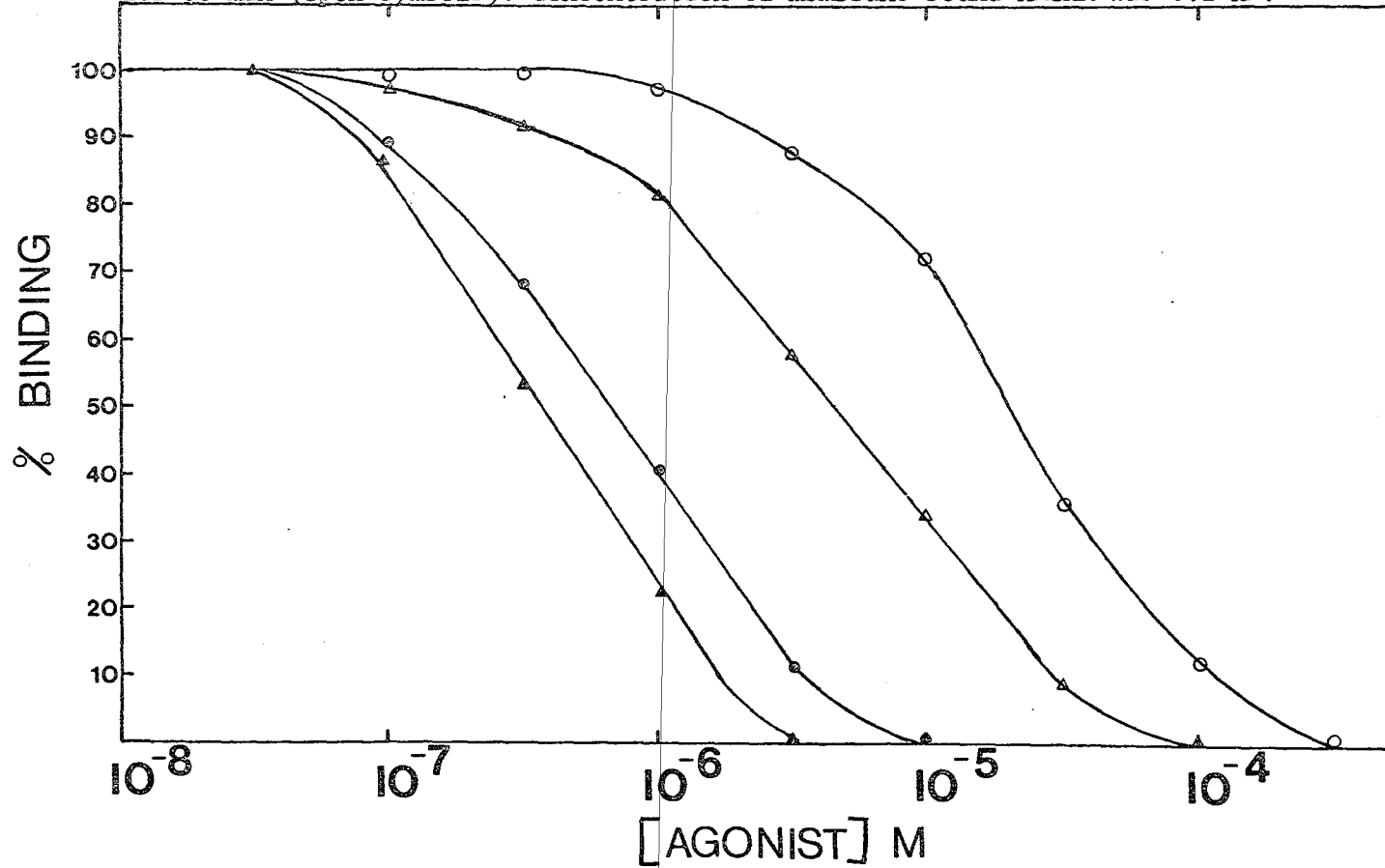


Figure 5-8

Competition of acetylcholine (circles) and nicotine (triangles) against 0.8 nM ^3H - α -bgt, with either 30 min pre-equilibration (solid symbols) before addition of toxin or coincubation for 60 min (open symbols). Concentration of membrane-bound nAChR was 0.2 nM.



and nicotine, is shown. This demonstrates that the toxin binding site responds to nicotinic compounds and thereby fulfills a pharmacological criterion of receptor specificity. Another point is indicated in the Figure. With increasing times of exposure to the agonists, the agonist potency against α -bgt increases, suggesting the time-dependent conversion of the nAChR to a form with higher agonist affinity. This process has been described in some detail (24,25,56) as an in vitro model of desensitization. Subsequent dilution of the agonist rapidly reverses the high-affinity state to the resting form (24,25,56).

The association rates for radiolabeled α -toxins are much slower than diffusion-limited processes (57). Figure 5-9 illustrates the association rates for ^3H - α -bgt and [$^{125}\text{I}_2$]- α -bgt on membrane-bound nAChR. Half-completion of the reaction with the tritiated toxin was reached at 7 min and with the diiodinated toxin at 21 min. Thus, diiodinated α -bgt is much slower in its initial receptor interaction. Since the dissociation of the toxin from the receptor is extremely slow (22,38), and the concentrations of both nAChR and radiolabeled toxins greatly exceed the true equilibrium K_d , the reverse reaction need not be included in the forward rate formulation. Thus, we can assume that ^3H - α -bgt binds irreversibly to a homogeneous population of non-interacting sites and the equation for the forward rate is given by:

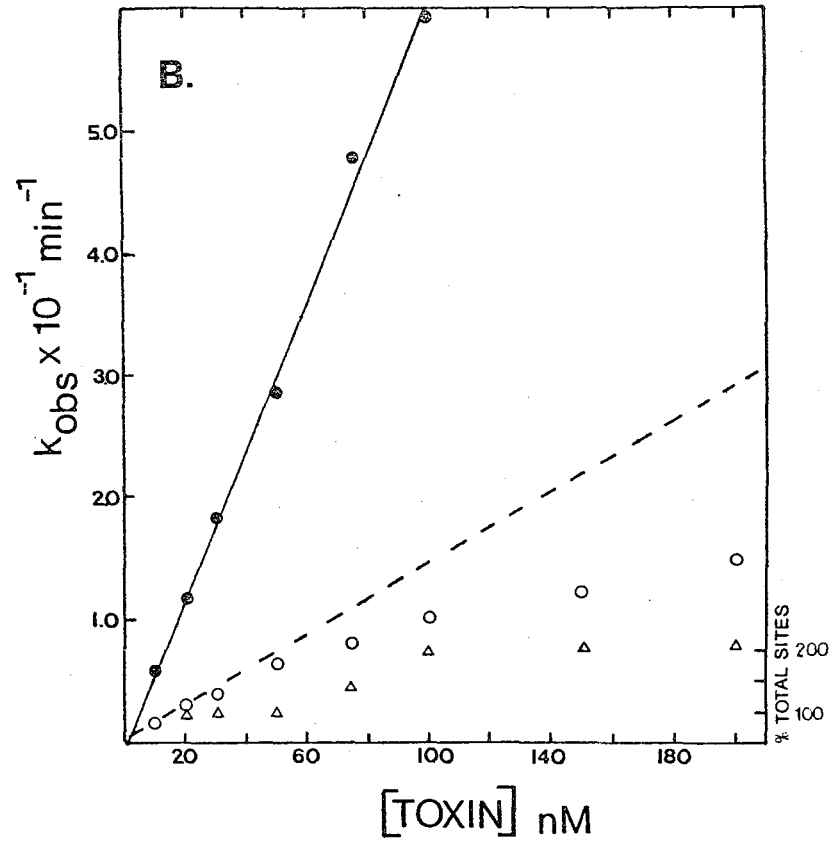
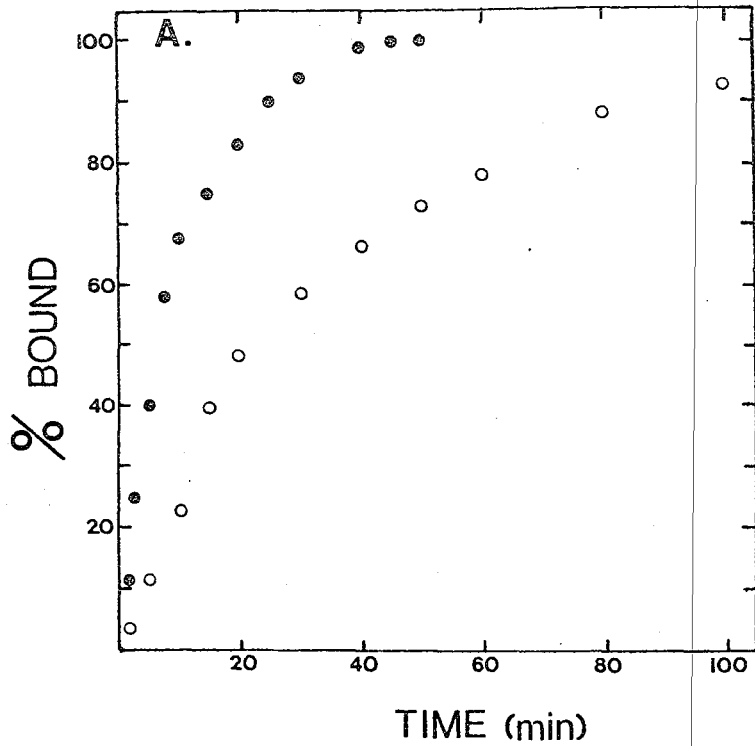
$$k_1 t = \frac{1}{R_0 - T_0} \cdot \ln[(T_0/R_0) \times (R_0 - B)/(T_0 - B)]$$

where k_1 = forward rate constant, t = time, R_0 = total α -toxin sites, T_0 = initial free toxin concentration, and B = the amount of bound toxin. Replotting of the data in Figure 5-9A gives a good straight line fit for the first 30 min with ^3H - α -bgt and 60 min for [$^{125}\text{I}_2$]- α -bgt. From the slopes of these replotted data, $k_1 = 5.95 (10^6) \text{ M}^{-1}\text{min}^{-1}$ for ^3H - α -bgt and $k_1 =$

Figure 5-9

A) Association rate for ^3H - α -bgt and $[^{125}\text{I}_2]$ - α -bgt on Torpedo membranes at concentration of 10 nM for toxins, 4.2 nM for nAChR.

B) Concentration dependence of initial binding rate (k_{obs}).
Solid circles- ^3H - α -bgt, open circles- $[^{125}\text{I}_2]$ - α -bgt, triangles-total sites at saturation.



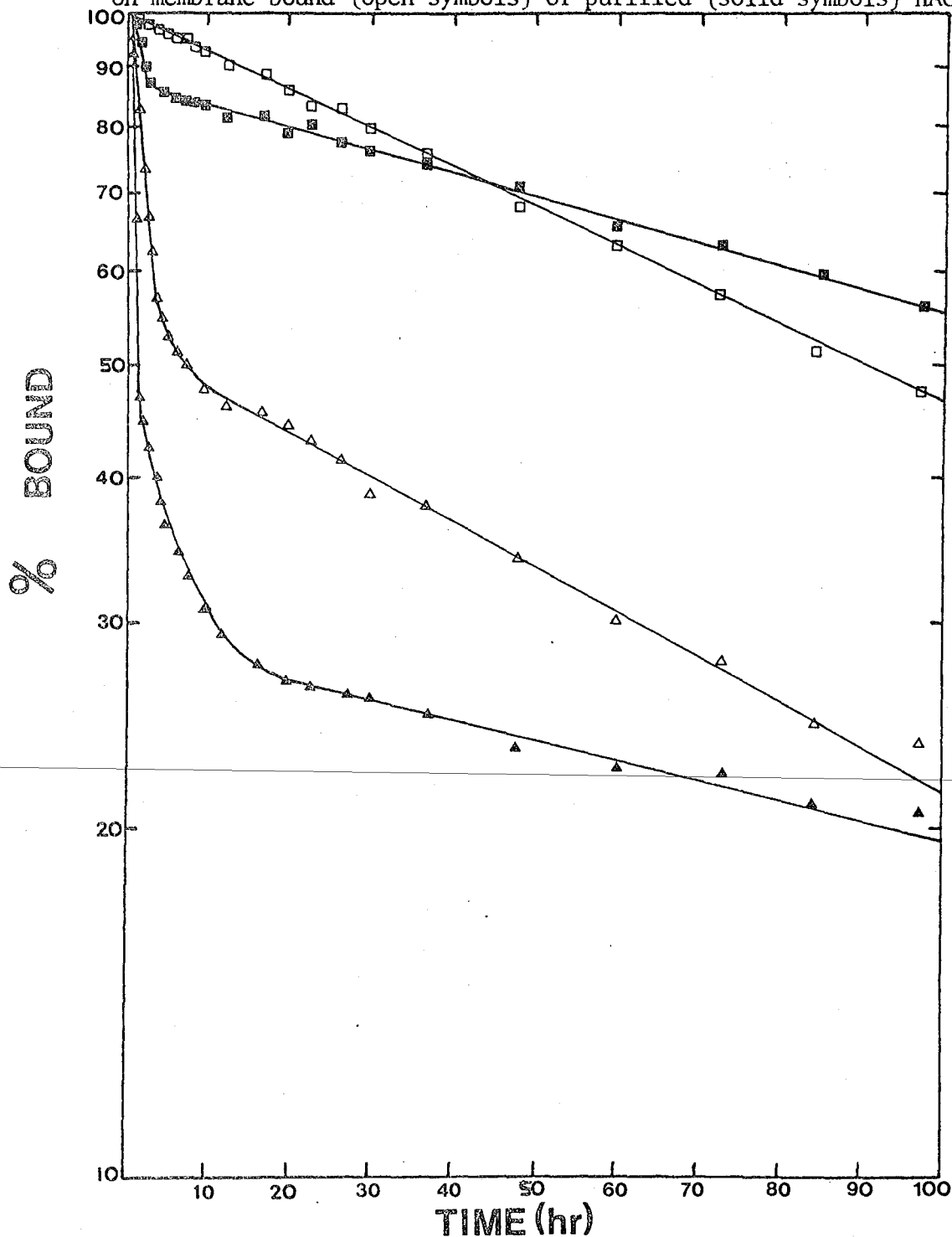
1.55 (10^6) $M^{-1}min^{-1}$ for [$^{125}I_2$]- α -bgt.

If the reaction is truly a simple bimolecular association, then the rate (k_{obs}) should be linearly dependent upon the initial concentration of the reactants. This is true for 3H - α -bgt over wide range of toxin concentrations (up to 100 nM), whereas the rates fall off from initial linearity for [$^{125}I_2$]- α -bgt at concentrations above 30 nM (see Figure 5-9B). At higher toxin concentrations, the rate appears to stabilize at a lower value as indicated by the stable slope. Calculating the slower rate gives $k_1 = 0.6$ (10^6) $M^{-1}min^{-1}$, a value less than half that observed at low concentrations for [$^{125}I_2$]- α -bgt. A linear concentration dependence of the initial rate has also been observed with 3H -Naja nigricollis toxin (38) and 3H -cobrotoxin (22), but monoiodinated α -bgt has been reported to give decreasing rates above 100 nM (58). Thus, both mono- and diiodinated α -bgt derivatives differ, not only in their rates from 3H - α -bgt, but also in the dependence of k_1 on toxin concentration. Another important difference is indicated in Figure 5-9B, which is the measured number of total sites appears to increase with increasing [$^{125}I_2$]- α -bgt concentration until the levels stabilize at twice the number of 3H - α -bgt sites. These results suggest that self-association of iodinated toxin derivatives might play a role in multiphasic kinetics observed at high concentrations (>10 nM). However, there are multiple phases observed with tritiated toxins as well, which are unlikely to be attributable to self-interaction (22).

Dissociation kinetics indicate further complexities in the toxin interactions. Figure 5-10 shows that 3H - α -bgt follows a single exponential relaxation process ($\tau_{1/2}=90$ hrs) in its release from membrane-bound nAChR sites, but when incubated with purified nAChR (in 0.1% Triton X-100), gives two phases, a fast ($\tau_{1/2}=9$ hrs) and a slow ($\tau_{1/2}=130$ hrs) rate. [$^{125}I_2$]-

Figure 5-10

Dissociation kinetics for ^3H - α -bgt (squares) and $[^{125}\text{I}]$ - α -bgt (triangles) on membrane-bound (open symbols) or purified (solid symbols) nAChR.



Radiolabeled toxins were incubated with Torpedo membranes at >10 nM, to insure saturation, for 4 hrs at 21°C , and were then sedimented at $100,000 \times g$ for 30 min. Membranes were diluted to 400 mL of 50 fmoles nAChR/mL with Torpedo Ringer. Ten mL aliquots were centrifuged at $100,000 \times g$ for 30 min at timed intervals, and the pellet solubilized for counting. Assays were in duplicate. Purified nAChR was assayed by DE81 disks (see Methods).

α -bgt, on the other hand, exhibits multiple phases of toxin-nAChR dissociation with both membrane-bound and purified receptors. With membrane-bound nAChR, there is a very rapid loss of one half the total toxin bound, followed by a single exponential process ($\tau_{1/2}=78$ hrs). With purified nAChR, [$^{125}\text{I}_2$]- α -bgt follows three sequential exponential decays. First, there is the rapid loss of half the total sites, followed by a slower loss ($\tau_{1/2}=12$ hrs), and a very slow final phase ($\tau_{1/2}=120$ hrs). For the diiodinated toxin, the very rapid initial phase involves the loss of the extra population of sites not detected with ^3H - α -bgt.

The experimental kinetics for the two radiolabeled toxin species binding to membrane-bound and purified nAChR are summarized in Table V-6. The values for ^3H - α -bgt agree closely with literature values (22,38), and the calculation of the true K_d , by k_{-1}/k_1 , gives $4.0 (10^{-11})$ M and $3.5 (10^{-11})$ M for membranes and purified receptor respectively. These values are similar to true K_d measurements for ^3H -Naja nigricollis toxin (38), $2 (10^{-11})$ M, and for [^{125}I]- α -bgt interaction with purified muscle nAChR, 2 to $4 (10^{-11})$ M (54). It should be noted that the use of this ratio for determining the true K_d assumes that the reaction is a reversible, bimolecular interaction. Another interpretation of the multiple decay phases is that there is an irreversible isomerization induced by the toxin after the initial interaction to give a long-lived toxin-receptor complex (59). However, this study used iodinated α -bgt, and Table V-6 clearly points out the experimental idiosyncracies of iodinated α -bgt. There is a very rapid loss of one half of the toxin sites, the rate of which has not been included in the Table because it is assumed to correspond to extra sites peculiar to the use of this toxin derivative. In both purified and membrane-bound nAChR, there are two decay rates with iodinated toxin. In

TABLE V-6
 MEASURED KINETIC PARAMETERS FOR RADIOLABELED α -BGT DERIVATIVES BINDING TO
 MEMBRANE-BOUND AND PURIFIED TORPEDO nAChR

	Purified nAChR				Membrane-bound nAChR			
	$k_1 M^{-1} \text{min}^{-1}$	$k_{-1} \text{min}^{-1}$	$K_d \text{ M}$	$K_d^{\text{app}} \text{ nM}$	$k_1 M^{-1} \text{min}^{-1}$	$k_{-1} \text{min}^{-1}$	$K_d \text{ M}$	$K_d^{\text{app}} \text{ nM}$
$^3\text{H-}\alpha\text{-Bgt}$	6.1 (10^6)	2.1 (10^{-4}) 2.5 (10^{-3})	3.5 (10^{-11})	0.3	6.0 (10^6)	2.4 (10^{-4})	4.0 (10^{-11})	0.5
$[^{125}\text{I}_2]\text{-}\alpha\text{-Bgt}$	3.0 (10^6)	2.2 (10^{-4}) 2.1 (10^{-3})	7.3 (10^{-11})	0.4	1.6 (10^6) 0.6 (10^6)	2.5 (10^{-4}) 1.3 (10^{-2})	0.16 (10^{-9}) 0.42 (10^{-9})	1.4

membranes, the fast phase gives a $k_{-1} = .013 \text{ min}^{-1}$, which is almost exactly the value for $k_{II} = .012 \text{ min}^{-1}$ determined by Bulger et al (59) for the hypothetical toxin-induced irreversible isomerization step. These data urge caution in imputing significance to measurements made only with iodinated α -bgt, and suggest that alternative explanations may be offered for this relaxation phase (see Discussion). The association rates for iodinated toxin are slower than that for the tritiated toxin, but are partially compensated for by the slow dissociation rates. Thus, the K_d s for ^3H - α -bgt and $[^{125}\text{I}_2]$ - α -bgt with purified nAChR are very similar whether measured under pre-equilibrium conditions (0.3 vs. 0.4 nM) or whether determined by the ratios of off-to-on rates (3.5 vs. 7.3 (10^{-11})M). Membrane-bound nAChR, however, binds ^3H - α -bgt more strongly than $[^{125}\text{I}_2]$ - α -bgt, whether determined by pre-equilibrium saturation analysis (0.5 vs. 1.4 nM) or kinetically (4.0 vs. 42 (10^{-11})M).

v. Chemical Modification of α -Bgt and the Effects on Lethality and nAChR Binding. Table V-7 summarizes the results for the effects of residue modification on two measures of biological activity, an in vitro test (receptor binding), and an in vivo test (mouse lethality). Five of the modification procedures lead to the complete abolition of any toxin activity: 1) extensive dansylation of amino groups, 2) complete reduction of cystines, 3) selective reduction of a single disulfide (assumed to be Type II-toxin specific fifth disulfide) and its alkylation by iodoacetic acid, 4) extensive modification of lys and arg by 2,4-pentanedione, and 5) selective blocking of two arg residues by 2,4-pentanedione. Previous results have indicated the importance of cystine residues (60), the general basic charge-character (61), and particular amino groups (62,63) to toxin activity. The dansylation of lys₂₆ and lys₄₆ in the short toxin Naja haje I

TABLE V-7
EFFECTS OF CHEMICAL MODIFICATIONS OF α -BGT ON THE LETHALITY AND nAChR AFFINITY

<u>Modification</u>	<u>Residues Modified</u>	<u>Evidence for Specific Modification</u>	LD [*] 50	K _d ^{app} nM
Native			0.14	0.3
Dansylation	1 Lys 2 Lys All Amino	Ninhydrin reactivity Ninhydrin reactivity Ninhydrin reactivity	0.5 2.9 0	1.0 5.6 0
2,4-Pentanedione + hydroxylamine	All Lys/2 Arg 2 Arg	Amino acid analysis Amino acid analysis	0 0	0 0
Dithiothreitol	All Cystines	DTNB titration	0	0
Borohydride Reduction +iodoacetic acid +iodoacetamide +iodoacetamide	Cys ₂₉ -Cys ₃₃ Cys ₂₉ -Cys ₃₃ + 1 mole of another Cys	Amino acid analysis: CM-cysteine CAM-cysteine CAM-cysteine	0 1.2 20.0	0 3.4 26.0
Catalytic Reduction (Pd/C)	Met ₂₇ Met ₂₇ + Cys ₂₉ - Cys ₃₃	Amino acid analysis	0.16 0.55	0.4 0.8
N-bromosuccinimide	Trp ₂₈	Fluorescence	1.6	2.9
Dimethyl-(2-hydroxy- 5-nitrobenzyl)sulfonium bromide	Trp ₂₈	Fluorescence	1.9	4.1
Photooxidation (Rose Bengal)	His ₄ , His ₆₇	Amino acid analysis	0.19	0.5
Iodination	1/Tyr ₅₄ 2/Tyr ₅₄	CNBr cleavage and resolution of peptides	0.14 X	0.3 0.4
N-acetyl imidazole	Tyr ₅₄	Spectrophotometry	X	0.3

*

μ g/g mouse after subcutaneous injections.

leads to a complete elimination of lethality, which apparently arises from a 200X reduction in the association rate without any change in its dissociation rate (43). Modification of two lys groups in α -bgt attenuates its toxicity by 20X and has the same effect on the pre-equilibrium K_d^{app} . Therefore, the most reactive lys residues in α -bgt are not as functionally important as those in the Naja haje short toxin, perhaps because the additions to the longer α -bgt polypeptide chain have conferred additional stabilization. The monodansylated derivative is very nearly like the native toxin in its potency, much as has been noted before for a singly-labeled tetramethyl-rhodamine derivative used in fluorescent localization experiments (62).

2,4-Pentanedione is a reagent that modifies both lys and arg residues, but can be made specific for arg by the restoration of lys by hydroxylamine treatment (45). When reacted with α -bgt, all the lys and two of the arg residues are reacted with complete loss of activity. However, the role of the arg residues cannot be independently judged unless the lys residues are regenerated. In this instance, the activity does not return, implicating at least one of the modified arg in an essential function. Modification of arg₃₀ and arg₃₃ in cobrotoxin was also noted to virtually abolish lethality (64). Thus, it may be that the speculated receptor-recognition residue arg₃₇ is one of the modified arg, and that its integrity is required for receptor binding.

The fifth disulfide, bridging cys₂₉ to cys₃₃, has been shown to be particularly sensitive to reduction and can be selectively opened by either timed exposure to sodium borohydride (43) or by a molar equivalent of dithioerythritol toxin (65). Although there is no direct supporting evidence, it is assumed that the single disulfide opened by borohydride treatment

or catalytic reduction is the fifth disulfide. In either treatment, considerable lethality remains and the receptor binding affinity is reduced by only 10X. However, with borohydride reduction, biological activity can only be preserved with iodoacetamide alkylation. As noted for Naja haje toxin III, the reduced disulfide generates an inactive derivative if alkylated with iodoacetic acid, which introduces negative charges. The catalytic reduction presumably produces a derivative with considerable activity because it reduces the cys residue to two ala residues and does not alter the charge. If the timed exposure to borohydride is continued, a second cystine is apparently cleaved. However, since there is no evidence for selectivity in the kinetics of subsequent disulfide reduction, this "single" disulfide is very likely a mixture of products. Thus, the presence of residual biological activity cannot be interpreted.

Several residues can be considered nonessential from the chemical modification results. The trp residue can be modified with either NBS or Koshland reagent I to give products with ~10% residual activity in both tests. Thus, although an invariant residue, the trp is not required for activity. A critical comparison of the status of the trp in Type I and Type II neurotoxins concluded that the latter were insensitive to trp modification, but that the former were completely inactivated (66). It might be that the extra loop in Type II toxins adds stability in the trp region, so that its modification is structurally less disruptive. The single met and two his residues are apparently unimportant. Lastly, the exposed tyr residue susceptible to iodination or N-acetyl imidazole modification is not essential, although its modification may have quantitatively significant effects arising from subtle structural changes on iodination

(see Discussion). This is important only inasmuch as iodinated toxins are frequently prepared in order to make radiolabeled derivatives.

vi. Application of a Reporter Group to the Study of Toxin-nAChR Interaction.

Modification of the single trp by Koshland reagent I gives a derivative with the environmentally-sensitive p-nitrophenolic group (67). Accordingly, this derivative was used to probe the binding region on the receptor. Because of its relatively weak extinction, the 2-hydroxy-5-nitrobenzyl chromophore was suitable for studies only in the micromolar concentration range, necessitating the use of purified nAChR. (The receptor was also equilibrated into Emulphogene BC-720 as an optically-transparent detergent.)

The difference spectrum of 2-hydroxy-5-nitrobenzyl- (HNB)-modified toxin vs. HNB-toxin + nAChR shows that there is a red shift and increase in extinction upon binding. These results suggest that the HNB-trp is being masked in a hydrophobic environment. Consistent with this, the bound HNB-chromophore is no longer sensitive to external pH manipulation, unlike the free HNB-toxin (Figure 5-11B). Examination of the intrinsic fluorescence emission spectrum of the toxin-receptor complex also shows a pronounced quenching of the receptor fluorescence, as well as a blue shift of its emission maximum (Figure 5-11C). These data suggest that there are trp residues near the toxin recognition site on the receptor, or that there is a conformational change masking trp residues upon toxin binding. However, because the quenching much weaker with NBS-modified toxin, it seems unlikely that this effect arises from a conformational change.

vii. α -Toxin Binding to Rat Brain Sites. Both [125 I]-ddt and radiolabeled derivatives of α -bgt bind to a small level of saturable sites in crude mitochondrial fraction (CMF) membranes (Figure 5-12). By comparing the binding in brain to that in Torpedo nAChR-rich membranes, it is apparent

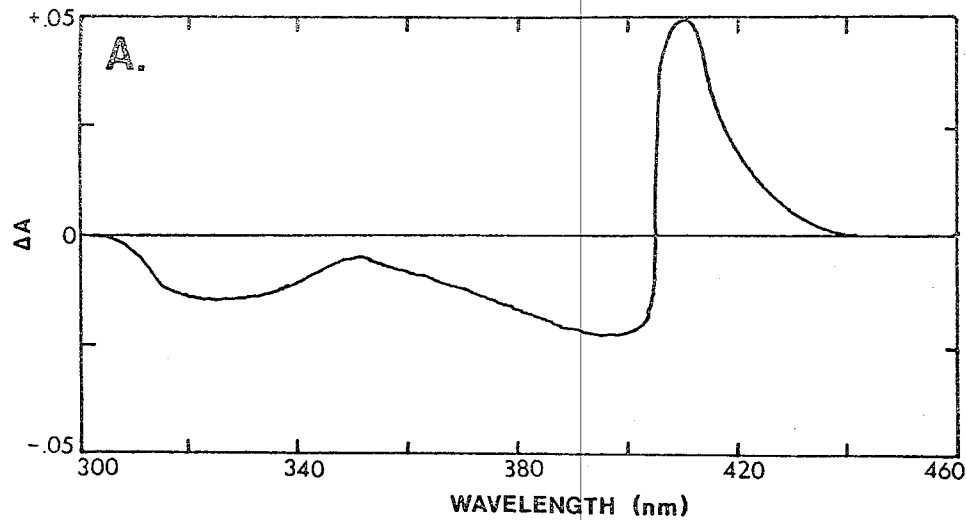
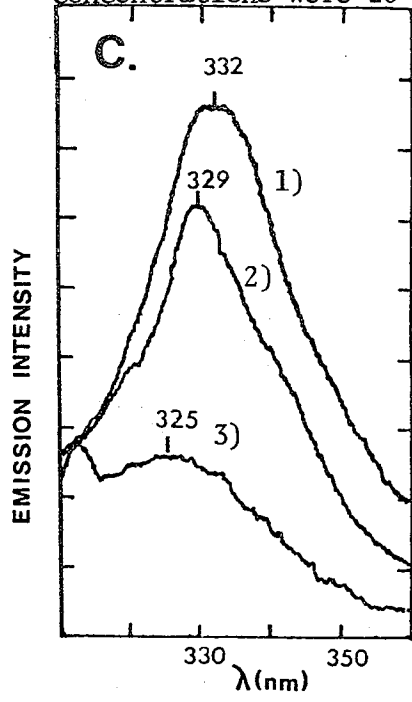
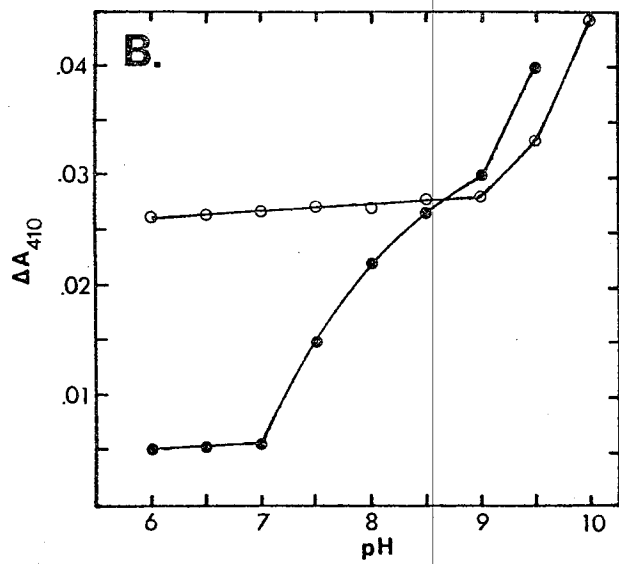


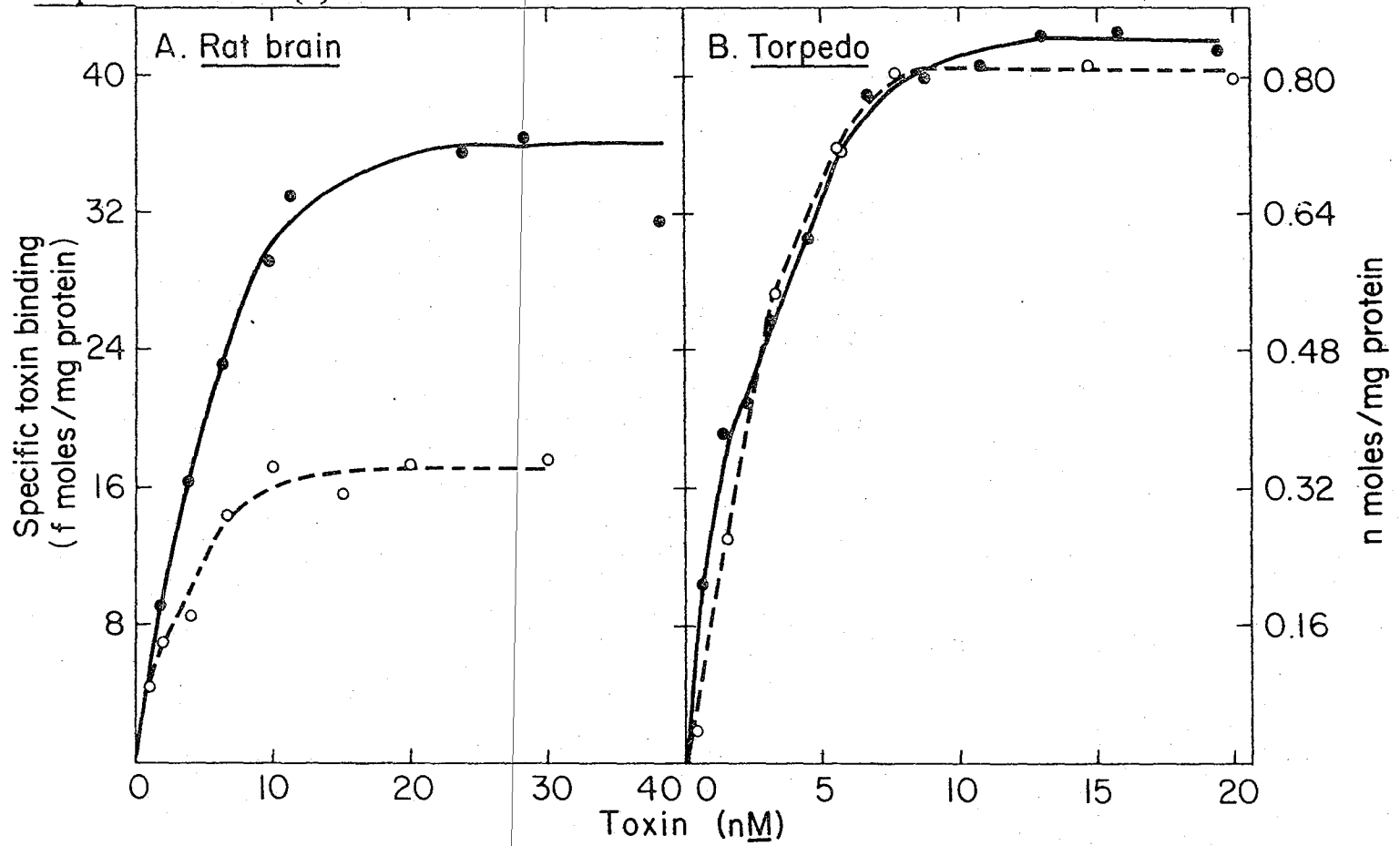
Figure 5-11
 HNB-modified α -bgt as a reporter of toxin receptor interaction.
 A) Differential absorption of 100 nM HNB-toxin + 100 nM purified nAChR in 0.1% Emulphogene BC-720 vs. HNB-toxin, minus nAChR, in detergent.
 B) pH sensitivity of HNB-toxin alone (solid circles) and HNB-toxin-nAChR complex (open circles) in 0.1% Emulphogene.
 C) Intrinsic fluorescence of nAChR-rich membranes in presence or absence of trp-modified toxins. Protein concentration of membranes was 10 μ g/mL (=7 nM nAChR). Toxin concentrations were 20 nM. Excitation at 287 nm.



- 1) Membranes alone
- 2) + NBS-trp toxin
- 3) + HNB-trp toxin

Figure 5-12

Comparison of saturation binding of ^3H - α -bgt (open circles) and $[^{125}\text{I}]$ -ddt (solid circles) to rat brain (A) and Torpedo membranes (B).

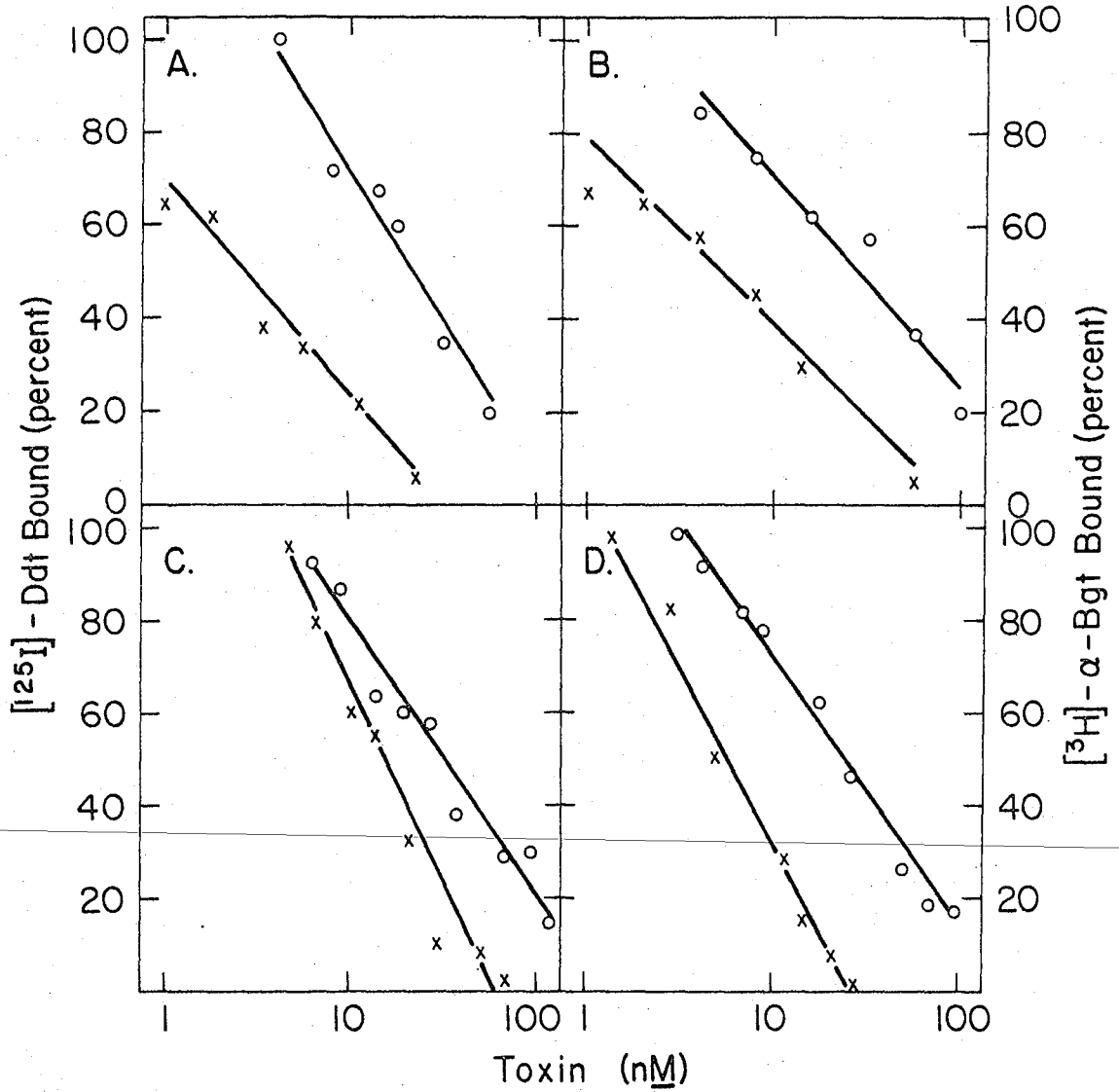


XBL 785-876

that specific binding levels in brain were twice as high for [^{125}I]-ddt as for ^3H - α -bgt, but were the same for binding saturation to Torpedo membranes. Analysis of Scatchard plots of a minimum of five independent saturation curves gave an average K_d^{app} for [^{125}I]-ddt of 4.0 ± 0.6 nM in brain and 4.1 ± 1.5 nM in Torpedo. These values can be compared with 4.0 ± 0.6 nM in brain and 0.5 ± 0.2 nM in Torpedo for ^3H - α -bgt. The proportion of non-specifically bound [^{125}I]-ddt increased with the degree of radioactive labeling. Typically, for [^{125}I]-ddt preparations, specific binding at saturation was 20-40% of the total in rat brain, and 50-80% of the total in Torpedo, compared to 70% and 99+% specific binding for ^3H - α -bgt in rat brain and Torpedo respectively. The larger proportion of non-specific binding in brain arose because of the vastly larger protein content required to obtain working levels of the receptor. Specific binding was apparently to a single homogeneous population of sites for both toxins in both tissues, although the higher non-specific binding of [^{125}I]-ddt in brain makes this conclusion tentative. Nevertheless, the specific binding levels and the two-to-one ratio of ddt to α -bgt sites at saturation were independent of the degree of radioactive labeling or overall iodination.

Data from experiments in which labeled and unlabeled toxins were co-incubated with membrane-bound sites indicated that unlabeled α -bgt and ddt quantitatively blocked specific binding of both the homologous and heterologous radiolabeled toxins in both tissues (Figure 5-13). K_d^{app} s calculated from the 50% inhibition values of these plots gave good agreement with the values derived from direct binding (4.6 nM in brain and 5.9 nM in Torpedo for ddt, and 2.2 nM in brain and 0.2 nM in Torpedo for α -bgt). In all cases, specific binding competition behavior indicated a single population of sites for each toxin.

Figure 5-13
 Competition of unlabeled α -bgt (-X-X-) and ddt (-o-o-) against [125 I]-ddt (graphs A and C) or 3 H- α -bgt (graphs B and D) in binding to rat brain membranes (graphs A and B) or Torpedo membranes (graphs C and D).



XBL 785-877

The nicotinic pharmacology of both toxin-binding sites was confirmed by the competition of cholinergic drugs towards toxin binding (Table V-8). Comparison of the data for toxin binding to sites in each tissue showed excellent agreement for individual ligands. Comparison between the two tissues showed that both carbachol and d-tubocurarine were markedly less effective in brain than in Torpedo, in agreement with other investigations (39,68). Muscarinic and other non-nicotinic drugs were ineffective on the binding of either toxin. Recent work by Lukasiewicz and Bennett (39,69) has shown that brain membrane α -toxin sites can show the same type of "agonist-conditioning" effect as that seen in Torpedo membrane-bound nAChR. Since the time-dependent changes in agonist affinity are thought to be an in vitro model for desensitization, as noted earlier, one can conclude that nicotinic agonists can also induce desensitization affinity-changes in brain sites. Table V-8 also includes examples of this conditioning effect by nicotine and acetylcholine on both toxin sites in both tissues. Thus, the ddt sites are also sensitive to state changes of their receptor.

With solubilization in deoxycholate, the binding saturation stoichiometries were preserved (Figure 5-14). Moreover, in both tissues, the specific binding activity was found to co-enrich (1.1X in brain, 2.1X in Torpedo) with solubilization. To rule out the possibility that a peculiar sub-population of sites was being selectively extracted from brain with the low solubilization yield (20% of total sites), several extraction conditions were tested. The [125 I]-ddt and 3 H- α -bgt binding activities increased or decreased coordinately (Table V-9), but were unfortunately not enriched in toxin sites. Thus, since solubilization yields followed the total membrane protein extraction yields, this approach did not give unequivocal information as to the presence of the

TABLE V-8
 COMPARATIVE PHARMACOLOGY OF [¹²⁵I]-DDT and ³H-α-BGT MEMBRANE-BOUND BINDING SITES IN RAT BRAIN AND TORPEDO

Drug *	Torpedo K_d^{app} (μM) [¹²⁵ I]-ddt	³ H-α-bgt K_d^{app} (μM)	K_i for purified nAChR (22)	Rat brain K_d^{app} (μM) [¹²⁵ I]-ddt	³ H-α-bgt K_d^{app} (μM)
Acetylcholine **					
Preincubation	1.1 ± 0.3 (2)	0.5 ± 0.2 (2)	0.8	1.0 ± 0.5 (5)	0.8 ± 0.2 (3)
Coincubation	14.6 ± 2.3 (2)	7.4 ± 1.2 (2)		6.8 ± 2.0 (2)	24.0 ± 3.5 (2)
Nicotine					
Preincubation	0.4 ± 0.1 (2)	0.2 ± 0.1 (2)	0.1	0.4 ± 0.2 (4)	0.25 ± 0.05 (3)
Coincubation	2.7 ± 0.8 (2)	2.5 ± 0.6 (2)		0.6 ± 0.2 (2)	1.1 ± 0.2 (2)
Carbachol	0.4 ± 0.1 (2)	0.6 ± 0.2 (2)	0.7	4.6 ± 1.2 (3)	2.5 ± 0.2 (3)
d-Tubocurarine	0.1 ± 0.05 (2)	0.1 ± 0.05 (2)	0.1	2.9 ± 2.0 (5)	4.4 ± 2.5 (3)
Atropine	>100 (1)	>100 (1)		>100 (1)	>100 (1)

*

All drugs were pre-equilibrated for 30 min prior to the addition of radiolabeled toxin, except "coincubation" samples in which both drug and toxin were added coordinately. K_d^{app} was calculated as described elsewhere (22) assuming a strictly competitive interaction of the ligands at homogeneous sites. This calculation is the simplest method for correcting in differences in affinities and incubation concentrations of the radiolabeled toxins. Comparison of these data to corrected K_i s from Electrophorus purified nAChR (22) shows good agreement. Negative at 0.1 mM: GABA, glutamate, glycine, histamine, neuroleptics, noradrenaline.

**

Executed in the presence of either 0.02 M BW-284c51, 0.02 M neostigmine, or 0.1 M eserine (10 min preincubation before acetylcholine addition) which quantitatively suppresses acetylcholine enzymatic breakdown, but has no effect on toxin binding.

TABLE V-9
SOLUBILIZATION OF α -TOXIN BINDING SITES FROM RAT BRAIN CRUDE MITOCHONDRIAL FRACTIONS

Treatment ^a	% Protein ^b Solubilized	¹²⁵ I]-ddt sites		³ H- α -bgt sites		
		% Solubilized ^c	SAE ₁ ^d	% Solubilized ^c	SAE ₂ ^d	SAE ₁ /SAE ₂
0.1% sodium deoxycholate, 4°C	12	15	1.25	16	1.33	0.94
1% sodium deoxycholate, 4°C	20	22	1.10	23	1.15	0.96
1% sodium deoxycholate, 37°C	32	44	1.38	43	1.34	1.03
1% sodium deoxycholate + 2 M NaCl 37°C	39	42	1.08	40	1.03	1.05
1% Emulphogene BC-720, 4°C	25	35	1.40	37	1.48	0.95
1% Emulphogene BC-720, 37°C	29	42	1.45	40	1.38	1.05
0.1% Triton X-100, 4°C	38	25	0.66	28	0.74	0.89
1% Triton X-100, 4°C	53	40	0.75	44	0.83	0.90
1% Triton X-100, 37°C	71	80	1.13	82	1.15	0.98

a

All detergent extractions were done for 90 min using 10% (w/w) suspensions of crude mitochondrial fractions (see Methods). All detergents were made up in 5 mM sodium phosphate buffer (pH 7.4) + 0.02% NaN₃ + 0.1 mM PMSF. Samples were then clarified by centrifugation at 100,000 X g for 60 min.

b

By Lowry determination with standards and controls treated under the same conditions. Where interference was pronounced, samples were checked against a fluorescamine-filter disk method.

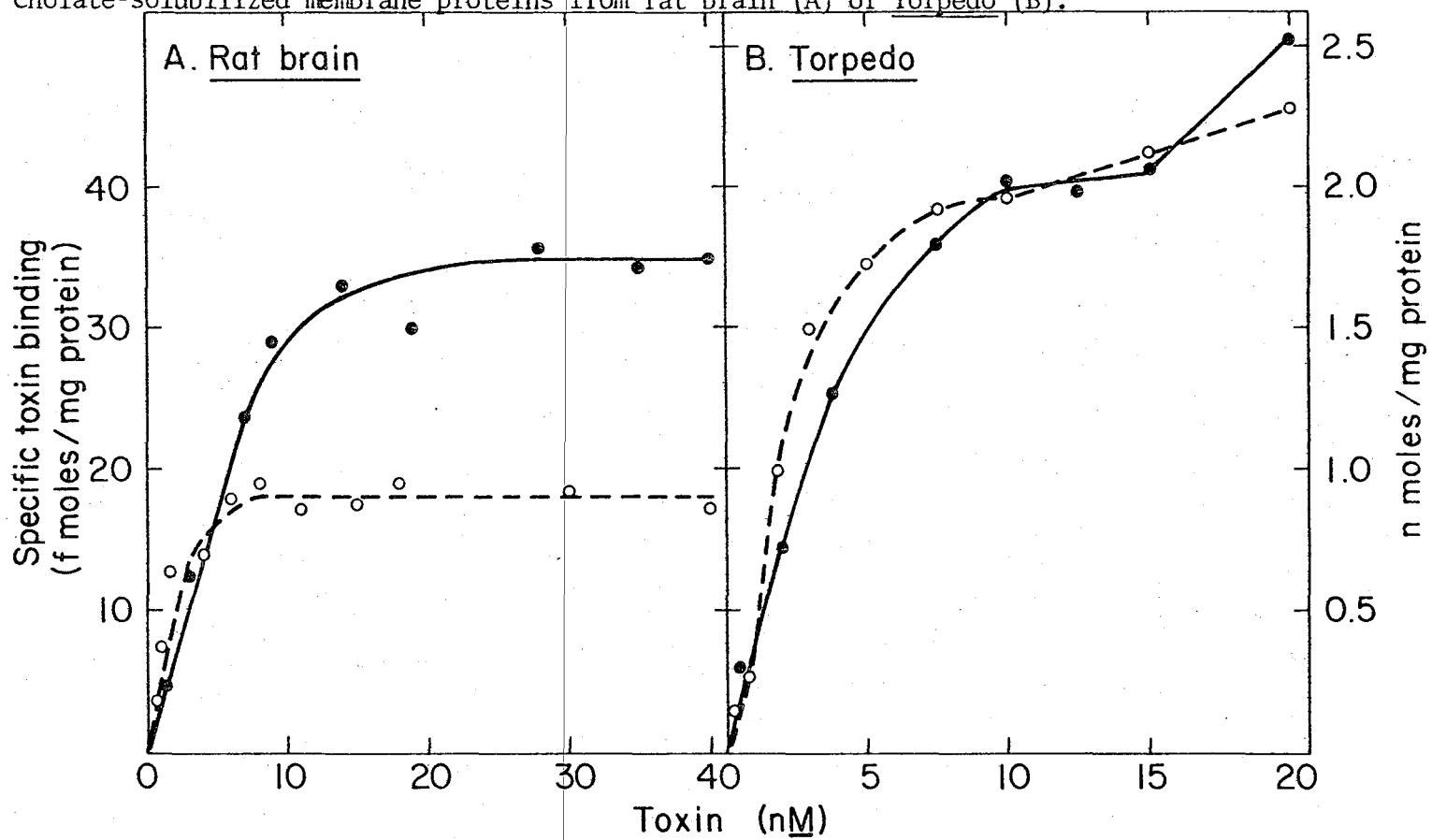
c

Determined relative to aliquots taken from original crude mitochondrial fraction before extraction. Binding assays are given in Methods, using saturating concentrations of [¹²⁵I]-ddt (14.0 nM) and ³H- α -bgt (13.5 nM).

^dSpecific Activity Enrichment (SAE) given by ratio of the specific binding activity (fmoles α -toxin bound/mg protein) of detergent extracts vs. original fraction homogenate.

Figure 5-14

Comparison of binding saturation of ^3H - α -bgt (open circles) and $[^{125}\text{I}]$ -ddt (solid circles) to deoxycholate-solubilized membrane proteins from rat brain (A) or Torpedo (B).



XBL 785-875

two sites on the same receptor.

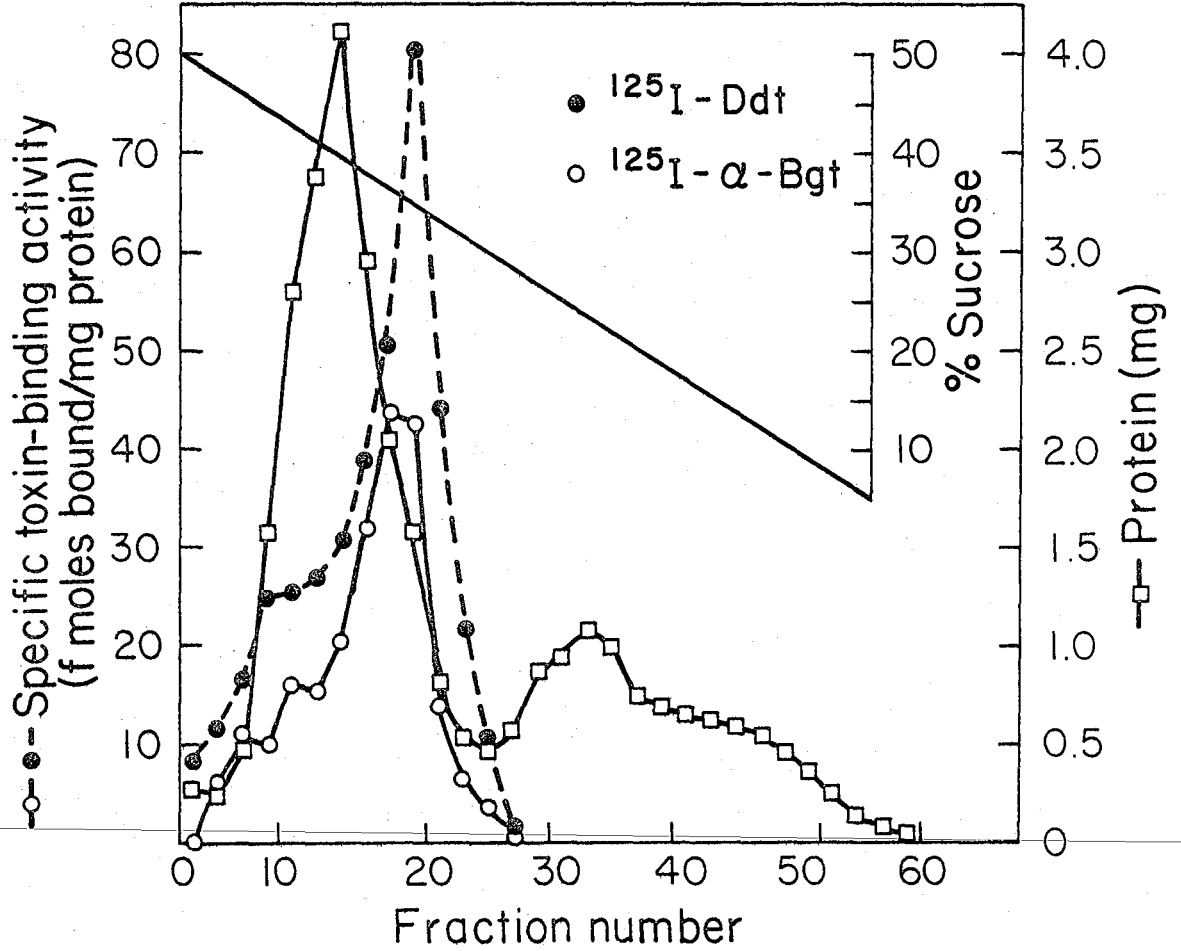
Another approach to the localization of the toxin sites was pursued by equilibrium sucrose gradient centrifugation of heterogeneous brain particulate fractions (containing both synaptic and microsomal membranes). Figure 5-15 shows that maximum specific activity for both toxins, enriched 2.3X over the CMF membranes, was detected at a buoyant density of 1.146 g/mL, somewhat higher than the density of 1.112 g/mL for a microsomal sub-fraction enriched in [^{125}I]- α -bgt binding sites (70). The radioactivity profiles show that both toxins follow the same distribution in the gradient, and do not follow total protein levels. Furthermore, the two-to-one site stoichiometry appeared to be retained in the gradient fractionation. It should be emphasized that this procedure involved the use of separate gradients to correct for the pronounced effect of non-specific trapping of radiolabeled toxins by high concentrations of protein. Thus, when this gradient fractionation was run under double-labeling conditions, the toxin-binding activities followed the total protein levels owing to high non-specific binding backgrounds. It is the variability between separately-run gradients that accounts for the small deviation from perfect two-to-one stoichiometry of toxin sites across the binding peak.

DISCUSSION.

Many applications of the α -toxins demand that the toxins be suitably modified, and the most frequent such modification is the incorporation of a radioactive label. Radiolabeling permits the detection of very small levels of toxins in binding assays, as well as localization in both the light and electron microscope by autoradiography (71,72). ^3H -Naja nigricollis toxin α (38,53), ^3H - (22) or ^{125}I -labeled cobra toxins (25), and [^{125}I]- (54,58), [$^{125}\text{I}_2$]- (7,11,17,56) or ^3H - α -bgt (33,35,73) have been the toxin derivatives that have experienced the greatest application to the

Figure 5-15

Equilibrium sucrose gradient centrifugation of pre-labeled crude brain membranes. Specific toxin binding was given by subtraction of non specific binding from total binding for each toxin using separate gradients. Thus, the reported figures are derived from a minimum of four separate gradients.



characterization of the toxin-receptor interaction. There are differences between results obtained by iodinated and tritiated cobra neurotoxins (22, 25). The former gives a slower on-rate and a faster dissociation rate than the latter. Thus, neglecting complications from differences in methodology, the difference may indicate that the toxins are sensitive to the nature of the radioactive substitution. Unlike Naja nigricollis toxin (74) which is iodinated at a his residue, cobra neurotoxin appears to be modified at a tyr residue (25), like α -bgt. Any kinetic anomalies described for iodinated α -bgt might be applicable to other homologous toxins used to monitor the nAChR. At the simplest qualitative level, mono- or diiodination of tyr₅₄ does little because the animal lethality and pre-equilibrium K_D^{app} are virtually unchanged (33). This does not indicate whether more subtle changes may have occurred. Examination of the kinetics of ^3H - α -bgt vs. [$^{125}\text{I}_2$]- α -bgt (Table V-6) reveals that the latter is much slower in its association rate, and faster in its dissociation rate. Further, its k_{obs} for association is not linear with increasing toxin concentration and falls to a stable value of $0.6 (10^6) \text{ M}^{-1}\text{min}^{-1}$ at high concentrations. Lastly, there is a concentration dependence in the observed number of sites. At high concentrations, [$^{125}\text{I}_2$]- α -bgt gives twice the number of ^3H - α -bgt sites. In dissociation rate studies, this second population of sites has a very rapid relaxation rate. There are several interpretations for these data. When on-rates fail to follow a linear concentration dependence, it is taken as evidence that the rate-limiting step is altered. Hess and his group have interpreted the effect as an allosteric change in the receptor mediated by the toxin (59). Alternatively, iodinated toxin might be detecting a second population of lower-affinity binding sites. Both of these explanations assume the change occurs in the target and not

in the toxin. However, there is a third possibility that a concentration-dependent self-association of the iodinated toxin gives a bulkier, slower-associating solution species. The enhanced tendency of iodinated polypeptide hormones to undergo self-association has been documented (75). If only a tendency to form dimers is increased in iodinated toxins, it may, in fact, be somewhat surprising that the consequences of iodination are not more dramatic. Tyr₅₄ is located at the end of a loop stacked onto the recognition-site loop by a domain of β -sheets. Perturbations in the recognition-site region were shown in the previous Chapter to be sensitively detected in the spectral properties of tyr₅₄. It would not be unreasonable to expect a reciprocal influence of modification in this tyr on the hypothesized active-site loop. In this regard, recall that diiodination leads to widespread CD changes (Chapter IV and ref. 33) that, in the far-UV, can be interpreted as the loss of some β -structure. Localized loss of β -sheet hydrogen-bonding patterns could result from the substitution of bulky iodine atoms for phenolic hydrogens, and further disruption could occur by ionization of the tyr, as the pK_a of diiodotyrosine is below pH 7.0. From the loss of activity by alkylation of the nearby "fifth" disulfide with iodoacetic acid, but its retention by iodoacetamide alkylation, it has been established that this region of the molecule is acutely sensitive to the introduction of negative charges, such as the diiodinated tyr residue might introduce. Thus structural considerations indeed point to the possibility of functional disruption by iodination of α -bgt. Kinetic data derived exclusively from the use of iodinated toxin, and not corroborated by an independent technique, must be considered tentative. In particular, the kinetic values determined by Hess and his colleagues for the "irreversible isomerization" step of toxin interaction may have alternative interpretations. The rate for this isomerization,

$k_{II} = .012 \text{ min}^{-1}$, may correspond to the off-rate of iodinated toxin dimer dissociation, and the K_d for initial nAChR interaction, $K_2 = 100 \text{ nM}$, may correspond to the K_d for monoiodinated-toxin dimer formation. Calculating the on-rate assuming microreversibility, $k_1 = 0.12 \text{ M}^{-1}\text{min}^{-1}$, it proves to be slower than the observed on-rate for receptor at even high toxin concentrations. It is obvious that more extensive binding and physical experiments must be made before an unequivocal determination of the role of toxin dimers in these data can be inferred.

The chemical modification data have two important uses that develop from the two types of limiting cases, modifications that have no effect and modifications that cause complete loss of activity. The modifications that have no effect are useful because they offer the possibility of finding residues that can incorporate reporter groups, radioactive labels, or spacer arms for immobilization, without disturbing the activity. Thus, the single trp, the exposed tyr₅₄, the two his, the single met, and the fifth disulfide cys₂₉-cys₃₃ are all potential candidates for non-disruptive modification. One group has exploited the his residue by reacting it with diazotized p-aminobenzoylhexylamino-Sepharose 6B to bind the toxin to the column, which was successfully used for neuron isolation (76). Similarly, another group has shown the suitability of introducing a radioactive label by the selective alkylation of the reduced fifth disulfide (44). In this Chapter, the trp residue was modified with the 2-hydroxy-5-nitrobenzyl (HNB) chromophore which is sensitive to both the local charge and polarity of its environment. In the toxin, the bound HNB-chromophore has an altered pH sensitivity, giving an apparent pK_a of 8.5 for its ionization, as compared to the normal 10.9 (77). This points to the strong influence exerted by the nearby basic groups. Upon

interaction with purified nAChR in non-absorbing detergent, there is a red shift and intensity enhancement of the absorption spectrum, consistent with the masking of the reporter in a hydrophobic domain. Further, in support of this evidence for isolation from the solvent, the reporter is no longer responsive to external pH manipulation once bound. Studying the other half of the interaction, one can take advantage of the elimination of the toxin's trp residue by using intrinsic protein fluorescence as a specific monitor for the nAChR. The emission spectrum of the membrane-bound nAChR is due to trp residues in hydrophobic membrane proteins (77). There is a significant quenching and blue shift of the emission maximum with reaction with NBS- α -bgt, pointing to either the involvement of trp residues in the binding site or the modification of trp environments by a toxin-induced conformational change. HNB-toxin has a much more dramatic quenching effect, which suggests that the differences between the two toxins must be a physical one, since they bind with similar affinities and would be expected to induce identical changes in the receptor. Thus, the additional size of the HNB-substituent may bring it into more effective quenching proximity to trp residues responsible for a large proportion of the intrinsic fluorescence of nAChR-rich membranes. The current evidence is very good that there are trp residues in the toxin-binding 40,000 dalton subunit of the receptor (80) which give efficient energy transfer to the affinity label dansyl-choline (79), and are significantly quenched by cholinergic ligand binding (80).

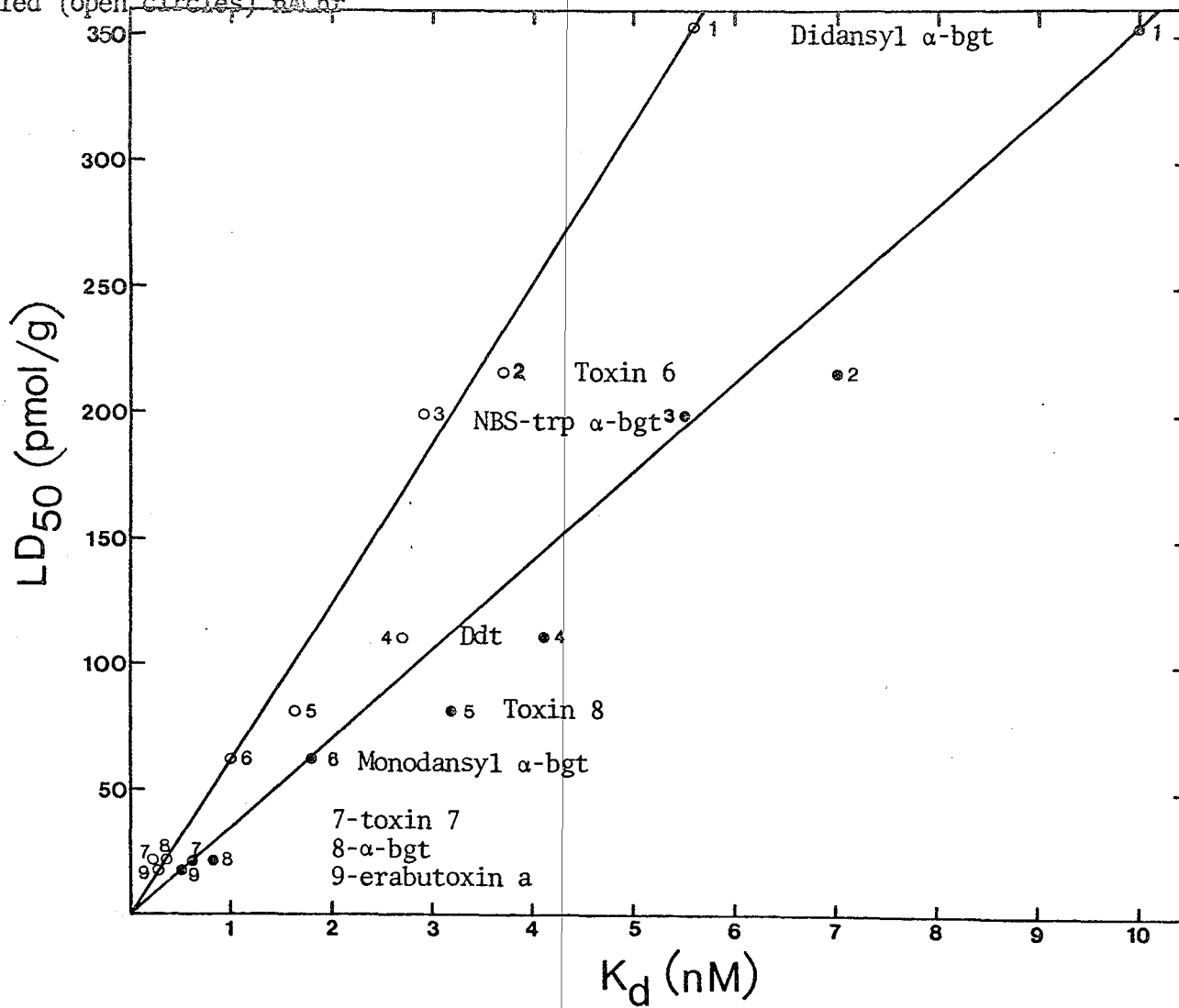
Modifications that abolish activity are useful in the identification of structurally or functionally important residues. Thus, the cystines are essential for activity because of their structural role, and activity loss with lys or arg modification implicates these residues in the receptor recognition site.

A recurring theme in this Chapter has been the comparison of membrane-bound and purified receptors in terms of their toxin-binding properties. Table V-6 indicates several differences. With purified receptors, ^3H - α -bgt exhibits a second, faster decay rate in dissociation studies that is not found in the membrane-bound nAChR. Indeed, the kinetic behavior of ^3H - α -bgt binding to membrane-bound receptor fits a bimolecular reaction with simple monophasic association and dissociation rates. This is not true for any other condition tested. The use of either iodinated toxins or purified receptor introduces other kinetic phases. Purified nAChR does not appear to quantitatively discriminate between iodinated and tritiated toxins (note the agreement of both experimental and kinetically-derived K_d 's), which might be evidence for a subtle "relaxation" of a strict binding site geometry upon solubilization and purification. On-rates for both types of radiolabeled toxins are slightly faster, off-rates slightly slower, and overall true K_d 's slightly stronger in the purified nAChR. This might indicate the presence of a subtle access barrier for toxin binding to the receptor in its native membrane environment, or point to a systematic difference arising from the assay techniques. In a previous investigation of the binding properties of solubilized vs. membrane-bound Torpedo nAChR, the conclusion was that there were no changes in toxin binding, but that agonists had decreased affinity for the solubilized receptor (81). However, other work has shown agonists to be more effective in binding to solubilized receptor (82,83). Whatever the nature of the change in the agonist-binding properties, one interpretation is that such changes are the result of the loss of a structural constraint normally imposed by the membrane (82). It may be that this hypothetical change is detectable only by detailed comparisons of the kinetics of closely-related

ligands, such as different derivatives of α -bgt. The effectiveness of a variety of native and modified toxins has been tested in a simple way by comparing toxin K_d^{app} values to their lethal potencies by LD_{50} s. Previous work has shown there is a linear correspondence between LD_{50} and equilibrium K_d for receptor binding (54). In Figure 5-16, the potencies of several toxins against both purified and membrane-bound nAChR have been plotted vs. their LD_{50} s. In this Figure, the potencies are the K_d^{app} values determined under pre-equilibrium conditions by competition against 3H - α -bgt. In both receptor states, there is a reasonable fit to a straight line, but the two lines have different slopes. The toxins are uniformly more potent on the purified than on the membrane-imbedded receptor, although the rank order is not disturbed. The fact that three toxins (6,8, and ddt) fall off both straight lines in the same direction (towards lower K_d^{app} s) suggests a significant difference between Torpedo and muscle receptors to which these toxins are responding; these toxins appear to prefer the muscle nAChR.

~~The interpretation of toxin binding sites in vertebrate ganglia and brains has become controversial with the recent demonstrations that the toxins fail to have an electrophysiological activity in neural test systems (15,17,18,84). Thus, the fact that the α -toxins bind to a membrane component with similar physical properties (85,86), drug binding responsiveness (39,87), and state changes (39) as that of the peripheral nAChR, and with a histochemical distribution confined to discrete and appropriate regions of the vertebrate brain (19,20), has become an unresolved paradox. Further, recent EM results have localized the toxin sites to the synaptic membrane (88,89). An alternative to discarding the identification of the α -toxin site as a brain nAChR is to consider the failure of the toxins to block central synapses as~~

Figure 5-16
 Correlation of LD_{50} with K_d^{app} for several native and modified toxins on membrane-bound (solid circles) or purified (open circles) nAChR



a functional difference between central and peripheral receptor pharmacology. There is a precedent for this suggestion in the nAChR literature. Specifically-targeted antibodies can bind with great selectivity to nAChR determinants in two different species, yet have a physiological effect in one case and not the other (90). A very significant but unexploited tool in this problem is an α -toxin which has been shown to have a synaptic blocking activity on a central nicotinic junction, dendrotoxin 4.7.3 (16). Its physiological idiosyncrasy might be expected to have a biochemical correlate, and thus the binding properties of iodinated ddt have been compared with those of radiolabeled α -bgt, using the Torpedo nAChR as a peripheral model in which their binding should be qualitatively equivalent.

The two toxins apparently bind to the same population of rat brain receptors as judged by co-migration in sucrose gradients of brain membranes, and mutual competition effectiveness. However, there are twice as many [125 I]-ddt sites as 3 H- α -bgt sites at saturation in rat brain. This is unlike the binding characteristics of the two toxins to Torpedo membranes wherein they exhibit identical pharmacological properties and saturation levels. These observations have two important consequences.

The first is that the Torpedo and rat brain nAChR are distinguishable by the specific features of α -toxin recognition. Thus, although Torpedo and rat brain sites appear superficially alike in their physical behavior (85,86), the pharmacological responsiveness and site binding properties are different. It is tempting to suggest that the vertebrate brain nAChR is evolutionarily related, but significantly altered from the Torpedo receptor. There is a variation in toxin-binding properties of peripheral nAChR among species of Reptilia; some snake neuromuscular junctions

are immune to the action of the toxins because the toxins cannot bind to the receptor. Thus, it is not a wild leap to suppose that a functionally-cryptic binding could take place on central nAChR, particularly since it is never a physiological target site of the toxins. This leads to the thought that there may be other unique features of the brain receptor which could only be discovered by its direct study. From this perspective, the immunological discrimination between toxin-binding sites in PC-12 cells and Torpedo receptor may only point to the evolutionary difference of antigenic determinants on two related proteins.

The second major point is that the second population of sites recognized by [¹²⁵I]-ddt offers a possible explanation of its electrophysiological activity in vertebrate central nervous system. The specifics of how additional sites relate to the physiological observations is premature with the limited data reported here, but some speculations may be offered with which the current evidence agrees.

The binding of both toxins can be prevented by pre-equilibration of the sites with both nicotinic agonists and antagonists. Thus, agonists must directly bind to both classes of toxin sites, or binding at one set of sites alters the properties of all sites so that toxin can no longer bind. Because α -bgt is presumed to have no physiological effect, we can assume that the α -bgt sites are physically distinct from the important agonist sites. Therefore, agonist inhibition should be non-competitive, and may be linked to experimentally accessible changes in receptor state. Recent results by Lukasiewicz and Bennett (39,69) agree with these predictions. The potency of unlabeled ddt towards displacement of both toxins would therefore suggest an overlap of its binding specificity with both agonist and α -bgt sites, giving twice as many sites as α -bgt.

However, a severe complication is the ability of α -bgt to inhibit all the [^{125}I]-ddt binding; it is assumed to overlap with only one half of the ddt sites. One explanation would be to suggest a physical congruence of these sites, and invoke that blocking activity requires site occupancy by a specific dimer of ddt. Alternatively, α -bgt causes a state change that non-competitively inhibits ddt binding to the non-overlapping sites, but has no effect on agonist binding(!). Another difficulty is that the pharmacological results with several nicotinic drugs reveal no differences such as might be expected with two different sites with different toxin recognition properties. However, the results with iodinated vs. tritiated toxins indicated that important differences may be subtle, and can be missed in simple competition experiments. Several key experiments on brain toxin sites are underway: 1) the inhibition of agonist sites by the irreversible affinity reagent MBTA (92); 2) the tritiation of [^{125}I]-ddt to improve its binding properties; 3) the description of other α -toxins that behave like ddt; and 4) kinetic and double-labeling experiments to determine if simultaneous occupancy or half-of-the-sites reactivity can occur with toxins and small ligands.

In general, the wide natural diversity of curarimimetic toxins has not been exploited to study differences in physical states of the peripheral nAChR, or to identify differences in receptors from different species or tissues. Results in this Chapter suggest that comparative studies of the interaction of different toxins may reveal important changes in receptor state or recognize tissue-specific sites.

REFERENCES.

1. Changeux, J.-P., Kasai, M., and Lee, C.-Y. (1970) Proc.Nat.Acad.Sci., 67, 1241.

2. Miledi, R., and Potter, L. (1971) *Nature*, 233, 599.
3. Berg, D.K., Kelly, R.B., Sargent, P.B., Williamson, P., and Hall, Z. W. (1972) *Proc.Nat.Acad.Sci.*, 69, 147.
4. Moore, W.J., and Loy, N.J. (1972) *Biochem.Biophys.Res.Communs.*, 46, 2093.
5. Eterovic, V.A., and Bennett, E.L. (1974) *Biochim.Biophys.Acta*, 362, 346.
6. Patrick, J., McMillan, J., Wolfson, H., and O'Brien, J.C. (1977) *J.Biol.Chem.*, 252, 2143.
7. Patrick, J., and Stallcup, W.B. (1977) *J.Biol.Chem.*, 252, 8629.
8. Greene, L.A., Sytkowski, A.J., Vogel, Z., and Nirenberg, M. (1973) *Nature*, 243, 163.
9. Chiappinelli, V.A., and Zigmond, R.E. (1978) *Proc.Nat.Acad.Sci.*, 75, 2999.
10. Wilson, S.P., and Kirshner, N. (1977) *J.Neurochem.*, 28, 687.
11. Vogel, Z., and Nirenberg, M. (1976) *Proc.Nat.Acad.Sci.*, 73, 1806.
12. Kao, I., and Drachman, D.B. (1976) *Science*, 195, 74.
13. Shain, W., Greene, L.A., Carpenter, D.O., Sytkowski, A.J., and Vogel, Z. (1974) *Brain Res.*, 72, 225.
14. Dudai, Y. (1977) *FEBS Lett.*, 76, 211.
15. Duggan, A.W., Hall, J.G., and Lee, C.-Y. (1976) *Brain Res.*, 107, 166.
16. Miledi, R., and Szczepaniak, A.C. (1975) *Proc.Roy.Soc.*, 190, 267.
17. Carbonetto, S.T., Fambrough, D.M., and Muller, K.J. (1978) *Proc.Nat. Acad.Sci.*, 75, 1016.
18. Patrick, J., and Stallcup, W.B. (1977) *Proc.Nat.Acad.Sci.*, 74, 4689.
19. Polz-Tejera, G., Schmidt, J., and Karten, H.J. (1975) *Nature*, 258, 349.
20. Segal, M., Dudai, Y., and Amsterdam, A. (1978) *Brain Res.*, 148, 105.
21. Szczepaniak, A.C. (1974) *J.Physiol.*, 241, 55P.
22. Maelicke, A., Fulpius, B.W., Klett, R.P., and Reich, E. (1977) *J. Biol.Chem.*, 252, 4811.
23. Weber, M., and Changeux, J.-P. (1974) *Mol.Pharmacol.*, 10, 15.
24. Weber, M., David-Pfeuty, T., and Changeux, J.-P. (1975) *Proc.Nat. Acad.Sci.*, 72, 3443.

25. Weiland, G., Georgia, B., Wee, V.T., Chignell, C., and Taylor, P.W. (1976) *Mol.Pharmacol.*, 12, 1091.
26. Adams, P.R., and Sakmann, B. (1978) *Proc.Nat.Acad.Sci.*, 75, 2994.
27. Sugiyama, H., and Changeux, J.-P. (1975) *Eur.J.Biochem.*, 55, 505.
28. Chothia, C., and Janin, J. (1975) *Nature*, 256, 705.
29. Litchfield, J.T., and Wilcoxon, F. (1949) *J.Pharm.Exp.Ther.*, 96, 99.
30. Hazelbauer, G.L., and Changeux, J.-P. (1974) *Proc.Nat.Acad.Sci.*, 71, 1479.
31. Hess, G.P., and Andrews, J.P. (1977) *Proc.Nat.Acad.Sci.*, 74, 482.
32. Popot, J.L., Sugiyama, H., and Changeux, J.-P. (1976) *J.Mol.Biol.*, 106, 469.
33. Lukasiewicz, R.J., Hanley, M.R., and Bennett, E.L. (1978) *Biochemistry*, 17, 2308.
34. Banks, B.E.C., Miledi, R., and Shipolini, R.A. (1974) *Eur.J.Biochem.*, 45, 457.
35. Eterovic, V.A., Aune, R.G., and Bennett, E.L. (1975) *Anal.Biochem.*, 68, 394.
36. Schmidt, J., and Raftery, M.A. (1973) *Biochemistry*, 12, 852.
37. Gray, E.G., and Whittaker, V.P. (1962) *J.Anat.*, 96, 79.
38. Weber, M., and Changeux, J.-P. (1974) *Mol.Pharmacol.*, 10, 1.
39. Lukasiewicz, R.J., and Bennett, E.L. (1978) *Biochim.Biophys.Acta* (in press).
40. Schmidt, J., and Raftery, M.A. (1973) *Anal.Biochem.*, 52, 349.
41. Horton, H.R., and Tucker, W.P. (1970) *J.Biol.Chem.*, 245, 3397.
42. Westhead, E.W. (1965) *Biochemistry*, 4, 2139.
43. Chicheportiche, R., Vincent, J.-P., Kopeyan, C., Schweitz, H., and Lazdunski, M. (1975) *Biochemistry*, 14, 2081.
44. Simpson, R.T., Riordan, J.F., and Vallee, B.L. (1963) *Biochemistry*, 2, 616.
45. Gilbert, H.F., and O'Leary, M.H. (1975) *Biochemistry*, 14, 5194.
46. Chang, C.C., and Lee, C.-Y. (1963) *Archs.Int.Pharmacodyn.Ther.*, 144, 241.

47. Lee, C.-Y., Chang, S.L., Kau, S.T., and Luh, S.-H. (1972) *J.Chromatog.*, 72, 71.
48. Cooper, D., and Reich, E. (1972) *J.Biol.Chem.*, 247, 3008.
49. Hanley, M.R. (1978) *Biochem.Biophys.Res.Communs.*, 82, 392.
50. Andreasen, T.J., and McNamee, M.G. (1977) *Biochem.Biophys.Res.Communs.*, 79, 958.
51. Jenkinson, D.H. (1960) *J.Physiol.*, 152, 309.
52. Scatchard, G. (1949) *Ann.N.Y.Acad.Sci.*, 51, 660.
53. Ishikawa, Y., Menez, A., Hori, H., Yoshida, H., and Tamiya, N. (1977) *Toxicon*, 15, 477.
54. Brockes, J.P., and Hall, Z.W. (1975) *Biochemistry*, 14, 2092.
55. Moody, T., Schmidt, J., and Raftery, M.A. (1973) *Biochem.Biophys.Res. Communs.*, 53, 761.
56. Quast, U., Schimerlik, M., Lee, T., Witzemann, V., Blanchard, S., and Raftery, M.A. (1978) *Biochemistry*, 17, 2405.
57. Weber, G. (1975) *Adv.Prot.Chem.*, 29, 2.
58. Bulger, J.E., and Hess, G.P. (1973) *Biochem.Biophys.Res.Communs.*, 54, 677.
59. Bulger, J.E., Fu, J.-J.L., Hindy, E.F., Silberstein, R.L., and Hess, G.P. (1977) *Biochemistry*, 16, 684.
60. Yang, C.C. (1965) *Toxicon*, 3, 19.
61. Yang, C.C. (1974) *Toxicon*, 12, 1.
62. Ravdin, P., and Axelrod, D. (1977) *Anal.Biochem.*, 80, 585.
63. Chicheportiche, R., Rochat, C., Sampieri, F., and Lazdunski, M. (1972) *Biochemistry*, 11, 1681.
64. Yang, C.C., Chang, C.C., and Liou, I.F. (1974) *Biochim.Biophys.Acta*, 365, 1.
65. Botes, D.P. (1974) *Biochim.Biophys.Acta*, 359, 242.
66. Karlsson, E., Eaker, D., and Drevin, H. (1973) *Biochim.Biophys.Acta*, 328, 510.
67. Horton, H.R., and Koshland, D. (1965) *J.Am.Chem.Soc.*, 87, 1126.
68. Salvaterra, P.M., and Mahler, H.R. (1976) *J.Biol.Chem.*, 251, 6327.
69. Lukasiewicz, R.J., and Bennett, E.L. (1978) *J.Neurochem.* (in press).

70. DeBlas, A., and Mahler, H.R. (1978) *J.Neurochem.*, 30, 563.
71. Fertuck, H.C., and Salpeter, M.M. (1974) *Proc.Nat.Acad.Sci.*, 71, 1376.
72. Arimatsu, A., Seto, A., and Amano, T. (1978) *Brain Res.*, 147, 165.
73. Barnard, E.A., Coates, V., Dolly, J.O., and Mallick, B. (1977) *Cell Biol.Int.Rep.*, 1, 99.
74. Bourgeois, J.P., Ryter, A., Menez, A., Fromageot, P., Boquet, P., and Changeux, J.-P. (1972) *FEBS Lett.*, 25, 127.
75. Yalow, R., and Berson, S.A. (1966) *Trans.N.Y.Acad.Sci.*, 28, 1033.
76. Dvorak, D.J., Gipps, E., and Kidson, C. (1978) *Nature*, 271, 564.
77. Frey, P.A., Kokesh, F.C., and Westheimer, F.H. (1971) *J.Am.Chem.Soc.*, 93, 7266.
78. Eftink, M.R., and Ghiron, C.A. (1976) *Biochemistry*, 15, 672.
79. Cohen, J.B., and Changeux, J.-P. (1973) *Biochemistry*, 12, 4855.
80. Barrantes, F.J. (1978) *J.Mol.Biol.*, 124, 1.
81. Franklin, G.I., and Potter, L.T. (1972) *FEBS Lett.*, 28, 101.
82. Meunier, J.-C., and Changeux, J.-P. (1973) *FEBS Lett.*, 32, 143.
83. Eldefrawi, M.E., Eldefrawi, A.T., Seifert, S., and O'Brien, R.D. (1972) *Archs.Biochem.Biophys.*, 150, 210.

84. Bursztajn, S., and Gershon, M.D. (1977) *J.Physiol.*, 269, 17.
85. Lowy, J., McGregor, J., Rosenstone, J., and Schmidt, J. (1976) *Biochemistry*, 15, 1522.
86. Seto, A., Arimatsu, A., and Amano, T. (1977) *Neurosci.Lett.*, 4, 115.
87. Schmidt, J. (1977) *Mol.Pharmacol.*, 13, 283.
88. Lentz, T.L., and Chester, J. (1977) *J.Cell Biol.*, 75, 258.
89. Hunt, S.P., and Schmidt, J. (1978) *Brain Res.*, 142, 152.
90. Karlin, A., Holtzman, E., Valderrama, R., Damle, V., Hsu, K., and Reyes, F. (1978) *J.Cell Biol.*, 76, 577.
91. Burden, S.J., Hartzell, H.C., and Yoshikami, D. (1975) *Proc.Nat.Acad.Sci.*, 72, 3245.
92. Reiter, M.J., Cowburn, D.A., Prives, J.M., and Karlin, A. (1972) *Proc. Nat.Acad.Sci.*, 69, 1168.
93. Almon, R.R., Andres, C.G., and Appel, S.H. (1974) *Science*, 186, 55.

CHAPTER VI.

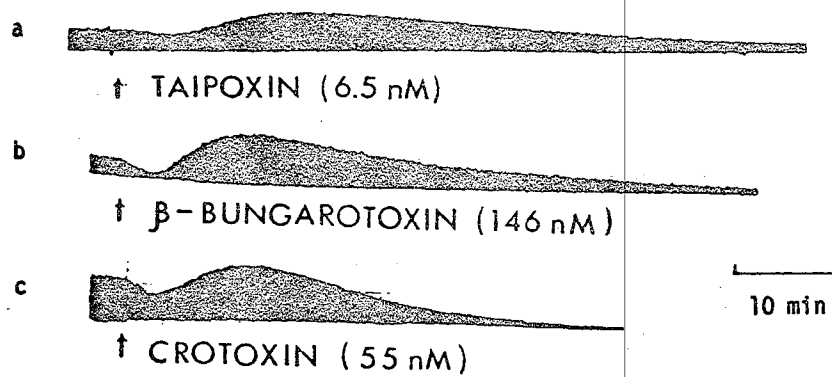
APPLICATIONS AND FUNCTIONAL
STUDIES OF THE β -TOXINS.

VI. INTRODUCTION.

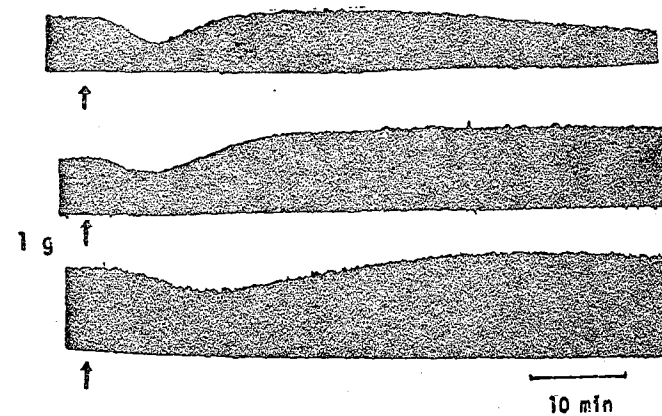
The class of toxic phospholipase A₂ (PhA) enzymes has emerged as one of the most intriguing areas in venom research. The β -type bungarotoxins are all potent blockers of transmitter release from the neuromuscular junction and are therefore regarded as "pre-synaptic" neurotoxins, although it should be noted that there are related toxic PhA enzymes which do not produce their toxic effects through an action on neural tissue. The relationship between the PhA activity and neurotoxicity is the major focus of current work on β -bgt and similar toxins (1,2). Several lines of evidence, particularly selective chemical modifications (3,4), have implicated the PhA digestion in the mechanism of the irreversible blockade. More extensive descriptions of the time course of physiological events from toxin application to junctional failure show three discrete phases. The simplest method to observe the multiple phases is the measurement of muscle tension with repetitive stimulation through the connecting nerve to an isolated nerve-muscle preparation (7). In such experiments, all of the characterized pre-synaptic snake toxins (Table III-2) block in qualitatively the same way: an initial depression, a secondary enhancement, and a final progressive depression to an irreversible final blockade (Figure 6-1). Intracellular recording has revealed that these events are paralleled by changes in the end-plate potential quantal content with evoked release, and in the miniature synaptic potential frequency with spontaneous release (6,8). Either the removal of external calcium, or the chemical modification of calcium binding to β -bgt by p-bromophenacyl bromide leads to the abolition of the final decline phase, but retains the characteristic initial inhibition followed by a slow rebound "recovery", although the recovery will not reach control levels if exposed to high concentrations of modified toxin (8,9). It has been suggested therefore that the initial response

Figure 6-1
Effects of pre-synaptic toxins on mouse phrenic nerve-diaphragm preparation in either low calcium (0.45 mM) (I) or with substitution of 3.6 mM $\text{Sr}(\text{NO}_3)_2$ for 1.8 mM CaCl_2 (II). Data from ref. 7.

I. LOW Ca^{+2}



II. Sr^{+2}



XBL 788 - 4118

reflects binding of the toxin to the pre-synaptic terminal (8-10), and that the other phases may be the result of the enzymatic activity. However, one complication is that in vitro PhA assays require the presence of non-physiological concentrations of calcium (>1 mM) and a surfactant in order to give high digestive rates (2), which has been interpreted as evidence that significant phospholipolytic damage could not occur under physiological conditions on the time scale of transmission blockade (2). Thus, the role of the enzymatic activity remains controversial (2,13). The actual cause of transmission failure has been attributed to a disruption of calcium metabolism in the nerve terminal (14), an accumulation of lysophosphatides (5,15), the uncoupling of pre-synaptic energy metabolism by liberated fatty acids, the inhibition of high-affinity choline uptake leading to a depletion of transmitter stores (17), and a depolarization of the nerve terminal (18). There have been claims to have mimicked β -bgt's action on central nervous system synaptosomes by fatty acids alone (16) or on the neuromuscular junction by direct application of lysolecithin (19). Clearly, the specifics of the molecular mechanism, the role of phospholipid degradation, and the basis for apparent pre-synaptic selectivity have all to be resolved.

Uncertainty about the mechanism of β -bgt has inevitably slowed its application as a synaptic tool (see Table VI-1). However, there have been several reports which have taken advantage of the degenerative effect of its chronic application to selectively delete neurons (20,21). Its apparent peripheral specificity for the chemical denervation of neuromuscular junctions has also been exploited (22). Attempts to use it as a specific nerve-terminal labeling agent have not been successful, not even at the neuromuscular junction where ultrastructural data suggests that it is highly localized (3). On the other hand, immunohistochemical lo-

TABLE VI-1

APPLICATIONS OF β -TYPE TOXINS

1. Molecular events in neurotransmitter release (3,5,15).
 2. Chemical denervation of neuromuscular junctions (5,22).
 3. Neuropathology of neuromuscular junctions (20).
 4. Structure-function studies of membrane-directed toxins (71).
 5. Central neuronal lesioning (this Chapter).
-

calization of bound β -bgt by a specific anti-toxoid antibody shows some regional variation in its binding to chick brain neuron cell bodies (24).

Results in this Chapter are addressed to several comparative aspects of the enzymatic activities, and membrane effects of the β -type bungarotoxins. Data is reported on the attempt to introduce a new application for pre-synaptic toxins as neuronal lesioning agents in vertebrate brain.

METHODS.

i. Toxicology. Peripheral toxicity was measured as described in Chapter V Methods (see also ref. 25). For intraventricular administration, toxins were injected in 1 μ L of artificial cerebrospinal fluid (26) with a Hamilton syringe. To prevent local edema, toxins were injected slowly over a two minute interval by a peristaltic pump. Controls with artificial cerebrospinal fluid alone were negative.

ii. Preparation of Excitable Vesicles and their Use in Sodium-22 Efflux Assays. These were described in Chapter V Methods.

iii. Preparation of Rat Brain Synaptosomes. Pinched-off nerve endings that are able to function in vitro as models for pre-synaptic endings can be isolated from homogenates of mammalian brain by differential centrifugation (29). Crude mitochondrial fractions contain these pinched-off nerve endings ("synaptosomes") and were prepared from rat brain as described in Chapter V Methods. Synaptosomes were purified by resuspension of the crude mitochondrial fraction in 5 mL of 0.32 M sucrose (pH 7.4 phosphate buffered) and layering over 20 mL of 0.8 M sucrose, followed by centrifugation at 9,000 X g for 30 min. The white band at the 0.32 M-0.8 M sucrose interface was taken and recentrifuged at 20,000 X g for 20 min. The resulting pellet was resuspended in rat Ringer to the required final concentration. Samples of the final pellet were processed for electron microscopy by a

30 min fixation in 2% glutaraldehyde at 4°C, followed by post-fixation with 1% osmium tetroxide in Ringer. The fixed pellets were dehydrated through graded ethanol and embedded in Spurr resin. Thin sections were cut with a diamond knife, stained with uranyl acetate, and viewed in a Siemens I electron microscope. The fraction was ~70% synaptosomes as judged by representative field surveys at various points through the thickness and width of the original pellet. Contaminants included myelinated axon fragments, ruptured membranes, and free mitochondria and vesicles.

iv. Fluorescence Monitoring of Synaptosome Membrane Potential with Merocyanine Dyes. 3,3'-Dipentyl-2,2'-oxacarbocyanine (CC₅, gift of Dr.A.S. Waggoner) was used to test effects of toxins on the maintenance of membrane potentials in intact synaptosomes (30). The dye's emission intensity has been shown to be a sensitive monitor of cellular membrane potentials (30,31) by alterations in its absorbance and fluorescence properties with potential changes. Excitation was at 475 nm and emission was recorded at 500 nm using 6 nm slitwidths in a Hitachi Perkin-Elmer MPF 2A recording fluorimeter. To 1 mL quartz cuvettes, 25 µL of the enriched synaptosome suspension (10 mg membrane protein/mL) was added to 1 mL of rat Ringer containing 5 µL of a 2 mg/mL standard solution of CC₅ in absolute ethanol. Integrity of the synaptosomes was routinely checked by depolarization with successive aliquots of 2 µL of a 3 M KCl solution. When toxins were added, they were introduced in 10 µL of Ringer, and mixed with the dye-stained suspension.

v. Phospholipase A Assay. The assay was modified from the basic procedure of Salach et al (27) which involves the rapid measurement of the rate of pH change over a narrow interval brought about by the release of titratable fatty acids. Unless otherwise noted, all assays were conducted at 37°C under

a nitrogen stream in a final volume of 2 mL of 100 mM NaCl, 1 mM CaCl₂, 0.05 mM EDTA, and 2.5 mM sodium deoxycholate, adjusted to pH 8.0 with 1 N NaOH. The substrate was 0.7 mL of emulsified egg yolk (1 egg yolk/100 mL), or 20 μmole of purified phospholipid (lecithin (Calbiochem) or phosphatidyl serine (Sigma)), or 50 to 100 μmole of liposome suspension activated by pre-treatment with 50 mM n-hexanol (69). Substrate and other solutions were always prepared fresh on the day of use saturated with argon to prevent oxidative lipid damage (28). Control tests on the production of fluorescent oxidative products were negative. The reaction was initiated by introducing the enzyme in 10 μL of assay medium. The rate of pH change was monitored by a Corning Digital 110 expanded scale pH meter coupled through a decade resistance box to a Moseley chart recorder. Rates were linear for the first 2 to 5 min and, in most instances, activity was measured from the rate of acid production from pH 8.00 to 7.90. In some experiments, enzymes were added in 1% BSA to prevent enzyme losses from adsorption, and the assay medium was supplemented with 0.1% BSA to sequester released fatty acids and prevent their accumulation. These modifications had no effect. It should be emphasized that these assay conditions were deliberately not optimized since it is not clear what the relationship of artificially enhanced in vitro activities is to the physiological digestion.

vi. Lipid Extractions. Total lipids were extracted from Torpedo excitable vesicles, rat brain synaptosomal membranes, or rat liver particulate fractions by 19 vol. of chloroform-methanol (2:1 v/v).

For the preparation of fatty acid or lysophosphatide extracts, a more extensive preparative scheme was followed. To suspensions of the membranes, 10 vol. of chloroform-methanol (3:1 v/v) was added for 1 hr at 20°C with constant stirring under a nitrogen barrier. The residue was re-extracted with 10 vol. of chloroform-methanol (2:1 v/v) for 30 min. Ten vol. each of

chloroform and water (deionized) were added and the phases broken by a brief centrifugation. The chloroform phase was removed and an equal volume of benzene added before drying the pooled organic phases under vacuum. The dry residue was taken up in 5 vol. acetone (with 0.2 vol of a solution of 5% $MgCl_2$ in methanol) and incubated at 4°C for one hr. The precipitate (containing polar lipids) was spun down at 5000 X g for 10 min, washed twice with 5 vol. of acetone, and dried on a rotary evaporator. The acetone supernatants (containing neutral lipids) were pooled and dried on a rotary evaporator. The polar lipid fraction was taken up in 1 vol. of chloroform and spotted on a preparative Silica Gel H (Brinkmann) plate. A parallel sample of standard lysolecithin (Sigma) was also applied as a mobility marker. The plate was developed in chloroform-methanol-acetic acid-water (25:15:4:2 v/v) and the marker position ($r_f = 0.1$) determined by staining with iodine vapors. The position corresponding to the mobility of the marker was scraped and eluted with 1 vol. of chloroform-methanol (1:1 v/v), dried, and taken up in 0.2 vol. chloroform. This stock was kept at 4°C under argon and is hereafter termed the "lysophosphatide" fraction. The neutral lipids were taken up in 1 vol. chloroform and applied in aliquots to preparative Silica Gel H plates. The plates were developed in heptane-isopropyl ether-acetic acid (60:40:4 v/v) using marker palmitic acid run in parallel to mark the position of fatty acids. The marker position ($r_f = 0.45$) was determined by spraying with 0.01% rhodamine 6G. The position corresponding to the marker was extracted with 0.5 vol. of chloroform. dried, and taken up in 0.2 vol. diethyl ether for storage under argon (4°C) as the "fatty acid" fraction.

vii. Liposome Preparation. A solution of the appropriate lipids in chloroform-methanol (2:1 v/v) was dried under a nitrogen stream, dissolved in

diethyl ether and dried again. The lipids were resuspended in aqueous solutions (to a 2% final lipid concentration) by vortexing and then sonicating at setting 4 on a Branson sonifier for 30 min at 4°C. The resulting clarified liposome preparation was freed from metal particles from the sonifier tip and multi-lamellar vesicles by centrifugation at 100,000 X g for 30 min.

viii. Stereotaxic Injection of Toxins. Male Sprague-Dawley rats were anesthetized with Equithesin and positioned in a stereotaxic apparatus. Toxin was injected in 0.5 mM sodium phosphate buffer (pH 7.0) containing 0.8% NaCl at a rate of 0.35 μ L/min until 1 μ L was injected. The cannula was positioned at L2.5, AP-3.2, V-3.0 for injections into the dentate gyrus, L0.5, AP-2.8, V-7.0 for injections into the diagonal band of the septum, L2.5, AP2.5, V-5.5 for injections into the corpus striatum, and L1.6, AP2.2, V-2.3 for injections into the substantia nigra. After 1 to 4 days, the rats were killed by decapitation, and the relevant regions removed for biochemical analyses or the brains were rapidly frozen as anterior and posterior halves in dry ice for histology.

ix. Enzyme, Uptake, and Receptor Binding Assays. Sodium-potassium-activated adenosine triphosphatase (Na-K-activated ATPase, Na pump, EC 3.6.1.3) was assayed in intact synaptosomes by the procedure of Forbush *et al* (32). Lactate dehydrogenase (LDH, EC 1.1.1.27) was assayed by a published procedure (43). Tyrosine hydroxylase (TOH, EC 1.14.16.2) was measured by the technique of Hendry and Iversen (33). Glutamic acid decarboxylase (GAD, EC 4.1.1.15) was assayed by the method of Fonnum *et al* (34). Choline acetyltransferase (ChA, EC 2.3.1.6) was measured by the technique of Fonnum (35). High affinity 3 H-choline uptake and high affinity, sodium-dependent 3 H- γ -amino butyric acid (GABA) uptake were measured in 200 X 200 μ brain region slices using published procedures (36,37). Muscarinic acetylcholine receptors

were monitored by the binding of ^3H -quinuclidinyl benzilate (^3H -QNB) by the technique of Hanley and Iversen (38). The binding of ^3H -etorphine and ^3H -spiroperidol were used to follow levels of opiate (39) and mixed aminergic (40,41) receptors respectively.

x. Histology. Frozen half-brains were sectioned at -20°C on a cryostat. Twenty five μ sections were taken at 50 μ intervals, air dried, formalin fixed, and stained for acetylcholinesterase (AChE, EC 3.1.1.7) by the procedure of Koelle and Friedenwald (42), and counter-stained with 0.1% cresyl-violet to visualize neuronal and glial cell bodies.

xi. Chemical Modifications. Chemical modifications followed published procedures which have been identified in the Methods sections of Chapters III-V.

RESULTS.

i. Toxicology. The quantitative characteristics of the β -toxins' lethality were reported in Tables V-3 and V-4. Toxin 12 as a representative member of this group shows their characteristic "lag" time before which death does not occur, even at the highest doses (Figure 5-2). Toxins 9A thru 13 all share this long minimum time-to-death, but toxin 14 at doses $>15 \times \text{LD}_{100}$ kills within 15 min, the time scale of curarimimetic effects. This could point to either cross-contamination with a post-synaptic toxin, or to the detection of a secondary activity at higher doses. In view of the physical evidence favoring the purification of toxin 14 away from post-synaptic toxins, the latter explanation is favored (toxin 14 can exhibit a post-synaptic activity, see section ii).

Toxin 9A had a particularly persistent action which was reflected in slow deaths (3 to 5 days after administration) at low doses. Even at the highest doses, toxin 9A was the slowest-acting of the β -toxins. The rank

order of the LD_{50} s was paralleled by the rank order of the minimum time-to-death. Persistence experiments using re-injection of surviving mice suggested that toxins 11 thru 14 were cleared more rapidly than the α -toxins since <35% of the previous day's dose could be detected by potentiation of the second dose. Toxin 9A was unique in that the potentiation of the lethality of a second dose suggested complete (100%) retention for more than 2 days.

Figure 6-2 shows that direct administration of β -bgt to the brain by injection into the lateral ventricles gives an LD_{50} over 10^3 X lower than that for peripheral lethality (0.02 ng/g vs. 50 ng/g respectively). Animals injected unilaterally with a lethal dose developed hyperactivity within 20 min, and frequently began contralateral circling. Within 30 min, righting ability was lost, and pronounced tremors began on the ipsilateral side. Up until death at 1 to 2 hrs, the tremors developed into spasmodic convulsive seizures that spread to the contralateral side, becoming more frequent and persistent until death occurred with complete muscular tetany. In all cases, there was a 20 to 30 min latent period before the development of symptoms, similar to the peripheral observations. However, the symptomology of the central action was otherwise utterly unlike the flaccid paralysis observed with peripheral injections.

ii. Sodium-22 Efflux from Excitable Vesicles. The β -toxins were screened for possible post-synaptic effects using the acceleration of ^{22}Na release from pre-loaded Torpedo excitable vesicles by cholinergic agonists as the test response. At a final concentration of 1 μM , toxins 9A and 14 blocked carbachol stimulation (Table VI-2). Interestingly, although they had no blocking action, the other β -toxins were nevertheless interacting in some way with the vesicles because they slowed the resting efflux rate. In view

Figure 6-2
Comparison of the central (intraventricular) and peripheral (subcutaneous) administration of β -bgt.

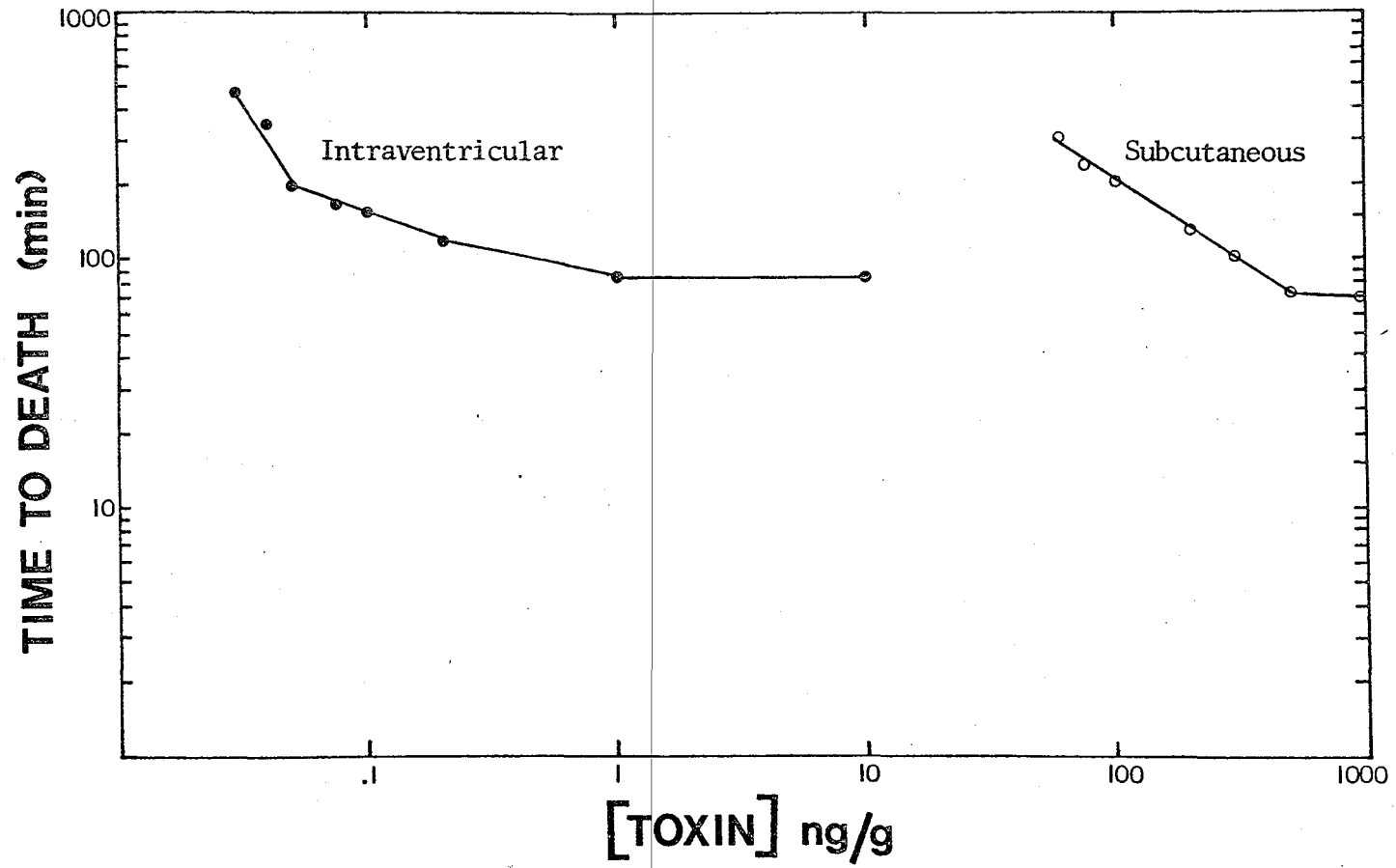


TABLE VI-2
SUMMARY OF SODIUM-22 EFFLUX EXPERIMENTS WITH β -TOXINS*

	θ_0 (min)	θ (min)	θ_0/θ
Control	9.3 \pm 1.0	1.0 \pm 0.1	9.3 \pm 1.0
β -Bgt	13.0	0.9	14.4
β -Bgt + 0.1 mM EGTA	14.9	1.1	13.5
β -Bgt (100 μ M)	13.8	5.5	2.5
9A	10.6	9.4	1.1
9A + 0.1 mM EGTA	10.2	1.2	8.5
9A (modified by p-bromophenacyl bromide)	9.8	1.1	8.9
9A (0.25 μ M)	10.2	3.5	2.9
9A (0.1 μ M, 30 min)	9.6	4.8	2.0
9A (0.1 μ M, 60 min)	9.2	9.0	1.0
11	12.9	1.0	12.9
12	12.3	1.1	11.2
13	13.1	1.0	13.1
14	9.7	9.6	1.0

*

Control values are the mean of ten separate determinations. All others are the mean of two determinations. All toxin incubations were for 15 min at 4°C at a final concentration of 1.0 μ M unless otherwise indicated. θ_0 and θ are the times for the resting and carbachol (0.1 mM)-stimulated efflux to reach 75% of the initial values.

of the calcium-dependent intrinsic PhA activity of these toxins (section iv), the experiments were repeated in 0.1 mM EGTA for toxin 9A and β -bgt. The blockade of carbachol stimulation by 9A was abolished in the absence of calcium, but the slowing of the resting efflux by β -bgt was not affected. Because less than stoichiometric amounts of 9A to receptor sites could produce a full block, and 10 X lower doses could produce a full block if the incubation was extended to 60 min, these results implicated the digestive activity of 9A, as had been proposed for crotoxin (44). Accordingly, the products of 9A membrane digestion of Torpedo vesicles were purified into "fatty acid" and "lysophosphatide" fractions, and added to excitable vesicles (Figure 6-3). The fatty acid fraction blocked carbachol stimulation and the lysophosphatide fraction disrupted the vesicles causing a rapid leakage of ^{22}Na . With protracted (>60 min at 1 μM) incubations with 9A or crotoxin, a gradual acceleration of the resting efflux rate was observed, suggesting accumulating membrane damage. The early phase of 9A action, the block of carbachol stimulation, was thus linked to fatty acid production, and the late phase, the increased resting leakage, was mimicked by lysophosphatides. The effects of the other β -toxins, the retardation of the resting efflux, were apparently not enzymatic in nature because calcium removal had no effect.

iii. Effects of β -toxins on Synaptosomes. Pre-synaptic nerve endings from the central nervous system can be isolated in a functional form from homogenates by differential centrifugation (45). These "synaptosomes" are commonly used as a biochemical test system for pre-synaptic effects. Previous results from a variety of laboratories indicated that not only was β -bgt active on synaptosomes, but it showed a complex range of effects (13,16-18,43).

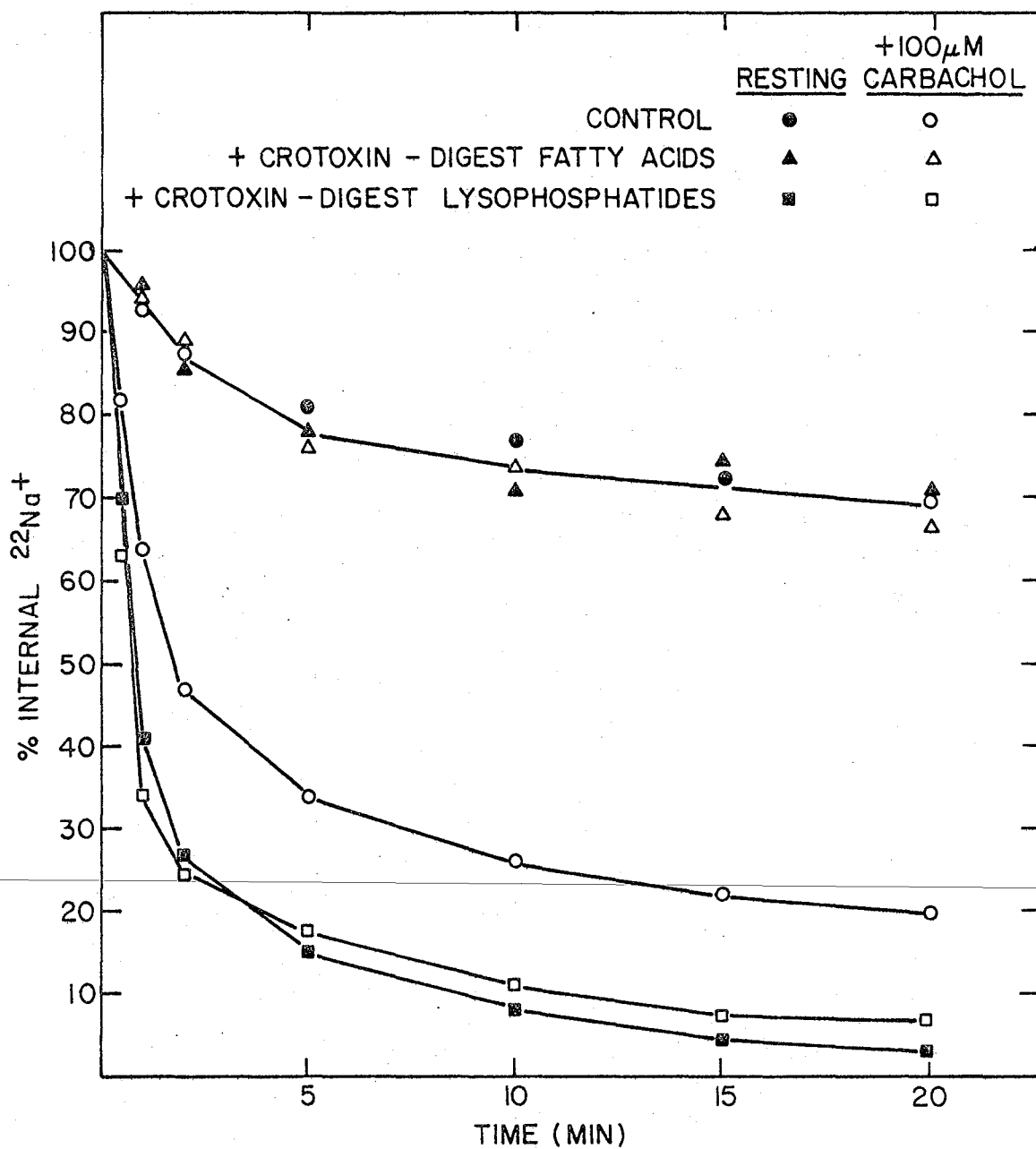


Figure 6-3

XBL7712-4791

Effects of the purified products of crotoxin digestion of Torpedo nAChR-rich membranes (60 min at 20°C) on the resting and carbachol-stimulated ^{22}Na efflux rates from excitable vesicles. Comparable results were obtained after a 60 min digestion of Torpedo membranes by $1\ \mu\text{M}$ bungarotoxin 9A.

Using lactate dehydrogenase (LDH) as a marker of synaptosomal integrity (43), β -toxins were incubated with enriched synaptosomes for 60 min and then the levels of the enzyme in the medium assayed. Under these conditions, the two-chain β -toxins were slightly disruptive. However, the single chain toxins 9A and 14 were more potent in releasing the intracellular LDH marker. As with Torpedo membranes, lysophosphatide and fatty acid fractions were purified from a 60 min digest of synaptosomes and added to test their effects. Lysophosphatides were able to almost completely mimic the quantitative rupturing elicited by 9A. These data are summarized in Table VI-3. Prolonged incubation with the other β -toxins (>3 hrs) gave eventual disruption of 70 to 80% of the synaptosomes, because 20 to 30% of the total LDH remained refractory to toxin-induced release at even very high concentrations or even longer incubation intervals.

Diffusion potentials are maintained in synaptosomes by an asymmetric distribution of ions which is maintained by the vectorial transport activity of the sodium pump (30). In intact synaptosomes, all pre-synaptic toxins completely abolished sodium pump activity within 30 min. Because this might in part be attributable to the consequences of partial lysis of the synaptosomes, β -bgt was tested on synaptosomal membranes and was found to have the same inhibitory effect. The kinetics of the inhibition was followed at 0.5 min intervals for all the β -toxins and the rapidity with which they produced enzymatic inhibition paralleled the rank order of their in vitro PhA activities (see Table VI-4).

Figure 6-4 shows that enriched synaptosomes maintain a diffusion potential that is sensitive to potassium depolarization, as expected (30,31). To demonstrate that the dye was not responding to changes in medium tonicity, similar additions of NaCl were without effect. Addition of 10 μ M β -bgt produced a decline in the resting potential after a 5 min lag period. The

TABLE VI-3

EFFECTS OF β -TOXINS ON SYNAPTOSOMAL ENZYMES MONITORING MEMBRANE PERTURBATIONS (SODIUM PUMP) AND SYNAPTOSOME LYSIS (LDH)

<u>Toxin</u>	<u>% LDH Released^a</u>	<u>$\tau_{1/2}$ for Na Pump Inhibition (min)^b</u>
9A	100	<1
β -Bgt	10	4.1
11	12	5.5
12	11	4.8
13	18	2.2
14	39	3.4
1% Triton X-100	100	x
9A Lysophosphatides ^c	87	x
9A Fatty acids ^c	0	x
9A (modified by p-bromophenacyl bromide)	0	No effect

a

Lactate dehydrogenase (LDH) is an intracellular enzyme used to monitor synaptosomal rupturing by the proportion of total activity released to the incubation medium compared to 100% value from 1% Triton X-100 solubilization (43). Control values were only 5-6% of the total values. Total values were 457 nmol substrate/min/mg membrane protein. All incubations with toxins were 60 min at 20°C in rat Ringer using enriched synaptosomes (see Methods) at a final concentration of 1 mg membrane protein/mL.

b

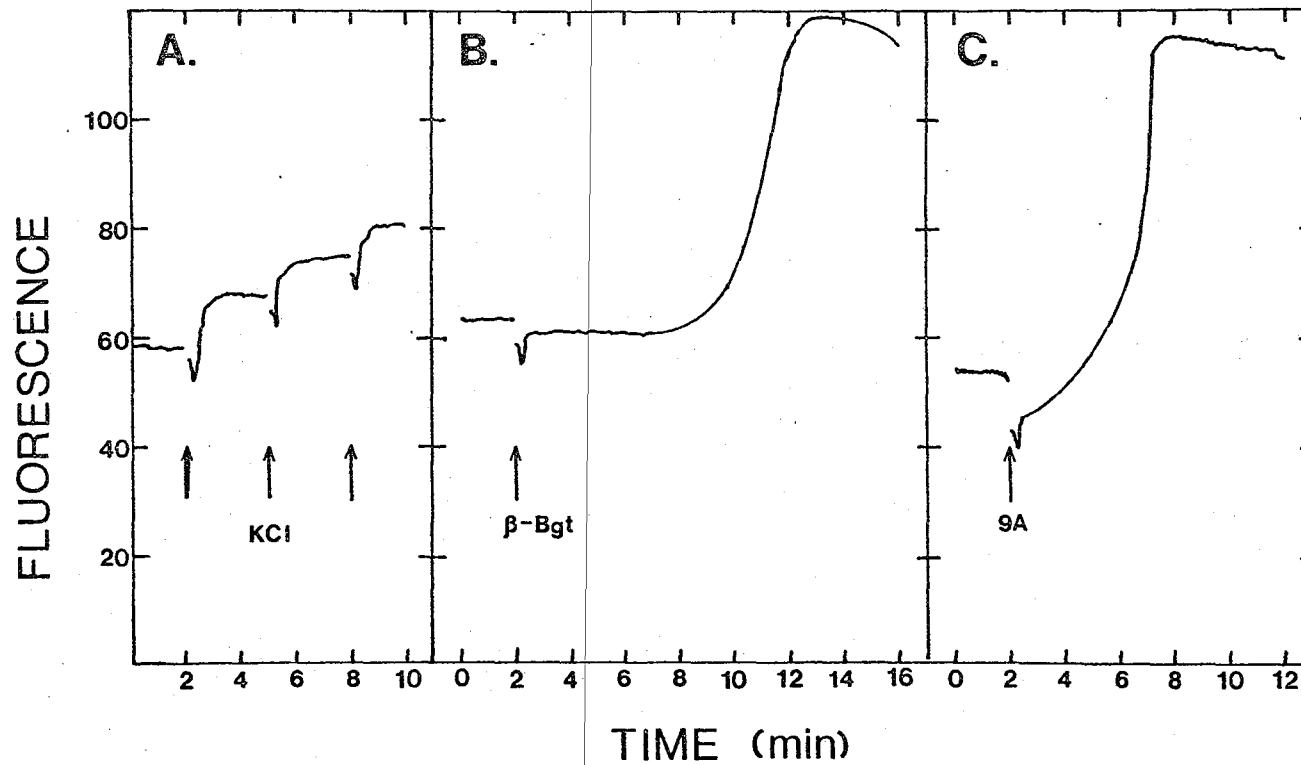
All toxins quantitatively abolished Na-K-activated ATPase (Na pump) activity within 30 min at 20°C. The reported numbers are the half-time for 100% inhibition from time course curves generated at 0.5 min intervals.

c

Purified from 60 min digests at 20°C of synaptosomal membranes by the procedures described in Methods.

X- not tested.

Figure 6-4
Effects of A) successive 2 μ L aliquots of 3M KCl, B) 10 μ M β -bgt, and C) 10 μ M toxin 9A on the membrane potential of enriched synaptosomes using CC_5 fluorescence. Note that increases in fluorescence intensity indicate depolarization (loss of membrane potential). Additions of 2 μ L aliquots of 3M NaCl had no effect on fluorescence.



changes it produced were irreversible and could not be compensated for by changes in the medium ionic composition. Toxins 9A and 14 were much more rapid in the onset and time course of membrane depolarization.

iv. Phospholipase A Activities. PhA activities of the various toxins were assayed by the rate at which they produced fatty acids, which was linear for the first 2 to 5 min at pH 8.0 in all cases. Using emulsified egg yolk as the substrate (2,46), the toxins 9A thru 14 exhibited negligible PhA activity in the absence of both calcium and a surfactant. With the addition of both 1 mM CaCl₂ and 2.5 mM sodium deoxycholate, the intrinsic activities were augmented to levels in the range of other PhA enzymes (47). Comparison of the toxins shows that the two-chain toxins give the same rank order of enzymatic activity as they do animal lethality, as has been reported elsewhere (8). However, the rank order for PhA/lethality was 12>13>11>β-bgt in the earlier study, compared to the order 13>β-bgt>12>11 reported here. Toxins 9A and 14 did not fit into the ranking scheme as they were weaker lethal agents but more potent PhA enzymes than the other toxins. Toxin 9A gave the highest activity under these conditions (Table VI-4). In an attempt to compare hydrolytic rates under defined model conditions that would also be suitable for spectroscopy, several conditions were tried. The highest in vitro hydrolysis rates were obtained using mixed detergent-lipid micelles, as documented by Dennis for Naja naja PhA (47). However, the substantial UV absorption of most detergents rendered them useless for spectral studies, and the UV-transparent detergent Emulphogene BC-720 produced scattering artifacts in both fluorescence and CD pilot experiments. Thus, liposomes were prepared from purified or tissue-extracted lipids and used as substrates. Liposomes were prepared under conditions designed to give maximum yields of homogeneous unilamellar products. Gel filtration

TABLE VI-4

Toxin	Activity ^a	CHARACTERISTICS OF INTRINSIC PHOSPHOLIPASE A ACTIVITIES OF β -TOXINS		Liposome Substrates ^d				Membranes ^e	
		Ca ⁺² Req. ^b	DOC Req. ^c	Lecithin	P-Serine	Liver	Synaptic	Liver	Synaptic
9A	250	Yes (0.16 mM)	Yes	26	9	4	19	10	82
β -Bgt	90	Yes (0.14 mM)	Yes	7	2	0	11	4	23
11	65	Yes (0.18 mM)	Yes						
12	76	Yes (0.15 mM)	Yes						
13	170	Yes (0.15 mM)	Yes	11	3	0	10	12	35
14	110	Yes (0.06 mM)	Yes	10	7	2	18	7	42

a

μ moles/min/mg protein on deoxycholate-dispersed egg yolk. All values for enzymatic activity are in the same units.

b

Hydrolysis undetectable in its absence. Numbers in parentheses are the estimated dissociation constants for calcium binding using the quenching of intrinsic fluorescence (8). All toxins were >50% activated by Eu⁺², 5 to 50% activated by Sr⁺², and were inhibited by Zn⁺² whether in the presence or absence of 1 mM CaCl₂. One mM CaCl₂ in the incubations. Eu⁺² and Sr⁺² activations were tested at 10 mM, as was Zn⁺² inhibition.

c

Sodium deoxycholate at 2.5 mM was necessary to achieve measurable rates. This does not imply a strict requirement for DOC, but rather the need for surfactant treatment of the substrate.

d

Liposomes were activated by the addition of 50 mM n-hexanol which retains liposome structure, but improves hydrolysis rates (69). DOC was not used because it favors liposome disruption and the formation of mixed detergent-lipid micelles. N-hexanol does not promote dissociation of titratable fatty acids, but rather improves substrate availability (69). Liver and synaptic membrane liposomes were prepared from "total lipid" extracts (chloroform-methanol 2:1 v/v).

e

Intact membranes were from a 100,000 X g pellet of lysed mitochondrial/microsomal fractions and were activated by 50 mM n-hexanol.

of liposome preparations on Sepharose 2B gave a single symmetric peak of light scattering at A_{300} .

Studies using liposome substrates focused on the two single chain toxins, 9A and 14, and two of the two-chain toxins, β -bgt and 13. In general, liposome substrates were not hydrolyzed with the high rates of mixed micelles or detergent-dispersed substrates. Nevertheless, usable rates were obtained under these conditions using the activator 50 mM n-hexanol (69). The first observation was that enriched homogeneous liposomes gave more satisfactory rates than had been noted with multilamellar substrates (48). Dimyristoyl phosphatidyl choline was used as a substrate because it was reported to give the highest hydrolysis rates of synthetic lecithins in the absence of detergent (48). The rank order of digestive rates on this substrate followed the rank order seen with emulsified egg yolk (Table VI-4). Purified brain phosphatidyl serine (PS) gave slower rates and a slightly different rank order of rates, toxin 14 being more potent than 13 on this substrate. It must be noted that PS liposomes were digested in the presence of 1 mM calcium, a condition which produced a marked turbidity indicative of the reduced solubility of the substrate. The fact that calcium forms an insoluble salt with PS and cross-links liposomes to produce aggregates that are poor PhA substrates have been discussed by Dennis et al (49). Further, the competition between PS and the toxin for calcium may reduce the concentration below the PhA's required level. Thus, the improved rates with toxin 14 relative to 13 may be attributable to the former's higher calcium-binding affinity. In order to detect any tissue specificity of cleavage rates, total lipid extracts from liver and synaptosomal membranes were used to prepare liposomes. The two-chain toxins were inactive on liver lipids and the single chain toxins gave reduced rates. However, faster hydrolysis rates were detected using

synaptosomal liposomes. Rates were slightly higher on this preparation than on the others tested. Liver membranes and intact synaptosomal membranes were not detectably degraded in the titration assay unless activated by the addition of 50 mM n-hexanol (69). All of the tested toxins worked better on synaptosomal than liver membranes, and single chain toxins were the most effective in terms of absolute rates.

Figure 6-5 shows the concentration dependence of the initial rates of fatty acid liberation on emulsified egg yolk substrates. The two-chain toxins gave a linear concentration dependence, but the single chain toxins' rates reached plateau values below 30 nM.

The toxins gave a variety of responses to different divalent cations in spectral or enzymatic assays. However, one universal feature of the PhA activities was that they were all effectively activated by Eu^{+2} substitution, partially activated by Sr^{+2} substitution, and inhibited by Zn^{+2} inclusion (independent of the presence of calcium). The Eu^{+2} substitution offers the possibility of studying the calcium-binding site by fluorescence and magnetic circular dichroism techniques.

Using the intrinsic fluorescence of β -bgt's single trp as a reporter, its interaction with liposomes was tested. There was no change of the fluorescence properties with up to a 20 X molar excess of phosphatidyl choline, phosphatidyl ethanolamine, or sphingomyelin in either the presence or absence of calcium. On the other hand, there was a 14 nm blue shift of the position of the emission maximum (338 to 324 nm) and a doubling of intensity upon exposure to liposomes of phosphatidyl serine (PS), phosphatidic acid (PA), and phosphatidyl inositol (PI) (Figure 6-6). The fluorescence changes saturated, on a mole lipid/mole protein basis, at 8 for PS, 12 for PA, and 22 for PI. The changes in the position of the

Figure 6-5
Dependence of phospholipase digestive rates in pH-change assay (see Methods) on toxin concentration. Emulsified egg yolk was used as substrate.

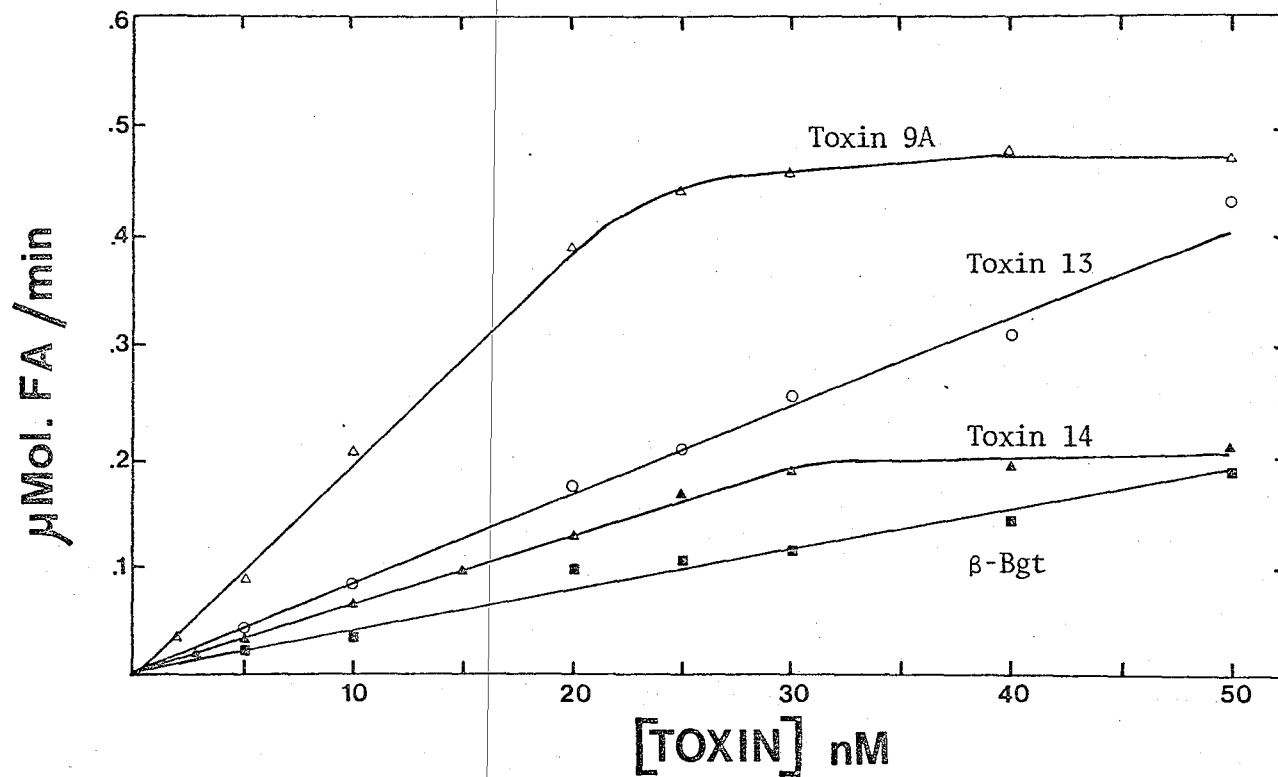
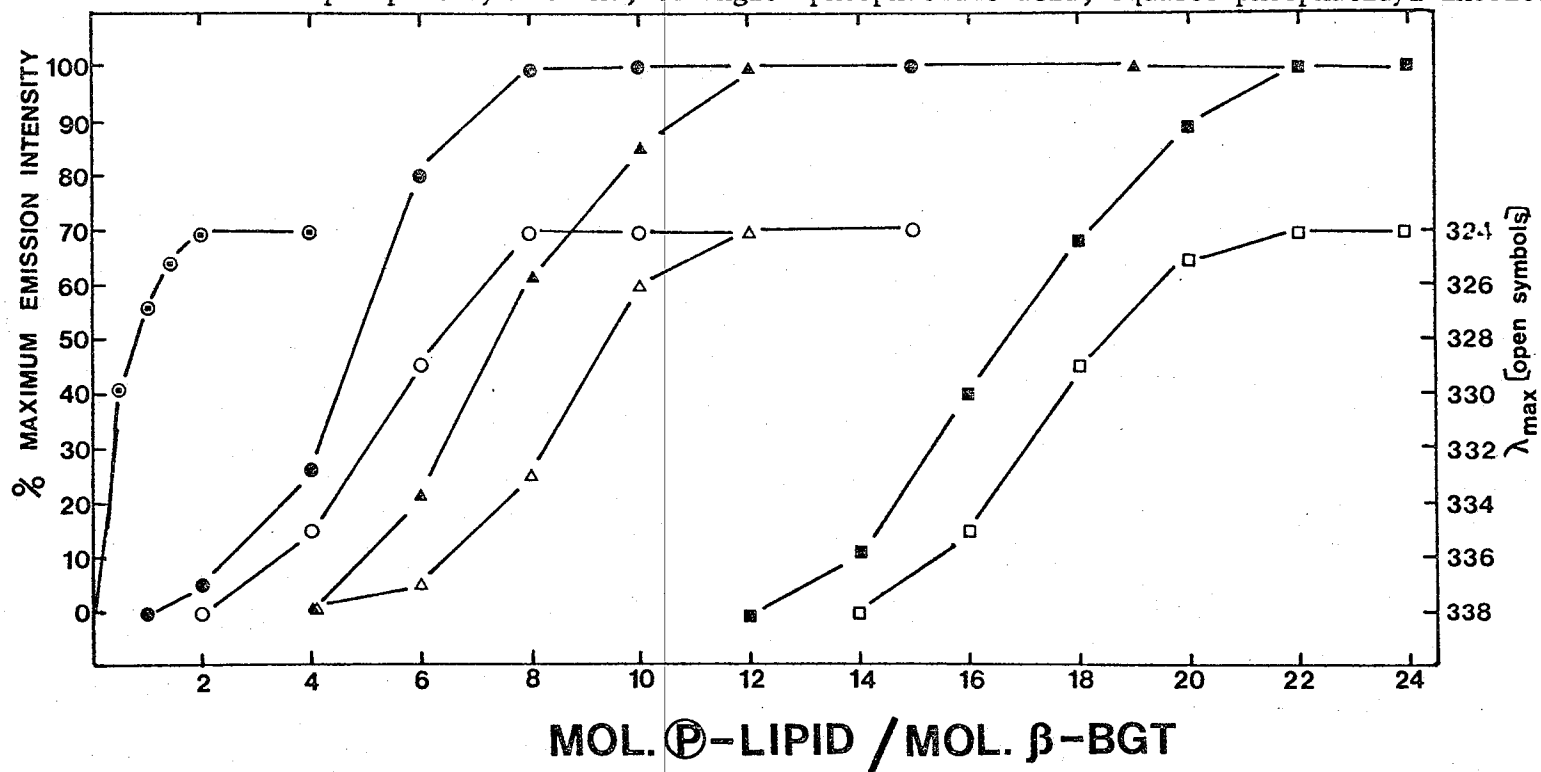


Figure 6-6

Interaction of 3.3 μM β -bgt with model liposomes monitored by changes in intrinsic emission maximum intensity (solid symbols) and wavelength (open symbols). All incubations were in 20 mM Tris buffer (pH 7.4) containing toxin to which aliquots of phospholipid suspensions were added. Circles-phosphatidyl serine, triangles-phosphatidic acid, squares-phosphatidyl inositol.



θ -phosphatidyl serine/gangliosides (total brain, Sigma) at 1:1 mole/mole in the presence of 1 mM CaCl_2 . Either the addition of calcium or gangliosides alone did not enhance the molar potency of liposomes to elicit the emission maximum wavelength shift. Excitation was at 287 nm using 6 nm emission and excitation slitwidths in all cases.

emission maximum paralleled those in the intensity, and were independent of the toxin concentration from 0.1 to 10 μM . The addition of 1 mM CaCl_2 quenched the fluorescence, as noted before (8), but did not dissociate the complex because the shifted position of the emission maximum was not altered. Mixed liposomes of PS and brain gangliosides (one-to-one on a molar basis) gave the same effects as PS liposomes alone, shifting the position of the emission maximum in proportion to the added molar proportion of PS in the liposomes. The addition of calcium to the PS-gangliosides preparation led to the saturation of fluorescence changes at one to two moles PS/mole protein.

v. Effects of Chemical Modifications of β -Bgt on Lethal and Enzymatic Activities. Table VI-5 summarizes the results of selective chemical modifications. As with the α -toxins, there are modifications which either abolish activity or have no effect. Both lethal and PhA activities were abolished by 1) modification of basic groups, 2) modification of arg residues after deblocking of lys residues with 2,4-pentanedione modification, 3) photochemical oxidation of three his and the single trp, and 4) reduction of cystines by dithiothreitol. Modification of tyr residues by N-acetyl imidazole is the only modification which had no effect on both lethal or PhA activities. One goal of chemical modification is to achieve a discrimination between the enzymatic and lethal functions, as has been claimed elsewhere (4,6), or to show that the activities are always modified in the same proportions (3). Unfortunately, the data do not fall into one pattern or the other. Modifications appear to most frequently cause a decline, but not a complete abolition, in both functions. N-bromosuccinimide oxidation and Koshland reagent I modification of the single trp reduced the lethal activity $\sim 90\%$, as has been seen with another PhA (50), but the former modification has 10 X more severe consequences

TABLE VI-5

EFFECTS OF SELECTIVE CHEMICAL MODIFICATIONS OF β -BGT ON LETHALITY AND PHOSPHOLIPASE ACTIVITIES AND PROTECTION AGAINST SELECTED MODIFICATIONS

<u>Modification</u>	<u>Modified Residues</u>	<u>Ev. for Specific Modification</u>	<u>% Lethality^a</u>	<u>% Pha^b</u>
N-bromosuccinimide	1 Trp	Fluorescence	10	0.6
Dimethyl-(2-hydroxy-5-nitrobenzyl) sulfonium bromide	1 Trp	Fluorescence	8	5
Tetranitromethane	4 Tyr	Amino acid analysis	75	54
N-acetyl imidazole	3 Tyr	Spectrophotometry	100	100
Dimethyl suberimidate	5 Amino Groups	Ninhydrin reactivity	50	40
Methyl butyrimidate	8 Amino Groups	Ninhydrin reactivity	20	33
Dansylation	7 Amino Groups	Ninhydrin reactivity	0	0
2,4-Pentanedione	8 Amino Groups	Ninhydrin reactivity	0	0
(after lys deblocking)	+ 4 Arg 4 Arg	Amino acid analysis Amino acid analysis	0	0
p-Bromophenacyl bromide	1 His	Spectrophotometry	2	0.1
Dithiothreitol (excess)	All Cystine	DTNB titration	0	0
Dithiothreitol (1 mole/ mole toxin)	0.8 Cystine	DTNB titration	1	2
Photochemical oxidation (Rose Bengal)	3 His, 1 Trp	Amino acid analysis	0	0
Photochemical oxidation (Methylene Blue)	2 Met, 1 Trp 4 Tyr (1 His ?)	Amino acid analysis	0	0

PROTECTION STUDIES

<u>Modification Reaction</u>	<u>Modified Residues</u>		
	<u>Native</u>	<u>+ 10 mM CaCl₂</u>	<u>+ PS Liposomes^c</u>
N-bromosuccinimide	1 Trp	1 Trp	None
Tetranitromethane	4 Tyr	3 Tyr	2.4 Tyr
p-Bromophenacyl bromide	1 His	1 His	0.3 His

a

Based on time-to-death at LD₁₀₀=0.08 μ g/g and an estimated LD₅₀ using ten mice. No lethality indicates no deaths at 10 X LD₁₀₀.

b

Phospholipase activity using emulsified egg yolk + 1 mM CaCl₂ + 2.5 mM deoxycholate.

^cPhosphatidyl serine liposomes + 1 mM CaCl₂ were added at a molar ratio of 10:1 to toxin

on the assayed PhA. Tetranitromethane treatment of exposed tyr residues (51) reduced both activities to a small extent, as did the introduction of an average of 2 to 3 cross-links by dimethylsuberimidate. Reduction of one disulfide by timed exposure to dithiothreitol reduced the activities to low levels. Similarly, photooxidation sensitized by methylene blue destroyed several different residues and led to a large loss of both activities. The most extensively used modification of toxic PhA has been the eradication of a single his implicated in calcium binding by p-bromophenacyl bromide (3,8,10-12,52). As has been reported for β -bgt (3,8), this modification extensively reduced, but did not abolish both activities.

In the effort to identify the origin of activity changes, modifications were repeated under protecting conditions with either 10 mM CaCl_2 or a ten-to-one suspension of phosphatidyl serine liposomes (moles lipid/mole protein). The NBS modification of trp could be prevented by liposomes, but not by calcium. Tetranitromethane modification of one of the four tyr residues it normally alters could be prevented by calcium, and two of the four could be protected by liposomes. The p-bromophenacyl bromide reaction was not blocked by calcium, but could be inhibited by liposomes.

vi. Application of β -Toxins as Lesioning Tools by Stereotaxic Injection into Rat Brain. Initial experiments tested the lesioning potential of β -bgt on rat corpus striatum and showed that doses as low as 0.1 ng could induce pronounced focal dégeneration on a time scale of days. Accordingly, more extensive studies were directed to the septal-hippocampal system, which has several attractive features: 1) a well-characterized central cholinergic projection (53), 2) a reproducible laminar staining pattern in the dentate gyrus which is a sensitive monitor of the integrity of pre- and post-synaptic elements, and 3) the availability of data on the effects of other lesioning agents (55,56). In-depth studies on the nigro-

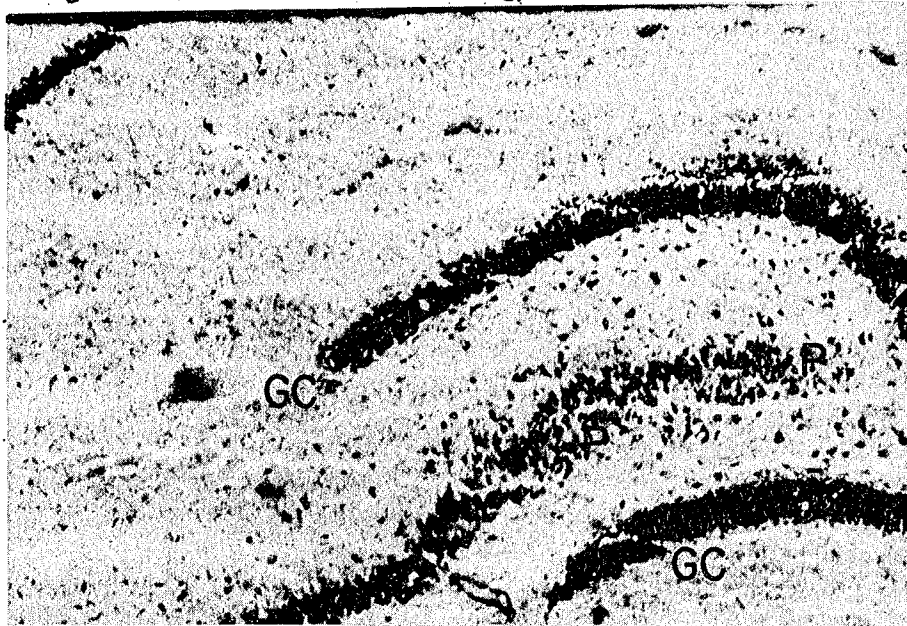
striatal system were complementary in that the striatum contains a population of cholinergic interneurons (57) and has been extensively studied by kainic acid lesioning (58,59).

Examination of cresyl violet-stained sections of the dentate gyrus (Figure 6-7A) indicated a focal lesion with both pyramidal cell and granule cell loss and glial cell proliferation. Acetylcholinesterase histochemistry (Figure 6-7B) of the dentate gyrus on the injected side showed a breakdown of the normal laminar distribution of AChE-positive product in this area, diffusion of the reaction product, and evidence of neuronal loss, particularly in the granule and pyramidal cell layers. All the histochemical observations indicated that like kainic acid, β -bgt can damage neuronal cell bodies. However, at low doses, the kainic acid lesion can be more selective, as for pyramidal cells in the hippocampus (56).

Nerve terminals have specific high-affinity uptake systems which serve to scavenge and recycle transmitters (60). High-affinity ^3H -choline uptake in both the diagonal band and the dentate gyrus was quantitatively inactivated by the time of the first measurement at day one. High-affinity ^3H -GABA uptake was also strongly attenuated by day one (Figure 6-8B), but recovered progressively over the next three days. This may reflect a contribution by the proliferating glial cells to the net uptake (61). The muscarinic receptor-labeling ligand ^3H -QNB is thought to be a strictly post-synaptic marker in the hippocampus (62), and thus was used as another indicator of cellular integrity. Its decline paralleled that of the enzymatic markers in the same area (Figure 6-9A).

Figure 6-9 shows the effects at one to four days after β -bgt injection on enzymatic markers in the dentate gyrus and the diagonal band. ChA activity checked the status of cell bodies in the diagonal band and nerve

Figure 6-7A
 Cresyl violet staining of β -bgt lesions at four days after injection
 of 1 ng of toxin into the dentate gyrus.

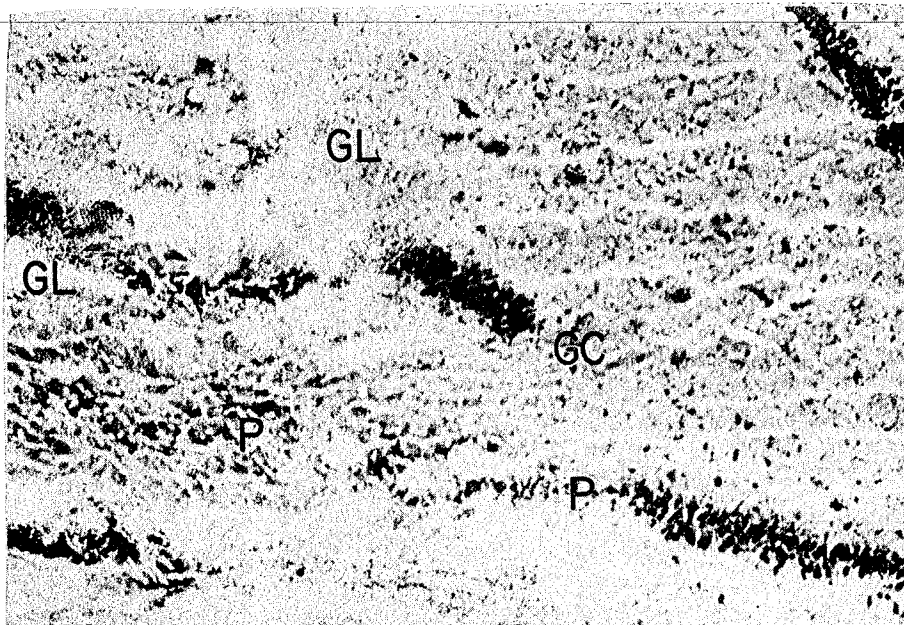


XBB 7812-15343a

Control side X 50 magnification.

P-pyramidal cell; GC-granule cells; GL-glia cells.

Note loss of pyramidal and granule cells (neurons) and glial proliferation in lesioned side vs. control side.



XBB 7812-15341a

Lesioned side X 50 magnification.

Figure 6-7B

Acetylcholinesterase staining of β -bgt lesions at four days after injection of 1 ng into the dentate gyrus.



Control side X 50 magnification.

XBB 7812-15342a

P-pyramidal cells; GC-granule cells.

Note disruption of staining around granule and pyramidal cell bands in lesioned side vs. control side.



Lesioned side X 50 magnification.

XBB 7812-15340a

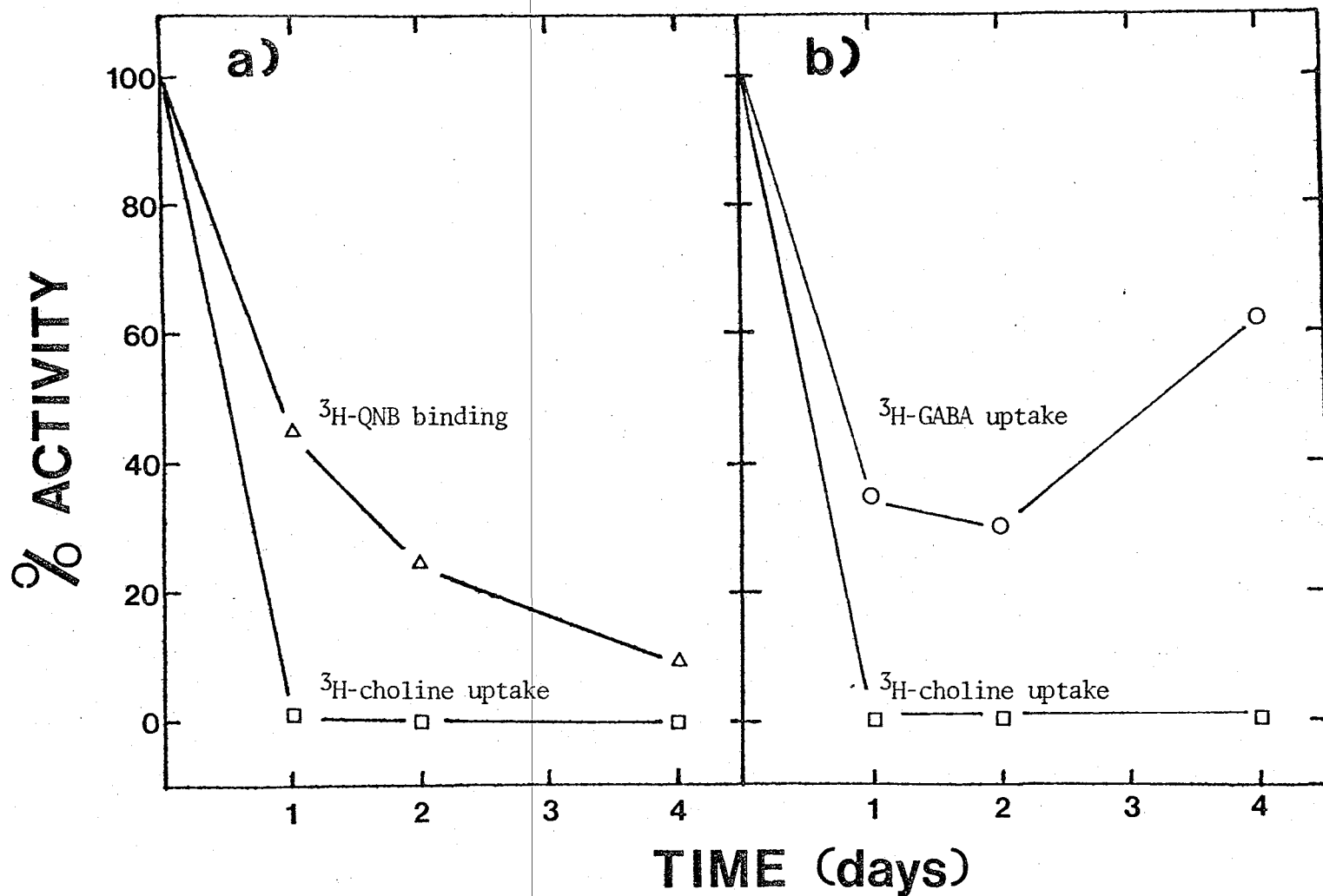


Figure 6-8

Declines in receptor and uptake markers in the dentate gyrus (a) and the diagonal band (b) with injection of 1.0 ng of toxin on day zero. Control activities were: $^3\text{H-choline}$ uptake (dentate gyrus), 2.2 pmoles/mg protein/min; $^3\text{H-choline}$ uptake (diagonal band), 0.8 pmoles/mg protein/min; $^3\text{H-QNB}$ binding (dentate gyrus), 0.42 pmoles/mg protein; $^3\text{H-GABA}$ uptake (diagonal band), 5.3 pmoles/mg protein/min.

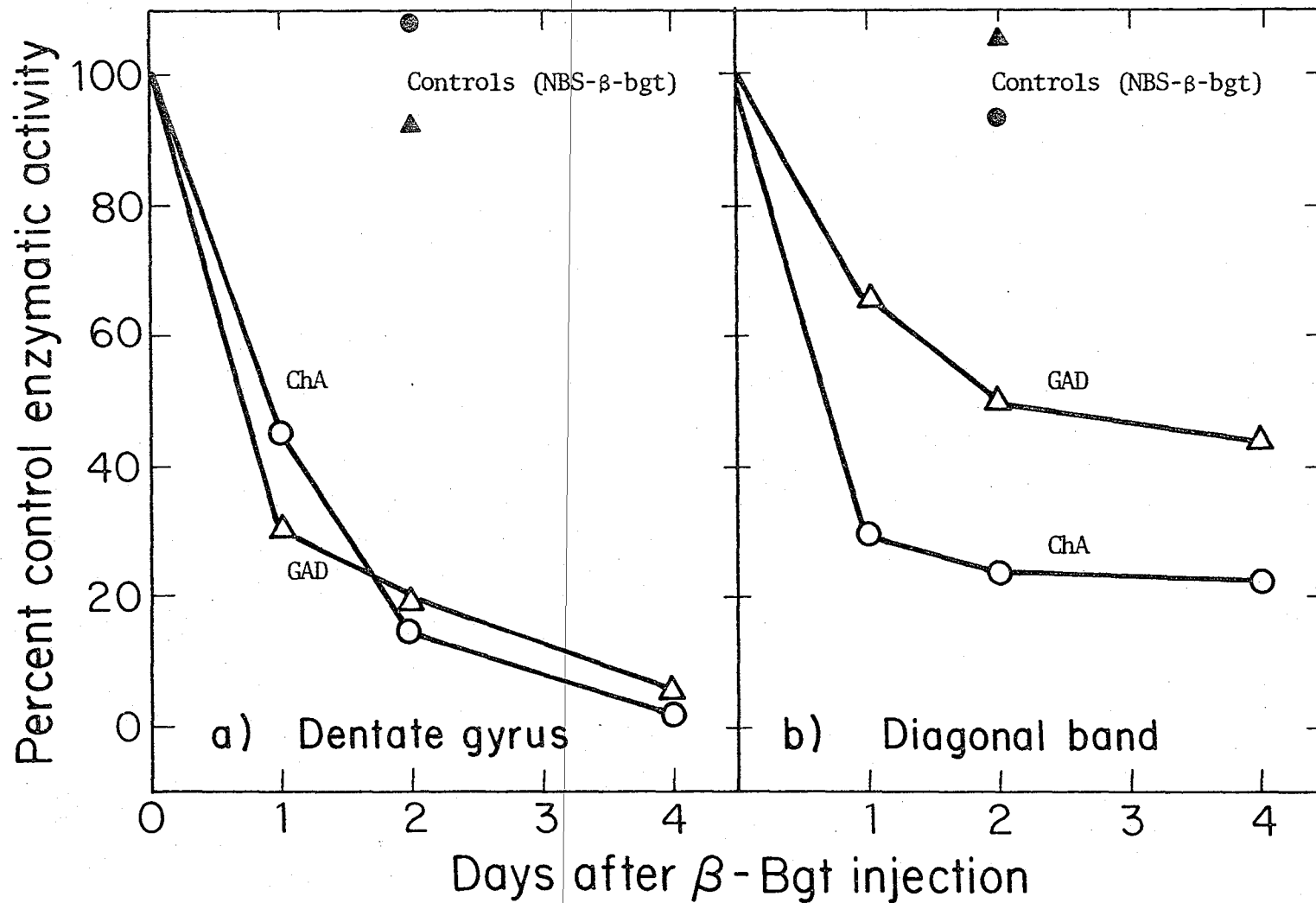


Figure 6-9

Declines in enzymatic markers in dentate gyrus (a) and the diagonal band (b) with XBL 785-942 injection of 1.0 ng of toxin on day zero. Control activities were: ChA (dentate gyrus), 69 nmoles/mg wet wt./hr; ChA (diagonal band), 182 nmoles/mg wet wt./hr; GAD (dentate gyrus), 59 nmoles/mg wet wt./hr; GAD (diagonal band), 80 nmoles/mg wet wt./hr.

terminals in the dentate gyrus, and GAD levels monitored the integrity of cell bodies of neurons in both the diagonal band and the dentate gyrus. Declines for both markers in both regions indicated no pre- or post-synaptic or cholinergic vs. non-cholinergic strict specificity.

ChA served as an indicator for intrinsic cholinergic interneurons in the striatum, TOH marked the integrity of the dopaminergic nerve terminals, and GAD reported on a population of cell bodies which send projections outside the striatum (63). Figure 6-10A shows that all three markers declined with the same time course after β -bgt injection. Histological observations of the substantia nigra had indicated little damage with β -bgt introduction. Accordingly, it was not surprising that there was only a 20% decline in the cell body marker TOH over four days (Figure 6-10B), but the pre-synaptic marker GAD was progressively reduced over the same period.

In the striatum, ^3H -choline uptake was again completely eradicated by the first day (Figure 6-11A). The decline of the receptor probes ^3H -etorphine (opiate receptors) and ^3H -QNB matched that of the enzymatic markers in the striatum (Figure 6-11A). In the nigra, the receptor label ^3H -spiroperidol (which labels dopaminergic receptors in this region (64)) declined only partially, to a level matching that of TOH on a percentage basis. ^3H -GABA uptake, however, was rapidly lost and was undetectable by day two. This indicates the loss of pre-synaptic function and may be indicative of nerve terminal damage (Figure 6-11B).

The role of the toxin's PhA activity in this effect was investigated in some preliminary experiments. To rule out a non-specific physical disruption, unrelated to β -bgt's enzymatic and toxic activities, the NBS-trp derivative was injected and found to be ineffective at even 10^3 X higher

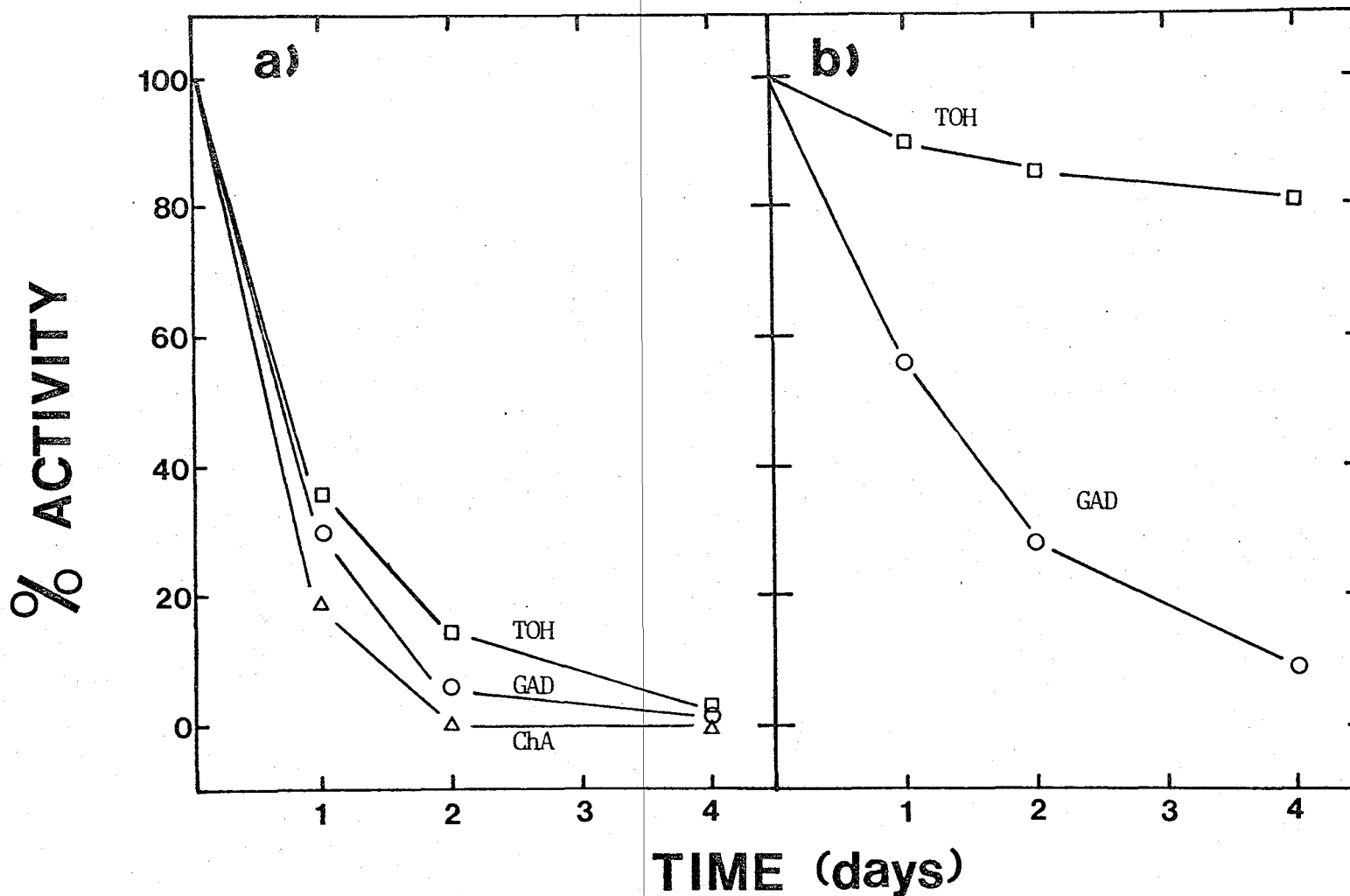


Figure 6-10

Declines in enzymatic markers in corpus striatum (a) and substantia nigra (b) with injection of 1.0 mg of toxin on day zero. Control activities were: TOH (corpus striatum), 172 pmoles/mg protein/hr; GAD (corpus striatum), 238 nmoles/mg protein/hr; ChA (corpus striatum) 188 nmoles/mg protein/hr; TOH (substantia nigra), 285 pmoles/mg protein/hr; GAD (substantia nigra), 285 nmoles/mg protein/hr.

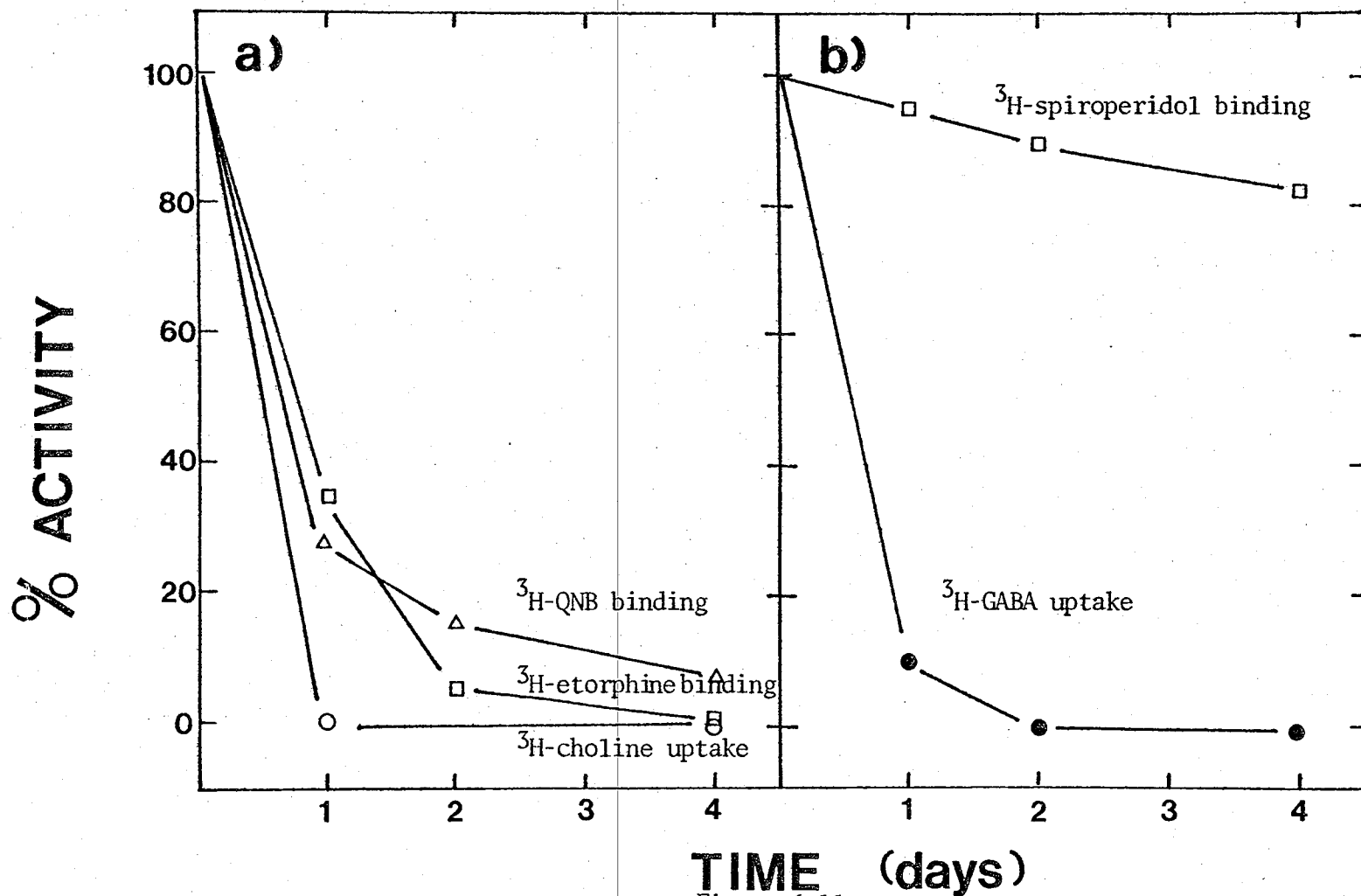


Figure 6-11

Declines in receptor and uptake markers in corpus striatum (a) and substantia nigra (b) with injection of 1.0 ng of toxin on day zero. Control activities were: ^3H -choline uptake (corpus striatum), 13.0 pmoles/mg protein/min; ^3H -QNB binding (corpus striatum), 0.89 pmoles/mg protein; ^3H -etorphine binding (corpus striatum), 90 fmoles/mg protein; ^3H -GABA uptake (substantia nigra), 7.8 pmoles/mg protein/min; ^3H -spiropiperidol binding (substantia nigra), 0.36 pmoles/mg protein.

doses than the native toxin. All other pre-synaptic bungarotoxins, either single chain or two-chain structures, produced similar lesions in the striatum, varying only in their time course, dose potency, and extent of non-neuronal cellular damage. Crotoxin was also found to share the lesioning capability. Thus, all phospholipolytic neurotoxins tested had the ability to induce neuronal lesions. A non-toxic PhA isoenzyme from Vipera russellii venom (65) was tested and found to cause no detectable histological or enzymatic marker damage in the striatum at doses up to 1 μ g. Thus, PhA activity cannot by itself account for the creation of lesions.

DISCUSSION.

Information about the toxic and non-toxic forms of PhA is accumulating at a rapid rate, but, as has been noted in earlier Chapters, few significant correlations have emerged from comparisons. Thus, the basic question of the relationship of the enzymatic activity, demonstrable in biochemical assays and in vitro incubations with natural and synthetic membranes, to the toxic activity is not understood. Clearly, at some level, it MUST be involved, because direct evidence from ultrastructural studies of the time course of β -toxin action (3,5) shows the breakup and withdrawal of the nerve ending at long incubation times. However, damage of this type is not seen in shorter incubations or in muscle endplates removed and fixed from experimental animals at the moment of death (66). Morphological studies on central nervous system slices or synaptosomes (13,43) have shown no damage when biochemical functions have been disrupted.

In order to consider the mechanism of β -toxin effects, it is convenient to distinguish between early and late events. The first category of initial events will be taken to include the pre-synaptic binding, the rapid depression

and facilitation phases of neuromuscular blockade, the rapid inhibition of choline and neurotransmitter uptake systems, and the loss of sodium pump activity. The second category of early effects includes perturbations in nerve terminal calcium compartmentation, the depletion of pre-synaptic energy stores, the gradual depolarization of synaptosomes, the interruption of synaptic vesicle recycling, and the irreversible decline in evoked transmitter release. In addition, a third class of events should be considered which are linked to prolonged exposure to the toxin: the lysis of synaptosomes or erythrocytes, effects on non-neural membranes, withdrawal of nerve terminals at the neuromuscular junction, and the production of neuronal lesions. The framework which must be organized is the relation of each class of events to the others, and the role of PhA activity.

Work in this Chapter has been directed to two aspects of the initial events, the role of phospholipids in the membrane recognition specificity of β -bgt, and the involvement of any catalytic differences on different model substrates. The liposome system was selected as the model because both binding and degradative functions could be separately studied under equivalent conditions. However, it should be noted that it is not clear what criteria should be used in selecting an appropriate model. The PhA literature offers different experimental systems (lipid monolayers, mixed micelles, immobilized lipids, liposomes) with different advantages, but with experimental disagreement and conflicting results. The liposome system was chosen because it could be directly used in both spectroscopic and enzymatic studies, and could be modified with defined components.

β -Bgt's interactions with liposomes were monitored by its intrinsic fluorescence because this was a sensitive way of using the native toxin directly in binding experiments. With negatively charged lipids (PS,PA,PI),

the trp emission both increased in intensity and shifted its emission maximum position to that of a more hydrophobic environment (338 to 324 nm), and other phospholipids caused no changes. The changes were identical whether 0.1 to 10 μM β -bgt was used. Comparing the group of the three negative lipids, they were effective in the order PS>PA>PI, with PS saturating the fluorescence effect at a molar ratio of 8-to-1 over toxin. Addition of calcium quenched the emission intensity, but did not dissociate the complex as indicated by the retention of the blue shift of λ_{max} ; Ca^{+2} also did not increase or decrease the molar potency of negative phospholipids in eliciting this change. However, the addition of gangliosides to the liposomes increased the molar effectiveness of complex formation, so that a molar ratio of PS over toxin of 2-to-1 saturated the change, and did so only in the presence of calcium. Thus, in protein-free, highly-idealized models, a gradient of binding preference is observed. It is not clear whether this is physical in nature (changes in fluidity, etc.) or due to a binding specificity. A remarkably similar type of association of toxins with liposomes has been reported for the bee venom toxin melittin (67) and for cobra cardiotoxin (68). In both cases, their interaction with phospholipids gave rise to enhanced intensity and a blue shift of the emission maximum of their trp residue fluorescence. This is particularly significant in view of the speculated evolution of cardiotoxins from toxic PhA (see Chapter I).

The model studies suggest that negatively charged lipids, particularly PS, may contribute to the observed catalytic preference with extracted lipids from liver and synaptosomes. What is intriguing is that ternary liposome mixtures of PS-gangliosides- Ca^{+2} are required to give most effective toxin binding, and an extraordinarily high surface packing density

must be achieved. Thus, tissues which present higher surface concentrations of PS and gangliosides might be expected to bind more toxin, not only with high affinity, but also at high local density, thus producing "patches" of rapid damage. Binding studies of radiolabeled β -bgt reported a low level of saturable sites on synaptosomal, liver, and red blood cell membranes (70), with a dissociation constant of 1 to 2 nM. The data on PS/gangliosides in models is not inconsistent with their participation in the " β -bgt receptor", particularly since current ideas of membrane asymmetry propose that little PS is normally at the surface (72); thus, one might expect a low level of binding. Further, the limited amount of external PS is thought to occur in association with membrane proteins (72) so that β -bgt would be placed very near vulnerable targets such as membrane pumps and uptake sites by this type of binding.

If PS were part of the recognition site, it should be refractory to toxin digestion because PS hydrolysis would act to dislodge the toxin from the membrane by destroying its own target. This has been observed in a variety of test systems (49,73) which have repeatedly indicated that PS is only slightly attacked by a variety of PhAs. The data on liposome hydrolysis reported here indicated that this was true for β -bgt as well. Intriguingly, crotoxin, which one would like to consider similar to β -bgt, is able to cause a more potent indirect hemolysis using PS than the customary PC (2), which can be taken as evidence of preferred digestion of PS.

If PS recognition were all that was involved in the neurotoxicity, then many more PhA enzymes would be neurotoxic. Therefore, there must be other contributing factors. Digestive experiments showed that synaptosomal liposomes were degraded more rapidly than liver liposomes. Further, if intact membranes are used, then the rate on synaptosomal membranes is the highest of the tested model conditions. This may indicate a role

for proteins, not only in the recognition specificity, but also in the catalytic efficiency of toxic PhA enzymes. Proteins could act directly as receptor sites, or indirectly, as organizational sites for unique lipid/glycolipid domains. Increased catalytic rates might also be interpreted as evidence for an endogenous membrane "activator" of PhA activity, specific for neurotoxic PhA.

The inhibition of the sodium pump, the interruption of several uptake processes, and the depolarization of synaptosomes have all been observed with both toxic and non-toxic forms of PhA (16,18,74). Thus, attempts to invoke these elements as the key features of the mechanism of β -bgt action in the periphery must reckon with the absence of peripheral toxicity in PhA enzymes that give identical synaptosomal effects to β -bgt. The explanation has been that there must be unique surface determinants that direct the peripheral actions of toxic PhA to different target tissues. One complication is that sequencing of a number of toxic and non-toxic forms of PhA shows that they vary little in the ~ 20 to 30 residues of the N-terminal sequence which is speculated to be the lipid-binding site for all PhA enzymes (71,75). However, it should be considered that the N-terminal region may only be a non-selective anchoring point for membrane attachment, and, perhaps, that binding selectivity arises from an orienting site located elsewhere in the primary structure, or from a conformational change that inhibits dissociation from specific targets. In this regard, it is tantalizing to speculate that this specificity may arise in part from a contribution of the light chain in β -bgt.

It is not clear how PhA enzymes block the sodium pump and uptake sites. The possibilities are the release of inhibitory fatty acids, the release of disruptive lysophosphatides, or the destruction of essential local lipids.

It is interesting to note that Dowdall (76) has recently shown that enzymatically-inactivated derivatives of pre-synaptic toxins are still capable of potent inhibition of high-affinity ^3H -choline uptake in T-sacs (peripheral synaptosomes), which may point to a purely physical basis for the inhibition. This physical basis could be a specific binding of the toxin to the immediate lipid domain near the choline uptake sites. It seems reasonable to suggest that the loss of membrane polarization arises from the cessation of sodium pump activity, and not from a direct effect of the PhA activity.

The chemical modifications did not resolve the relation of PhA activity to lethality. This may be because the egg-yolk/pH titration assay system is simply not a good model for physiological digestion. Nonetheless, protection studies implicated the single trp in the lipid-interface recognition site, in agreement with the fluorescence results, and tyr residues in both the catalytic and binding sites. Curiously, 10 mM CaCl_2 did not protect against p-bromophenacyl bromide modification, but this observation has also been made for the modification of crotoxin B by this reagent (11).

In earlier Chapters, attention was directed to the potential functional significance of structural differences of 9A and 14. In this Chapter, functional differences have indeed been documented differentiating these single chain toxins from the two-chain toxins. 9A, for example, has a unique toxicology which resembles that of Enhydrina schistosa myotoxin (77), a single chain toxic PhA, inasmuch as both exhibit more rapid lethality at high doses. 9A and 14 both have effects like crotoxin (44), unlike the other β -toxins, on excitable vesicles by causing a block of carbachol stimulation at low doses and rupturing the vesicles at higher doses. They have potent in vitro PhA activities like the other toxins, but attack

model liposomes, synaptosomal membranes, and intact synaptosomes more aggressively than the other toxins and show less tissue selectivity. 9A causes an immediate depolarization of synaptosomes and induces quantitative lysis within 1 hr. For comparison, β -bgt has a lag time before it brings about a slower rate of synaptosomal depolarization, and only causes 10% lysis at 1 hr. In lesioning experiments on the striatum, histological examination showed that 9A and 14 gave the most extensive areas of damage and also gave the highest proportions of non-neuronal damage to glial cells, connective tissue, and axons. There are two contexts in which these observations are important. The first is that the cross-contamination of β -bgt with toxin 9A would give the former a wider apparent spectrum of membrane action, and a more potent in vitro PhA. Dr. Cassian Bon (Pasteur Institute, Paris) has indeed noted in unpublished experiments that commercial β -bgt contaminated with 9A gave a potent block of the carbachol depolarization of the isolated electroplaque cell, whereas our purified β -bgt had no such effect. The second context is the description of toxin 14 as " β -bgt" by the Livengood et al group (6). These results show unequivocal pharmacological differences between these two toxins, and could account for the decline in miniature synaptic potential amplitude they have reported as a post-synaptic effect of this toxin (75). In addition to the differences mentioned in this Chapter, the binding of ^{125}I -labeled toxin 14 to synaptosomal membranes was inhibited by divalent cations (6), unlike the binding of ^{125}I -labeled β -bgt (70).

The original context in which β -bgt was studied was its potential utility as a specific pre-synaptic marker, and ideally, as a probe for a specific pre-synaptic protein to which it was hoped the toxin would bind. These goals have been complicated by the presence of the endogenous degradative activity. However, in this Chapter, this activity has been put to

direct use as a new tool for deleting central nervous system neurons. The search for selective degenerative neurotoxins has proven most successful with small molecule analogues of natural neurotransmitters, notably 6-hydroxydopamine(79), 5,7-dihydroxytryptamine (80), and kainic acid (58). Their use led to significant advances in the knowledge of neurotransmitter and receptor compartmentation, and transmitter pathway identification. In principle, protein toxins might be found that could add to the repertoire of chemical lesioning specificities. However, to date, protein toxins either have activities that do not produce lesions, or the lesions they produce are not usefully selective, as in the case of diptheria toxin (81). Because β -bgt produces a selective loss of pre-synaptic neuromuscular terminals, it was considered a candidate for a cholinergic neuron lesioning agent.

The biochemical and histological effects noted in the diagonal band of the septum, the dentate gyrus of the hippocampus, and the corpus striatum show a lack of specificity for either cholinergic or non-cholinergic cells, or for terminals over cell bodies. However, there is evidence for resistant cell bodies in the substantia nigra because the biochemical and histological tests show little evidence of degeneration. The incoming GABA terminals in the nigra, on the other hand, appear to be sensitive because both GAD and ^3H -GABA uptake are reduced to less than 10% of controls over a four-day period. Uptake markers, regardless of the brain region, were particularly vulnerable. ^3H -choline uptake was quantitatively abolished in every tested region by day one, and ^3H -GABA uptake underwent a precipitous drop. In the diagonal band, ^3H -GABA uptake appeared to recover because of the increased contribution of proliferating glial cells to the observed uptake. This was not seen in the nigra because the cell bodies were not extensively damaged and there was no glial cell increase.

With all of these markers, it is difficult to extricate cause and effect. For example, some of the rapidly lost biochemical markers may indicate contribute to the development of a lesion. Thus, it is not possible to identify the primary cause of neuronal loss.

Although all of the tested β -toxins caused lesions, a non-toxic PhA from Vipera russellii venom did not. Thus, there must be more than PhA activity per se in the mechanism of lesion induction. One possibility for the difference may be that non-toxic PhA have an altered cellular partitioning, or membrane binding specificity, from the toxic PhA, as has been suggested before. Alternatively, lesion creation may result from a secondary consequence of the ability to disrupt synaptic transmission by inducing a particular type of membrane damage. The degenerative damage in the brain occurs in both terminals and cell bodies unlike the restriction of the effects to terminals in the periphery. This may simply be due to unavailability of the cell bodies to peripheral β -bgt or, if there is a toxin recognition site conferring neuromuscular junction specificity, it may be a widespread surface feature of central neurons.

One striking aspect of β -bgt as a lesioning agent is its extraordinary potency. As little as 0.1 ng can produce complete neuronal deletion within a small area. Such a dose corresponds to 5 fmoles, making β -bgt over 10^6 X more potent than kainic acid on a molar basis (51,82). This extreme potency leads to the speculation that perhaps the products of β -bgt induce a self-propagating cascade of increasing damage, perhaps by inducing natural degradative mechanisms. The critical question is whether the synaptic blockade and lesioning activities are causally related or independent.

β -Toxins can be used as lesioning devices when complete and rapid removal of neurons is needed. In this way, these toxins can prove complementary to the action of kainic acid, which does not delete certain neurons (56,83).

REFERENCES.

1. Strong, P.N., Goerke, J., Oberg, S.G., and Kelly, R.B. (1976) Proc. Nat.Acad.Sci., 73, 178.
2. Jeng, T.-W., Hendon, R.A., and Fraenkel-Conrat, H.F. (1978) Proc. Nat.Acad.Sci., 75, 600.
3. Strong, P.N., Heuser, J.E., and Kelly, R.B. in Cellular Neurobiology, ed. by Hall, Z.W., Kelly, R.B., and Fox, C.F., Alan R. Liss, Inc., New York, New York, 1977, p.227.
4. Howard, B.D., and Truog, R. (1977) Biochemistry, 16, 122.
5. Abe, T., Limbrick, A.R., and Miledi, R. (1976) Proc.Roy.Soc., 194, 545.
6. Livengood, D.R., Manalis, R.S., Donlon, M.A., Masukawa, L.M., Tobias, G.S., and Shain, W. (1978) Proc.Nat.Acad.Sci., 75, 1029.
7. Chang, C.C., Su, M.J., Lee, J.D., and Eaker, D. (1977) Naunyn-Schmiedeberg's Archs.Pharmacol., 299, 155.
8. Abe, T., Alema, S., and Miledi, R. (1977) Eur.J.Biochem., 80, 1.
9. Abe, T., and Miledi, R. (1978) Proc.Roy.Soc., 200, 225.
10. Strong, P.N., Von Wedel, R.J., and Kelly, R.B. (1977) Neurosci.Abstacts, 3, 377.
11. Jeng, T.-W., and Fraenkel-Conrat, H.F. (1978) FEBS Lett., 87, 291.
12. Halpert, J., Eaker, D., and Karlsson, E. (1976) FEBS Lett., 61, 72.
13. Sen, I., Grantham, P., and Cooper, J.R. (1976) Proc.Nat.Acad.Sci., 73, 2664.
14. Wagner, G.M., Mart, P.E., and Kelly, R.B. (1974) Biochem.Biophys. Res.Communs., 58, 475.
15. Oberg, S.G., and Kelly, R.B. (1976) J.Neurobiol., 7, 129.
16. Wernicke, J.F., Vanker, A.D., and Howard, B.D. (1975) J.Neurochem., 25, 483.
17. Dowdall, M.J., Fohlman, J., and Eaker, D. (1977) Nature, 269, 700.
18. Sen, I., and Cooper, J.R. (1978) J.Neurochem., 30, 1369.
19. Albuquerque, E.X. (University of Maryland School of Medicine), personal communication, July, 1978.
20. Pittman, R.N., and Oppenheim, R.W. (1977) Neurosci.Abstacts, 3, 116.
21. Hirokawa, N. (1977) J.Cell Biol., 73, 27.

22. Chang, C.C., Chuang, S.-T., and Huang, M.C. (1975) *J.Physiol.*, 250, 161.
23. Kato, A.C., Pinto, J.E.B., Glavinovic, M., and Collier, B. (1977) *Can.J.Physiol.Pharmacol.*, 55, 574.
24. Hirokawa, N. (1978) *J.Comp.Neurol.*, 180, 449.
25. Eterovic, V.A., Hebert, M., Hanley, M.R., and Bennett, E.L. (1975) *Toxicol.*, 13, 37.
26. Elliott, K.A.C. in *Handbook of Neurochemistry*, ed. by Lajtha, A., volume 2, Plenum Press, New York, New York, 1969, p. 103.
27. Salach, J.I., Turini, P., Seng, R., Hauber, J., and Singer, T.P. (1971) *J.Biol.Chem.*, 246, 331.
28. Farnsworth, C.E., and Dratz, E.A. (1976) *Biochim.Biophys.Acta*, 443, 556.
29. Whittaker, V.P., and Barker, L.A. in *Methods of Neurochemistry*, ed. by Fried, R., volume 2, Marcel Dekker, New York, New York, 1972, p. 1.
30. Blaustein, M.P., and Goldring, J.M. (1975) *J.Physiol.*, 247, 589.
31. Sims, P.F., Waggoner, A.S., Wang, C.-H., and Hoffman, J.F. (1974) *Biochemistry*, 13, 3315.
32. Forbush, B., Kaplan, J.H., and Hoffman, J.F. (1978) *Biochemistry*, 17, 3667.
33. Hendry, I.A., and Iversen, L.L. (1971) *Brain Res.*, 29, 159.
34. Fonnum, F., Storm-Mathisen, J., and Walberg, F. (1970) *Brain Res.*, 20, 259.
35. Fonnum, F. (1969) *Biochem.J.*, 115, 465.
36. Iversen, L.L., and Neal, M.J. (1968) *J.Neurochem.*, 15, 1141.
37. Carroll, P.T., and Goldberg, A.M. (1975) *J.Neurochem.*, 25, 523.
38. Hanley, M.R., and Iversen, L.L. (1978) *Mol.Pharmacol.*, 14, 246.
39. Simon, E.J., Hiller, J.M., and Edelman, I. (1973) *Proc.Nat.Acad.Sci.*, 70, 1947.
40. Howlett, D.R., and Nahorski, S.R. (1978) *FEBS Lett.*, 87, 152.
41. Leysen, J.E., Niemegeers, C.J.E., Tollenaere, J.P., and Laduron, P.M. (1978) *Nature*, 272, 168.
42. Koelle, G.G., and Friedenwald, J.S. (1949) *Proc.Soc.Exp.Biol. Med.*, 70, 617.
43. Wernicke, J.F., Oberjat, T., and Howard, B.D. (1974) *J.Neurochem.*, 22, 781.

44. Hanley, M.R. (1978) *Biochem.Biophys.Res.Communs.*, 82, 392.
45. Whittaker, V.P., Michaelson, I.A., and Kirkland, R.J.A. (1964) *Biochem. J.*, 90, 293.
46. Breithaupt, H. (1976) *Toxicon*, 14, 221.
47. Dennis, E.A. (1973) *J.Lipid Res.*, 14, 152.
48. Strong, P.N., and Kelly, R.B. (1977) *Biochim.Biophys.Acta*, 469, 231.
49. Roberts, M.F., Otnaess, A.-B., Kensil, C.A., and Dennis, E.A. (1978) *J.Biol.Chem.*, 253, 1252.
50. Viljoen, C.C., Visser, L., and Botes, D.P. (1976) *Biochim.Biophys.Acta*, 138, 424.
51. Sokolovsky, M., Riordan, J.F., and Vallee, B.L. (1966) *Biochemistry*, 5, 3582.
52. Roberts, M.F., Deems, R.A., Mincey, T.C., and Dennis, E.A. (1977) *J.Biol.Chem.*, 252, 2405.
53. Krnjevic, K. (1969) *Fed.Proc.*, 28, 113.
54. Cotman, C.W., and Banker, G.A. (1974) *Revs.Neurosci.*, 1, 1.
55. Isaacson, R.L., and Pribram, K.H. (eds.) *The Hippocampus*, Plenum Press, New York, New York, 1975.
56. Nadler, J.V., Perry, B.W., and Cotman, C.W. (1978) *Nature*, 271, 676.
57. Hattori, T., Singh, V.K., McGeer, P.L., and McGeer, E.G. (1976) *Brain Res.*, 102, 164.
58. Coyle, J.T., and Schwarcz, R. (1976) *Nature*, 263, 244.
59. Minneman, K.P., Quik, M., and Emson, P.C. (1978) *Brain Res.*, 151, 507.
60. Kuhar, M.J. (1973) *Life Sci.*, 13, 1623.
61. Schrier, B.K., and Thompson, E.J. (1974) *J.Biol.Chem.*, 249, 1769.
62. Yamamura, H.I., and Snyder, S.H. (1974) *Brain Res.*, 78, 320.
63. Hattori, T., McGeer, P.L., Fibiger, H.C., and McGeer, E.G. (1973) *Brain Res.*, 54, 103.
64. Creese, I., Schneider, R., and Snyder, S.H. (1977) *Eur.J.Pharmacol.*, 46, 377.
65. Bennett, E.L., Morimoto, H., Lukasiewicz, R.J., Hanley, M.R., Hebert, M. (1977) *Proc.Intern.Soc.Neurochem.*, 6, 387.

66. Chen, I.L., and Lee, C.-Y. (1970) *Virchows Archs. B.Zellpathol.*, 6, 318.
67. Dufourcq, J., and Faucon, J.F. (1977) *Biochim.Biophys.Acta*, 467, 1.
68. Dufourcq, J., and Faucon, J.F. (1978) *Biochemistry*, 17, 1170.
69. Upreti, G.C., and Jain, M.K. (1978) *Archs.Biochem.Biophys.*, 188, 364.
70. Oberg, S.G., and Kelly, R.B. (1976) *Biochim.Biophys.Acta*, 433, 662.
71. Eaker, D. (1978) International Symposium on Proteins, Taipei, Taiwan.
72. Bergelson, L.D., and Barsukov, L.I. (1977) *Science*, 197, 224.
73. Adamich, M., and Dennis, E.A. (1978) *J.Biol.Chem.*, 253, 5121.
74. Sun, A.Y. (1974) *J.Neurochem.*, 22, 551.
75. Slotboom, A.J., and DeHaas, G.H. (1975) *Biochemistry*, 14, 5394.
76. Dowdall, M.J. (1978) Proc.Third Intern.Symp.Cytopharmacol., Venice, Italy.
77. Fohlman, J., and Eaker, D. (1977) *Toxicon*, 15, 385.
78. Masukawa, L.M., Tobias, G.S., Donlon, M.A., and Livengood, D.R. (1977) *Neurosci.Abstracts*, 3, 374.
79. Sachs, C., and Jonsson, G. (1975) *Biochem.Pharmacol.*, 24, 1.
80. Baumgarten, H.G., and Bjoklund, A. (1976) *Ann.Rev.Pharmacol.*, 16, 101.
81. Eames, R.A., Jacobson, S.G., and McDonald, W.I. (1977) *J.Neurol.Sci.*, 32, 381.
82. McGeer, E.G., and McGeer, P.L. (1976) *Nature*, 263, 517.
83. Hendron, R.M., and Coyle, J.T. (1977) *Science*, 198, 71.

CHAPTER VII.
SUMMARY AND PERSPECTIVES.

VII. Protein neurotoxins are very significant in contemporary neuroscience because they have elucidated aspects of nerve impulse conduction and synaptic transmission that were not accessible by other techniques. The most useful toxins have great specificity for particular targets, which either permits the detailed study of the target, or its selective inactivation. Further, unlike the alkaloid toxins (such as tetrodotoxin), protein neurotoxins have the advantage of the relative ease with which spectroscopic, radioactive, or electron-dense labels can be incorporated without the loss of biological activity.

Although the two major neurotoxins of the snake Bungarus multicinctus, α - and β -bungarotoxin, have been studied in detail, they are a long way from completely understood. The approach taken in this thesis program was the detailed comparative study of these two toxins in addition to the seven related bungarotoxins from the same venom. The two major goals were to discover new applications for these toxins and to understand the molecular details of their mechanism.

At the outset, the philosophy was adopted that concerted functional study is appropriate only on a firm foundation of rigorous purification and structural characterization. Accordingly, a considerable effort was devoted to obtaining extensively purified toxins, providing evidence for purity by several techniques, and then systematically determining the basic structural features of each toxin. By structural, and later functional, criteria, the toxins repeatedly fell into three categories: curarimimetic toxins similar to α -bungarotoxin, pre-synaptic toxins similar to β -bungarotoxin, and single-chain pre-synaptic toxins similar to notexin. In all cases, the neurotoxins were highly stable structures, due a large number of internal disulfide cross-links. Nonetheless, spectroscopic evidence identified local regions of conformational flexibility in all three classes.

α -Bungarotoxin will, in all likelihood, not differ dramatically from the recently reported X-ray structures of shorter sea snake neurotoxins. One exceptional feature, however, may be the long extended C-terminal tail. From hydrodynamic data, this tail adds to the overall solution asymmetry of the toxins so that they appear larger than their true molecular weight. The functional significance, if any, of this tail is unknown. The clustering of several charged amino acid residues that are invariably found in similar positions in post-synaptic toxin sequences leads to the proposition that the loop including residues 27-38 is the "active site". The term "active site" must be used cautiously, because few chemical modifications cause the complete abolition of all activity in all post-synaptic toxins. Therefore, it is likely that many residues make interaction contributions, and that several residues may have redundant functions so that any one of the residues may provide a necessary bond or spatial orientation. Surprisingly, the invariant tryptophan residue, found in the middle of the hypothesized active site, is not essential and can be modified in α -bungarotoxin with only a partial loss of activity. This is fortunate inasmuch as the residue can be used as a fluorescent reporter or be modified into another reporter group to allow spectroscopic analysis of the toxin binding to the receptor. The utility of this approach was demonstrated by preparing a 2-hydroxy-5-nitrobenzyl derivative of the tryptophan and showing that it was masked in a hydrophobic domain upon receptor binding.

The presence of α -toxin binding sites in a variety of tissues is now well-established. The significance of these sites is not. It was shown that sites in rat brain can bind another toxin, dendrotoxin 4.7.3, at a ratio of two-to-one over α -bungarotoxin sites, and that this difference in site recognition properties is not found in a peripheral receptor. Since den-

drotoxin has been reported to have a synaptic blocking activity in a central nervous system preparation, it seems likely that this observation on its binding is related to this functional difference. I have proposed that α -bungarotoxin and dendrotoxin bind to the same entity, which is a functional and significant brain acetylcholine receptor, but that the former toxin does not block agonist stimulation of the receptor. This implies that it is possible for α -bungarotoxin to occupy a population of specific receptor sites simultaneously with an agonist. Agonists, however, can prevent α -bungarotoxin binding by pre-equilibration with the brain sites. This suggests that toxin binding is lost under these conditions due to a non-competitive effect of the agonists in altering the toxin to a state refractory to toxin binding, possibly the desensitized state. If true, this would point to the brain and peripheral receptors as being fundamentally different in their desensitization responses.

The current state of curarimimetic research demands more details on ~~the chemical nature of toxin binding sites on the receptor.~~ It is now technically possible to map the receptive surface of the acetylcholine receptor using fluorescence energy transfer among various ligands (e.g. fluorescent rare-earth calcium analogues, fluorescent agonists, and fluorescent local anesthetics), or by saturation-transfer EPR using suitably modified derivatives. Photoaffinity derivatives of post-synaptic toxins can be used to probe the peptide composition in the binding site, and to detect the proximity of polypeptides speculated to be part of the functional receptor. Lastly, the major problem remains of proving that the toxin-binding site detected in vertebrate brains and ganglia is or is not a synaptic, functional acetylcholine receptor. To this end, radio-labeled agonists of extremely high specific activity must be prepared to

test whether dendrotoxin overlaps with agonist sites, but α -bungarotoxin does not. Much more extensive electrophysiology is necessary before clear statements can be made as to whether all toxins in all central nervous tissues have no synaptic blocking ability.

The pre-synaptic toxins have proven to be very complicated indeed. The fundamental question remains as to the relationship of the phospholipase activity to the toxicity, particularly since so many non-toxic phospholipase enzymes have virtually identical effects on test systems of several sorts. The recurring idea has been a binding specificity, and, to date, hypotheses have revolved around protein receptor sites. The extremely high density of β -bungarotoxin binding to liposomes composed of both phosphatidyl serine and brain gangliosides suggests surface features of this type would be an ideal target. One complication is that non-toxic phospholipases appear to share the preference for phosphatidyl serine. Accordingly, the following sequence of events is proposed: both toxic and non-toxic phospholipases share the same recognition step and bind to acidic lipids. However, toxic phospholipases are proposed to be able to undergo a conformational change, possibly triggered by a particular lipid or protein determinant, to stabilize their binding to target tissues. Non-toxic phospholipases dissociate and re-bind. The net result would be to spread non-toxic phospholipases randomly over a membrane, but to accumulate toxic phospholipases in patches. Furthermore, the proposed recognition element of combined PS-ganglioside contains two components that are known to preferentially associate with membrane proteins. It would therefore be the disruption of membrane functions by local lipid damage around protein sites that causes pre-synaptic failure. Single chain toxins are much more potent than two-chain toxins in several biochemical tests, yet are less toxic. This may be because they are less selective in their

tissue binding, perhaps because they are unable to undergo the conformational stabilization of site-specific binding, and are diluted by adsorption to non-neural tissues.

Intriguingly, a similar mechanism for a preferential binding of a phospholipase to the annular lipid zone is being considered for the post-synaptic effects of phospholipases in inhibiting acetylcholine receptor function. This might imply that there are entire families of affinity-directed phospholipases specific for different surface determinants of different tissues, and could provide an important new class of membrane probes.

The ability of pre-synaptic toxins to induce brain lesions correlates with peripheral lethality, in the small range of toxic and non-toxic phospholipases studied. Thus, if the proposal above is correct, the ability of these toxins to induce lesions must be related to a persistent binding of the toxins, and the patchwork damage effect. The resistance of neuronal cell bodies in the substantia nigra might point to the absence of the speculated "binding-validation" component which inhibits dissociation of the toxin. Once the missing element that explains the regional selectivity of pre-synaptic action is identified, there is the hope that it might be accessible to experimental modification so as to produce selective lesions of particular transmitter-types of neurons, or particular pre- or post-synaptic zones.

Some of the data on the central effects of both pre- and post-synaptic toxins may have unexpected dividends in elucidating the mechanisms of neuropathologies. For example, preliminary data has linked epilepsy to the occurrence of specific antibodies to the brain-specific toxin receptor. Also, selective loss of cholinergic neurons may mimic a pathological state, if this can be achieved by modifying the lesioning specificity of β -toxins.

This report was done with support from the Department of Energy. Any conclusions or opinions expressed in this report represent solely those of the author(s) and not necessarily those of The Regents of the University of California, the Lawrence Berkeley Laboratory or the Department of Energy.

TECHNICAL INFORMATION DEPARTMENT
LAWRENCE BERKELEY LABORATORY
UNIVERSITY OF CALIFORNIA
BERKELEY, CALIFORNIA 94720